TU/e EINDHOVEN UNIVERSITY OF TECHNOLOGY

# Olefin copolymerization via controlled radical polymerization : an insight

*Citation for published version (APA):*
Venkatesh, R. (2004). *Olefin copolymerization via controlled radical polymerization : an insight*. [Phd Thesis 1 (Research TU/e / Graduation TU/e), Chemical Engineering and Chemistry]. Technische Universiteit Eindhoven. https://doi.org/10.6100/IR574838

*DOI:*
10.6100/IR574838

*Document status and date:*
Published: 01/01/2004

*Document Version:*
Publisher's PDF, also known as Version of Record (includes final page, issue and volume numbers)

*Please check the document version of this publication:*

• A submitted manuscript is the version of the article upon submission and before peer-review. There can be important differences between the submitted version and the official published version of record. People interested in the research are advised to contact the author for the final version of the publication, or visit the DOI to the publisher's website.
• The final author version and the galley proof are versions of the publication after peer review.
• The final published version features the final layout of the paper including the volume, issue and page numbers.

Link to publication

*General rights*
Copyright and moral rights for the publications made accessible in the public portal are retained by the authors and/or other copyright owners and it is a condition of accessing publications that users recognise and abide by the legal requirements associated with these rights.

• Users may download and print one copy of any publication from the public portal for the purpose of private study or research.
• You may not further distribute the material or use it for any profit-making activity or commercial gain
• You may freely distribute the URL identifying the publication in the public portal.

If the publication is distributed under the terms of Article 25fa of the Dutch Copyright Act, indicated by the "Taverne" license above, please follow below link for the End User Agreement:

www.tue.nl/taverne

*Take down policy*
If you believe that this document breaches copyright please contact us at:

openaccess@tue.nl

providing details and we will investigate your claim.

Download date: 16. Nov. 2023

# Olefin Copolymerization via Controlled Radical Polymerization – An Insight

Rajan Venkatesh

**Cover:** Matrix assisted laser desorption/ionization – time of flight – mass spectrometry (MALDI-TOF-MS) spectrum of a statistical poly[(methyl acrylate)-co-(1-octene)] copolymer.

CIP-DATA LIBRARY TECHNISCHE UNIVERSITEIT EINDHOVEN

Venkatesh, Rajan

Olefin Copolymerization via Controlled Radical Polymerization : An Insight /
by Rajan Venkatesh. – Eindhoven : Technische Universiteit Eindhoven,
2004.
Proefschrift. – ISBN 90-386-2965-6
NUR 913

Trefwoorden: polymerisatie ; radicaalreacties / reactiekinetiek / radicaal-polymerisatie ; ATRP / ketenoverdracht ; RAFT / copolymeren ; chemische samenstelling / polymeerkarakterisatie
Subject headings: polymerization ; radical reactions /reaction kinetics / atom transfer radical polymerization ; ATRP / chain transfer ; RAFT / copolymers ; chemical composition / polymer characterization

© 2004, Rajan Venkatesh

Printed by the Eindhoven University Press, Eindhoven, The Netherlands.

This research was financially supported by the Dutch Polymer Institute (DPI).

An electronic copy of this thesis is available from the site of the Eindhoven University Library in PDF format (www.tue.nl/bib).

# Olefin Copolymerization via

# Controlled Radical Polymerization

# – An Insight

PROEFSCHRIFT

ter verkrijging van de graad van doctor aan de
Technische Universiteit Eindhoven, op gezag van de
Rector Magnificus, prof.dr. R.A. van Santen, voor een
commissie aangewezen door het College voor
Promoties in het openbaar te verdedigen
op maandag 19 april 2004 om 16.00 uur

door

Rajan Venkatesh

geboren te Mumbai, India

Dit proefschrift is goedgekeurd door de promotoren:

prof.dr. C.E. Koning
en
prof.dr. D.M. Haddleton

Copromotor:
dr.ir. L. Klumperman

*Dedicated*

*to*

*My Parents*

# Contents

**Chapter 1** General Introduction

1.1 Introduction 1

1.1.1 Copolymerization of (meth)acrylates with α-olefins 2

1.1.1.1 Brookhart Catalysts 3

1.1.1.2 Yasuda Catalysts 5

1.2 Objective and Challenge of the Project 7

1.3 Free radical polymerization (FRP) 8

1.4 Controlled radical polymerization (CRP) 9

1.4.1 Prerequisites for CRP 10

1.4.2 Atom transfer radical polymerization (ATRP) 10

1.4.2.1 Monomers 11

1.4.2.2 Initiators 11

1.4.2.3 Catalyst/Ligand 11

1.4.2.4 Solvents 12

1.4.3 Reversible addition-fragmentation chain transfer (RAFT) Polymerization 12

1.4.3.1 Choice of RAFT agent 14

1.4.3.2 Choice of Initiator 14

1.5 Outline of Thesis 14

1.6 References 15

**Chapter 2** Olefin Copolymerization via Controlled Radical Polymerization : Copolymerization of Acrylate and 1-Octene

2.1 Introduction 17

2.2 Experimental Section 20

2.2.1 Materials 20
2.2.2 Analysis and Measurements 20
Laboratory Experiments
2.2.2.1 Determination of Conversion and Molar Mass Distribution (MMD) 20
2.2.2.2 NMR 21
2.2.2.3 MALDI-TOF-MS 21
Online NMR Experiments
2.2.2.4 NMR 21
2.2.2.5 Determination of MMD 22
2.3 Synthetic Procedures 22
2.3.1 Copolymerization of MA and 1-Octene 22
2.3.2 Online NMR Experiments 23
2.4 Results and Discussion 23
2.4.1 Copolymerization of MA and 1-Octene 23
2.4.2 Reactivity ratios 26
2.4.3 Polymer Characterization 32
2.4.3.1 Atom Transfer Radical Polymerization 32
2.4.3.2 Free Radical Polymerization 37
2.5 Determination of Activation Rate Parameters 41
2.5.1 Materials 41
2.5.2 Method employed for determination of rate coefficient of activation ($k_{act}$) 42
2.5.3 Synthetic Procedures 43
2.5.3.1 Trapping Experiments 43
2.5.3.2 Synthesis of the model compound H-MA-Hexene-Br 43
2.5.4 Results and Discussion 45
2.6 Conclusions 49
2.7 Supporting Information 50

2.8 References 51

**Chapter 3** Olefin Copolymerization via Controlled Radical Polymerization : Copolymerization of Methyl Methacrylate and 1-Octene

3.1 Introduction 55
3.2 Experimental Section 57
3.2.1 Materials 57
3.2.2 Analysis and Measurements 57
3.2.2.1 Determination of Conversion and MMD 57
3.2.2.2 GPEC Analysis 58
3.2.2.3 MALDI-TOF-MS 58
3.2.2.4 DSC 59
3.3 Synthetic Procedures 59
3.3.1 ATR Copolymerization of MMA and 1-Octene 59
3.3.2 Bulk Polymerization of MMA (Chain transfer experiments) 59
3.4 Results and Discussion 60
3.4.1 Choice of initiator 60
3.4.2 Determination of Chain transfer constant ($C_{tr}$) for 1-octene in MMA 62
3.4.3 MMA / 1-Octene Copolymers 64
3.4.4 ATRP initiated by P[(MMA)-co-(1-Octene)]. Chain extension with MMA 69
3.4.5 Copolymer Characterization 70
3.4.5.1 MALDI-TOF-MS 71
3.4.5.2 DSC 73
3.5 Conclusions 74
3.6 References 75

**Chapter 4** Copolymerization of Acrylates and Methacrylates with 1-Octene using Reversible addition-fragmentation chain transfer (RAFT)

4.1 Introduction 79
4.2 Experimental Section 81
4.2.1 Materials 81
4.2.2 Analysis and Measurements 81
4.2.2.1 Determination of Conversion and MMD 81
4.2.2.2 GPEC Analysis 82
4.2.2.3 MALDI-TOF-MS 82
4.2.2.4 NMR 83
4.2.3 Choice of RAFT agent 83
4.3 Synthetic Procedures 83
4.3.1 RAFT copolymerization 83
4.4 Results and Discussion 84
4.4.1 RAFT copolymerization 84
4.4.2 Copolymer Characterization 88
4.4.2.1 Copolymers of BA/Octene 88
4.4.2.2 Copolymers of MMA/Octene 92
4.5 Conclusion 93
4.6 References 94

**Chapter 5** Reversible addition-fragmentation chain transfer (RAFT)**:** Fate of the Intermediate Radical

5.1 Introduction 95
5.2 Experimental Section 98
5.2.1 Materials 98
5.2.2 Analysis and Measurements 98
5.2.2.1 Determination of MMD 98

5.2.2.2 MALDI-TOF-MS 99
5.2.2.3 ESR 99
5.3 Synthetic Procedures 100
5.3.1 ESR 100
5.3.2 RAFT polymerization 100
5.3.3 ATR polymerization 100
5.3.4 Model reactions of PBA-Br with PBA-RAFT 101
5.4 Results and Discussion 101
5.4.1 ESR 101
5.4.1.1 BA System 102
5.4.1.2 Styrene System 105
5.4.2 Termination Reactions 109
5.4.2.1 Reactions with AIBN 113
5.4.2.2 Reactions with PBA-Br 116
5.5 Conclusions 126
5.6 References 127

**Chapter 6** Copolymerization of allyl butyl ether (ABE) with acrylates via controlled radical polymerization

6.1 Introduction 129
6.2 Experimental Section 131
6.2.1 Materials 131
6.2.2 Analysis and Measurements 132
6.2.2.1 Determination of Conversion and MMD 132
6.2.2.2 NMR 133
6.2.2.3 MALDI-TOF-MS 133
6.3 Synthetic Procedures 133
6.3.1 ATR Copolymerization of MA and ABE 133

6.3.2 RAFT Copolymerization of BA and ABE 134
6.4 Results and Discussion 134
6.4.1 Copolymerization of MA/ABE 134
6.4.2 RAFT Copolymerization of BA/ABE 136
6.4.3 Polymer Characterization 138
6.4.3.1 Copolymers of MA/ABE synthesized using ATRP 138
6.4.3.2 Copolymers of BA/ABE synthesized using RAFT 143
6.5 Conclusions 147
6.6 References 148

**Chapter 7** Novel 'bottle-brush' Copolymers via Controlled Radical Polymerization

7.1 Introduction 151
7.2 Experimental Section 152
7.2.1 Materials 152
7.2.2 Analysis and Measurements 153
7.2.2.1 Determination of Conversion and MMD 153
7.2.2.2 NMR 154
7.2.2.3 Preparative HPLC 154
7.2.2.4 Contact Angle Measurements 154
7.2.2.5 Scanning Force Microscopy (SFM) 154
7.2.2.6 HPLC-MS 154
7.2.2.7 Adhesion Measurements 155
7.3 Synthetic Procedures 156
7.3.1 Synthesis of 2-(2-bromoisobutyryloxy)ethyl methacrylate [BIEM] 156
7.3.2 RAFT polymerization 156
7.3.3 ATR polymerization 156

7.3.4 Sample Preparation 157
7.4 Results and Discussion 157
7.4.1 Homopolymerization of BIEM and 'grafting through' Copolymerization of BIEM/PEOMA 158
7.4.2 'Grafting from' polymerization using P(BIEM) and P(BIEM-co-PEOMA) as polyinitaitors 160
7.4.3 SFM characterization of brush polymers 163
7.4.4 Contact angle measurements 164
7.4.5 Adhesion measurements 165
7.5 Conclusions 169
7.6 References 169

**Chapter 8** Highlights and Technological Assessment

8.1 Highlights 171
8.2 Technological Assessment 173
8.3 References 174

SUMMARY 175

SAMENVATTING 179

Patents / Scientific Papers 183

Acknowledgements 185

Curriculum Vitae 187

# Chapter 1

# *General Introduction*

## *1.1 Introduction*

Presently, the world capacity for the higher alpha-olefins ($C_6$ – $C_{18}$ segment) is approx. 2.5 m tonnes / year. The main processes from which they are obtained are, **(i)** Ethylene oligomerization (or trimerization); **(ii)** Fischer-Tropsch ($CO/H_2$); **(iii)** Wax cracking (dehydrogenation of n-paraffin). The major producers are BP Amoco, Chevron/Phillips, Sasol and Shell. These alpha-olefins find applications in various fields

| | | | | | |
|---|---|---|---|---|---|
| (a) | $C_6$, $C_8$ | - | co-monomers for polyolefins (LLDPE) | | |
| (b) | $C_6$-$C_{10}$ | - | hydroformylation | → | plasticizers, solvents |
| | | | oligomerization | → | lubricants |
| (c) | $C_{10}$-$C_{13}$ | - | reaction with benzene | → | linear alkyl benzenes |
| (d) | $C_{11}$-$C_{14}$ | - | hydroformylation | → | detergent intermediates |

Copolymers of alpha-olefins with polar monomers with various architectures remain an ultimate goal in polyolefin engineering. Of the many permutations available for modifying the properties of polymers, the incorporation of polar functional groups into an otherwise nonpolar material is substantial.[1,2] Polar groups exercise control over important properties such as, adhesion, barrier properties, surface properties (paintability, printability, etc.), solvent resistance, miscibility with other polymers, and rheological properties. Although random copolymerizations of olefins with methyl methacrylate or vinyl acetate have been put to practical use as an amendment process, this traditional technique possesses only a limited utility because it produces elastomers with variable composition only under drastic conditions (high temperature and high pressure).[3] Grafting of polyolefins with polar poly(methyl methacrylate) or poly(acrylonitrile) also gave structurally rather complex branched polymers.[3] In this context, a more intelligent synthetic methodology is required for realizing structurally well-defined linear copolymers comprised of nonpolar and polar monomer units.

An important feature of successful copolymerization of two monomers is the ability to control the amount of the two monomers and their distribution over the polymer chains. Aside from monomer concentration, the other important determinant in this process is the relative reactivity of the monomer pair.

The next sections briefly discuss the work done in our area of interest.

## *1.1.1 Copolymerization of (meth)acrylates with α-olefins*

The high oxophilicity of early transition metal catalysts (titanium, zirconium or chromium) causes them to be poisoned by most functionalised vinyl monomers, particularly the commercially available polar comonomers. Simple coordination of the functional group of the monomer with the metal center may be a problem. For example, potential olefin copolymerization is inhibited by back chelation of the penultimate carbonyl after 1,2-insertions, a process that blocks monomer access to vacant coordination sites (Figure-1.1). Once the metal-oxygen enolate bond forms, however, insertion of olefins will not occur. An exception to this would be a metal enolate species that is capable of rearranging from the oxygen-bound enolate to another carbon-metal bound intermediate. Such a system based on Palladium (Pd) has been discovered. The lower oxophilicity and the presumed greater functional – group tolerance of the late transition metals relative to early metals make them likely targets for the development of catalysts for the copolymerization of ethylene and polar comonomers under mild conditions.

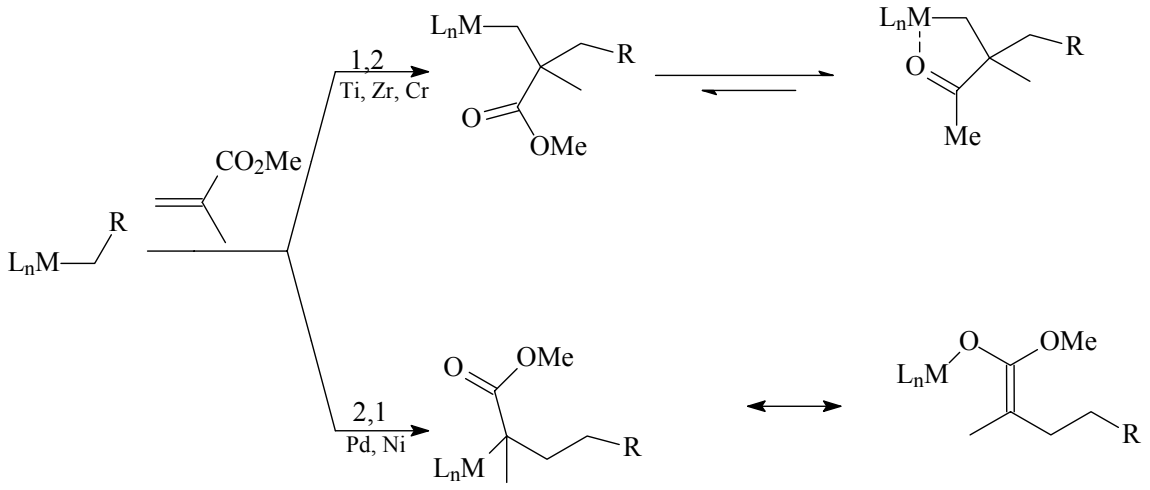


**Figure-1.1:** Insertion reactions

### *1.1.1.1 Brookhart Catalysts*

The area of alpha-olefins polymerization (especially ethylene polymerization) with late transition metal catalysts was rejuvenated when Brookhart and his group reported a family of new cationic Pd(II) and Ni(II) α-diimine catalysts for the polymerization of ethylene, α-olefins and cyclic olefins, and also the copolymerization of nonpolar olefins with a variety of functionalized olefins.[4]

Three key features of the original α-diimine polymerization catalysts are, **(i)** highly electrophilic, cationic nickel and palladium metal centers; **(ii)** the use of sterically bulky α-diimine ligands; and **(iii)** the use of non-coordinating counterions or the use of reagents to produce non-coordinating counterions.[5] The electrophilicity of the late metal center in these cationic complexes results in rapid rates of olefin insertion. The use of bulky ligands favors insertion over chain transfer. The use of non-coordinating counterions provides an accessible coordination site for the incoming olefins.

***α-Diimine based catalysts***

The easily varied steric and electronic properties of the α-diimine ligands are an important feature of the nickel α-diimine catalyst system. The α-diimine ligands are well known to stabilize organometallic complexes.[6,7] E.g. (I) neutral Ni catalysts derived from [ArN=C(R)-C(R)=NAr]$NiBr_2$ (i) plus methylaluminoxane (MAO) are quite active for polymerization of α-olefins in toluene.[8] Poly(α-olefins) with relatively high molar mass (MM) and very narrow molar mass distributions (MMDs) are produced.

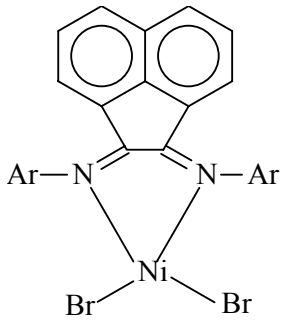


a) Ar = 2,6-(i-Pr)$_2$C$_6$H$_3$-; b) Ar = 2-t-Bu C$_6$H$_4$-

**(i)**

(II) Cationic palladium and nickel complexes with sterically bulky α-diimine ligands polymerize ethylene and α-olefins to high MM polymers of unique microstructure.[8] Copolymers of ethylene or α-olefins with alkyl acrylates and other functionalised monomer can also be obtained employing Pd catalysts (ii).

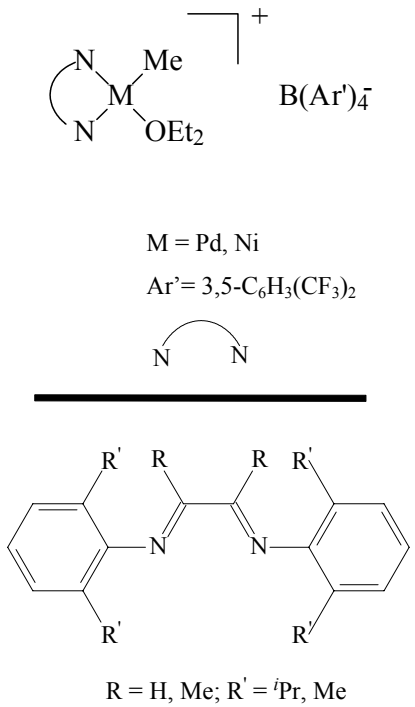


**(ii)**

The cationic palladium α-diimine complexes are remarkably functional-group tolerant. These complexes catalyze the copolymerizations. Acrylate insertion occurs predominantly in a 2,1-fashion, yielding a strained four-membered chelate ring in which the carbonyl oxygen atom is coordinated to the palladium atom. This insertion is followed by a series of β-hydride eliminations and readditions, expanding the ring stepwise to the six-membered chelate complex; this is the catalyst resting state shown in Figure-1.2.

Considering an example of copolymerization of ethylene ($C_2H_4$) with methyl acrylate (MA), the relative ratios of incorporation of ethylene and methyl acrylate into the copolymers are governed by both the equilibrium ratio of the alkyl ethylene and alkyl methyl acrylate complexes, and their relative rates of migratory insertion as shown in Figure-1.2. The composition of the copolymer depends upon the feed concentrations of both ethylene and methyl acrylate. There is an overwhelming preference for binding ethylene to the electrophilic Pd(II) center relative to the

electron-deficient methyl acrylate. Thus, to achieve significant incorporation of methyl acrylate into the copolymer, very large ratios of MA : $C_2H_4$ ratios must be used. A consequence of increasing the MA concentrations is that the overall rate of polymerization decreases due to increased concentrations of the chelate complex. Decreasing the bulk of the diimine ligand, or incorporating more electron-donating substituents on the diimine, increase acrylate incorporation, probably through improved binding of MA to the catalyst center.

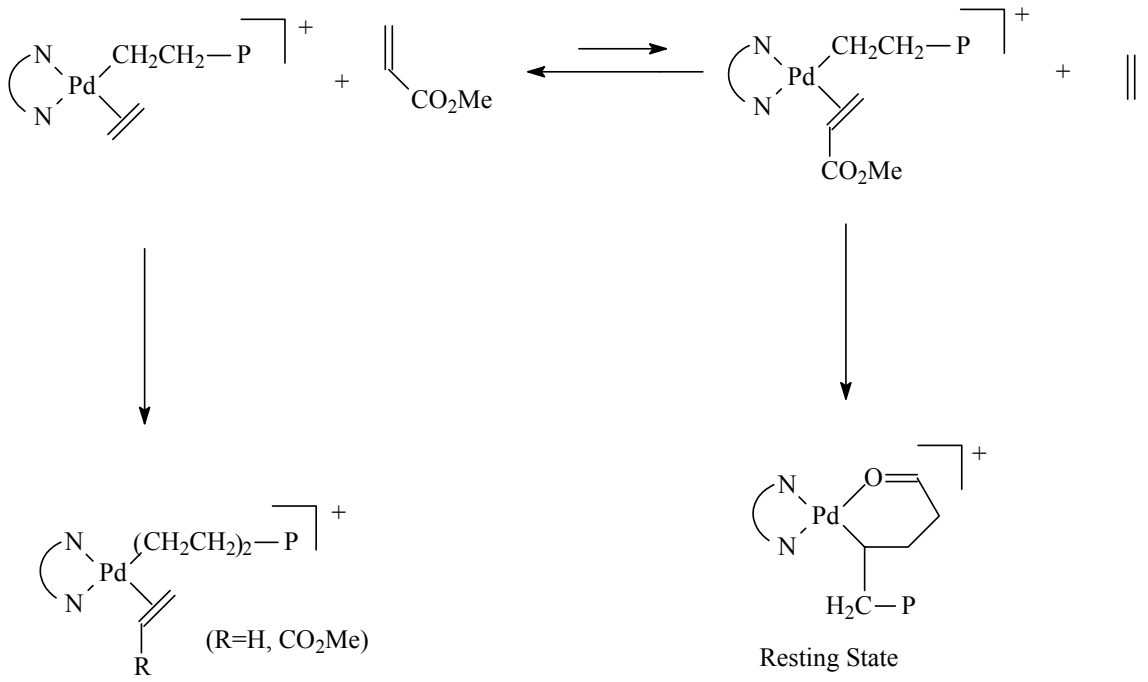


**Figure-1.2:** Mechanistic studies of the copolymerization of ethylene and methyl acrylate [9]

### *1.1.1.2 Yasuda Catalysts*

A polymerization system based on neutral lanthanocenes, particularly $(C_5Me_5)_2SmR$ (iii) complexes,[3,10] has been developed by Yasuda et al. In this case, the large and highly electropositive organosamarium center can serve simultaneously as both the initiator (insertion) and catalyst (monomer activation) components of the group transfer polymerization. A second Lewis acid equivalent (co-catalyst) is not required.

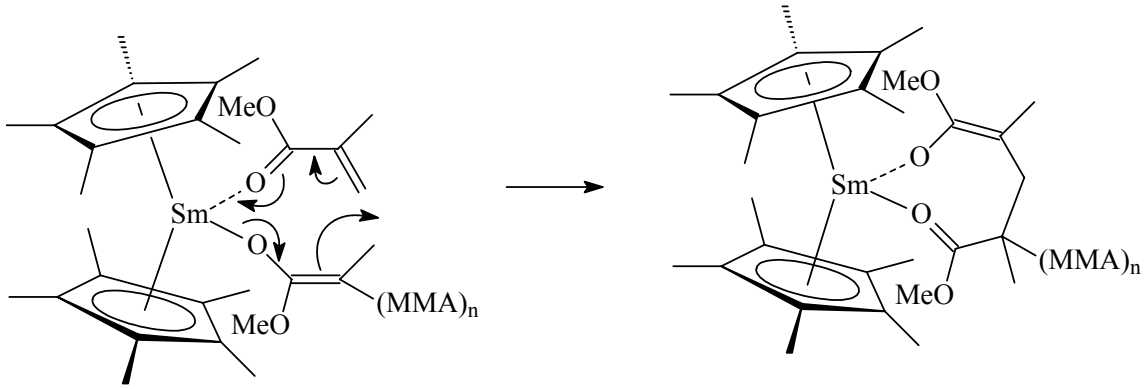


**Figure-1.3:** Mechanism on using organosamarium centered catalyst.

Mechanistic crossover from olefin polymerization to group transfer polymerization is possible with lanthanocene catalysts, since the insertion of an acrylate into the propagating metal alkyl to form an enolate is energetically favored. Block copolymers of ethylene with MMA, methyl acrylate, or ethyl acrylate have been prepared by sequential addition of the respective monomers to the lanthanide catalysts. The reverse order of monomer addition, i.e., (meth)acrylate followed by ethylene, does not give diblocks since the conversion of an enolate to an alkyl is not favored.

The more open ligand sphere provided by the $C_5Me_5$/ER ligand set (refer **iii** & **iv**), could explain why the present systems are more active than the corresponding metallocene catalysts. Polystyrene or poly(methyl methacrylate) content in the block copolymers can be easily adjusted by changing the feeding amount of the monomers.

$C_5Me_5$, $C_5Me_5$, Sm—R

R=H, Me

**(iii)**

$C_5Me_5$, ER, Sm, $C_5Me_5K(THF)n$, L

1: ER=$OC_6H_3{}^iPr_2$-2,6, L=THF, n=2

2: ER=$OC_6H_2{}^iBu_2$-2,6-Me-4, L=none, n=2

3: ER=$SC_6H_2{}^iPr_3$-2,4,6, L=THF, n=1

**(iv)**

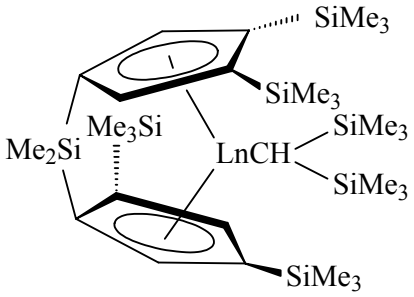


Ln=Sm

**(v)** [11]

*In conclusion, to the author's limited knowledge, although catalyst systems showing excellent behavior for both olefins and polar monomers do exist, true (random/statistical) copolymerization of these two types of monomers is difficult to achieve due to the very unfavorable reactivity ratios in conjunction with these catalyst systems.*

## *1.2 Objective and Challenge of the Project*

***The main objective of the current project is to develop an approach, based on conventional and controlled radical polymerization (CRP) [CRP enables to control MMD] that allows the statistical incorporation of α-olefins in vinyl polymers.***

From the free-radical perspective, the homopolymerization of α-olefins and allylic monomers like allyl acetate or allyl butyl ether is very unlikely and if it does occur, it polymerizes at considerably low rates. This effect is a consequence of degradative chain transfer, wherein, the propagating radical in such a polymerization is very reactive, while the allylic C-H in the monomer is quite weak, resulting in chain transfer to monomer. The weakness of the allylic C-H bond arises from the high resonance stability of the allylic radical that is formed. This formed allylic radical is too stable to reinitiate polymerization and will undergo termination by reaction with another allylic radical or more likely, with propagating radicals.[12,13] Recently, it was observed that 1-octene and allyl ethyl ether both act as a strong retarder for the polymerization of methyl methacrylate initiated by α,α'-azobisisobutyronitrile.[14,15]

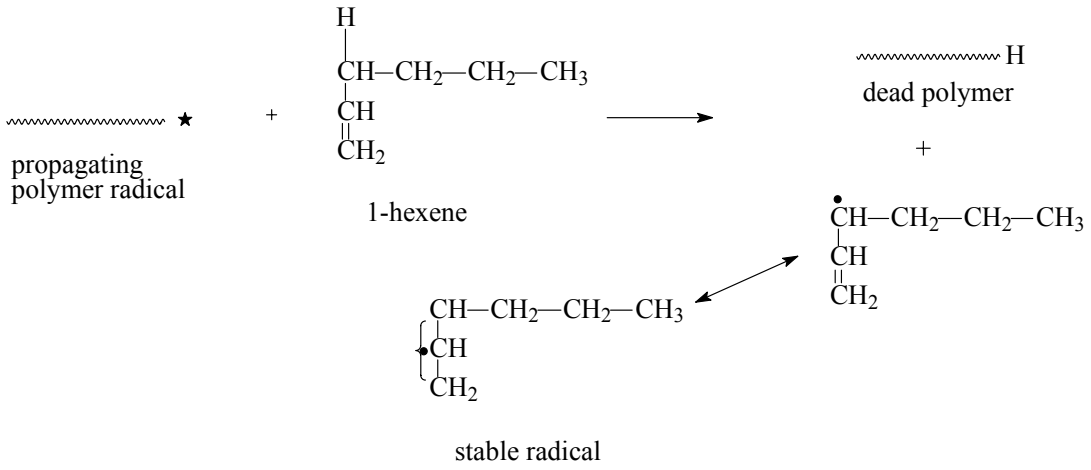


**Figure-1.4:** Formation of stable allylic radical

## *1.3 Free radical polymerization (FRP)*

Of all the types of polymerization, free-radical processes are commercially the most important and scientifically the most thoroughly investigated. One of the reasons for this is the fact that useful high-molar mass polymers and copolymers can be prepared from a wide variety of monomers. Also, these processes are generally the easiest to carry out and control. Thus, the free-radical polymerization provides a convenient route to polymers with a wide variety of properties. In the western countries alone, current production of all polymers is around $10^8$ tonnes / year and approximately 30% (by weight) of these polymers have been prepared by free-radical polymerization means.[16] In the USA, free-radical polymerization contributes 46% (by weight) of the total production of plastics.[5]

Polymerization of monomers of general structure $CH_2 = CXY$ are commonly carried out using free radical techniques. In the first quarter of the 20th century, Staudinger recognized the nature of these reactions and put forward a correct interpretation for the mechanism of radical polymerization.[17] Later, in 1937, Flory published a comprehensive paper on quantitative aspects of the kinetics and mechanism of the free-radical polymerization.[18] Subsequently free-radical polymerization has been extensively studied and considerable progress has been made.[19,20,21,22,23]

In common with other types of chain polymerizations, free-radical polymerization can be divided into three distinct stages: initiation, propagation and termination. In the first stage an initiator is used to produce free-radicals, which react with the olefinic monomer to initiate the polymerization. Each polymer chain propagates by rapid sequential addition of monomer molecules

to the terminal radical reactive site, which is known as the active center for polymerization. Consequently upon every addition of monomer, the active center is transferred to the last attached monomeric species. Termination of the growth of polymer chains results from the reactions between actively growing polymer chains, or between growing polymer chains and primary radicals. An important feature of free-radical polymerization is that the partially polymerized mixture mainly consists of high molar mass polymer molecules and unreacted monomer molecules.

The advantages of the free radical polymerization are, **(i)** compatible with many monomers including functional monomers, **(ii)** versatile with regard to reaction conditions, and **(iii)** widely applied in industry for the above reasons.

The clear limitations being, **(i)** due to diffusion-controlled termination reactions between growing radicals, little control over molar mass distribution (MMD), **(ii)** since, the typical life time of a propagating chain is very short, in the range of 1 s, it is not possible to synthesize block copolymers or other chain topologies, and **(iii)** there is no control over the polymer tacticity.

Now, so as to retain the advantages of conventional free radical polymerization (FRP) and minimize its disadvantages, controlled radical polymerization (CRP) techniques were developed. The main similarity between CRP and FRP is the participation of free radicals in the chain growth. The main difference between CRP and FRP is that, in CRP the steady concentration of free radicals is established by balancing rates of activation and deactivation, but in FRP this is realized by balancing the rates of initiation and termination. Accordingly, in CRP the rates of initiation, activation and deactivation are much larger than that of termination. The exchange between active and dormant chains also enables an extension of the lifetime of propagating chains from ~ 1 s in FRP to >> 1 h in CRP. This enables synthesis of polymers with different chain topologies (e.g. block, graft).

## *1.4 Controlled radical polymerization (CRP)*

Currently, the three most effective methods of CRP include nitroxide mediated polymerization (NMP),[24] atom transfer radical polymerization (ATRP)[25] and reversible addition-fragmentation chain transfer (RAFT) pplymerization.[26] In this section a brief insight is given into two of these techniques, which have been employed in this work, namely, ATRP and RAFT.

### *1.4.1 Prerequisites for CRP*

The prerequisites for CRP in general can be summarized as follows, **(1)** Fast initiation as compared to propagation, since all chains should begin to grow essentially at the same time and retain functionality. **(2)** Concentration of the propagating radicals should be sufficiently low ($[P^*] < 10^{-7}$ M) to enable chain growth on one hand and reduce termination events on the other. **(3)** Fast exchange between active and dormant species, so that majority of the growing chains are in the dormant state and only a small fraction is present as propagating free radicals.

### *1.4.2 Atom Transfer Radical Polymerization (ATRP)*

The name ATRP comes from the atom transfer step, which is the key elementary reaction responsible for the uniform growth of polymeric chains. ATRP originates in atom transfer radical addition (ATRA) reactions, which target the formation of 1:1 adducts of alkyl halides and alkenes, which are catalyzed by transition metal complexes.[27] In copper mediated ATRP, the carbon-halogen bond of an alkyl halide (RX) is reversibly cleaved by a $Cu^{I}X$/ligand system resulting in a radical (R*) and $Cu^{II}X_2$/ligand (deactivator). The radical will mainly either reversibly deactivate, add monomer or irreversibly terminate (Figure 1.5).

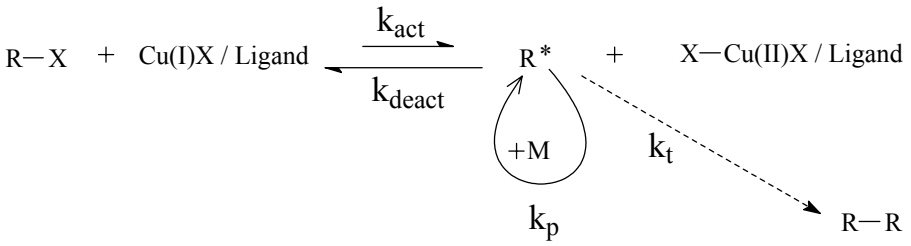


**Figure 1.5:** Simplified ATRP Mechanism

The role of the different ingredients like monomers, alkyl halide initiators, catalyst, ligand and solvent employed during ATRP is of paramount importance. *But as always, a reliable working formulation with all the necessary ingredients can only be developed after extensive laboratory reactions.* Recently published reviews [25] give an excellent insight into various aspects of ATRP.

### *1.4.2.1 Monomers*

A variety of monomers have been successfully polymerized using ATRP. The polar monomers used for the current study predominantly constitute of acrylates and methacrylates, which contain substituents that can stabilize the propagating radicals. ATR homopolymerization of α-olefins and allyl butyl ether was tried but without success. The reason is that, as there are no substituents present to stabilize the formed radicals, the propagating radicals are too reactive, leading to excessive termination as a result of side reactions. For each specific monomer, the concentration of propagating radicals and the rate of radical deactivation need to be adjusted to maintain polymerization control.

### *1.4.2.2 Initiators*

In ATRP, alkyl halides (RX) are typically used as initiators. Initiation should be fast and quantitative. The structure of the R group and halide atom X must be carefully selected depending on the monomer and catalyst/ligand employed. For the present work, the initiators employed were; *acrylates* – ethyl-2-bromoisobutyrate (EBriB), *methacrylates* – 2,2,2-trichloroethanol (TCE) and *p*-toluenesulphonyl chloride (pTsCl).

### *1.4.2.3 Catalyst/Ligand*

The key to achieve the desired atom transfer equilibrium and the rate of exchange between dormant and active species is the appropriate choice of the catalyst/ligand combination. Some important prerequisites for a suitable catalyst are, that the metal center should have reasonable affinity towards a halogen and the coordinating sphere around the metal should be expandable on oxidation to selectively accommodate the halide. The ligand, should strongly complex with the catalyst, solubilize the transition metal salt and adjust the redox potential of the metal center forming the complex. Various transition metals have been studied. In this research, for the ATRP reactions of acrylates, *copper (I) bromide* was employed, and for the methacrylate reactions, *copper (I) chloride* was used. Similarly, in literature, several ligands have been employed, the most extensive being 2,2'-bipyridine derivatives, 2-iminopyridine derivatives and some aliphatic polyamines. In the present case, *N,N,N',N'',N''*-pentamethyldiethylenetriamine (PMDETA) has been extensively employed.

#### *1.4.2.4 Solvents*

The choice of the solvent is as important, since there is a possibility that the structure of the catalyst complex may change in different solvents, which in turn directly influences the atom transfer equilibrium and the polymerization reaction rate. Polar solvents are known to improve the solubility of the catalyst complex. During this research, *p*-xylene had been employed as the solvent in most cases, in conjunction with PMDETA, thus resulting in a heterogeneous ATRP system.

### *1.4.3 Reversible Addition-Fragmentation Chain Transfer (RAFT) Polymerization*

It was found that simple organic compounds possessing the thiocarbonylthio moiety (figure 1.6) were effective in controlling the polymerization by reversible addition-fragmentation chain transfer.[28,29] There have been a number of publications ever since, clearly indicating the versatility of the RAFT systems using various monomers in both homogeneous and heterogeneous environments. A recently published book on radical polymerization, comprises a chapter, which deals with the work done in the RAFT field.[26] There are four classes of thiocarbonylthio RAFT agents, depending on the nature of the activating (Z) group: **(i)** dithioesters (Z = aryl or alkyl), **(ii)** trithiocarbonates (Z = substituted sulfur), **(iii)** dithiocarbonates (xanthates), **(iv)** dithiocarbamates (Z = substituted nitrogen). Representative examples for the thiocarbonylthio RAFT and the preferred combination of the activating and leaving groups are given in Figure 1.6. It is also shown, which combination would be the best suited for specific monomers.

In a RAFT mechanism, initiation occurs via the decomposition of the free radical initiator leading to formation of propagating chains. This is followed by addition of the propagating radical to the RAFT chain transfer agent. Further, the fragmentation of the intermediate radical occurs, giving rise to a polymeric RAFT agent and a new radical. This radical reinitiates the polymerization to form new propagating radicals. The RAFT process relies on this rapid central addition-fragmentation equilibrium between propagating and intermediate radicals, and chain activity and dormancy as shown in Figure 1.7.

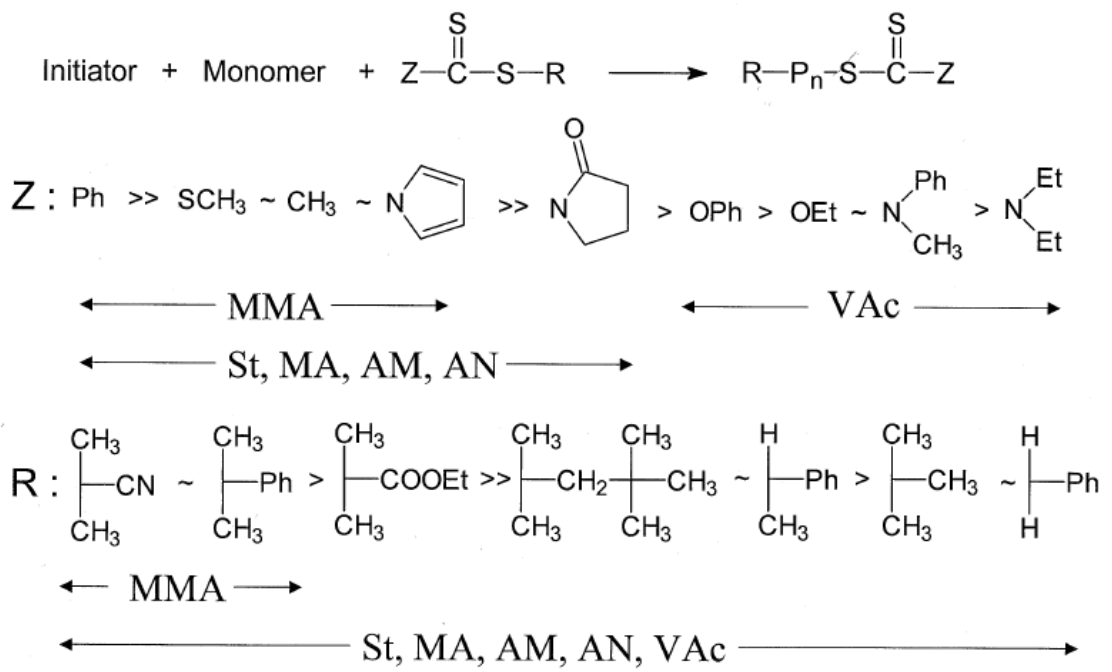


**Figure 1.6:** Examples of different RAFT agents in relation to the monomers that can be polymerized in a well-controlled way. (St = styrene, MMA = methyl methacrylate, MA = methyl acrylate, AM = acrylamide, AN = acrylonitrile, VAc = vinyl acetate).

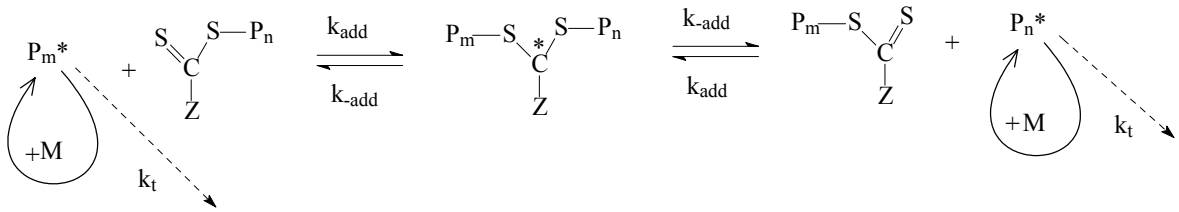


**Figure 1.7:** The central RAFT equilibrium

In a RAFT system, the important parameters are, (1) choice of the RAFT agent depending upon the monomer to be polymerized, (2) a high ratio of RAFT agent to initiator consumed and (3) a low radical flux during the polymerization.

#### *1.4.3.1 Choice of RAFT agent*

The RAFT agent must be chosen such that its chain transfer activity is appropriate to the monomer to be polymerized. The electronic properties of the activating (Z) group and the stereoelectronic properties of the leaving (R) group determine the chain transfer activity of the RAFT agent. The Z group in the RAFT agent must be chosen such that it activates the double bond towards radical addition, but at the same time not provides a too great stabilization influence on the intermediate radical. The R group should be a good leaving group, relative to the radical of the propagating species, and should also preferentially reinitiate the polymerization. The influence and choice of the Z and R groups are discussed in detail in recent publications.[30,31]

#### *1.4.3.2 Choice of Initiator*

The choice of the thermal initiator is also an important factor in obtaining control over a RAFT polymerization. High ratios of the RAFT agent to initiator should be employed, so as to maintain a low radical flux. The choice of the initiator is dependent on its half-life at the desired reaction temperature and its initiation ability relative to the monomer employed. The longer the half-life of the initiator at the desired temperature, the longer is the duration of radical production and thereby, the RAFT polymerization is kept active for a longer time.

The areas of immense interest, research and debate are focused to the initial stages of the RAFT polymerization (inhibition or initialization) and the retardation effects observed during the RAFT polymerization, which is related to the fate of the intermediate radical.

## *1.5 Outline of the thesis*

*Chapter 2* describes the conventional free radical polymerization (FRP) and atom transfer radical copolymerization (ATRP) of methyl acrylate (MA) and 1-octene (Oct). *Chapter 3* details the successful copolymerization of methyl methacrylate (MMA) and 1-octene. *Chapter 4* tackles the reversible addition-fragmentation chain transfer (RAFT) polymerization of acrylates and methacrylates with 1-octene. *Chapter 5* deals with the intriguing area of RAFT kinetics. *Chapter 6* looks into the copolymerization aspects of acrylates with allyl butyl ether (ABE) using both ATRP

and RAFT. *Chapter 7* utilizes the previously described chemistry for the synthesis of novel copolymers, which can for example, be applied as adhesion promoting agents. *Chapter 8* highlights the important findings and is a technology assessment on the probable industrial utilization of these copolymers.

## *1.6 References*


1) Padwa, A. R., *Prog. Polym. Sci.*, **14**, 811 (1989).
2) *Functional Polymers: Modern Synthetic Methods and Novel Structures*; Patil, A. O., Schulz, D.N., Novak,B. M. (Eds.); ACS Symposium Series 704; American Chemical Society: Washington, DC (1998).
3) Yasuda, H., Furo, M., Yamamoto, H., *Macromolecules*, **1992**, *25*, 5115, and references therein.
4) Ittel, S. D., Johnson, L. K., Brookhart, M., *Chemical Reviews*, **2000**, *100*, 1169.
5) Ittel, S. D., Johnson, L. K., Brookhart, M., *J. Am. Chem. Soc.*, **1995**, *117*, 6414.
6) tom Dieck, H., Svoboda, M., Grieser, T., *Z. Naturforsh*, **1981**, *36b*, 832.
7) Van Koten, G., Vrieze, K., *Adv. Organomet. Chem*., **1982**, *21*, 151.
8) Killian, C. M., Tempel, D. J., Johnson, L. K., Brookhart, M., *J. Am. Chem. Soc.*, **1996**, *118*, 11664.
9) Mecking, S., Johnson, L. K., Wang, L., Brookhart, M., *J. Am. Chem. Soc.*, **1998**, *120*, 888.
10) Yasuda, H., Ihara, E., *Macromol. Chem. Phys.*, **1995**, *196(8)*, 2417.
11) Hou, Z., Tezuka, H., Zhang, Y., Yamazaki, H., Wakatsuki, Y., *Macromolecules*, **1998**, *31*, 8650.
12) Odian, G, *Principles of Polymerization*; John Wiley: New York, **1991**, p. 266.
13) *The Elements of Polymer Science and Engineering*; Rudin, A; 2nd Edition, Academic Press **1999**, p 218.
14) Bevington, J. C., Huckerby, T. N., Hunt, B. J., Jenkins, A. D.; *J. Macromol. Sci.-Pure Appl. Chem.*, **2001**, *A38(10)*, 981.
15) Venkatesh, R., Klumperman, B.; *Macromolecules*, **2004**, *37*, 1226.
16) Gilbert, R. G., in *Emulsion Polymerization: A Mechanistic Approach,* Academic Press, London, **1995**, *Chapter 1*, p. 1.
17) Staudinger, H.; *Ber.*, **1920**, *53*, 1073; **1924**, *57*, 1203.
18) Flory, P. J.; *J. Am. Chem. Soc*., **1937**, *57*, 241.

19) Flory, P. J.; *Principles of Polymer Chemistry*, Cornell University Press, Ithaca, New York **1953**.

20) Bamford, C. H., Tipper, C. F. H.; in *Comprehensive Chemical Kinetics,* Elsevier, Amsterdam, **1976**, *Volume 14A*.

21) Bamford, C. H.; in *Encyclopaedia of Polymer Science and Engineering,* Mark, H. F., Bikales, N. M., Overberger, C. G., Menges, G., (Eds.), Wiley-Interscience, New York, **1988**, *Volume 13*.

22) Eastmond, G. C., Ledwith, A., Russo, S., Sigwalt, P., in *Comprehensive Polymer Science*, Sir Allen, G., Bevington, J. C., (Eds.), Pergamon Press, **1989**, *Volume 3*.

23) *Handbook of Radical Polymerization*, Matyjaszewski, K., Davis, T. P., (Eds.), John Wiley and Sons Inc., Hoboken, **2002**.

24) Hawker, C. J.; in *Handbook of Radical Polymerization*, Matyjaszewski, K., Davis, T. P., (Eds.), John Wiley and Sons Inc., Hoboken, **2002**, *Chapter 10*.

25) Kamigaito, M., Ando, T., Sawamoto, M.; *Chem. Rev*., **2001**, *101*, 3689. Matyjaszewski, K., Xia, J.; *Chem. Rev*., **2001**, *101*, 2921.

26) Chiefari, J., Rizzardo, E.; in *Handbook of Radical Polymerization*, Matyjaszewski, K., Davis, T. P., (Eds.), John Wiley and Sons Inc., Hoboken, **2002**, *Chapter 12*, p.

27) Curran, D. P.; *Synthesis*, **1988**, 489.

28) Le, T. P., Moad, G., Rizzardo, E., Thang, S. H.; *PCT Int Appl*., **1998**, WO98/01478.

29) Chiefari, J., Chong, Y. K., Ercole, F., Krstina, J., Jeffery, J., Le, T. P. T., Mayadunne, R. T. A., Meijs, G. F., Moad, C. L., Moad, G., Rizzardo, E., Thang, S. H.; *Macromolecules*, **1998**, *31*, 5559.

30) Chong, Y. K., Krstina, J., Le, T. P. T., Moad, G., Postma, A., Rizzardo, E., Thang, S. H.; *Macromolecules*, **2003**, *36*, 2256.

31) Chiefari, J., Mayadunne, R. T. A., Moad, C. L., Moad, G., Rizzardo, E., Postma, A., Skidmore, M. A., Thang, S. H.; *Macromolecules*, **2003**, *36*, 2273.

# Chapter 2

## *Olefin Copolymerization via Controlled Radical Polymerization : Copolymerization of Acrylate and 1-Octene*

**Abstract:** The atom transfer radical copolymerization (ATRP) of methyl acrylate (MA) with 1-octene was investigated in detail. Well-controlled copolymers containing almost 25 mol% of 1-octene were obtained using ethyl-2-bromoisobutyrate (EBriB) as initiator. Narrow molar mass distributions (MMD) were obtained for the ATRP experiments. The feasibility of the ATRP copolymerizations was independent of the ligand employed. Copolymerizations carried out using 4,4'-dinonyl-2,2'-bipyridine (dNbpy) resulted in good control, with significant octene incorporation in the polymer. The lower overall conversion obtained for the dNbpy systems as compared to the PMDETA systems, was attributed to the redox potential of the formed copper(I)-ligand complex. The comparable free radical (co)polymerizations (FRP) resulted in broad MMDs. An increase in the fraction of the olefin in the monomer feed, led to an increase in the level of incorporation of the olefin into the copolymer, at the expense of the overall conversion. There was a good agreement between the values of the reactivity ratios determined for the ATRP and FRP systems. The formation of the copolymer was established using matrix assisted laser desorption / ionization – time of flight – mass spectrometry (MALDI-TOF-MS). From the obtained MALDI-TOF-MS spectra for the ATRP systems, it was evident that several units of 1-octene were incorporated into the polymer chain. This was attributed to the rapidity of crosspropagation of octene-terminated polymeric radicals with acrylates. In ATRP polymerizations, only one pair of end groups was observed. On comparison, in the FRP systems, due to the multitude of side reactions occurring, several end groups were obtained.

## *2.1 Introduction*

Copolymers of alpha-olefins with polar monomers remain a pivotal area in polymer research, since the effect of incorporation of functional groups into an otherwise nonpolar material is substantial.[1,2]

---

Venkatesh,R., Harrisson, S., Haddleton, D. M., Klumperman, B.; submitted to *Macromolecules.*

In the area of metal-catalyzed insertion polymerization, the Brookhart Pd-based diimine catalyst[3] has been shown to copolymerize ethylene and higher alpha-olefins with acrylates and vinyl ketones.[4] Other late transition-metal-based complexes are also known to tolerate the presence of polar functional groups.[5] Block copolymers of ethylene with acrylates and methacrylates using group 4 metals are known.[6] Recently published reviews cover the work done in this field.[7] However, true (random) copolymerization of these two types of monomers is difficult to achieve due to the very unfavorable reactivity ratios in conjunction with these catalyst systems. Recent developments from Novak[8] indicated that olefins could be copolymerized with vinyl monomers via a free radical mechanism. This was followed up by a communication indicating the feasibility of the copolymerization of methyl acrylate (MA) with 1-alkenes using copper mediated controlled polymerization.[9]

This chapter is a very detailed study on the copolymerization of an alpha-olefin (1-octene) with an acrylate (methyl acrylate, MA). Comparison of reaction kinetics between free radical polymerization (FRP) and atom transfer radical polymerization (ATRP) was carried out. A heterogeneous transition metal/ligand system was employed for the ATR polymerizations. Reactivity ratios were measured using an online NMR technique. $^{1}H$ nuclear magnetic resonance (NMR) spectroscopy was employed to monitor the individual monomer conversion over time, similar to work reported by Haddleton et al.[10] The reaction was carried out within the cavity of the NMR spectrometer. From the data obtained, the reactivity ratios were calculated. The effect of monomer feed composition and of ligand was investigated. Chemical composition distributions (CCDs) were assessed using mass spectrometry for both ATRP and conventional free radical polymerization (FRP). To ascertain the preferred radical reactivity path during the ATR copolymerization, the relevant activation rate parameters for an ATRP copolymerization of methyl acrylate (MA) and octene system are investigated using model compounds. The influence of the terminal and penultimate units are discussed.

ATRP[11,12] is one of the techniques employed to obtain living (or controlled) radical polymerization. In copper mediated ATRP, the carbon-halogen bond of an alkyl halide (RX) is reversibly cleaved by a $Cu^{I}X$/ligand system resulting in a radical (R*) and $Cu^{II}X_2$/ligand (deactivator). The radical will mainly either reversibly deactivate, add monomer or irreversibly terminate (Scheme 2.1, equations 1-8).

**Scheme 2.1:** General scheme for ATRP

*Initiation*

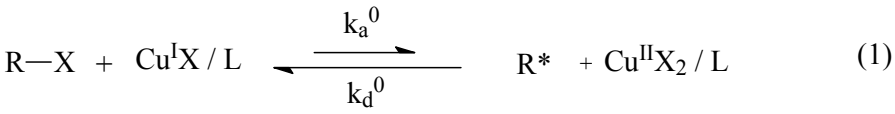


(1)

(2)

*Propagation*

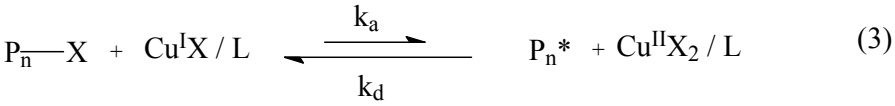


(3)

(4)

*Solubilization*

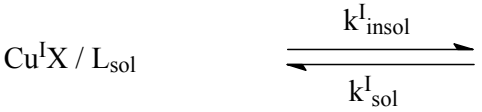


(5)

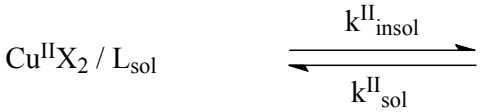


(6)

*Termination*

(7)

(8)

where, R* and $P_n$* are radicals from initiator and polymer, respectively, R-X and $P_n$-X are halogen terminated initiator and polymer chains with halide end group, M is monomer, $D^H$ and $D^=$ are the dead polymer chain with a hydrogen and vinyl-end group respectively and $D_{m+n}$ are the dead chains formed as a result of termination via combination. Rate coefficients for activation ($k_a$), deactivation ($k_d$), polymerization ($k_p$), solubilization ($k_{sol}$), insolubilization ($k_{insol}$), chain length dependent termination via combination ($k_{tC}^{m.n}$) and chain length dependent termination via disproportionation ($k_{tD}^{m,n}$).

## 2.2 Experimental Section

### 2.2.1 Materials:

Methyl acrylate (MA, Merck, 99+%) and 1-octene (Oct, Aldrich, 98%) were distilled and stored over molecular sieves. *p*-Xylene (Aldrich, 99+% HPLC grade) was stored over molecular sieves and used without further purification. N,N,N',N'',N''-pentamethyldiethylenetriamine (PMDETA, Aldrich, 99%), 4,4'-dinonyl-2,2'-bipyridine (dNbpy, Aldrich, 97%) ethyl-2-bromoisobutyrate (EBriB, Aldrich, 98%), copper (I) bromide (CuBr, Aldrich, 98%), copper (II) bromide ($CuBr_2$, Aldrich, 99%), aluminum oxide (activated, basic, for column chromatography, 50-200 μm), tetrahydrofuran (THF, Aldrich, AR) and 1,4-dioxane (Aldrich, AR) were used as supplied. α,α'-Azobisisobutyronitrile (AIBN, Merck, >98%) was recrystallized twice from methanol before use. For online NMR experiments - toluene-$d_8$ (Cambridge Isotope Labs Inc.) and toluene (Hi-Dry™, anhydrous solvent, Romil Ltd.) were used as supplied. Copper (I) bromide (CuBr, Aldrich, 98%) was purified according to the method of Keller and Wycoff.[13]

### 2.2.2 Analysis and Measurements

#### Laboratory Experiments

***2.2.2.1 Determination of Conversion and MMD:*** Monomer conversion was determined from the concentration of residual monomer measured via gas chromatography (GC). A Hewlett-Packard (HP-5890) GC, equipped with an AT-Wax capillary column (30 m × 0.53 mm × 10 μm) was used. *p*-Xylene was employed as the internal reference. The GC temperature gradient used is given in Figure 2.1.

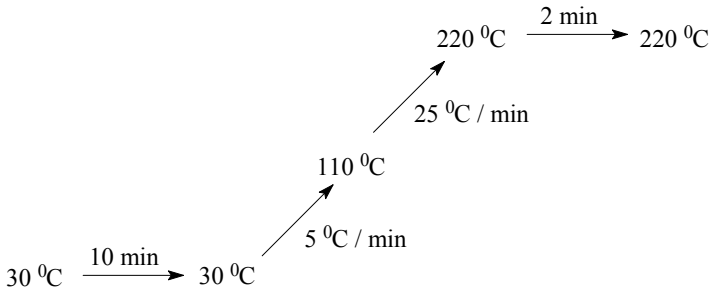


**Figure 2.1:** GC temperature gradient.

Molar mass (MM) and molar mass distributions (MMD) were measured by size exclusion chromatography (SEC), at ambient temperature using a Waters GPC equipped with a Waters model 510 pump, a model 410 differential refractometer (40 ºC), a Waters WISP 712 autoinjector (50 μL injection volume), a PL gel (5 μm particles) 50 × 7.5 mm guard column and a set of two mixed bed columns (Mixed-C, Polymer Laboratories, 300 × 7.5 mm , 5 μm bead size, 40 ºC) was used. THF was used as the eluent at a flow rate of 1.0 mL/min. Calibration was carried out using narrow MMD polystyrene (PS) standards ranging from 580 to $7 \times 10^6$ g/mol. The MM was calculated using the universal calibration principle and Mark-Houwink parameters [14] [PMA: $K = 1.95 \times 10^{-4}$ dL/g, a = 0.660; PS: $K = 1.14 \times 10^{-4}$ dL/g, a = 0.716]. The molecular weights were calculated relative to PMA homopolymer. Data acquisition and processing were performed using Waters Millenium 32 software.

***2.2.2.2 NMR:*** $^1H$ and $^{13}C$ nuclear magnetic resonance (NMR) spectra were recorded on a Varian 400 spectrometer, in deuterated chloroform ($CDCl_3$) at 25 ºC. All chemical shifts are reported in ppm downfield from tetramethylsilane (TMS), used as an internal standard (δ=0 ppm).

***2.2.2.3 MALDI-TOF-MS:*** Measurements were performed on a Voyager-DE STR (Applied Biosystems, Framingham, MA) instrument equipped with a 337 nm nitrogen laser. Positive-ion spectra were acquired in reflector mode. Dithranol was chosen as the matrix. Sodium trifluoracetate (Aldrich, 98%) was added as the cationic ionization agent. The matrix was dissolved in THF at a concentration of 40 mg/mL. Sodium trifluoracetate was added to THF at typical concentrations of 1 mg/mL. The dissolved polymer concentration in THF was approximately 1 mg/mL. For each spectrum 1000 laser shots were accumulated. In a typical MALDI experiment, the matrix, salt and polymer solutions were premixed in the ratio: 5 μL sample: 5 μL matrix: 0.5 μL salt. Approximately 0.5 μL of the obtained mixture was hand spotted on the target plate.

## ***Online NMR Experiments***

***2.2.2.4 NMR:*** $^1H$ NMR spectra were recorded on a Bruker ACP 400 spectrometer. Polymerization kinetics, followed by $^1H$ NMR, was recorded using the Bruker built-in kinetics software. Toluene (Hi- Dry™) was employed as the internal reference.

***2.2.2.5 Determination of MMD:*** Molar mass (MM) and molar mass distributions (MMD) were measured by size exclusion chromatography (SEC), at ambient temperature using a Polymer Laboratories system. For **SEC-1** [high MM], THF/triethyl amine (95:5) was used as the eluent at a flow rate of 1.0 mL/min, with a Polymer Laboratories (PL-gel) 5 μm (50 × 7.5 mm) guard column. A set of two linear columns [Mixed-C, Polymer Laboratories, 5 μm (300 × 7.5 mm)] with a refractive index detector was employed. Calibration was carried out using narrow polydispersity poly (methyl methacrylate) (PMMA) standards ranging from 200 to $1.577 \times 10^6$ g/mol. For **SEC-2** [low MM], THF was used as the eluent at a flow rate of 1.0 mL/min, with a Polymer Laboratories (PL-gel) 3 μm (50 × 7.5 mm) guard column. A set of two linear columns [Mixed-E, Polymer Laboratories, 3 μm (300 × 7.5 mm)] with a refractive index detector was employed. Calibration was carried out using narrow polydispersity PMMA standards ranging from 200 to $2.8 \times 10^4$ g/mol. MM was calculated by comparing the samples with the PMMA standards and by using Mark-Houwink parameters [14] [PMA: $K = 1.95 \times 10^{-4}$ dL/g, a = 0.660; PMMA: $K = 9.55 \times 10^{-5}$ dL/g, a = 0.719].

## *2.3 Synthetic Procedures*

***2.3.1 Copolymerization of MA and 1-Octene:*** A typical polymerization was carried out in a 100 mL three-neck round-bottom flask. *p*-Xylene (23.2 g, 0.2 mol), MA (4.67 g, 0.05 mol), 1-octene (6.1 g, 0.05 mol), CuBr (0.19 g, 1.0 mmol) and $CuBr_2$ (0.07 g, 0.3 mmol) were accurately weighed and transferred to the flask. The ligand, PMDETA (0.29 g, 1.6 mmol) was then added. The reaction mixture was degassed by sparging with argon for 30 min. The flask was immersed in a thermostated oil bath maintained at 80 °C and stirred for 10 min. A light green, slightly heterogeneous system was obtained. The initiator, EBriB (0.65 g, 0.3 mmol), was added slowly via a degassed syringe. The reactions were carried out under a flowing argon atmosphere. Samples were withdrawn at suitable time periods throughout the polymerization. A pre-determined amount of the sample was transferred immediately after withdrawal into a GC vial and diluted with 1,4-dioxane, so as to determine the monomer conversion using GC. The remaining sample was diluted with THF, passed through a column of aluminum oxide prior to SEC and MALDI-TOF-MS measurements.

***2.3.2 Online NMR Experiments:*** In a typical ATRP, CuBr (0.03 g, 0.2 mmol) and $CuBr_2$ (0.01 g, 0.06 mmol) were added to a pre-dried Schlenk tube, which was sealed with a rubber septum. The tube was evacuated and flushed with nitrogen three times to remove oxygen. Then MA (1.4 g, 16 mmol), 1-octene (0.6 g, 5.4 mmol), toluene-$d_8$ (4.0 g, 40 mmol), toluene (0.2 g, 2.2 mmol), PMDETA (0.05 g, 0.3 mmol) and EBriB (0.13 g, 0.66 mmol) were added via oven dried, degassed syringes. The liquid reagents in the Schlenk tube were degassed by three freeze-pump-thaw cycles. An aliquot of 2 mL of this solution was transferred to a NMR tube. So as to determine the initial monomer concentration at the onset of the reaction, the first scan at time = 0 s was taken at room temperature, before heating the sample to the required reaction temperature. After the experiment, the sample was diluted with THF and passed through a column of aluminum oxide prior to SEC.

## *2.4 Results and Discussion*

The synthesis of the copolymers and comparison of the ATRP results with the conventional free radical systems will be examined. The influence of the monomer feed composition and of the ligand will be highlighted. Determination and comparison of the obtained reactivity ratios from ATRP and FRP are carried out using an online NMR technique. Detailed chemical composition distributions (CCDs) for the copolymers synthesized by ATRP, determined by MALDI-TOF-MS are discussed. The various end groups obtained during the free radical reactions are assigned, and their mode of production is explained. An interesting pattern in the sequence distribution of the monomers, obtained from the MALDI data, is examined.

***2.4.1 Copolymerization of MA and 1-octene:*** AIBN-initiated and ATR copolymerizations of MA and 1-octene were examined as summarized in Table 2.1.

**Table 2.1:** Copolymers of MA/1-Octene

| Entry | MA (mol%) | 1-Octene (mol%) | 1-Octene incorporated (mol%)[d] | $M_n$ (g/mol) | PDI ($M_w/M_n$) |
|---|---|---|---|---|---|
| 1[*,a] | 75 | 25 | 11.6 | $2.4 \times 10^3$ | 1.3 |
| 2[#,b] | 75 | 25 | 12.1 | $8.1 \times 10^3$ | 3.5 |
| 3[*,a] | 50 | 50 | 25.5 | $1.9 \times 10^3$ | 1.3 |
| 4[#,b] | 50 | 50 | 23.6 | $6.2 \times 10^3$ | 2.8 |
| 5[*,c] | 75 | 25 | 9.0 | $1.8 \times 10^3$ | 1.2 |

*-ATRP reactions; #-Free radical polymerization (FRP) using AIBN as initiator.

*a* Targeted $M_n$ = 3000 g/mol; [monomer]:[EBriB]:[CuBr]:[PMDETA] = 32:1:0.5:0.5; Reaction time = 22 hrs.; Reaction temperature = 80 ºC.

*b* AIBN (10 mmol/L); Reaction time = 22 hrs.; Reaction temperature = 80 ºC.

*c* Targeted $M_n$ = 3000 g/mol; [monomer]:[EBriB]:[CuBr]:[dNbpy] = 32:1:0.5:1; Reaction time = 48 hrs.; Reaction temperature = 80 ºC.

*d* Calculated from values obtained from GC measurements and proton NMR.
Volume ratio solvent:monomer = 2:1

Some observations can be made from the data in Table 1: **(i)** 1-octene copolymerizes via a free radical mechanism. Homopolymerization of 1-octene was attempted in both FRP and ATRP, but no polymer was obtained. This could be attributed to the fact that alpha-olefins undergo degradative chain transfer of allylic hydrogens.[15] The stable allylic radical derived from the monomer is slow to reinitiate and prone to terminate. **(ii)** Copolymerizations under FRP conditions produce relatively low molecular weight polymer compared to MA homopolymerization under similar conditions. The tendency for 1-octene to behave as a chain transfer agent under FRP conditions has been reported for MMA systems.[16] **(iii)** The experimentally determined molar masses (MM) for polymerizations under ATRP conditions are close to the calculated values (Figure 2.2). The linearity clearly indicates that there were a constant number of growing chains during the polymerization. **(iv)** Narrow molar mass distributions (MMDs) were obtained in the ATRP experiments, which suggested conventional ATRP behavior, with no peculiarities caused by the incorporation of 1-octene. **(v)** As the fraction of the alpha-olefin was increased in the monomer feed, its incorporation was higher in the copolymer (*compare entries 1 & 3, 2 & 4*). Two effects can cause

this phenomenon. Due to composition drift, the fraction of 1-octene in the remaining monomer increases, which leads to a decrease in average propagation rate constant. When the fraction 1-octene increases, the probability of endcapping a 1-octene moiety at the chain end with a bromide increases. When this happens the chain will be virtually inactive, as shown in the latter part of this chapter with the model experiments. Thus, increasing the mol% of alpha-olefin in the monomer feed decreased the overall conversion (Figure 2.3). **(vi)** It is largely coincidental that the rates of polymerization in ATRP and in conventional FRP shown in Figure 2.3 are nearly identical. The choice of initiator concentration and polymerization conditions happens to be such that this coincidence occurs. However, the fact that the ratios at which the two comonomers are consumed seem to be in close agreement, points to a great similarity between the reactivity ratios. This will be further discussed below. **(vii)** To indicate the feasibility of the copolymerization under homogenous ATRP conditions, the copolymerization was also carried out using 4,4'-dinonyl-2,2'-bipyridine (dNbpy) as the ligand (Table 2.1, entry 5). This resulted in a good control over the polymerization. MM increased linearly with overall conversion (Figure 2.2), though the overall conversion and hence the incorporation of 1-octene was slightly lower as compared to the PMDETA systems. The lower the redox potential, the larger the apparent equilibrium constant for the oxidation of copper(I) to copper(II), and therefore the higher the activity in catalyzing the polymerization. The redox potential of a copper(I)-PMDETA complex was lower than that of the copper(I)-dNbpy complex, hence the PMDETA systems exhibit a higher polymerization rate.[17]

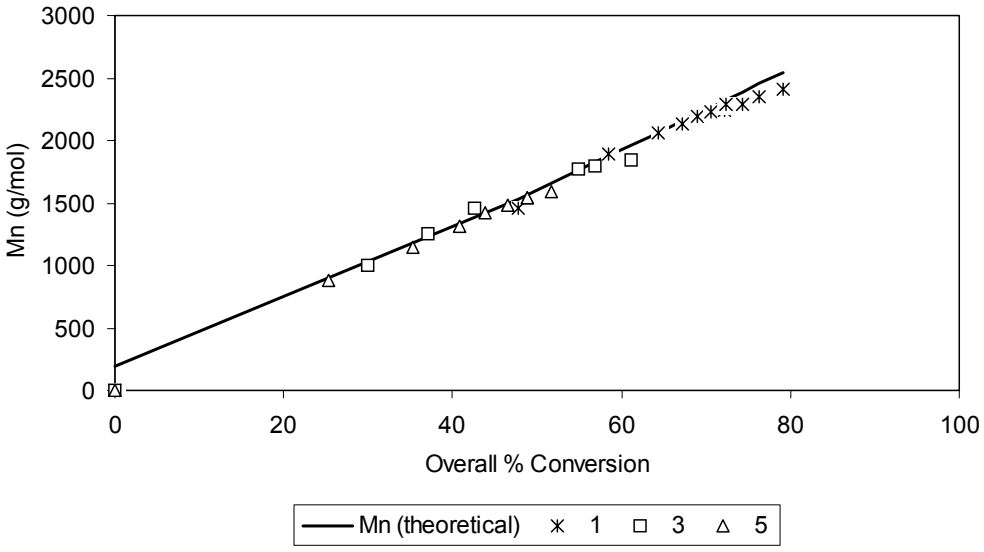


**Figure 2.2:** Plot of $M_n$ *vs* overall conversion for the ATRP copolymerizations of MA-Octene. For the labels, it is referred to the entries in Table 2.1.

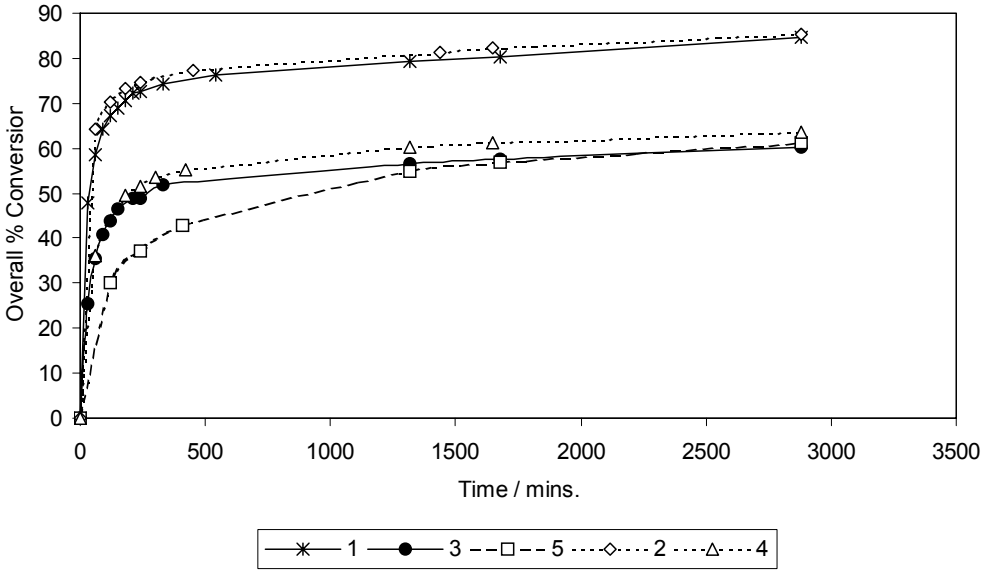


**Figure 2.3:** Plot of overall conversion *vs*. time for MA-Octene copolymerizations. For the labels, it is referred to the entries in Table 2.1.

### *2.4.2 Reactivity ratios:*

AIBN-initiated and ATR copolymerizations of MA with 1-octene, followed in-situ by $^{1}$H NMR, were examined as summarized in Table 2.2. The trend obtained for the copolymerizations from the online NMR experiments (Table 2.2), was comparable to that observed in the laboratory-scale experiments (Table 2.1). Narrow MMDs were obtained for the ATRP experiments, suggesting conventional ATRP behavior with no peculiarities caused by the incorporation of 1-octene.

Individual monomer conversions were monitored online using NMR. Figure 2.4 shows, sample spectra of the polymerization mixture after various reaction times (0 to 540 minutes). In order to quantify the results and track the fractions of the two monomers in the residual monomer mixture, the various vinylic protons were integrated with respect to the protons present in the aromatic region from toluene, which was employed as the internal standard. Integration of the signals yields relative amounts of residual monomer in the polymerization mixture. These amounts can easily be converted into comonomer fractions. The fraction of MA in the residual monomer was plotted as a function of overall monomer conversion (Figure 2.5). This type of experimental data can be described by the integrated copolymerization equation, also known as the Skeist-equation (Equation 9).[18]

$$\xi = 1 - \left(\frac{f_A}{f_A{}^0}\right)^{\frac{r_B}{1-r_B}} \left(\frac{1-f_A}{1-f_A{}^0}\right)^{\frac{r_A}{1-r_A}} \left(\frac{f_A{}^0 - \delta}{f_A - \delta}\right)^{\frac{1-r_B}{2-r_A-r_B}} \qquad (9)$$

where ξ is the fractional total conversion on a molar basis, $f_A^0$ is initial mole fraction of monomer A based on the total amount of monomer and δ is the following function of the monomer reactivity ratios, $r_A$ and $r_B$ (Equation 10):

$$\delta = \frac{1 - r_A r_B}{(1 - r_A)(1 - r_B)} \qquad (10)$$

**Table 2.2:** Copolymers of MA/1-Octene

| Entry | MA (mol%) | 1-Octene (mol%) | $M_n$ (g/mol) | PDI ($M_w/M_n$) |
|---|---|---|---|---|
| 1*,a | 90 | 10 | $2.2 \times 10^3$ | 1.11 |
| 2#,b | 90 | 10 | $3.2 \times 10^4$ | 4.9 |
| 3*,a | 75 | 25 | $2.2 \times 10^3$ | 1.14 |
| 4#,c | 75 | 25 | $1.1 \times 10^4$ | 5.2 |
| 5*,a | 50 | 50 | $1.6 \times 10^3$ | 1.2 |
| 6#,d | 50 | 50 | $1.4 \times 10^4$ | 3.6 |

*-ATRP reactions; #-Free radical polymerization (FRP) using AIBN as initiator.

*a* Targeted $M_n$ = 3000 g/mol; [monomer]:[EBriB]:[CuBr]:[PMDETA] = 32:1:0.5:0.5; Reaction time = 12 hrs.

*b* AIBN (3 mmol/L); Reaction time = 9 hrs.

*c* AIBN (10 mmol/L); Reaction time = 9 hrs.

*d* AIBN (3 mmol/L); Reaction time = 12 hrs.

Reaction temperature = 80 °C. Solvent:monomer = 2:1 by volume.

From Figure 2.5, it can be seen that, **(i)** an increase in the fraction of 1-octene in the monomer feed leads to a decrease in the overall conversion. **(ii)** As the fraction of MA in the monomer feed is decreased, there is a better accordance for the monomer conversion between FRP and ATRP reactions (compare 5 & 6 and 1 & 2). The deviation is much larger between 1 & 2 as compared to 5 & 6. It is known that deviations from the steady state ratio between the two propagating radicals may occur during the initial stages of an ATR copolymerization.[19] It is most likely that this is also the origin of the observed deviations between ATRP and conventional free radical copolymerization in this case. Additional research is currently being carried out in our labs to prove the general character of this phenomenon in living radical copolymerization.

The data from Figure 2.5 can be used for the estimation of reactivity ratios. It is well documented that the best way of estimating reactivity ratios from experimental data is via the use of a nonlinear least squares method.[20] The method of choice in the present work calculates the sums of squares in a relevant $r_1 - r_2$ space.[21] The minimum in the $r_1 - r_2$ sum of squares surface is then easily found. This point estimate is used to calculate the drawn curves shown in Figure 2.5. 95% joint confidence intervals are subsequently determined as the curve of intersection between the $r_1 - r_2$ sum of squares surface and a horizontal plane, the height of which is determined according to a method previously described. The resulting point estimates and confidence intervals for the six different experiments are shown in Figure 2.6. The point estimates are summarized in Table 2.3. It is clear that experiment 1, (ATRP, $f_{MA} = 0.10$) is poorly described by the Skeist equation. The uncertainty in the reactivity ratios for this experiment is correspondingly larger than that of the other experiments. As indicated above, the most probable explanation for this observation is the more frequently observed deviation from steady state equilibrium in ATR copolymerizations. Separately, the effect of chain transfer reactions on the quality of the predictions was examined, no significant deviations were observed.

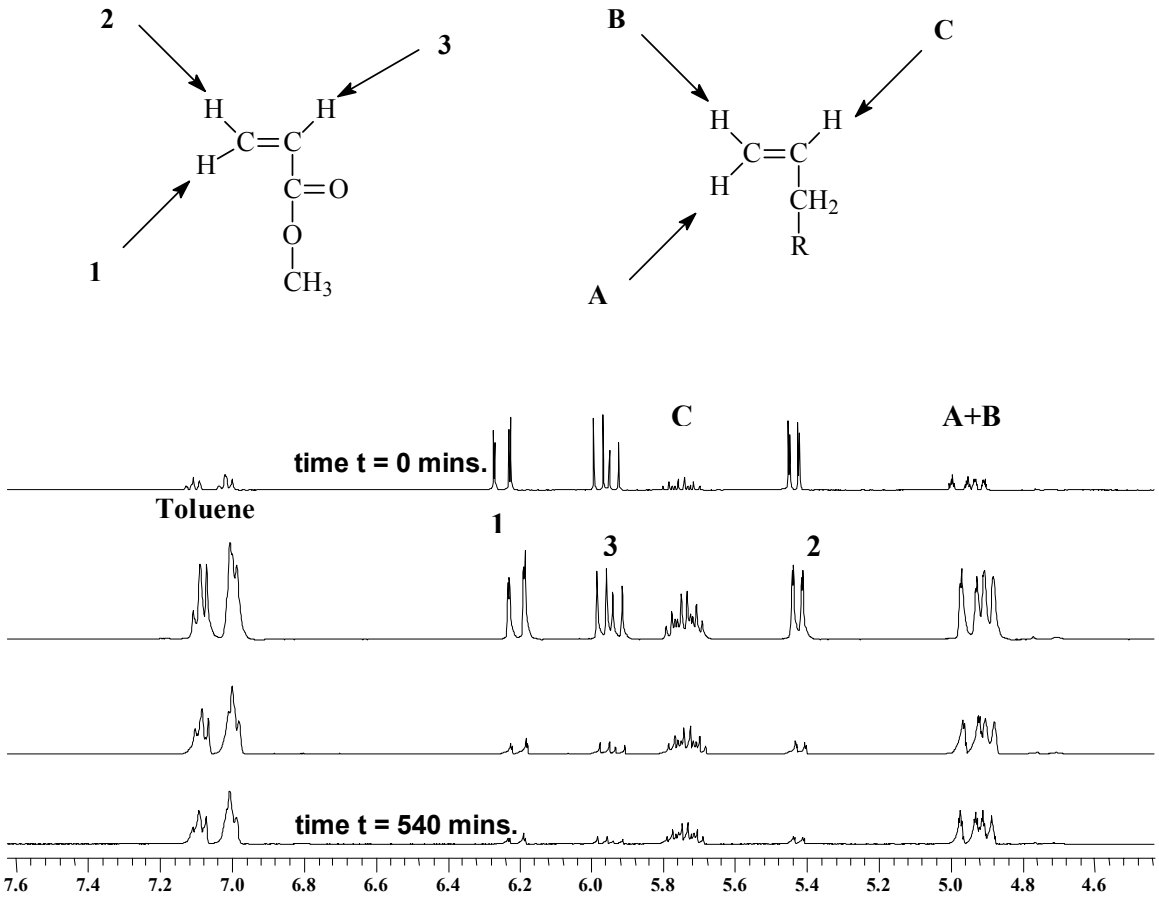


**Figure 2.4:** $^{1}$H NMR spectra of a MA–1-Octene copolymerization, measured *on line* during the polymerization experiment. [Free radical polymerization - $f_{octene}$ = 0.25. AIBN = 10 mmol/L. Reaction time = 9 hrs., Reaction temperature = 80 °C]

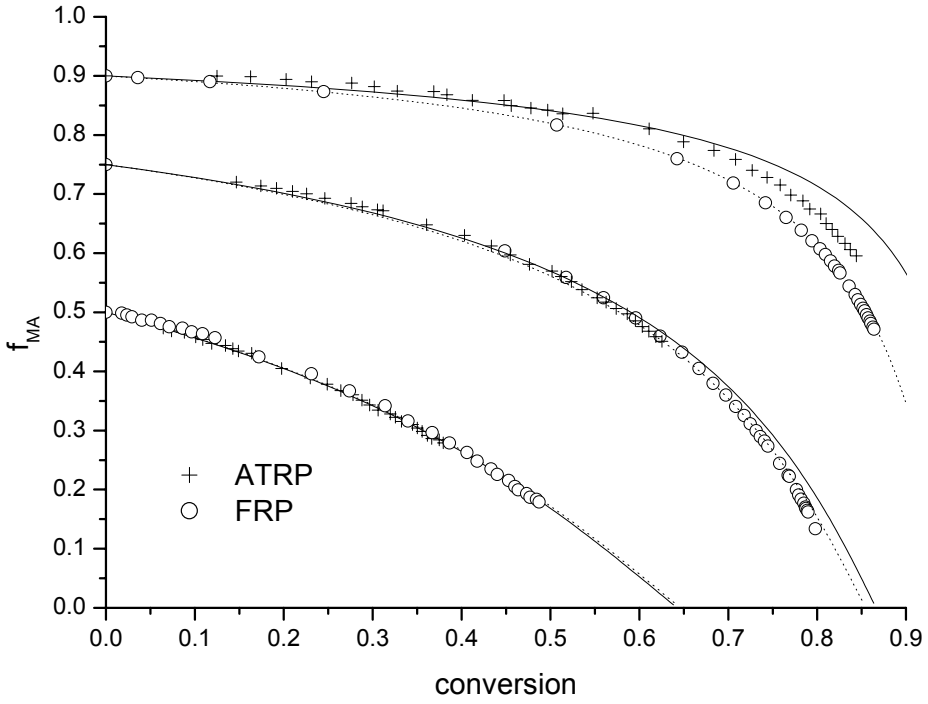


**Figure 2.5:** Plot of fraction of MA in the residual monomer as a function of overall monomer conversion. Solid lines are best fits according to the reactivity ratio point estimates as given in Table 2.3 for ATRP experiments. Dotted curves are the equivalent for conventional free radical copolymerizations.

**Table 2.3:** Determined reactivity ratios for MA/1-Octene

| Entry | MA (mol%) | 1-Octene (mol%) | $r_{MA}$ | $r_{1\text{-Octene}}$ |
|---|---|---|---|---|
| 1*,a | 90 | 10 | 3.36 | 0 |
| 2#,b | 90 | 10 | 7.52 | 0 |
| 3*,a | 75 | 25 | 5.92 | 0 |
| 4#,c | 75 | 25 | 6.77 | 0 |
| 5*,a | 50 | 50 | 7.55 | 0 |
| 6#,d | 50 | 50 | 7.13 | 0 |

*-ATRP reactions; #-Free radical polymerization (FRP) using AIBN as initiator.

*a* Targeted $M_n$ = 3000 g/mol; [monomer]:[EBriB]:[CuBr]:[PMDETA] = 32:1:0.5:0.5; Reaction time = 12 hrs.

*b* AIBN (3 mmol/L); Reaction time = 9 hrs.

*c* AIBN (10 mmol/L); Reaction time = 9 hrs.

*d* AIBN (3 mmol/L); Reaction time = 12 hrs.

Reaction temperature = 80 $^{o}$C. Solvent:monomer volume ratio = 2:1

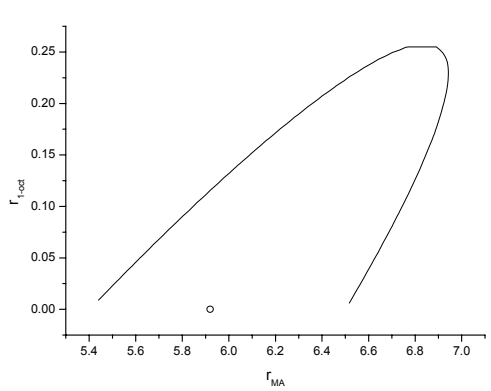


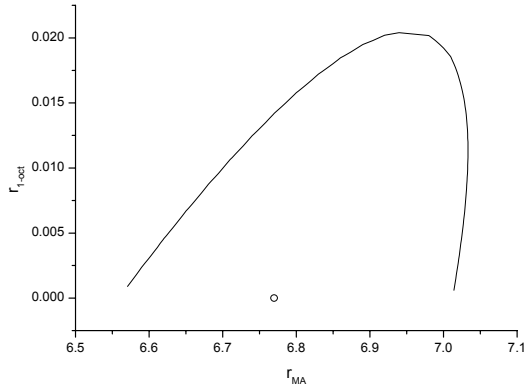


$f_{Octene}$ = 0.25 ATRP FRP

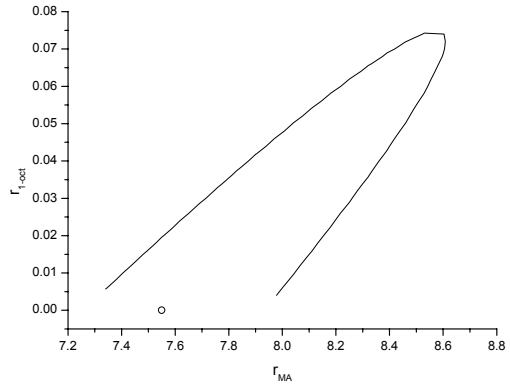


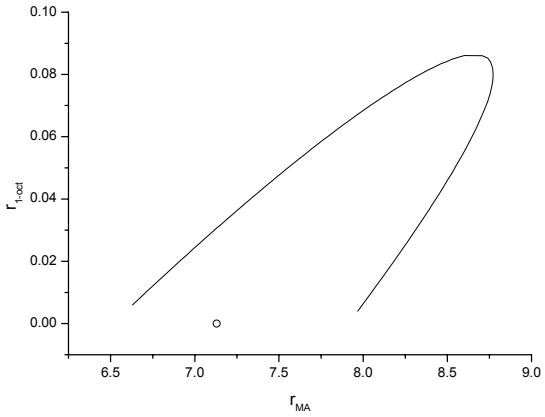


$f_{Octene}$ = 0.50 ATRP FRP

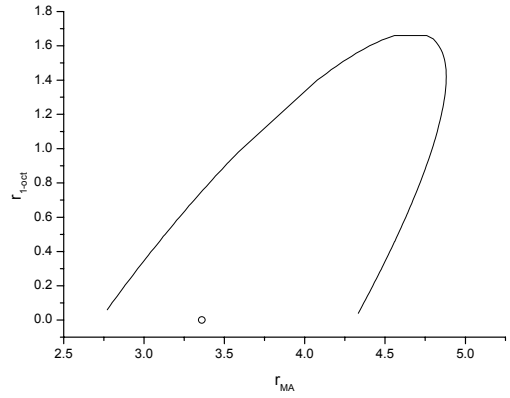


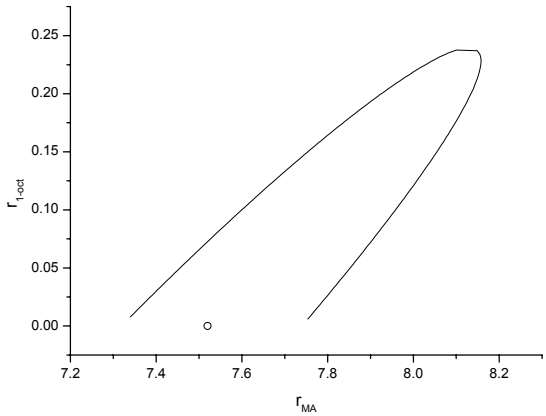


$f_{Octene}$ = 0.10 ATRP FRP

**Figure 2.6:** Point estimates and confidence intervals for the different copolymerization calculated using the method described in the text. (For experimental details, refer to Table 2.3).

### *2.4.3 Polymer Characterization:*

The synthesized copolymers were characterized using matrix assisted laser desorption / ionization – time of flight – mass spectrometry (MALDI-TOF-MS). Determination of the accurate (relative) molar masses of synthetic polymers is often difficult to achieve. Detailed information of molecular structure, such as identification of end groups, can be even more difficult. Even though polymers with a molecular weight of several hundred thousand Daltons can be characterized by MALDI-TOF-MS, most of the investigations with this technique focus on the mass range where single polymer chains are resolved.[22] The resolved mass range depends on the molar mass range of the repeating units and on the resolution of the mass spectrometer. In favorable cases, the polymer composition can be deduced directly from the absolute mass of each signal of the polymer distribution.

MALDI-TOF-MS spectra allow the determination of the variation in chemical composition between individual copolymer chains and comparison of the chemical composition distribution (CCD) in different mass ranges, coupled with very clear peak assignment with respect to end-group, theoretical mass and isotopic mass distribution.

#### *2.4.3.1 Atom Transfer Radical Polymerization:*

Figure 2.7 shows the MALDI-TOF-MS spectrum for the MA/1-octene copolymer (Table 2.1, entry 1). The overlap of several distributions is clearly visible. This is typical for the resolved mass distribution of a copolymer and is due to the heterogeneity of the degree of polymerization, corresponding to the chain length distribution, coupled with the heterogeneity in the chemical composition.

Figure 2.8 is an expansion of a selected portion of the spectrum shown in Figure 2.7. The peak assignments of Figure 2.8, described in Table 2.4, are made using the following strategies; **(i)** comparison with the homopolymer spectrum of MA, **(ii)** comparison of the experimental masses and those theoretically calculated, and **(iii)** comparison of the theoretical isotopic distribution with the observed distributions. The polymer chains were cationized with sodium, therefore were detected at a m/z value of 23 Daltons above the theoretically calculated mass.

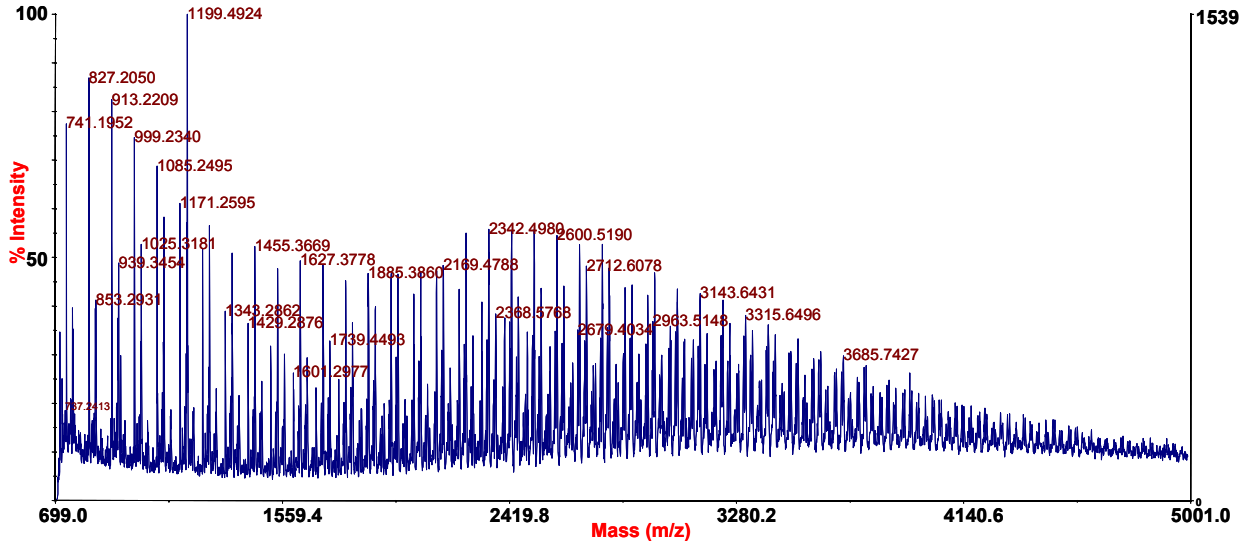


**Figure 2.7:** MALDI-TOF-MS spectrum for MA/Oct copolymer, $f_{octene}$ = 0.25, $F_{Octene}$ = 0.11. (Table 2.1, entry 1). [Spectrum acquired in the Reflector mode, Matrix : Dithranol].

After subtraction of the mass of the cationization reagent, the detected signals should be in agreement with the expected masses of the copolymer chains, which can be calculated according to Equation 11:

$$M_{copo} = 115.15 + [(m \times 86.09) + (n \times 112.21)] + 79.90 \qquad (11)$$

where 115.15 and 79.9 are the average masses of the end groups from the initiator fragment and bromine respectively (since EBriB was used as the ATRP initiator), 86.09 and 112.21 are the average masses of the MA and 1-octene repeating units, respectively, and m and n the numbers of the monomers in the chain.

However the agreement between the theoretical and observed masses is improved when equation 12 is employed. In this equation, the terminal bromine atom is not included.

$$M_{copo} = 115.15 + [(m \times 86.09) + (n \times 112.21)] \qquad (12)$$

During ATRP, most of the polymer chains are halide end-capped. This is of paramount importance, since, in its absence, the reaction will be uncontrolled. It has been already shown in this chapter that $M_n$ increases linearly with overall conversion for the ATRP copolymerizations (Figure 2.2), and that a low PDI is obtained. Hence, the reaction is certainly well controlled and this in turn

implies the presence of the halide at the copolymer chain end. In MALDI-TOF-MS, during ionization (in the range of laser intensity used in this work) it is observed that the terminal Br gets dislodged. Other groups have already reported the loss of the HBr during MALDI-TOF-MS analysis of poly(acrylates) produced by ATRP.[23] A careful choice of the laser intensity is extremely important for the spectral quality in MALDI-TOF-MS. There is an obvious trade-off between obtaining a spectrum with enough intensity (high laser power) and obtaining a spectrum without signs of fragmentation or distortions.[24]

It is evident from the data in Table 2.4 that several units of 1-octene were incorporated into the polymer chain. This indicates that the octene is behaving as a comonomer, and not simply as a chain transfer agent. There is an excellent correlation between the theoretical mass and that experimentally observed, which further validates the presence of the olefin in the copolymer. Moreover, the theoretical isotopic mass distribution is in good agreement with the observed distribution (Figure 2.9). Since only one pair of end groups is evident, and no chains seem to have been initiated by octene radicals, it can be concluded that chain transfer to 1-octene in the targeted MM range was negligible.

**Table 2.4:** Peak assignment of the MALDI-TOF-MS spectrum shown in Figure 2.8

| Peak No. | MA units | 1-octene units | Observed Mass (Da) | Theoretical Mass (Da) | $Na^+$ |
|---|---|---|---|---|---|
| 34-2 | 34 | 2 | 3289.56 | 3289.64 | 1 |
| 33-3 | 33 | 3 | 3315.65 | 3315.77 | 1 |
| 32-4 | 32 | 4 | 3341.73 | 3341.89 | 1 |
| 30-5 | 30 | 5 | 3282.44 | 3281.93 | 1 |
| 29-6 | 29 | 6 | 3308.54 | 3308.05 | 1 |
| 28-7 | 28 | 7 | 3334.62 | 3334.18 | 1 |
| 27-8 | 27 | 8 | 3360.67 | 3360.31 | 1 |

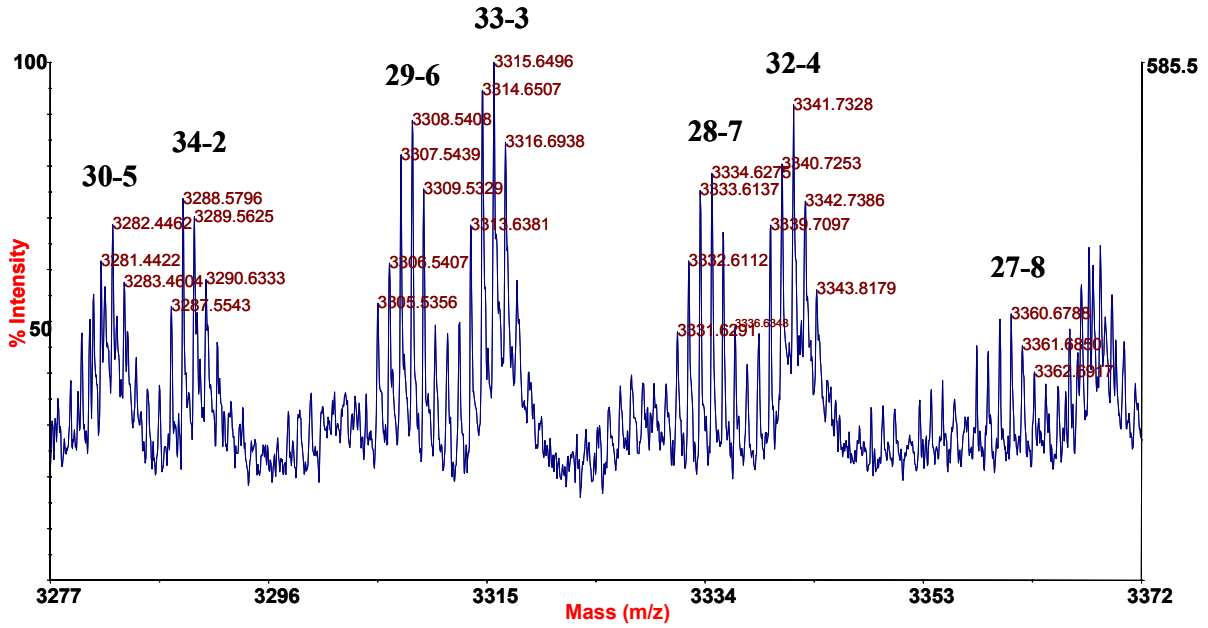


**Figure 2.8:** MALDI-TOF-MS spectrum for MA/Oct copolymer, $f_{octene}$ = 0.25, $F_{Octene}$ = 0.11. (Table 2.1, entry 1). [Spectrum acquired in reflector mode, Matrix : Dithranol].

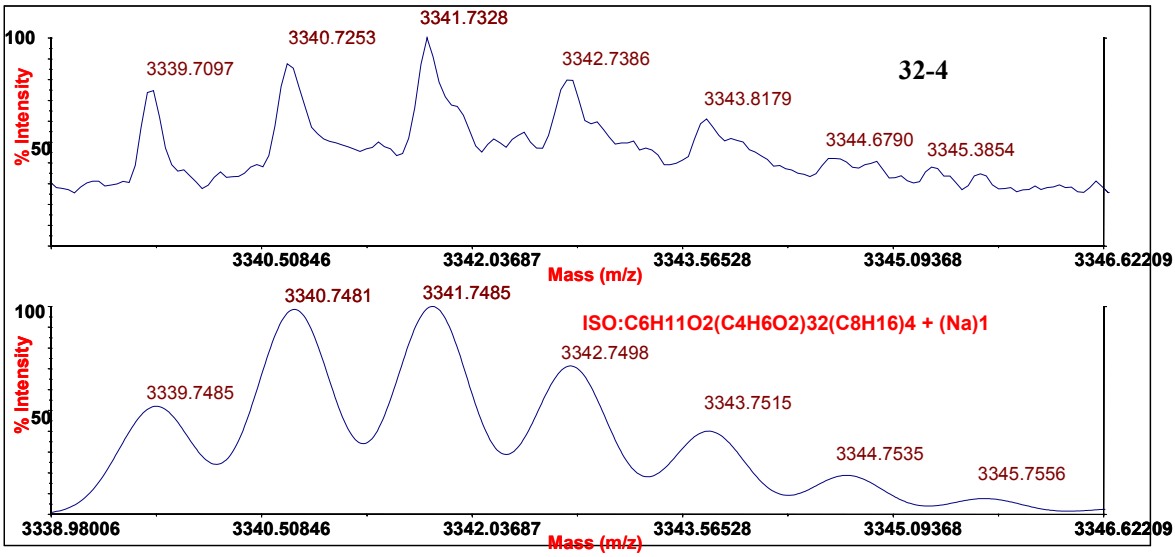


**Figure 2.9:** MALDI-TOF-MS spectrum of MA/Oct copolymer, $f_{octene}$ = 0.25, $F_{Octene}$ = 0.11. (Table 2.1, entry 1). Observed distribution (above) & theoretical isotopic distribution (below).

It has previously been established by $^{13}C$ NMR spectroscopy, that during the free radical copolymerization of acrylate and hexene, the olefin was randomly distributed in the copolymer chain.[8,10] Now, from the acquired MALDI-TOF-MS data, a clear pattern in the sequence distribution is observed. This was achieved by selecting regions of increasing mass from the obtained MALDI-TOF-MS spectrum (Figure 2.7) and expanding them to similar scale ranges for easy comparison. The peak assignments are made using equation 12. From Figure 2.10, an interesting trend is observed. In the low MM region, the homopolymer peak of MA has the highest intensity. In the progressively higher MM regions, the copolymer peaks increases in intensity and the homopolymer peak decreases in intensity. So, in essence, a gradient copolymer type pattern is observed. This was further confirmed by the copolymer fingerprint contour plots obtained for samples withdrawn at different time intervals during the ATR copolymerization (Supporting Information, Figure 2.19). There was a clear broadening observed in the contour plots for samples withdrawn at later stages during the copolymerization. From the plots, it was clear that as the copolymerization progressed, more octene was getting incorporated. Moreover, it is evident that number of octene units incorporated is greater than the expected number. That is, if for a polymer chain with a degree of polymerization (DP) of 10 say one unit of octene is incorporated, then for a chain with DP of 20, only 2 units should be expected to be incorporated. This most certainly is not the case.

The origin of a gradient-type comonomer incorporation has been discussed previously for the copolymerization of acrylate – methacrylate copolymerization. In that case, there is a large difference in the activation rate parameters between dormant chains that carry an acrylate terminal group *versus* those with a methacrylate terminal group. In the present case the situation is somewhat different, although the result is similar. It is likely that for propagating radicals with a terminal 1-octene unit, the time constant for crosspropagation is smaller than that for deactivation. In other words, chains with a 1-octene terminal unit exclusively undergo crosspropagation. Relevant activation rate parameters for α-olefin copolymerizations will be discussed in more detail in the latter part of this chapter. The resulting gradient in copolymer composition, or the relationship between composition and molar mass may be interpreted as follows. At the onset of the copolymerization, predominantly homopolymerization of MA occurs (since MA is a more reactive monomer). During the copolymerization, due to composition drift, the fraction of 1-octene in the remaining monomer increases, hence the probability of 1-octene being incorporated into the polymer chain increases. The addition of an α-olefin is followed by a very rapid crosspropagation, causing the chain that incorporates the α-olefin to gain chain length faster than the *homo*-MA chain.

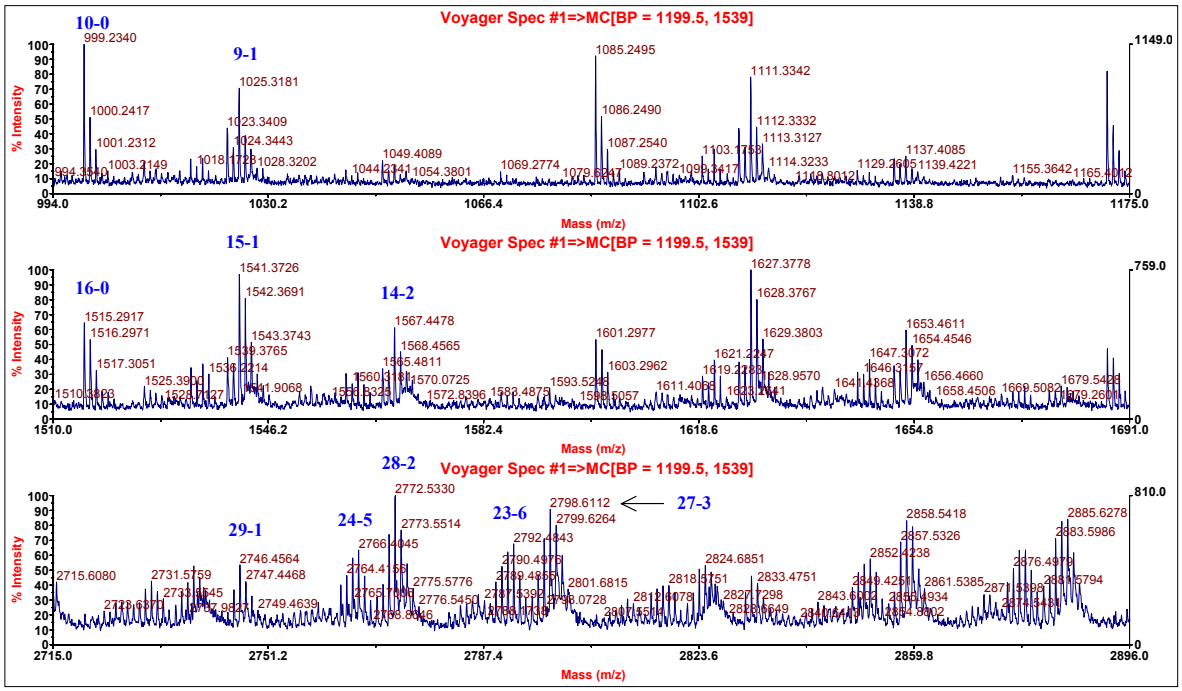


**Figure 2.10:** Expansion in different mass regions from a MALDI-TOF-MS spectrum of MA/Oct copolymer, $f_{octene}$ = 0.25, $F_{Octene}$ = 0.11. (Table 2.1, entry 1). [Spectrum acquired in Reflector mode; Matrix : Dithranol]

***2.4.3.2 Free Radical Polymerization:*** It has been found that MM estimates provided by MALDI-TOF-MS agree with the values obtained by conventional techniques only in the case of samples with narrow MMD,[25] whereas, with polydisperse polymers MALDI-TOF-MS does not give reliable results. Hence the polydisperse samples obtained in this work were fractionated by SEC, yielding narrow MMD samples which, when analyzed by MALDI-TOF-MS, resulted in reasonably well-resolved mass spectra.

Figure 2.11 depicts the MALDI-TOF-MS spectrum for a fractionated portion (by SEC) of a MA/Oct copolymer synthesized using AIBN as initiator (Table 2.1, entry 2). The copolymer was investigated to compare the CCD between the FRP and ATRP systems. Figure 2.12 is an expansion of a selected portion of the spectrum shown in Figure 2.11. The peak assignments in the FRP case are far more difficult than in the ATRP case. This is primarily due to the multitude of different end groups, which are present, in addition to the heterogeneity normally present for copolymers.

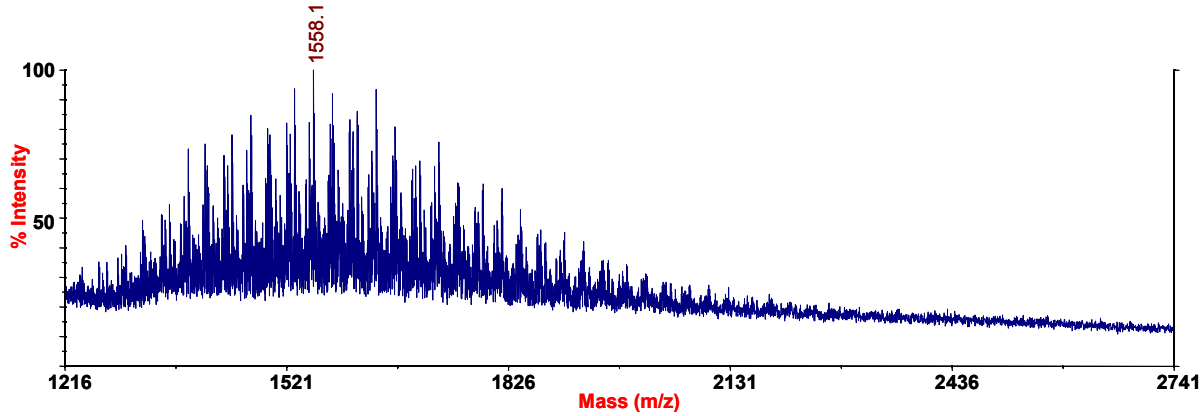


**Figure 2.11:** MALDI-TOF-MS spectrum for the fractionated sample of a MA/Oct copolymer, $f_{Octene}$ = 0.25. (Table 2.1, entry 2). [Spectrum acquired in reflector mode, Matrix : Dithranol].

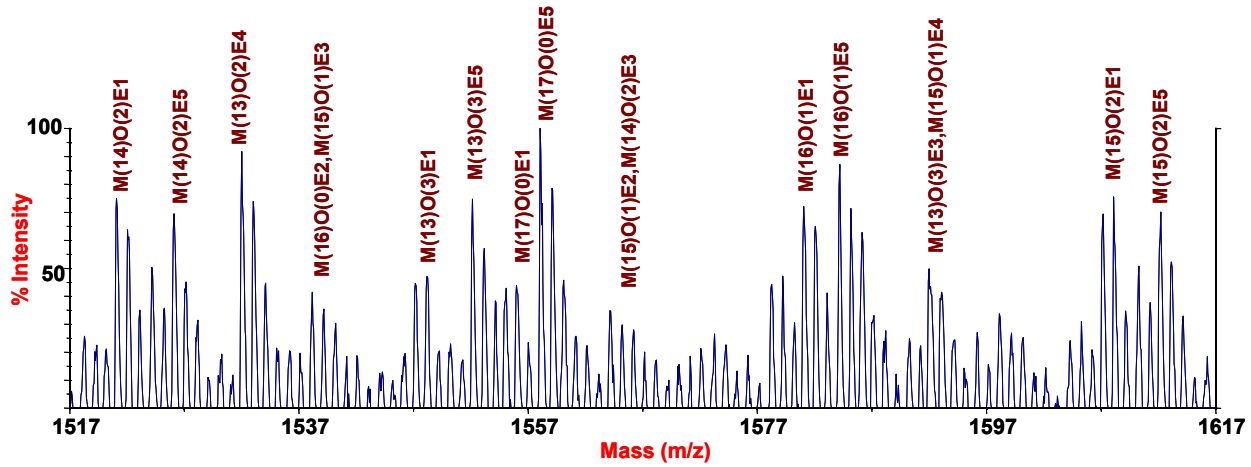


**Figure 2.12:** MALDI-TOF-MS spectrum for the fractionated sample of a MA/Oct copolymer, $f_{Octene}$ = 0.25. (Table 2.1, entry 2). [Spectrum acquired in reflector mode, Matrix : Dithranol].

The peak assignments were made using the following strategies; **(i)** predicting the possible end groups, which result normally during a free radical reaction, **(ii)** comparison of the observed mass with those theoretically calculated. The polymer chains were all cationized with sodium, hence were detected at a m/z value 23 Daltons above the theoretically calculated mass. All polymer chains were assigned to various chemical compositions, constituting of varying methyl acrylate (M) and octene (O) units. All the copolymer chains can be divided into having five pairs of end groups

(E1, E2, E3, E4, E5) [see Fig. 2.12]. The different end groups observed originate from the various side reactions, which occur during conventional free radical polymerization.

End group 1 (E1) was obtained as a result of chain transfer to monomer or polymer. It has been shown that octene acts as a chain transfer agent during free radical polymerization (increasing the fraction of octene in the monomer feed, resulted in lower overall conversion and lower MM [Table 2.1, compare entries 2 & 4]). Further, previous work in the area of chain transfer to polymer for acrylate monomers has clearly revealed that abstraction of the backbone proton from a dead polymer chain may take place. [26] The resulting end groups for the polymer chain can be assigned according to equation 13,

$$M_{copo} = 68.09 + [(m \times 86.09) + (n \times 112.21)]+1.00 \qquad (13)$$

where 68.09 and 1.00 are the average masses of the end groups from the initiator fragment (2-cyanoprop-2-yl radical from AIBN) and the abstracted hydrogen from octene or dead polymer respectively, 86.09 and 112.21 are the average masses of the MA and 1-octene repeating units, respectively, and m and n the numbers of the monomers in the chain.

The polymer chains having end group 2 (E2) were obtained due to termination *via* combination of the propagating chains. Solomon and Moad [27,28] conclude that despite the sparsity of reliable data, termination of polymerizations involving vinyl monomers occurs predominantly via combination. Equation 14 represents the product of termination via combination.

$$M_{copo} = 68.09 + [(m \times 86.09) + (n \times 112.21)]+68.09 \qquad (14)$$

where 68.09 is the average mass of the end group from the initiator fragment (AIBN fragment), 86.09 and 112.21 are the average masses of the MA and 1-octene repeating units, respectively, and m and n the numbers of the monomers in the chain.

The octene radical formed via chain transfer to monomer can also initiate the polymerization, though the rate coefficient of initiation by this stable allylic radical is very slow. These initiated chains also terminate as a result of chain transfer from monomer or polymer (equation 15), producing end group 3 (E3).

$$M_{copo} = 111.20 + [(m \times 86.09) + (n \times 112.21)]+1.00 \qquad (15)$$

where 111.20 and 1.00 are the average masses of the end groups from the octene allylic radical and the abstracted hydrogen from an octene or via chain transfer to polymer respectively, 86.09 and 112.21 are the average masses of the MA and 1-octene repeating units, respectively, and m and n the numbers of the monomers in the chain.

Chain transfer to polymer occurring during free radical polymerization of acrylates can lead to β-scission in the temperature range of 80 ºC to 240 ºC (Figure 2.13).[29] Abstraction of a proton from a dead polymer chain backbone results in the formation of an intermediate radical, which in turn can undergo β-scission. As a result of this, a new propagating radical and a macro-monomer are formed. The new propagating radical may also be terminated as a result of transfer events. Thus, two polymer chains with two different pairs of end groups are obtained. The polymer chains with end groups 4 (E4) and 5 (E5) were assigned as shown in Figure 2.13.

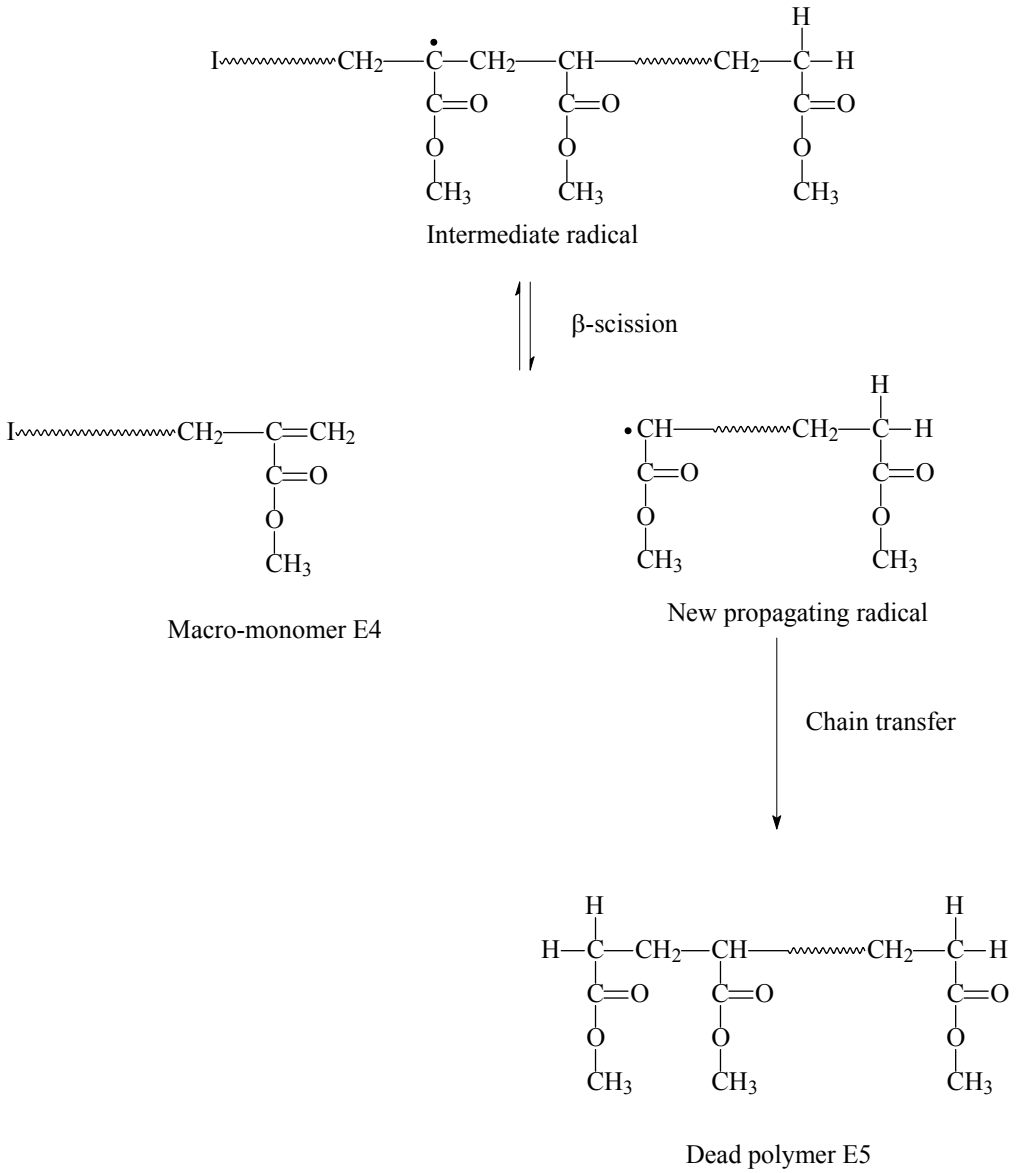


**Figure 2.13:** Mechanism for β-scission (I in end group E4 is the 2-cyanoprop-2-yl fragment from AIBN).

On comparison of data obtained from the MALDI-TOF-MS spectra for the free radical and ATRP systems, the important observation that can be made is, since, for the ATRP systems, only one pair of end groups was evident, and no chains seemed to have been initiated by the octene radicals, it can be concluded that chain transfer events if any, in the targeted MM range were negligible.

## *2.5 Determination Of Activation Rate Parameters*

In spite of the obvious limitations of the olefins under free radical conditions, copolymerization of the 1-octene with polar monomers using controlled radical techniques, resulted in excellent control on the polymerizations coupled with significant olefin incorporation in the polymer chains. This was attributed to the preferred crosspropagation ability for propagating radicals with a terminal 1-octene unit. Under controlled radical conditions, it was expected that the time constant for crosspropagation is smaller than that for deactivation. In other words, chains with a 1-octene terminal unit exclusively undergo crosspropagation. The only other possibility for the successful copolymerization, would be the result of fast reactivation/reinitation of the polymeric chains with the terminal octene unit.

To clarify this issue and ascertain the preferred radical reactivity path during the copolymerization, in this section, the relevant activation rate parameters for an ATRP copolymerization of methyl acrylate (MA) and octene system are investigated, using model compounds.

### *2.5.1 Materials*

Methyl-2-bromopropionate (MBrP, Aldrich, 98 %), 1-hexene (Aldrich, 98 %), 2-bromobutane (BrB, Aldrich, 98 %) were distilled under reduced pressure before use. Acetonitrile-$d_3$ (Aldrich, 99.8 atom % D, containing 0.03 % v/v TMS) and chloroform-*d* ($CDCl_3$, Cambridge Isotope Laboratories, 99,9+%, stabilized with silver, containing 0,05% v/v TMS) were used as received. *p*-Xylene (Aldrich, 99+%, HPLC grade) and methyl ethyl ketone (MEK, Aldrich, 99+%, HPLC grade) were stored over molecular sieves and used without further purification. N,N,N',N'',N''-pentamethyldiethylenetriamine (PMDETA, Aldrich, 98%), copper (I) bromide (CuBr, Aldrich, 99.98%), 4-hydroxy-2,2,6,6-tetramethyl-1-piperidinyloxy (hydroxy-TEMPO, Aldrich), 2,2,6,6-tetramethyl-1-piperidinyloxy (TEMPO, Aldrich), aluminum oxide (activated,

basic, for column chromatography, 50-200 μm) and tetrahydrofuran (THF, Aldrich, AR) were used as received.

### *2.5.2 Method employed for determination of rate coefficient of activation ($k_{act}$):*

The procedure employed for the determination of rate coefficient of activation ($k_{act}$) is based on the method reported by Fukuda et al.[30] The radicals originating from the alkyl halide initiator (I) are irreversibly trapped by a stable nitroxide radical (hydroxy-TEMPO) to yield the corresponding alkoxyamine. A 10-fold excess of the OH-TEMPO as compared to the initiator was used to ensure that no deactivation via the $CuBr_2$ would occur, and in this way pseudo-first-order kinetics were obtained. Also a 10-fold excess of Cu(I)/PMDETA was used to make these pseudo-first-order kinetics more straightforward. The decrease in the initiator [I] concentration will follow the differential equation (1) in this case.

$$-\frac{d[I]}{dt} = k_{act}[I][Cu(I)/PMDETA] \qquad (1)$$

It has to be taken into account that the catalyst concentration [Cu(I)/PMDETA] decreases in time as well.[31] When this is done, the general solution of equation (1) is found in equation (2),

$$\ln\left(\frac{[I]_0}{[I]_t}\right) + \ln\left(\frac{[Cu(I)/PMDETA]_0 - [I]_0 + [I]_t}{[Cu(I)/PMDETA]_0}\right) = \left([Cu(I)/PMDETA]_0 - [I]_0\right)k_{act}t \qquad (2)$$

where, $[I]_0$ and $[I]_t$ are the initial concentration and concentration at a time t of the alkyl-halide initiator respectively. The catalyst copper (I) bromide is designated as Cu(I) and PMDETA is the ligand employed for the ATRP polymerization. $k_{act}$ is the rate coefficient of activation.

The above equation can be simplified as

$$\ln(A)+\ln(B) = C\,k_{act}\,t \qquad (3)$$

The decrease in [I] can be monitored by $^1$H-NMR, where the ratio of the initiator towards an internal standard is decreasing in time. When the left hand of equation 2 is plotted *versus* time, a linear relationship is obtained with a slope equal to $([Cu(I)/Ligand]_0-[I]_0)k_{act}$. Thus $k_{act}$ can be calculated.

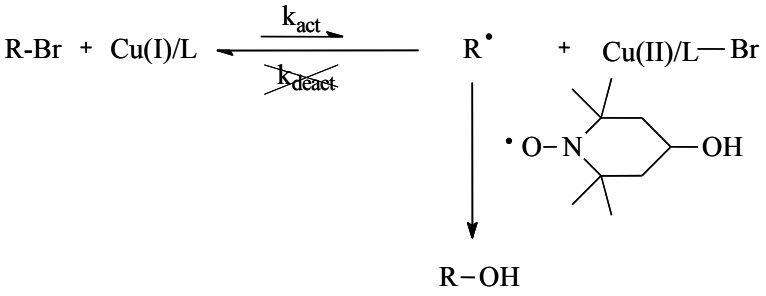


**Scheme 2.2:** Trapping experiments of model bromine – functional initiators in the presence of a large excess of TEMPO.

## *2.5.3 Synthetic Procedures*

***2.5.3.1 Trapping experiments:*** In a typical exchange experiment, acetonitrile-$d_3$ (4.23 g, 0.01 mol), PMDETA (0.31 g, 1.8 mmol), *p*-xylene (0.03 g, 0.3 mmol) and hydroxy-TEMPO (0.31 g, 1.8 mmol) were accurately weighed, transferred to a 25 mL round bottom flask and then purged with argon for 30 minutes. Hereafter, CuBr (0.26 g, 1.8 mmol) was added and the solution was purged for another 15 minutes. The flask was then immersed in an ice bath and maintained at 0 °C under a flowing argon atmosphere. A dark green homogeneous solution was obtained. The alkyl-halide initiator (MBrP) (0.18 mmol) was added quickly via a degassed syringe and a sample was taken immediately as a reference time 0 sample. Further, samples were withdrawn at regular time intervals throughout the reaction and immediately quenched in 1 g $CDCl_3$.

***2.5.3.2 Synthesis of the model compound H-MA-Hexene-Br:*** H-MA-Hexene-Br was synthesized using Atom Transfer Radical Addition (ATRA) method. MEK (6.45 g; 8.0 mL), 1-hexene (3.02 g; 36 mmol), PMDETA (1.04 g; 6 mmol) and toluene (1.00 g; 11 mmol) were accurately weighed and then added to a 25 mL round bottom flask. This mixture was purged with argon through a needle for 15 minutes. Then, Cu(I)Br (0.86 g; 6 mmol) was added and the solution

was purged for another 15 minutes. The needle was then removed and the reaction mixture was placed under an argon atmosphere and heated to 70 °C. MBrP (2.00 g; 12 mmol) was added via a degassed syringe through the septum and a sample (0.5 mL) was taken immediately as a reference time 0 sample. Further samples were taken at regular time intervals and quenched in 4 g THF. The reaction was carried out for 6 h.

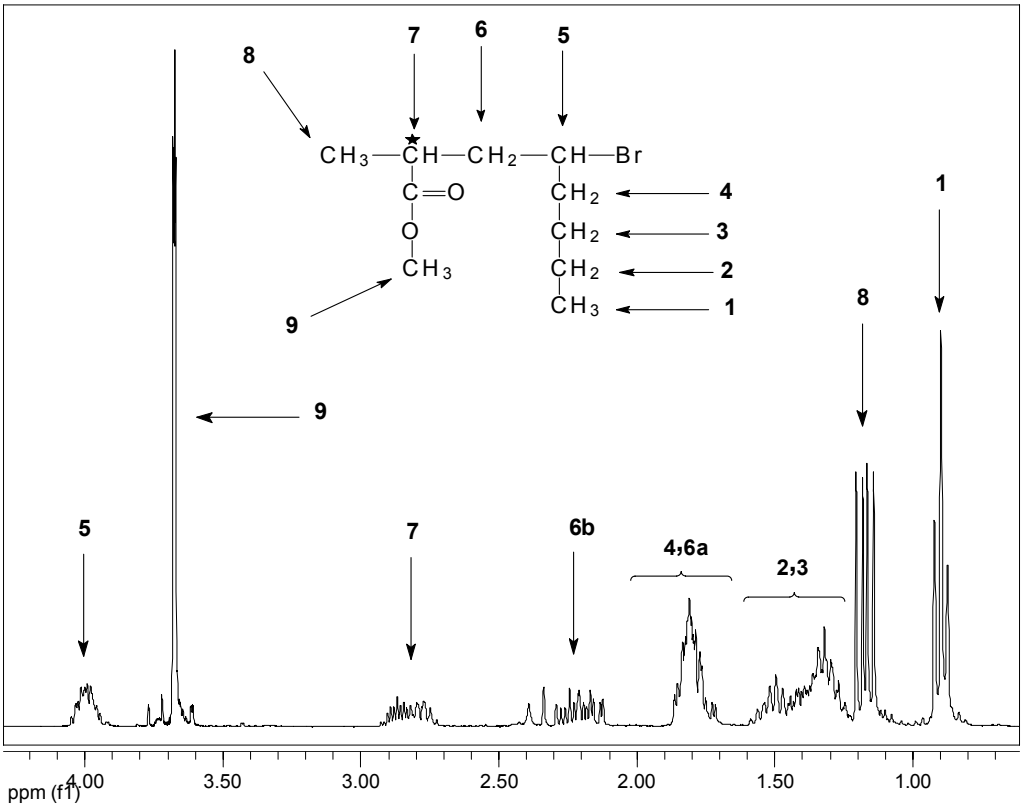


**Figure 2.14:** [1]H NMR spectrum for the model compound H-MA-Hexene-Br. The star sign at position 7, indicates the chiral carbon center and hence the formation of diastereomers. 6a and 6b are assigned to the methylene protons on the carbon at position 6.

The individual conversions for MBrP and hexene, and the formation of H-MA-Hexene-Br were determined using GC. The GC profile employed is detailed in Section 2.2.2.1. The final conversions for MBrP and hexene were found to be 91% and 34% respectively. In GC, two signals were obtained for the H-MA-Hexene-Br, associated to the presence of a diastereomer (i.e., the

mixture of racemic and meso forms). In a previous publication, formation of diastereomers was also reported during model compound synthesis.[32]

The $^{1}H$ NMR in Figure 2.14 confirmed that H-MA-Hexene-Br was obtained. The peak around 4.0 ppm is assigned to the α-methine proton on the terminal carbon attached to the bromine. This is the peak of importance, since after TEMPO trapping reactions, this would be the peak, which would be expected to decrease with time, clearly indicating that initiation occurred.

Prior, to the trapping reactions, the above reaction mixture was passed through an aluminum oxide column, so as to remove the copper. The solvents were evaporated using a rotary evaporator.

### *2.5.4 Results and Discussion*

The alkyl halides employed in this study are analogous to the terminal and penultimate units formed during the ATRP copolymerization of MA/1-Octene. Methyl-2-bromopropionate (MBrP), 2-bromobutane (BrB) and the synthesized model compound mimic the chain ends having methyl acrylate (MA) and octane as the terminal units, and MA as the penultimate group and octene as the terminal unit respectively. Therefore, these model compounds should provide a good insight about the atom transfer processes during polymerization and initiation. The activation constants were measured initially at 0 ºC for all the model compounds. In some cases, the temperature was also raised to a maximum of 70 ºC (representative of the reaction temperature employed during the ATRP copolymerization), to observe the influence of temperature on activation. PMDETA was used as the ligand and acetonitrile was the chosen solvent so as to solubilize the Cu(I)/PMDETA complex in the reaction media.

Figure 2.15 shows the $^{1}H$ NMR spectra (in the range 4.5-4.25 ppm) for the samples withdrawn during the trapping reactions for MBrP. The signals at 4.41 and 4.32 ppm are assigned to the α-methine proton of the MBrP and the corresponding TEMPO trapped product. As is evident, the intensities of the signals become smaller for the MBrP and larger for the TEMPO trapped product, as the reaction progressed. The peak for the MBrP completely disappeared in 300 s, indicating that the reaction proceeded quantitatively and very rapidly even at 0 ºC. The conversions in time for the MBrP were calculated by integrating the proton peak with respect to the $–OCH_3$ which is present in the MBrP side chain, since the $–OCH_3$ does not participate in the trapping reactions. Thus the concentration of MBrP in time can be calculated.

Figure 2.16 shows the plot according to the simplified form of equation 2 for the MBrP system at 0 ºC. The plot is almost linear passing through the origin, and its slope with the known concentration of the $[Cu(I)/Ligand]_0$ and $[MBrP]_0$ gives $k_{act} = 0.018$ (±0.001) L $mol^{-1}$ $s^{-1}$.

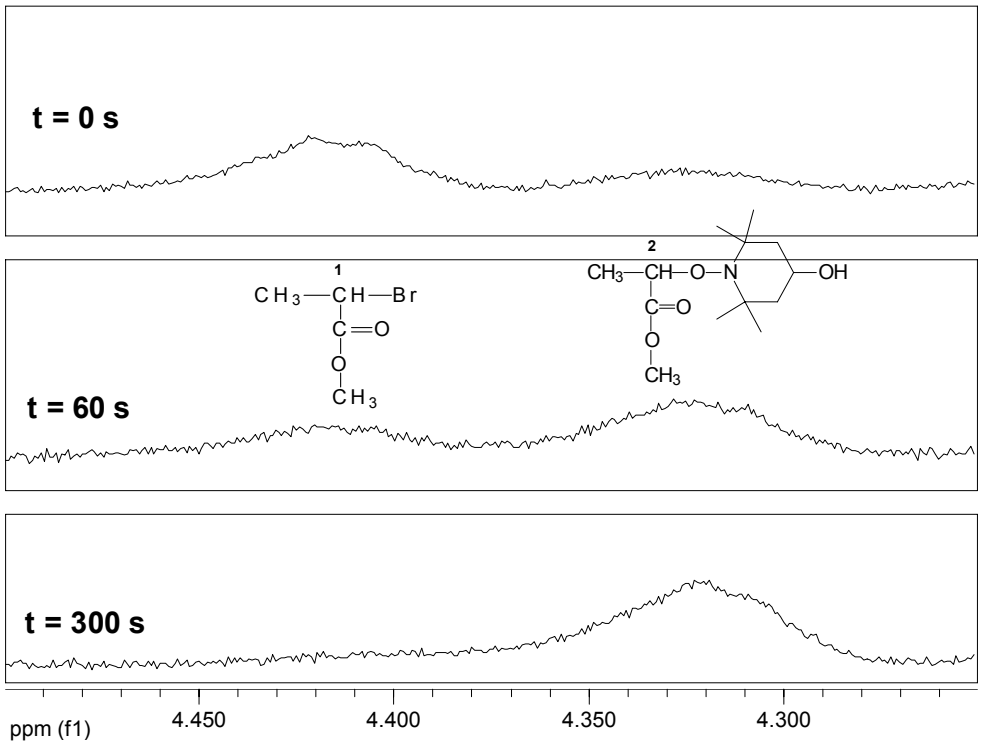


**Figure 2.15:** $^1H$ NMR spectra (in the range 4.5-4.25 ppm) for the MBrP/Cu(I)Br/PMDETA/hydroxy TEMPO (1/10/10/10) mixture in acetonitrile – $d_3$ at 0 ºC.

The trapping reactions for BrB and H-MA-Hexene-Br were performed using normal TEMPO, since the signals from the –CH next to the –OH group in the hydroxy TEMPO overlaps with the α-methine protons from BrB and H-MA-Hexene-Br. In Figure 2.17, the NMR spectra (in the range 4.15-4.0 ppm) for the samples withdrawn during the trapping reactions of BrB at 35 ºC are shown. No trapped product was observed. There is no decrease in the signal intensity of the peak from the BrB α-methine proton. Initially, this reaction was carried out at 0 ºC. The reaction temperature was raised to 35 ºC so as to increase the probability of activation. This result is indeed not surprising, since the activation of BrB is very unlikely, as there are no substituent groups in

butane to stabilize the formed radical. Hence, the initiation equilibrium as shown in Scheme 2.1 prefers to be on the dormant side. This trend would apply for most of the alkyl-substituted olefins.

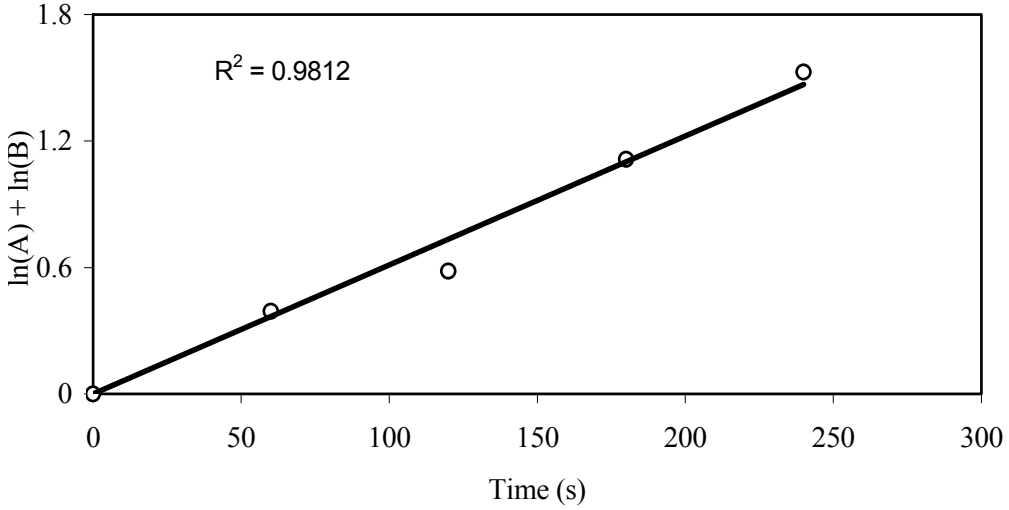


**Figure 2.16:** Plot of ln(A)+ln(B) *vs* time for the activation of MBrP catalyzed by Cu(I)Br in acetonitrile – $d_3$ at 0 ºC.

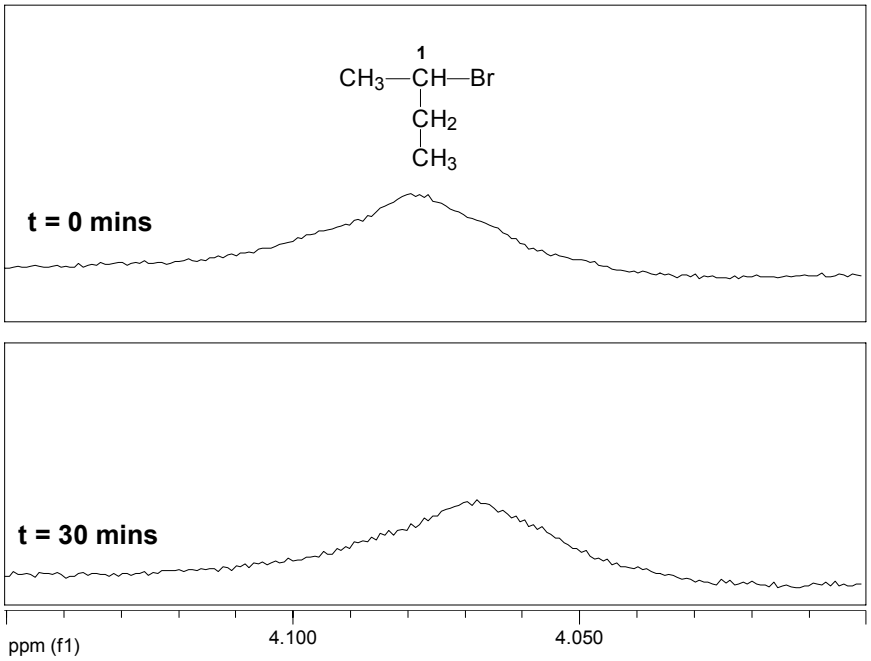


**Figure 2.17:** $^1$H NMR spectra (in the range 4.15-4.0 ppm) for the BrB/Cu(I)Br/PMDETA/TEMPO (1/10/10/10) mixture in acetonitrile – $d_3$ at 35 ºC.

So as to observe the influence of the penultimate group on the activation of the alkyl-substituted olefins, trapping reactions with the synthesized H-MA-Hexene-Br were performed. Recently published work indicated that there was a negligible penultimate unit effect of H or H-MA on the reactivity of secondary bromoesters.[12] The current reactions were initially performed at 0 ºC and then at elevated temperature of 70 ºC. Figure 2.18 entails the $^1$H NMR spectra (in the range 4.15-3.75 ppm) for the H-MA-Hexene-Br trapping reactions. Also here, like in the case of BrB, no trapped product was observed for a long period of time. After 18 h, there was change in the peak shape, clearly indicating that some of the H-MA-Hexene-Br was indeed trapped. Unfortunately, the calculation of the decrease in the concentration of H-MA-Hexene-Br proved to be difficult, since the two signals are overlapping.

Hence, it can be concluded that there was a negligible penultimate unit effect of H-MA on the activation of the terminal olefin. Further, the very slow activation rate can be attributed to the same phenomena as explained for BrB.

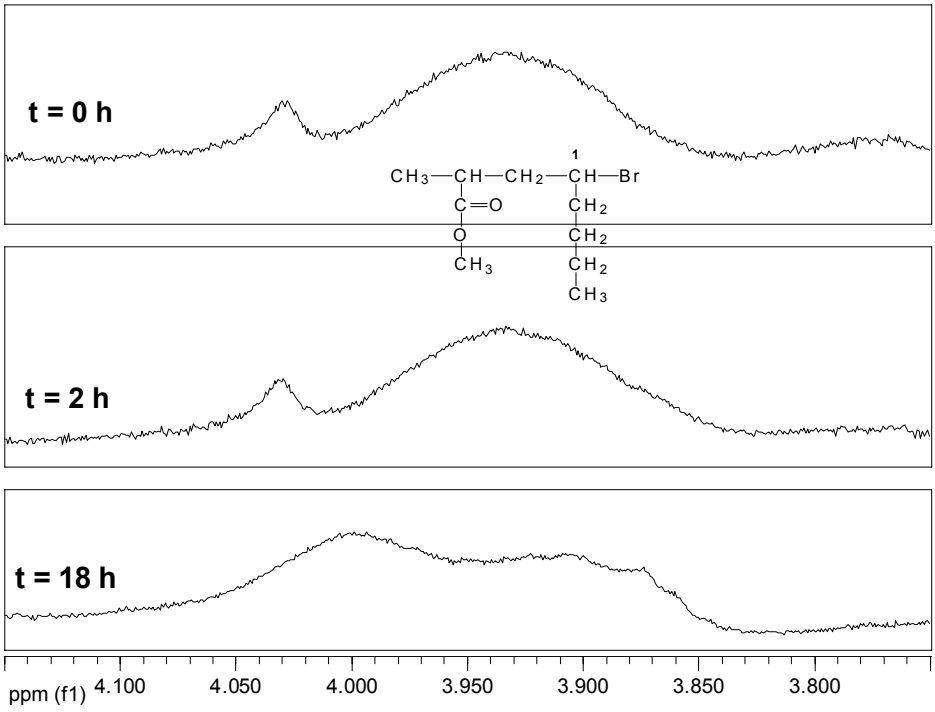


**Figure 2.18:** $^1$H NMR spectra (in the range 4.15-3.75 ppm) for the H-MA-Hexene-Br/Cu(I)Br/PMDETA/TEMPO (1/10/10/10) mixture in acetonitrile – $d_3$ at 70 ºC.

Thus, the only preferred radical pathway for the successful ATR copolymerization of MA and octene is the rapid crosspropagation of the octene terminal radicals. That is, for propagating radicals with a terminal octene unit, the time constant for crosspropagation is indeed smaller than that for deactivation. In other words, chains with an octene terminal unit exclusively undergo crosspropagation with MA. Because, as shown by the model compound studies, when the chain is end-capped with an olefin, it will be virtually inactive or extremely slow to re-initiate.

## *2.6 Conclusions*

The atom transfer radical copolymerization (ATRP) of methyl acrylate (MA) with 1-octene was investigated in detail. Well-controlled copolymers constituting almost 25 mol% of 1-octene were obtained using ethyl-2-bromoisobutyrate (EBriB) as initiator. Narrow molar mass distributions (MMD) were obtained for the ATRP experiments, which suggests conventional ATRP behavior, with no peculiarities caused by the incorporation of 1-octene. The feasibility of the ATRP copolymerizations was found to be independent of the ligand employed. Copolymerizations carried out using 4,4'-dinonyl-2,2'-bipyridine (dNbpy) resulted in good control, with significant octene incorporation in the polymer. The lower overall conversion obtained for the dNbpy systems as compared to the PMDETA systems was attributed to the redox potential of the formed copper(I)-ligand complex. The comparable free radical (co)polymerizations (FRP) resulted in broad MMDs. Increasing the fraction of the olefin in the monomer feed led to an increase in the level of incorporation of the olefin in the copolymer, at the expense of the overall conversion.

There was a good agreement between the reactivity ratios determined for the ATRP and FRP systems.

The formation of the copolymer was established using MALDI-TOF-MS. From the obtained MALDI-TOF-MS spectra for the ATRP systems, it was evident that several units of 1-octene were incorporated into the polymer chain. A gradient trend in the monomer sequence distribution was observed during the copolymerization. This was attributed to the rapidity of crosspropagation of 1-octene-terminated polymeric radicals with MA, as confirmed by the model compound studies. In ATRP polymerizations, only one pair of end groups was observed. By comparison, for the FRP systems, due to the multitude of side reactions occurring, several end groups were obtained.

## *2.7 Supporting Information*

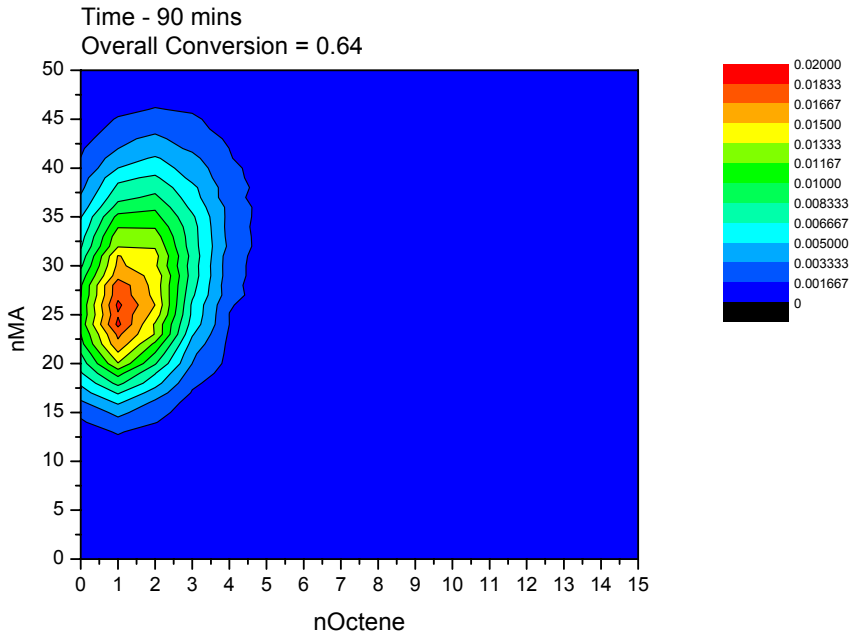


**(a)**

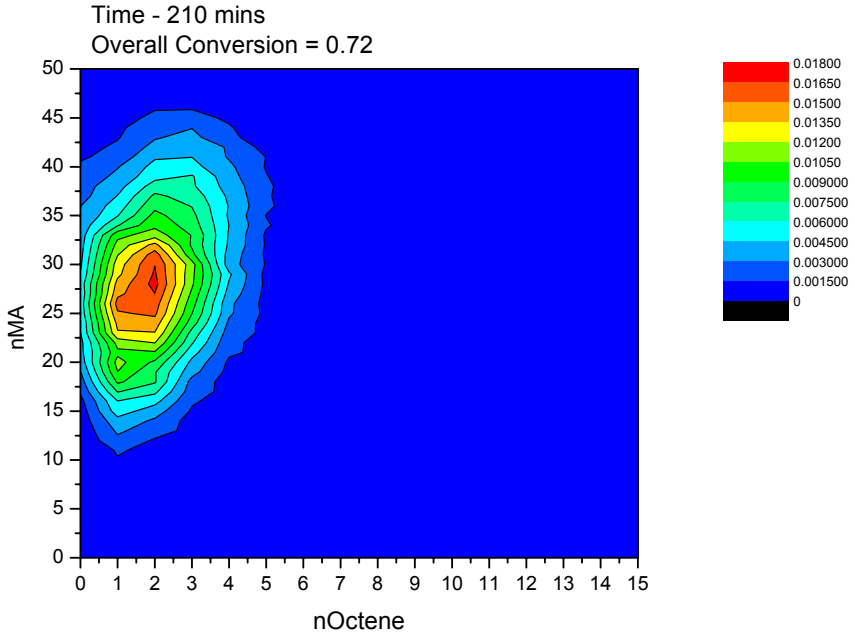


**(b)**

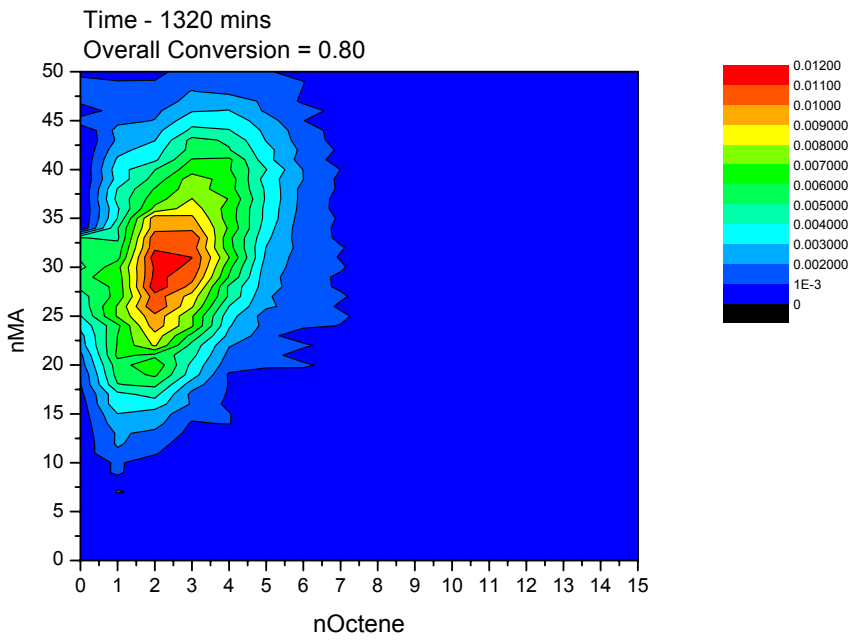


**(c)**

**Figure 2.19:** Copolymer fingerprint contour plots calculated from the acquired MALDI-TOF-MS spectra for samples withdrawn at various time intervals during the ATR copolymerization of MA/Octene, $f_{Octene}$ = 0.25. (Table 2.1, entry 1). [MALDI-TOF-MS spectra acquired in Reflector mode; Matrix **:** DCTB (trans-2-[3-(4-tert-butylphenyl)-2-methyl-2-propenylidene]malonitrile)]

## *2.8 References*

1) Padwa, A. R.; *Prog. Polym. Sci.*, **1989**, *14*, 811.

2) *Functional Polymers: Modern Synthetic Methods and Novel Structures*; Patil, A. O.; Schulz, D.N.; Novak, B. M.; (Eds.); ACS Symposium Series 704; American Chemical Society: Washington, DC, **1998**.

3) Johnson, L. K.; Killian, C. M.; Brookhart, M.; *J. Am. Chem. Soc.*, **1995**, *117*, 6414. Killian, C. M.; Temple, D. J.; Johnson, L. K.; Brookhart, M.; *J. Am. Chem. Soc.*, **1996**, *118*, 11664.

4) Johnson, L. K.; Mecking, S.; Brookhart, M.; *J. Am. Chem. Soc.*, **1996**, *118*, 267. Mecking, S.; Johnson, L. K.; Wang, L.; Brookhart, M.; *J. Am. Chem. Soc.*, **1998**, *120*, 888.

5) Wang, C.; Friedrich, S.; Younkin, T. R.; Li, R. T.; Grubbs, R. H.; Bansleben, D. A.; Day, M. W.; *Organometallics*, **1998**, *17*, 3149.

6) Yasuda, H.; Furo, M.; Yamamoto, H.; *Macromolecules*, **1992**, *25*, 5115. Yasuda, H.; Ihara, E.; Macromol. Chem. Phys., **1995**, *196*, 2417.

7) Ittel, S. D.; Johnson, L. K.; Brookhart, M.; *Chem. Rev.*, **2000**, *100*, 1169. Boffa, L. S.; Novak, B. M.; *Chem. Rev.*, **2000**, *100*, 1479.

8) Tian, G.; Boone, H. W.; Novak, B. M.; *Macromolecules*, **2001**, *34*, 7656.

9) Liu, S; Elyashiv, S.; Sen, A; *J. Am. Chem. Soc.*, **2001**, *123*, 12738.

10) Haddleton, D. M.; Sebastian, P.; Bon, S. A. F.; *Abstr. Pap.-Am. Chem. Soc.*, **2001**, 221st POLY-194.

11) Kato, M.; Kamigaito, M.; Sawamoto, M.; Higashimura, T.; *Macromolecules*, **1995**, *28*, 1721.

12) Wang, J. S.; Matyjaszewski, K.; *Macromolecules*, **1995**, *28*, 7901.

13) Keller, R. N.; Wycoff, H. D.; *Inorg. Synth.*, **1947**, *2*, 1.

14) Beuermann, S.; Paquet, D. A., Jr.; McMinn, J. H.; Hutchinson, R. A.; *Macromolecules*, **1996**, *29*, 4206.

15) Rudin, A.; *The Elements of Polymer Science and Engineering*; 2nd Edition, Academic Press, **1999**, p 218.

16) Venkatesh, R., Klumperman, B.; *Macromolecules*, **2004**, *37*, 1226.

17) Xia, J.; Matyjaszewski, K.; *Macromolecules*, **1997**, *33*, 7697. Qui, J.; Matyjaszewski, K.; Thouin, L.; Amatore, C.; *Macromol. Chem. Phys*., **2000**, *201*, 1625.

18) Skiest, I.; *J. Am. Chem. Soc.*, **1946**, *68*, 1781.

19) Chambard, G., Klumperman, B., Brinkhuis, R.H.G.; *ACS Symp. Ser.* **2003**, *854*, 180.

20) Mortimer, P.M., Mortimer, G.A.; *J.M.S. – Rev. Macromol. Chem* **1970**, *C4*, 281.

21) van Herk, A.M.; *J. Chem. Ed.*, **1995**, *72*, 138.

22) Nielen, M. W. F.; *Mass Spectrom. Rev*., **1999**, *18*, 309.

23) Matyjaszewski, K, Nakagawa, Y., Jasieczeck C. B.; *Macromolecules*, **1998**, *31*, 1535. Coessens, V., Matyjaszewski, K.; *J. Macromol. Sci.- Pure Appl. Chem.*; **1999**, *A 36*, 653. Coessens, V., Matyjaszewski, K.; *J. Macromol. Sci.- Pure Appl. Chem.*; **1999**, *A 36*, 667.

24) Axelsson, J., Scrivener, E., Haddleton, D. M., Derrich, P. J.; *Macromolecules*, **1996**, *29*, 8875.

25) Montaudo, G., Montaudo, M. S., Puglisi, C., Samperi, F., *Rapid Commun. Mass Spectrom*; **1995**, *9*, 453; *Macromolecules*; **1995**, *28*, 4562.

26) Ahmad, N. M., Heatley, F., Lovell, P. A.; *Macromolecules*; **1998**, *31*, 2822.

27) Moad, G., Solomon, D. H.; in *Comprehensive Polymer Science : The Synthesis, Characterization, Reactions and Applications of Polymers*; Allen, G. A., Bevington, J. C., (Eds.); Pergamon: Oxford, England, **1989**; Vol. 3; p 97.

28) Moad, G., Solomon, D. H.; in *Comprehensive Polymer Science : The Synthesis, Characterization, Reactions and Applications of Polymers*; Allen, G. A., Bevington, J. C., (Eds.); Pergamon: Oxford, England, **1989**; Vol. 3; p 147.

29) Chiefari, J., Jeffery, J., Mayadunne, R. T. A., Moad, G., Rizzardo, E., Thang, S.H.; *Macromolecules*; **1999**, *32*, 7700.

30) Goto, A.; Fukuda, T. *Macromol. Rapid Commun.* **1999**, *20*, 633.

31) Chambard, G.; Klumperman, B; German A.L. *Macromolecules,* **2000**, *33*, 4417.

32) Nanda, A. K., Matyjaszewski, K.; *Macromolecules*, **2003**, *36*, 8222.

# Chapter 3

## *Olefin Copolymerization via Controlled Radical Polymerization: Copolymerization of Methyl Methacrylate and 1-Octene*

**Abstract:** The atom transfer radical (co)polymerization (ATRP) of methyl methacrylate (MMA) with 1-octene was investigated. Well controlled homopolymer of MMA was obtained with 2,2,2-trichoroethanol (TCE) and p-toluenesulphonyl chloride (pTsCl), although, uncontrolled copolymerization occurred when pTsCl was employed in the presence of higher mol% of 1-octene in the monomer feed. Well-controlled copolymers constituting of almost 20 mol% of 1-octene were obtained using TCE as initiator. Narrow molar mass distribution (MMD) was obtained in the ATRP experiments. The comparable free radical (co)polymerizations (FRP) resulted in broad MMDs. Increasing the mol% of the olefin in the monomer feed, led to an increase in the level of incorporation of the olefin in the copolymer, at the expense of the overall conversion. The formation of the copolymer was established using matrix assisted laser desorption / ionization – time of flight – mass spectrometry (MALDI-TOF-MS). Evident from the MALDI-TOF-MS spectra was that most polymer chains contained at least one 1-octene unit. The glass transition temperature ($T_g$) of the copolymer was 16 ºC lower than that for the homopolymer of MMA. Block copolymer was synthesized and further characterized using gradient polymer elution chromatography (GPEC). The shift in the retention time between the macro-initiator and the formed block, clearly indicated the existence of the block copolymer structure and also confirmed the high macro-initiator efficiency.

## *3.1 Introduction*

Copolymers of alpha-olefins with polar monomers with various architectures remain an ultimate goal in polyolefin engineering. Of the many permutations available for modifying the properties of the polymers, the incorporation of functional groups into an otherwise nonpolar material is substantial.[1,2] Pioneering work in this field of olefin copolymerization with polar monomers, has

---

Venkatesh, R., Klumperman, B.; *Macromolecules*, **2004**, *37*, 1226.

been carried out in the area of metal-catalyzed insertion polymerization. The Brookhart Pd-based diimine catalyst[3] has been shown to copolymerize ethylene and higher alpha-olefins with acrylates and vinyl ketones.[4] Other late transition-metal-based complexes are also known to tolerate the presence of polar functional groups.[5] Block copolymers of ethylene with acrylates and methacrylates using group 4 metals are known.[6] Recently published reviews encompass the work in this field.[7] Although catalyst systems showing excellent behavior for both olefins and polar monomers do exist, due to differences in the reactivity between the two monomers, still energetically compatible mechanisms must be satisfied in order for true (random) copolymerization of these two types of monomer to occur. Very recent developments from Novak[8] were indicative of the fact that olefins could be copolymerized with vinyl monomers via a free radical mechanism. This was followed up by a publication detailing the copolymerization of methyl acrylate (MA) with 1-alkenes under atom transfer radical polymerization (ATRP) conditions.[9]

The present chapter deals with the copolymerization of methyl methacrylate (MMA) [a monomer having a high equilibrium constant ($K_{eq}$) under ATRP conditions and a lower rate constant for propagation ($k_p$) as compared to the acrylates] with 1-alkenes (in particular, 1-octene). Due to MMA's low $k_p$, coupled with the fact that, alpha-olefins undergo degradative chain transfer of allylic hydrogens,[10] the copolymerization reaction is highly unlikely. A heterogeneous transition metal/ligand system is employed for the ATR polymerizations. Results of the successfully controlled copolymerization and characterization by spectroscopic techniques are presented. A comparison of the ATRP results with conventional free radical polymerization using azo initiators is made. The choice/influence of initiator during the copolymerization in presence of the olefin will be highlighted. Further, the synthesized P[(MMA)-co-(1-octene)] is used as a macro-initiator for block polymer synthesis. The macro-initiator efficiency is monitored using Gradient Polymer Elution Chromatography (GPEC).

ATRP[11,12] is one of the techniques employed to obtain living (or controlled) radical polymerization. In copper mediated ATRP, the carbon-halogen bond of an alkyl halide (RX) is reversibly cleaved by a $Cu^{I}X$/ligand system resulting in a radical (R*) and $Cu^{II}X_2$/ligand (deactivator). The radical will mainly either reversibly deactivate, add monomer or irreversibly terminate. (See Scheme 2.1)

## 3.2 Experimental Section

### 3.2.1 Materials

Methyl methacrylate (MMA, Merck, 99+%) and 1-octene (Aldrich, 98%) were distilled and stored over molecular sieves at –15 ºC. *p*-Xylene (Aldrich, 99+% HPLC grade) was stored over molecular sieves and used without further purification. N,N,N',N'',N''-pentamethyldiethylenetriamine (PMDETA, Aldrich, 99%), 2,2,2-trichloroethanol (TCE, Aldrich, 99%), p-toluenesulphonyl chloride (pTsCl, Aldrich, 99%), copper (I) bromide (CuBr, Aldrich, 98%), copper (II) bromide ($CuBr_2$, Aldrich, 99%), copper (I) chloride (CuCl, Aldrich, 98%), copper (II) chloride ($CuCl_2$, Aldrich, 98%), aluminum oxide (activated, basic, for column chromatography, 50-200 μm), tetrahydrofuran (THF, Aldrich, AR), 1,4-dioxane (Aldrich, AR) were used as supplied. α,α'-Azobisisobutyronitrile (AIBN, Merck, >98%) was recrystallized twice from methanol before use. 1,1'-Azobis(cyclohexane-1-carbonitrile) (Vazo 88, Dupont, >98%) was used as procured.

### 3.2.2 Analysis and Measurements

***3.2.2.1 Determination of Conversion and MMD:*** Monomer conversion was determined from the concentration of the residual monomer measured via gas chromatography (GC). A Hewlett-Packard (HP-5890) GC, equipped with an AT-Wax capillary column (30 m × 0.53 mm × 10 μm) was used. *p*-Xylene was employed as the internal reference. The GC temperature gradient used is given in Figure 3.1.

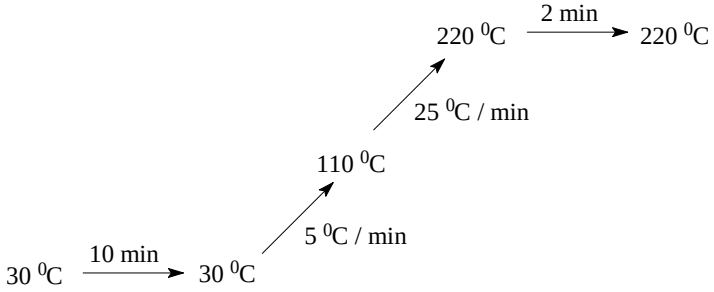


**Figure 3.1:** GC temperature gradient.

Molar mass (MM) and molar mass distributions (MMD) were measured by size exclusion chromatography (SEC), at ambient temperature using a Waters GPC equipped with a Waters model 510 pump, a model 410 differential refractometer (40 ºC), a Waters WISP 712 autoinjector ( 50 μL

injection volume), a PL gel (5 μm particles) 50 × 7.5 mm guard column and a set of two mixed bed columns (Mixed-C, Polymer Laboratories, 300 × 7.5 mm , 5 μm bead size, 40 ºC) . THF was used as the eluent at a flow rate of 1.0 mL/min. Calibration was carried out using narrow MMD polystyrene (PS) standards ranging from 580 to 7 × $10^6$ g/mol. The molecular weights were calculated using the universal calibration principle and Mark-Houwink parameters [13] [PMMA: K = 9.55 × $10^{-5}$ dL/g, a = 0.719; PS: K = 1.14 × $10^{-4}$ dL/g, a = 0.716]. The molecular weights were calculated relative to PMMA homopolymer. Data acquisition and processing were performed using Waters Millenium 32 software.

***3.2.2.2 GPEC Analysis:*** GPEC measurements were carried out on an Alliance Waters 2690 separation module with a Waters 2487 dual λ absorbance detector and a PL-EMD 960 ELSD detector (Nitrogen flow 5.0 ml/min, temperature 70 ºC). A Zorbax silica 5 μm column (4.6 mm × 150 mm, Dupont Chromatography) was used at 40 ºC. The gradient employed is detailed in Table 3.1. The column was reset at the end of the gradient to initial conditions between 25 and 30 mins. HPLC grade solvents were obtained from BioSolve. A Varian 9010 solvent delivery system was used to maintain a stable flow rate of the eluents. Dilute polymer solutions were made in THF (10 mg/mL) and a sample of 10 μL was used for analysis. Chromatograms were analyzed using the Millennium 32 software version 3.05.

**Table 3.1:** Linear Binary gradient used for GPEC

| Step | Time (min) | $\Phi_{heptane}$ | $\Phi_{THF}$ | Flow (ml/min) |
|---|---|---|---|---|
| 1 | Initial | 1 | 0 | 0.5 |
| 2 | 15 | 0 | 1 | 1.0 |
| 3 | 25 | 0 | 1 | 0.5 |
| 4 | 30 | 1 | 0 | 0.5 |

The eluent compositions are given in volume fraction (Φ).

***3.2.2.3 MALDI-TOF-MS:*** Measurements were performed on a Voyager-DE STR (Applied Biosystems, Framingham, MA) instrument equipped with a 337 nm nitrogen laser. Positive-ion spectra were acquired in reflector mode. DCTB (trans-2-[3-(4-tert-butylphenyl)-2-methyl-2-propenylidene]malononitrile) was chosen as the matrix. Potassium trifluoracetate (Aldrich, 98%) was added as the cationic ionization agent. The matrix was dissolved in THF at a concentration of 40 mg/mL. Potassium trifluoracetate was added to THF at a concentration of

1 mg/mL. The dissolved polymer concentration in THF was approximately 1 mg/mL. For each spectrum 1000 laser shots were accumulated. In a typical MALDI experiment, the matrix, salt and polymer solutions were premixed in the ratio: 5 μL sample: 5 μL matrix: 0.5 μL salt. Approximately 0.5 μL of the obtained mixture was hand spotted on the target plate.

***3.2.2.4 DSC:*** Scans were done on a TA Instruments Advanced Q1000 standard differential scanning calorimeter. The instrument was calibrated according to the standard procedure suggested by TA Instruments based on indium, saffire and standard polyethylene. The standards were all supplied by TA Instruments. The DSC temperature gradient used was, 20 ºC to 150 ºC at a rate of 10 ºC / min. The step change in the heat flow during the second heating run was considered for the glass transition temperature determination. The Tg was calculated at the inflection (inflection is the portion of the curve between the first and third tangents with the steepest slope).

## *3.2 Synthetic Procedures*

***3.3.1 ATR Copolymerization of MMA and 1-octene:*** A typical polymerization was carried out in a 50 mL three-neck round bottom flask. *p*-Xylene (11.05 g, 12.7 mL, 0.10 mol), MMA (2.42 g, 2.5 mL, 0.02 mol), 1-octene (2.71 g, 3.8 mL, 0.02 mol), CuCl (0.037 g, 0.4 mmol) and $CuCl_2$ (0.003 g, 0.02 mmol) were accurately weighed and transferred to the flask. The ligand, PMDETA (0.07 g, 0.1 mL, 0.4 mmol) was then added. After the reaction mixture was bubbled with argon for 30 min, the flask was immersed in a thermostated oil bath maintained at 90 ºC and stirred for 10 min. A light green, slightly heterogeneous system was then obtained. The initiator, TCE (0.15 g, 0.10 mL, 1.00 mmol) was added slowly via a degassed syringe. The reactions were carried out under a flowing argon atmosphere. Samples were withdrawn at suitable time periods throughout the polymerization. A pre-determined amount of the sample was transferred immediately after withdrawing into a GC vial and diluted with 1,4-dioxane, so as to determine the monomer conversion using GC. The remaining sample was diluted with THF, passed through a column of aluminum oxide prior to SEC and MALDI-TOF-MS measurements.

### *3.3.2 Bulk Polymerization of MMA (Chain transfer experiments):*

Solutions of varying [MMA]/[1-octene] ratios were prepared (Table 3.3). The initiator (Vazo 88) [Initiator – 10 mmol/L] was separately weighed for each of the formulations and transferred into Schlenk tubes. The monomer solutions were then added to the respective Schlenk tubes. The tubes were then degassed by three freeze – pump – thaw cycles and then heated to 90 ºC. All polymerizations for the determination of $C_{tr}$ were restricted to low conversions (< 2%), with reaction mixtures being quenched by rapid cooling and the addition of hydroquinone prior to gravimetric determination of final conversions. Molecular weights were determined using SEC.

## *3.4 Results and Discussion*

The choice of the initiator for the copolymerization is very briefly dealt with, followed by the determination of chain transfer constant ($C_{tr}$) for 1-octene in MMA. Then, the synthesis of the copolymers and comparison of the ATRP results with the conventional free radical systems will be discussed. The influence of the olefin during the copolymerization is highlighted. Further, copolymer characterization using MALDI-TOF-MS is discussed. Also, the synthesis of block copolymer with clear insight into the macro-initiator efficiency is explained.

***3.4.1 Choice of initiator:*** The CuCl/PMDETA catalyst system was used in the copolymerization. PMDETA was selected because **(i)** the catalyst complex is highly active, leading to faster rates of polymerization (especially useful since a very non-reactive monomer like 1-octene was present), **(ii)** readily available, **(iii)** cheap, and most importantly, **(iv)** the catalyst complex can be easily separated from the polymer, which is aided by the fact that a heterogeneous system was obtained when a non-polar solvent (eg. *p*-xylene, toluene) is employed for the polymerization. Now, since, the CuX/PMDETA (X=Cl,Br) is known to be a highly active catalyst system, more so with monomers such as MMA or in general methacrylates, with high observed propagation rate constants ($k_p^{obs} = k_p \times K_{eq}$; $K_{eq} \sim 10^{-7}$ to $10^{-6}$ for MMA with PMDETA/CuBr),[14] the choice for the initiator is crucial to avoid slow initiation and possible side reactions.

Percec[15] and coworkers were the first to demonstrate the use of arenesulphonyl halides as universal initiators for heterogeneous and homogeneous metal-catalyzed living radical polymerization of styrene, methacrylates and acrylates. 2,2,2-Trichloroethanol (TCE) was used as an initiator, which resulted in a fast and nearly quantitative initiation of MMA using the CuCl/bpy

catalyst system.[16] ATRP of MMA using an EBriB/CuCl system also led to a good control of molecular weight and narrow MMD.[17]

For the present work, the initiators employed were restricted to p-toluenesulphonyl chloride (pTsCl) and TCE. Table 3.2 details the results obtained for the homopolymerization of MMA using the selected initiators in a CuCl/PMDETA system.

**Table 3.2:** Homopolymerization of MMA (ATRP)

| Entry | Initiator | Reaction time (mins.) | Conversion (%) | $M_n$ (g/mol) | PDI |
|---|---|---|---|---|---|
| 1 | pTsCl [a,b] | 230 | 74.0 | $7.1 \times 10^3$ | 1.08 |
| 2 | TCE [a,b] | 180 | 45.0 | $2.8 \times 10^3$ | 1.25 |

a) Targeted $M_n$ = 5000 g/mol; [Initiator]:[CuCl]:[PMDETA] = 1:0.5:0.5, Reaction temperature = 90 °C.

b) Volume {*p*-xylene}/{monomer} = 1/0.5

The homopolymerizations were performed in 50 vol% *p*-xylene at 90 °C. The molar ratio of initiator to catalyst to ligand was chosen to be the same for both the entries 1 and 2, which enabled to compare the reactions. A typical semilogarithmic kinetic plot of the homopolymerization is shown in Figure 3.2. The linearity clearly indicates that there were a constant number of growing chains during the polymerization. The MM increases linearly with conversion (Figure 3.3) and the final MMD was ≤ 1.25. Though, the initiator efficiency in the case of pTsCl was only 50%, as compared to that of TCE of 80%, the initiator efficiency for the pTsCl can be improved by decreasing the copper (I) to initiator ratio (Table 3.5, entry 2).

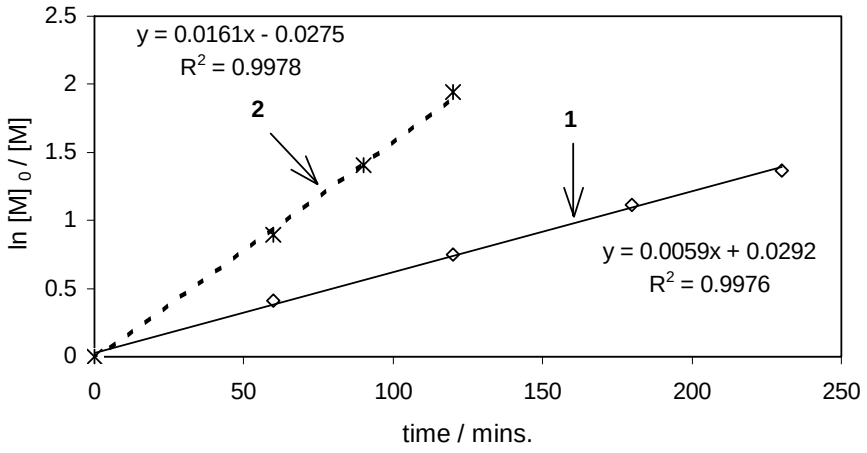


**Figure 3.2:** Plot of ln $[M]_0/[M]$ for the homopolymerization of MMA. (1) pTsCl initiated, **(**2) TCE initiated. (For details, see Table 3.2).

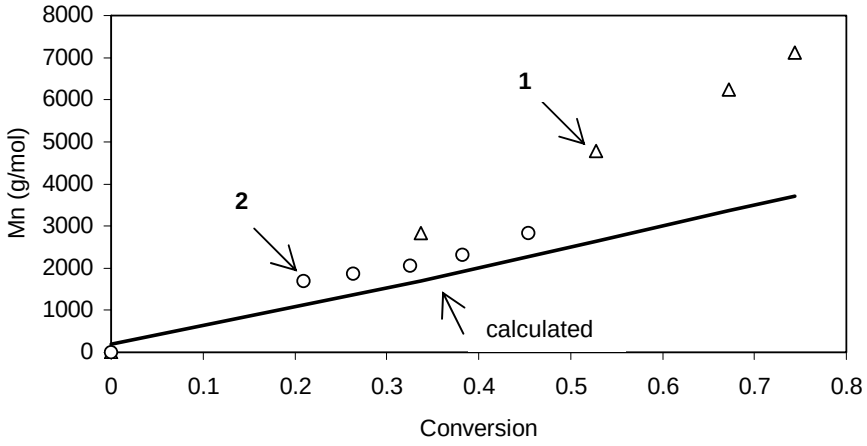


**Figure 3.3:** Plot of $M_n$ vs conversion for the homopolymerizations (For labels see Table 3.2).

### *3.4.2 Determination of Chain transfer constant ($C_{tr}$) for 1-octene in MMA:*

Higher alpha-olefins are known to act as chain transfer agents in radical polymerization.[10] Hence, it was interesting to determine the chain transfer constant for 1-octene during the radical polymerization of MMA. The activity of chain transfer is usually measured as the ratio between the transfer rate coefficient ($k_{tr}$) and the propagation rate coefficient ($k_p$). The Mayo method,[18] was employed, which expresses the reciprocal of the number-average degree of polymerization ($DP_n$), as a function of the rates of chain-growth and chain-termination;

$$\frac{1}{DP_n} = \frac{1}{DP_{no}} + C_{tr}\frac{[1\text{-Octene}]}{[MMA]} \qquad (1)$$

where, [1-octene] and [MMA] are the concentrations of the 1-octene and MMA respectively, and $DP_{no}$ is the number average degree of polymerization obtained in the absence of the transfer agent (in this case 1-octene).

Usually, the Mayo procedure involves the determination of $DP_n$ at low conversion for a range of [1-octene]/[MMA] values and the plot of 1/ $DP_n$ vs [1-octene]/[MMA] should yield a straight line with slope $C_{tr}$. Values for the $DP_n$ are commonly obtained by SEC. Since, the determination of number average molar mass ($M_n$) by SEC, is very sensitive to baseline fluctuations, it is prudent to consider the weight average molar mass ($M_w$), because it depends more on the high molar mass region of the distribution, which is better defined. Assuming that $M_w/M_n$ = 2 in a chain transfer dominated system at low conversions, the Mayo procedure can now be applied by plotting $1/(DP_w/2)$ versus [1-octene]/[MMA].[19,20]

The polymerizations were carried out in MMA at 90 ºC for 5 minutes. A wide range of [MMA]/[1-octene] ratios were employed. Low initiator concentration was used ([Vazo 88] = 10 mmol/L), so that chain transfer and not bimolecular termination largely occurred as chain stopping events. The polymerizations were stopped at low conversion, that is below 2%, so that the [MMA]/[1-octene] ratios were kept relatively constant and thus accurate $C_{tr}$ values could be obtained.

Table 3.3 gives the various mol% of MMA and 1-octene employed and also the $M_w$ obtained from SEC. $M_w$ values shift to lower MM with increasing 1-octene concentrations, clearly indicating that 1-octene does act as a transfer agent in free radical polymerization. Also clear was that, as the mol% of 1-octene increased in the monomer feed, the % conversion decreased. This can be attributed to the fact that, more allylic radicals were obtained as a result of chain transfer, and these formed radicals were slow to re-initiate the polymerization. Hence, retardation in the rate of polymerization was obtained. Now, using equation 1, the value for the $C_{tr}$ was obtained (Figure 3.4). The value for the $C_{tr}$ was $9 \times 10^{-4}$. On comparison with the chain transfer to monomer value of $0.1 \times 10^{-4}$ for methyl methacrylate at 90 ºC,[21] it turned out that the chain transfer constant to 1-octene is approximately two orders of magnitude larger.

**Table 3.3:** $C_{tr}$ experiments

| Entry | MMA (mol%) | 1-Octene (mol%) | % Conversion | $M_w$ (g/mol) |
|---|---|---|---|---|
| 1 | 100 | - | 1.1 | $6.4 \times 10^5$ |
| 2 | 98 | 2 | 1.1 | $6.3 \times 10^5$ |
| 3 | 95 | 5 | 1.0 | $6.0 \times 10^5$ |
| 4 | 90 | 10 | 0.8 | $4.8 \times 10^5$ |
| 5 | 75 | 25 | 0.6 | $3.3 \times 10^5$ |

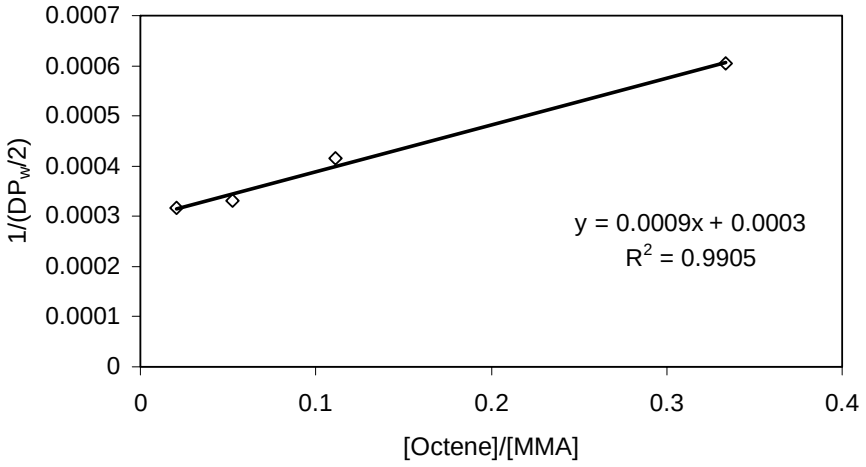


**Figure 3.4:** Plot of $1/(DP_w/2)$ *vs* [1-octene]/[MMA] ratios for determination of $C_{tr}$

### *3.4.3 MMA / 1-octene Copolymers:*

Free radical copolymerization (FRP) initiated by AIBN and Vazo 88, and ATR copolymerization of MMA in the presence of 1-octene using TCE as initiator were examined as summarized in Table 3.4.

In table 3.4, copolymerizations are listed at different comonomer ratios. Each of the comonomer ratios was polymerized under ATRP as well as under FRP conditions. A couple of observations can be made; **(i)** 1-octene does copolymerize via a radical mechanism. Homopolymerization of 1-octene was attempted in both FRP and ATRP, but no polymer was obtained. This is attributed to the fact that alpha-olefins undergo degradative chain transfer of allylic hydrogens.[10] The stable allylic radical derived from the monomer is slow to reinitiate and prone to terminate. The presence of the formation of the stable allylic radical is further confirmed by electron spin resonance.[22] **(ii)** The copolymerizations under FRP conditions show relatively low MM as compared to the MMA homopolymerization under the same conditions (*compare entry 1 with 2, 3, 6 & 7*). Broad MMDs were obtained for all FRP systems. In this chapter itself, the tendency for octene to behave as a chain transfer agent under FRP conditions was reported. The value for the $C_{tr}$ was found to be $9 \times 10^{-4}$, in the case of MMA systems. **(iii)** The experimentally determined MM in the case of polymerizations under ATRP conditions coincide nicely with the calculated values (Figure 3.5). The linearity clearly indicates that there were a constant number of growing chains during the polymerization. **(iv)** Narrow MMDs were obtained in the ATRP experiments, which points at ordinary ATRP behavior, i.e. no peculiarities caused by the incorporation of octene.

**Table 3.4:** Copolymers of MMA / 1-octene (TCE initiator)

| Entry | MMA (mol%) | 1-octene (mol%) | Overall % conversion | 1-octene incorporation (mol%) [f] | $M_n$ (g/mol) | PDI |
|---|---|---|---|---|---|---|
| 1 [a] | 100 | - | 47.0 | - | $6.6 \times 10^4$ | 2.0 |
| 2 [b] | 75 | 25 | 73.0 | **6.4** | $1.8 \times 10^4$ | 1.9 |
| 3 [c] | 75 | 25 | 79.0 | **8.2** | $1.7 \times 10^4$ | 2.7 |
| 4 [d] | 75 | 25 | 73.0 | **6.4** | $4.6 \times 10^3$ | 1.2 |
| 5 [e] | 75 | 25 | 78.0 | **7.0** | $6.2 \times 10^3$ | 1.3 |
| 6 [b] | 50 | 50 | 47.5 | **16.2** | $1.0 \times 10^4$ | 2.0 |
| 7 [c] | 50 | 50 | 58.0 | **18.2** | $9.4 \times 10^3$ | 2.7 |
| 8 [d] | 50 | 50 | 46.5 | **19.2** | $2.3 \times 10^3$ | 1.3 |

For all solution (co)polymerizations listed above, p-xylene was used as the solvent. Volume {solvent}/{monomer} = 1/0.5; Reaction temperature = 90 ºC; Reaction time = 25 hrs.

***a*** - FRP; Initiator = Vazo88 (10 mmol/L), Reaction time = 2 hrs. ***b*** - FRP; Initiator = AIBN (10 mmol/L). ***c*** - FRP; Initiator = Vazo88 (10 mmol/L). ***d*** - ATRP; Targeted $M_n$ = 5000 g/mol; [TCE]:[CuCl]:[PMDETA] = 1:0.4:0.4. ***e*** - ATRP; Targeted $M_n$ = 5000 g/mol; [TCE]:[CuCl]:[PMDETA] = 1:1:1**.** ***f*** - Calculated from monomer conversions, obtained from GC measurements.

**(v)** As the mol% of the alpha-olefin was increased in the monomer feed, its incorporation was higher in the copolymer (*compare entries 3 & 6, 4 & 7 and 5 & 8*). Two effects can cause this phenomenon. Due to composition drift, the fraction of 1-octene in the remaining monomer increases, which leads to a decrease in average propagation rate constant. When the fraction 1-octene increases, the probability of endcapping a 1-octene moiety at the chain end with a bromide increases. When this happens the chain will be virtually inactive as we learned from model experiments. Thus, increasing the mol% of alpha-olefin in the monomer feed decreased the overall % conversion (Figure 3.6). **(vi)** Varying the Cu(I) to initiator, does influence the reaction kinetics (*compare entries 4 & 5*). A higher Cu(I) concentration, leads to an increase in the initial radical concentration, and in turn to slightly faster polymerization rates (Figure 3.7). But as observed, it does not alter the final amount of 1-octene incorporated. Now, it is known that $k_t \propto [R^*]^2$ and $R_p \propto [R^*]$, where $k_t$ and $R_p$ are the rate coefficient of termination and rate of polymerization respectively. $[R^*]$ stands for radical concentration. Hence, a higher initial radical concentration, would lead to

some portion of the initiator radicals being lost due to bimolecular termination at the onset of the polymerization and hence to a lower initiator efficiency.

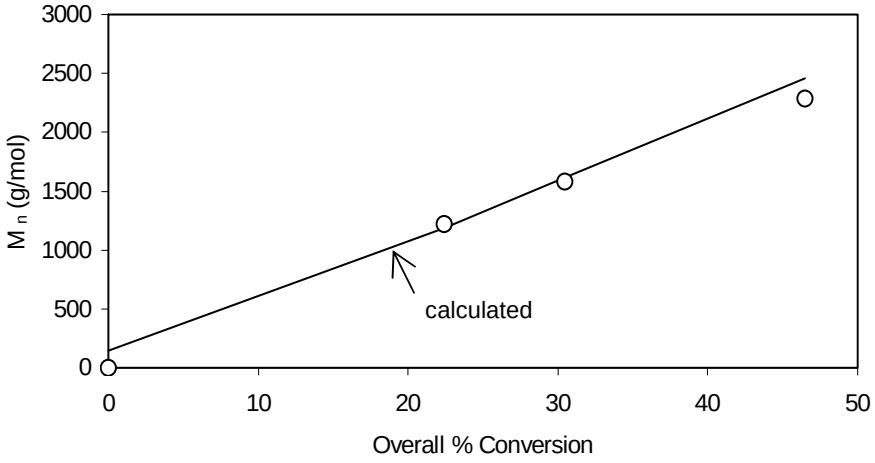


**Figure 3.5:** Plot of $M_n$ *vs* overall conversion for entry 8. (For labels, see Table 3.4).

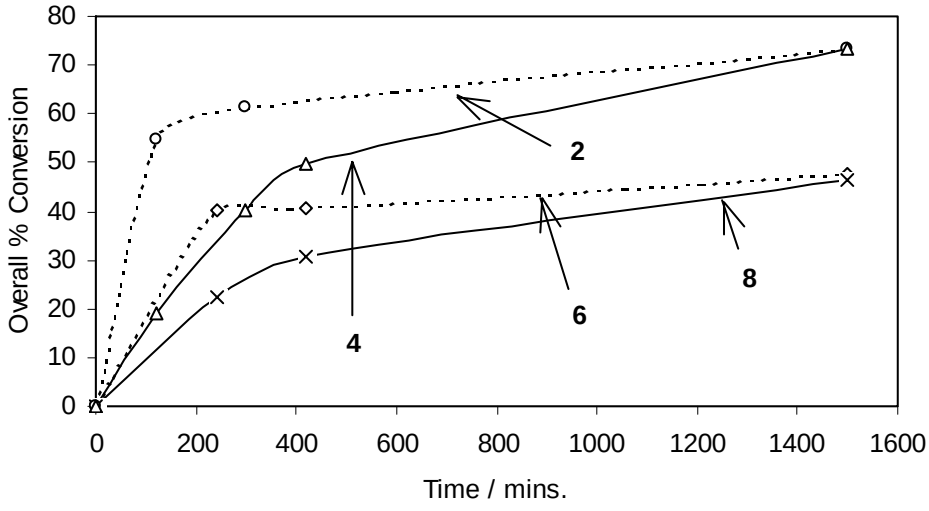


**Figure 3.6:** Plot of overall conversion *vs* time for the described copolymerizations. (For the labels, see Table 3.4).

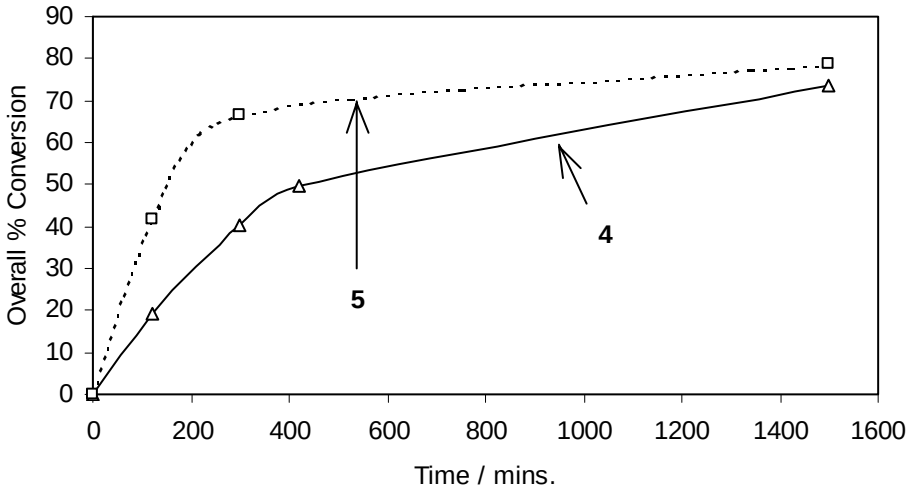


**Figure 3.7:** Influence of [Cu(I)] on conversion. Plot of overall conversion vs time for the described copolymerizations. (For the labels, see Table 3.4).

The copolymerizations were also performed using pTsCl as initiator, since for the homopolymerization of MMA narrower MMDs were obtained (Table 3.2). The trend obtained for the copolymerization described in Table 3.5, was comparable to that observed in Table 3.4. Narrow MMDs were obtained in the ATRP experiments, which points at ordinary ATRP behavior.

**Table 3.5:** Copolymers of MMA and 1-octene (pTsCl initiator)

| Entry | MMA (mol%) | 1-octene (mol%) | Overall % Conversion | 1-octene incorp. (mol%) [d] | $M_n$ (g/mol) | PDI |
|---|---|---|---|---|---|---|
| 1 [a] | 90 | 10 | 80.0 | **2.0** | $7.4 \times 10^3$ | 1.1 |
| 2 [b] | 75 | 25 | 66.0 | **7.3** | $8.6 \times 10^3$ | 1.1 |
| 3 [c] | 50 | 50 | 30.0 | **25.8** | $1.2 \times 10^3$ | 1.3 |

For all solution ATR(co)polymerizations listed above, p-xylene was used as the solvent. Volume {solvent}/{monomer} = 1/0.5; Reaction temperature = 90 ºC.

a *Targeted $M_n$ = 5000 g/mol; [pTsCl]:[CuCl]:[PMDETA] = 1:0.5:0.5; Reaction time = 9 h 30 min.*

*b* Targeted $M_n$ = 10000 g/mol; [pTsCl]:[CuCl]:[HMTETA] = 1:0.285:0.285; Reaction time = 70 h.

*c* Targeted $M_n$ = 10000 g/mol; [pTsCl]:[CuCl]:[HMTETA] = 1:0.285:0.285; Reaction time = 81 h.

*d* Calculated from monomer conversions, obtained from GC measurements.

The only exception is entry 3, where the MMD was relatively broad and very low molecular weight was obtained. The plot of overall conversion versus time (Figure 3.8) indicates that, in the presence of higher 1-octene in the monomer feed, a drastic decrease in the overall conversion was observed. This was coupled with the fact that there was no linear increase in the molecular weight with conversion (Figure 3.9), clearly indicating that the reaction was not controlled.

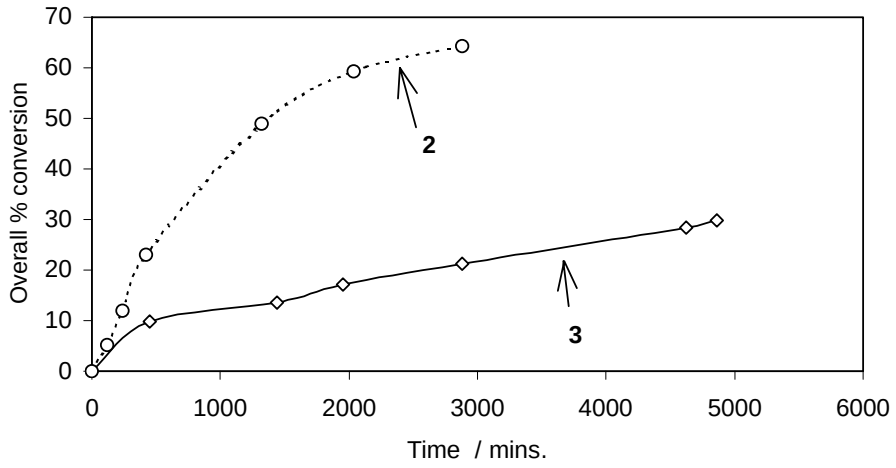


**Figure 3.8:** Plot of overall conversion *vs* time. (For the labels, see to Table 3.5).

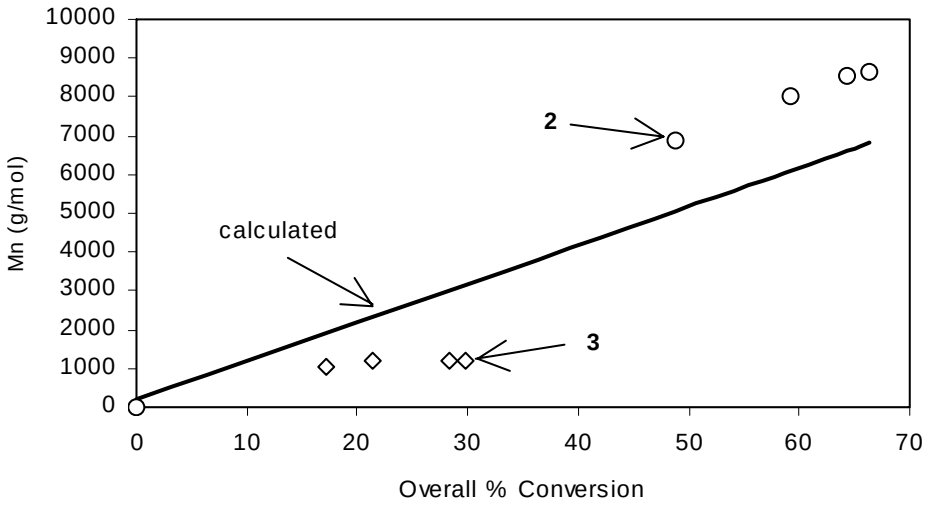


**Figure 3.9:** Plot of $M_n$ *vs* overall conversion. (For the labels, see to Table 3.5).

The important difference between alkyl halides and arylsulfonyl halides arises from the initiation mechanism (Scheme 3.1, Equations 1-3).[23] The arylsulfonyl halides undergo faster reduction to the corresponding sulfonyl radical, which in turn results in the faster addition of the sulfonyl radicals to the monomer. This addition is reversible, and the equilibrium of the reversible

addition is determined by the nature of the substituent attached to the monomer and its ability to stabilize the resulting radical. As in the present case, when there is more 1-octene in the monomer feed (Table 3.5, entry 3), then the probability of 1-octene adding to the sulfonyl radical in the initiation step is increased. If that occurs, then re-initaition of this monoadduct (with the 1-octene as the terminal group), is very unlikely, since there are no substituent groups in the 1-octene to stabilize the obtained radical. Hence, the equilibrium is shifted to the dormant side. Work on activation rate parameters using a 1-octene type alkyl halide as a model compound resulted in no initiation (refer Section 2.5). Thus, the result obtained for entry 3 can be explained due to the addition of the sulfonyl radicals to 1-octene, which in turn do not re-initiate the polymerization.

**Scheme 3.1:** Initiation Mechanism for substituted phenylsulfonyl chlorides [23]

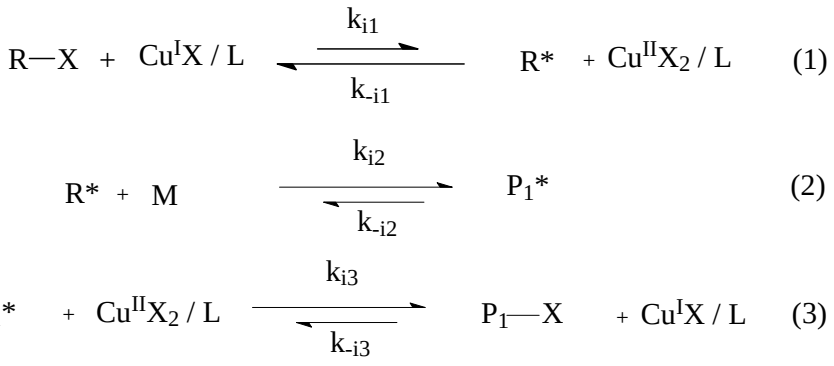


### *3.4.4 ATRP initiated by P[(MMA)-co-(1-octene)]. Chain extension with MMA:*

The synthesized copolymer (table 3.4, entry 8) comprising 19 mol% of 1-octene in the copolymer was used as the macroinitiator for block copolymerization. The resulting molecular weight and polydispersity was as summarized in table 3.6. The living character of the copolymer was demonstrated by chain extension with MMA. High-performance liquid chromatography was employed for selective separation. It has been used previously for selective separation and characterization of block and random copolymers.[24] In this paper, the term gradient polymer elution chromtography (GPEC) is used.[25] In GPEC, separation of the polymers is based on differences in column interactions, as in the case of isocractic chromatography, but also depends on precipitation and redissolution mechanisms as the eluent composition changes gradually in time. Hence, it is possible to separate polymers depending on molar mass, chemical composition and chain(-end) functionality. In the current study, normal phase GPEC with THF and n-heptane as

eluent was employed. The gradient used was shown in Table 3.1. The GPEC trace in Figure 3.10 clearly indicates well-resolved peaks from the macroinitiator and the block copolymer. The complete shift of the entire block polymer peak from the macroinitiator peak was evidence for the block copolymer formation. The difference in the elution behavior was a direct indication of chemical composition difference between the macroinitiator and the block copolymer. The clear shift of the block copolymer peak to higher retention time, also indicated the high macroinitiator efficiency, which is characteristic of a living polymerization. This was coupled with the fact that there was a reasonable match between the theoretical and experimentally determined molecular weights.

**Table 3.6:** Block copolymer

| Entry | M:I:Cu:L | Reaction time (hr) | Conversion (%) | Theoretical $M_n$ (g/mol) [a] | Experimental $M_n$ (g/mol) [b] | PDI |
|---|---|---|---|---|---|---|
| 1 | 77:1:1:1 | 11 | 64 | $6.4 \times 10^3$ | $5.5 \times 10^3$ | 1.5 |

Volume {solvent}/{monomer} = 1/0.5. Targeted Molecular weight = 10000 g/mol.

*a* $[(([MMA]_0/[Macroinitiator]_0) \times conversion) \times M_{MMA}] + M_{Macroinitiator}$

*b* From SEC analysis, using universal calibration for PMMA with PS standards.

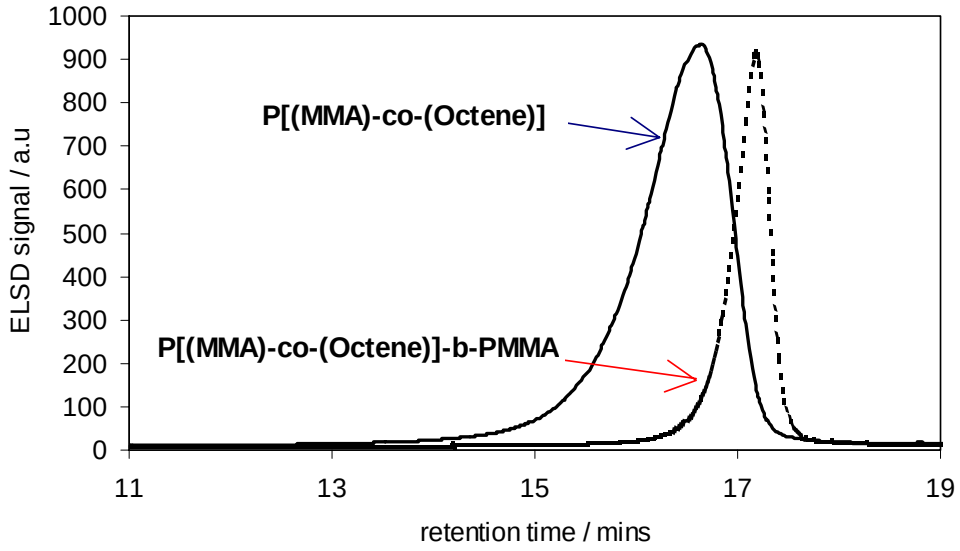


**Figure 3.10:** GPEC traces of the macroinitiator and the block copolymer respectively.

### *3.4.5 Copolymer Characterization:*

The formation of the copolymer was established using the matrix assisted laser desorption / ionization – time of flight – mass

spectrometry (MALDI-TOF-MS). Differential scanning calorimetry (DSC) was also employed to identify the difference in glass transition temperature (Tg) between the homopolymer of MMA and the formed copolymer.

***3.4.5.1 MALDI-TOF-MS:*** Figure 3.11 depicts the MALDI-TOF-MS spectrum for the MMA/1-octene copolymer (Table 3.5, entry 2). The copolymer obtained using pTsCl as initiator was only investigated, primarily due to the relative ease in peak assignment. The overlap of several signal distributions is clearly visible. This is typical for the resolved mass distributions of a copolymer, since copolymers have, in comparison with homopolymers, two types of heterogeneity. Like homopolymers, they have the heterogeneity in the degree of polymerization, corresponding to a distribution of the chain length. Additionally, there is the heterogeneity of the chemical composition.

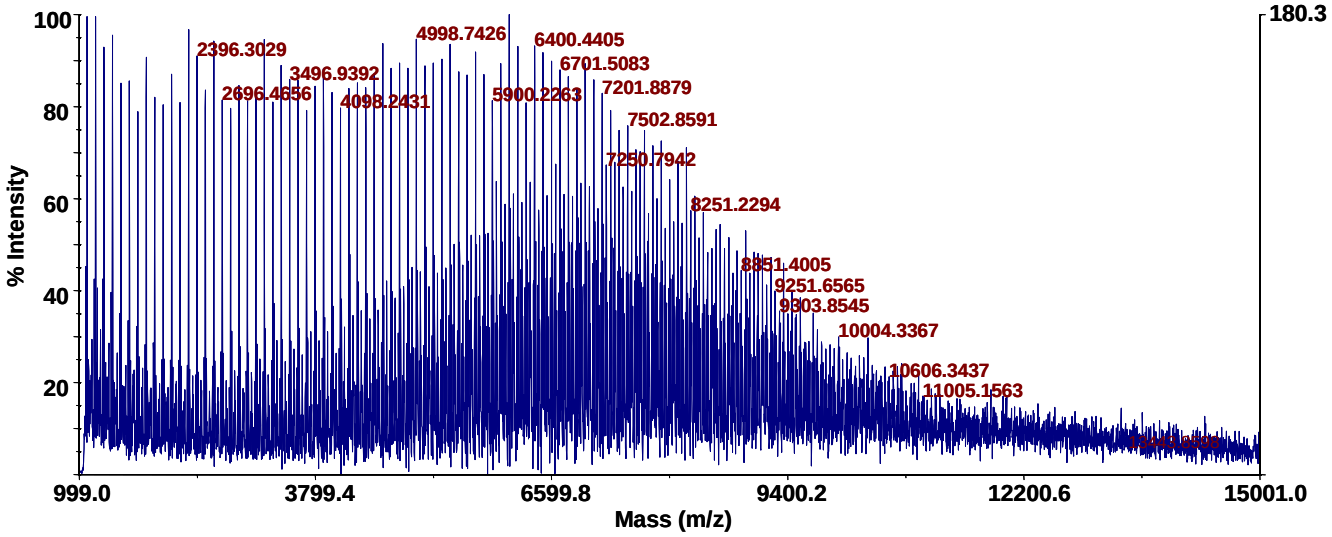


**Figure 3.11:** MALDI-TOF-MS spectrum for MMA/Oct copolymer (table 3.5, entry 2). [Spectrum acquired in the Reflector Mode, Matrix : DCTB (trans-2-[3-(4-tert-butylphenyl)-2-methyl-2-propenylidene]malononitrile)].

Figure 3.12 is an expansion of a selected portion of the spectrum shown in Figure 3.11. The peak assignments were made using the following strategies; **(i)** comparison with the MMA homopolymer spectrum, **(ii)** comparison of the observed masses with those theoretically calculated.

The polymer chains were cationized with potassium, therefore were detected at a m/z value 39 Daltons above the theoretically calculated mass. All the polymer chains were assigned to various chemical compositions, constituting of varying MMA (M) and 1-octene (O) units. Interestingly, all copolymer chains can be divided into having three pairs of end groups (E1, E2, E3) [Fig. 3.12].

Usually, the detected signals, after subtraction of the mass of the cationization reagent, should be in agreement with the expected masses of the copolymer chains, which can be calculated according to Equation I. End group E1 was assigned to equation I.

$$M_{copo} = 155.19 + [(m \times 100.12) + (n \times 112.21)] + 35.45 \qquad (I)$$

where, 155.19 and 35.45 are the average masses of the end groups from the initiator fragment and the chloride respectively (since pTsCl was used as the ATRP initiator), 100.12 and 112.21 are the average masses of the MMA and 1-Octene repeating units, respectively, and m and n the numbers of the monomers in the chain.

In MALDI-TOF-MS, during ionization (in the employed range of laser intensity) it is observed that some of the terminal halide fragments. Other groups have also reported the loss of the halide during MALDI-TOF-MS analysis.[26] Recently, it was reported that during MALDI-TOF-MS of PMMA synthesized by ATRP, a dissociation reaction occurred to form $CH_3Br$, followed by cyclization of the terminal two repeat units of the polymer chain, giving rise to a lactone end group.[27]

End group E2 arises due to the loss of the terminal halide. To explain end group E2, Equation II can be employed, which is a slight modification to equation I. The difference between the two equations is, that Eq-I accounts for the Cl at the chain end and Eq-II does not.

$$M_{copo} = 155.19 + [(m \times 100.12) + (n \times 112.21)] \qquad (II)$$

where, 155.19 is the average mass of the end group from the initiator fragment, 100.12 and 112.21 are the average masses of the MMA and 1-Octene repeating units, respectively, and m and n the numbers of the monomers in the chain.

End groups E3 is assigned to the polymer chains having a lactone group on one end and the p-toluenesulphonyl initiator fragment on the other end (Equation III). The lactone end group, as explained, resulted from a loss of $CH_3Cl$ followed by cyclization of the terminal two repeat units of the polymer chain.

$$M_{copo} = 155.19 + [(m \times 100.12) + (n \times 112.21)] + 185.2 \qquad (III)$$

where, 155.19 and 185.2 are the average masses of the end groups from the initiator fragment and the lactone ring respectively, 100.12 and 112.21 are the average masses of the MMA and 1-Octene repeating units, respectively, and m and n the numbers of the monomers in the chain.

The important point from Figure 3.12 is that, 1-octene got incorporated into the polymer chain during the copolymerization.

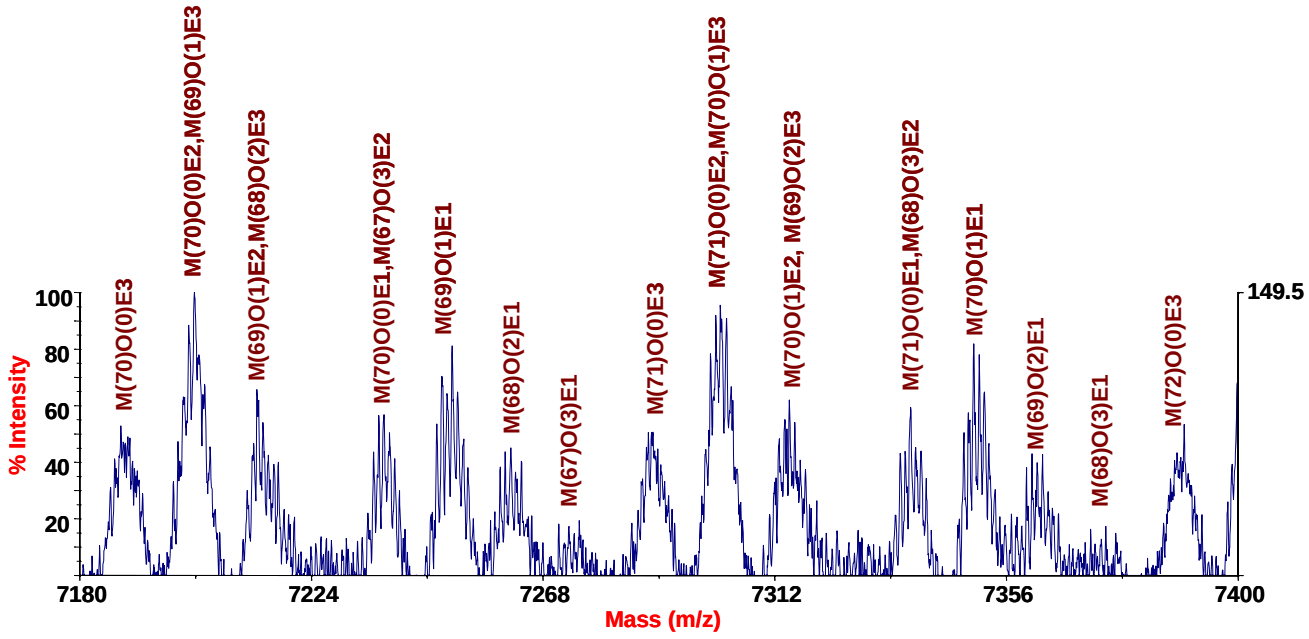


**Figure 3.12:** MALDI-TOF-MS spectrum for MMA/Oct copolymer (table 3.5, entry 2). [Spectrum acquired in the Reflector Mode, Matrix : DCTB (trans-2-[3-(4-tert-butylphenyl)-2-methyl-2-propenylidene]malononitrile)].

***3.4.5.2 DSC:*** DSC measurements were performed on the PMMA homopolymer (table 3.2, entry 2) and the poly[(MMA)]-co-(1-octene)] copolymer (table 3.4, entry 8). Now, since the molecular weight of the two polymers under consideration were similar, coupled with the fact that the end groups for the two polymers were the same (since the same initiator/catalyst system was employed for both the polymerizations), it was possible to compare the obtained glass transition temperatures ($T_g$). Now from literature,[28] the $T_g$ reported for the homopolymers of MMA and 1-octene was 100 ºC and – 41 ºC respectively. Since, the molecular weights of the polymers currently under consideration were much lower than those employed in literature, the $T_g$ values will

be lower. But, the important point is that if 1-octene gets incorporated into the polymer, the $T_g$ would be expected to be lower for the copolymer, as compared to that for the homopolymer of MMA. It is very clear from Figure 3.13 that the $T_g$ decreases by around 16 ºC for the copolymer. This was further evidence that the 1-octene got incorporated during the polymerization.

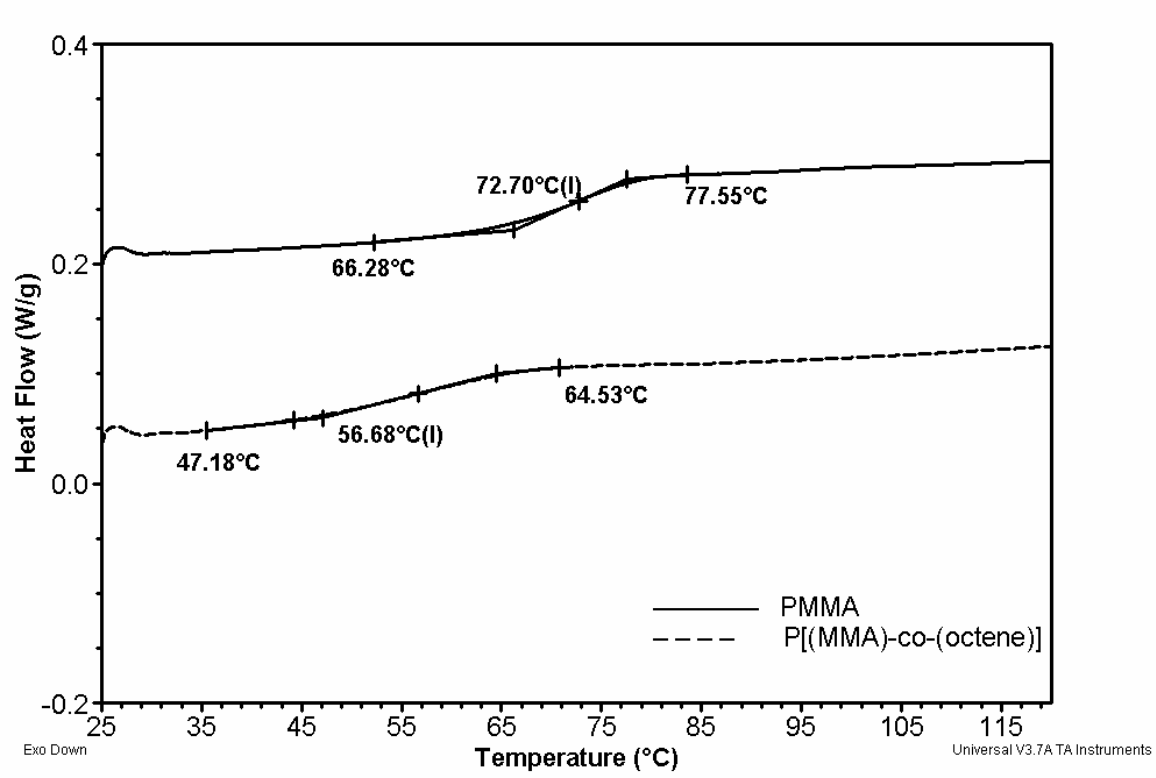


**Figure 3.13:** DSC curves comparing the difference in the obtained Tg for the homopolymer of PMMA and the copolymer of P[(MMA)-co-(1-Octene)].

## *3.5 Conclusions*

The atom transfer radical (co)polymerization (ATRP) of methyl methacrylate (MMA) with 1-octene was investigated. The importance of the initiator employed and the initiation mechanism in the presence of the olefin is highlighted. 2,2,2-Trichoroethanol (TCE) and p-toluenesulphonyl chloride (pTsCl) were efficient initiators due to higher initiation rates compared to the propagation rates. But, during copolymerization, uncontrolled polymerization occurred when pTsCl was

employed in the presence of higher mol% of 1-octene in the monomer feed. This could be explained by the difference in the initiation mechanism between TCE and pTsCl.

Well-controlled copolymers constituting of almost 20 mol% of 1-octene were obtained using TCE as initiator. Narrow molar mass distribution (MMD) was obtained in the ATRP experiments, which points at ordinary ATRP behavior, i.e. no peculiarities are caused by the incorporation of 1-octene**.** The comparable free radical (co)polymerizations (FRP) resulted in broad MMDs. An increased fraction of the olefin in the monomer feed, leads to an increased level of incorporation of the olefin in the copolymer, at the expense of the overall conversion.

The formation of the copolymer was established using the matrix assisted laser desorption / ionization – time of flight – mass spectrometry (MALDI-TOF-MS). Differential scanning calorimetry (DSC) was also employed to identify the difference in glass transition temperature ($T_g$) between the homopolymer of MMA and the formed copolymer. Evident from the MALDI-TOF-MS spectra was, that most polymer chains contained at least one 1-octene unit. The glass transition temperature of the copolymer was 16 ºC lower than that for the homopolymer of MMA of similar molar mass. Both results were clearly indicative of the fact that, 1-octene got incorporated into the polymer chains.

Block copolymer was synthesized using P[(MMA)-co-(1-octene)] as the macro-initiator and further characterized using gradient polymer elution chromatography (GPEC). The shift in the retention time between the macro-initiator and the formed block, clearly indicated the existence of the block copolymer structure, and also confirmed the high macro-initiator efficiency.

## *3.6 References*

References

1) Padwa, A. R.; *Prog. Polym. Sci.*, **1989**, *14*, 811.

2) *Functional Polymers: Modern Synthetic Methods and Novel Structures*; Patil, A. O.; Schulz, D.N.; Novak,B. M.; (Eds.); ACS Symposium Series 704; American Chemical Society: Washington, DC, **1998**.

3) Johnson, L. K.; Killian, C. M.; Brookhart, M.; *J. Am. Chem. Soc.*, **1995**, *117*, 6414. Killian, C. M.; Temple, D. J.; Johnson, L. K.; Brookhart, M.; *J. Am. Chem. Soc.*, **1996**, *118*, 11664.

4) Johnson, L. K.; Mecking, S.; Brookhart, M.; *J. Am. Chem. Soc.*, **1996**, *118*, 267. Mecking, S.; Johnson, L. K.; Wang, L.; Brookhart, M.; *J. Am. Chem. Soc.*, **1998**, *120*, 888.

5) Wang, C.; Friedrich, S.; Younkin, T. R.; Li, R. T.; Grubbs, R. H.; Bansleben, D. A.; Day, M. W.; *Organometallics*, **1998**, *17*, 3149.

6) Yasuda, H.; Furo, M.; Yamamoto, H.; *Macromolecules*, **1992**, *25*, 5115. Yasuda, H.; Ihara, E.; *Macromol. Chem. Phys.*, **1995**, *196 (8)*, 2417.

7) Ittel, S. D.; Johnson, L. K.; Brookhart, M.; *Chem. Rev.*, **2000**, *100*, 1169. Boffa, L. S.; Novak, B. M.; *Chem. Rev.*, **2000**, *100*, 1479.

8) Tian, G.; Boone, H. W.; Novak, B. M.; *Macromolecules*, **2001**, *34*, 7656.

9) Liu, S; Elyashiv, S.; Sen, A; *J. Am. Chem. Soc.*, **2001**, *123*, 12738.

10) *The Elements of Polymer Science and Engineering*; Rudin, A; 2nd Edition, Academic Press, **1999**, p 218.

11) Kato, M.; Kamigaito, M.; Sawamoto, M.; Higashimura, T.; *Macromolecules*, **1995**, *28*, 1721.

12) Wang, J. S.; Matyjaszewski, K.; *Macromolecules*, **1995**, *28*, 7901.

13) Beuermann, S.; Paquet, D. A., Jr.; McMinn, J. H.; Hutchinson, R. A.; *Macromolecules*, **1996**, *29*, 4206.

14) Snijder, A., Klumperman, B., van der Linde, R.; *Macromolecules*, **2002**, *35(12)*, 4785.

15) Percec, V., Barboiu, B.; *Macromolecules*, **1995**, *28*, 7970.

16) Destarac, M., Matyjaszewski, K., Boutevin, B.; *Macromol. Chem. Phys.*, **2000**, *201*, 265.

17) Matyjaszewski, K., Wang, J. L., Grimaud, T., Shipp, D. A.; *Macromolecules*, **1998**, *31*, 1527.

18) Mayo, F. R.; *J. Am. Chem. Soc.*; **1943**, *65*, 2324.

19) Moad, G., Moad, C. L.; *Macromolecules*, **1996**, *29*, 7727.

20) Heuts, J. P. A, Kukuj, D., Forster, D. J., Davis, T. P.; *Macromolecules*, **1998**, *31*, 2894.

21) Ueda, A., Nagai, S.; in *Polymer Handbook*, Brandrup, A., Immergut, E. H., Grulke, E. A., (Eds.), 4th Edition, John Wiley and Sons, New York (1999), Section II.

22) Unpublished results. Work done in collaboration with Kajiwara, A.

23) Percec, V., Barboiu, B., Kim, H.-J., *J. Am. Chem. Soc.*; **1998**, *120*, 305.

24) *Handbook of HPLC*, Katz, E., Eksteen, R., Schoenmakers, P., Miller, N., Marcel Dekker, New York, **1979**. Karanam, S., Goossens, H., Klumperman, B., Lemstra, P.; *Macromolecules*, **2003**, *36*, 3051.

25) Philipsen, H. J. A., De Cooker, M. R., Claessens, H. A., Klumperman, B., German, A. L.; *J. Chromatogr. A*, **1997**, *761*, 147.

26) Matyjaszewski, K, Nakagawa, Y., Jasieczeck C. B.; *Macromolecules*, **1998**, *31*, 1535. Coessens, V., Matyjaszewski, K.; *J. Macromol. Sci.- Pure Appl. Chem.*; **1999**, *A 36*, 653. Coessens, V., Matyjaszewski, K.; *J. Macromol. Sci.- Pure Appl. Chem.*; **1999**, *A 36*, 667.

27) Borman, C. D., Jackson, A. T., Bunn, A., Cutter, A. L., Irvine, D. J.; *Polymer*, **2000**, *41*, 6015.

28) Andrews, R. J., Grulke, E. A.; in *Polymer Handbook*, Brandrup, A., Immergut, E. H., Grulke, E. A., (Eds.), 4th Edition, John Wiley and Sons, New York (1999), Section VI.

# Chapter 4

## *Copolymerization of Acrylates and Methacrylates with 1-Octene using Reversible addition-fragmentation chain transfer (RAFT)*

**Abstract:** The RAFT copolymerizations of butyl acrylate (BA) and methyl methacrylate (MMA) with 1-octene were investigated. Well-controlled copolymers with 25 mol% incorporation of the olefin into the polymer chain were obtained. Narrow molar mass distributions (MMD) were obtained for the RAFT experiments. S,S'-Bis(α,α'-dimethyl-α''-acetic acid)trithiocarbonate and 2-cyanopropyl-2-yl dithiobenzoate were found to be the suitable RAFT agents for the BA/Octene and MMA/Octene RAFT copolymerizations respectively. The formation of the copolymer was established using matrix assisted laser desorption/ionization - time of flight - mass spectrometry (MALDI-TOF-MS), $^{13}C$ NMR and gradient polymer elution chromatography (GPEC). The fact that several units of octene were incorporated, clearly indicated that octene acts as a comonomer as opposed to a chain transfer agent. This was attributed, to the rapidity of the crosspropagation of octene-terminated polymeric radicals with the polar monomers.

## *4.1 Introduction*

Copolymers of α-olefins with polar monomers with various architectures are of great consequence in polymer chemistry. Since, of the many possibilities available for modifying the properties of polymers, the incorporation of functional groups into an otherwise nonpolar material is substantial.[1] It is known that α-olefins cannot be homopolymerized via a free radical mechanism. This is attributed to the fact that α-olefins undergo degradative chain transfer of allylic hydrogens.[2] The stable allylic radical derived from the monomer is slow to reinitiate and prone to terminate. On the other hand, polar vinyl monomers polymerize readily via a free radical mechanism. Copolymerization of methyl acrylate and α-olefin has been reported using metal-catalyzed insertion mechanism.[3] Catalyst systems showing excellent behavior for both olefins and polar monomers exist. However, true (random) copolymerization of these two types of monomer is difficult to achieve due to the very unfavorable reactivity ratios in conjunction with these catalyst systems. Recent developments were indicative of the fact that α-olefins maybe copolymerized with vinyl

Venkatesh, R., Staal, B. B. P., Klumperman, B.; submitted *Chem. Commun.*

monomers via a free radical technique.[4] But, polymers with broad molar mass distributions (MMDs) were obtained, as a result of chain transfer and termination events, which normally occur during free radical polymerization. The only other documented example has been the copolymerization of methyl acrylate with α-olefins using a copper-mediated polymerization technique.[5,6]

The chapter deals with the copolymerization of an acrylate (butyl acrylate, BA) with an α-olefin (1-octene), followed by the copolymerization of methyl methacrylate (MMA) also with an α-olefin (1-octene) using reversible addition-fragmentation chain transfer (RAFT) mediated polymerization. The RAFT process is a highly versatile controlled radical polymerization technique that can be applied to most monomers that can be polymerized under free radical conditions.[7,8,9,10,11] The RAFT process relies on the rapid central addition-fragmentation equilibrium between propagating and intermediate radicals, and chain activity and dormancy as shown in Scheme 4.1.

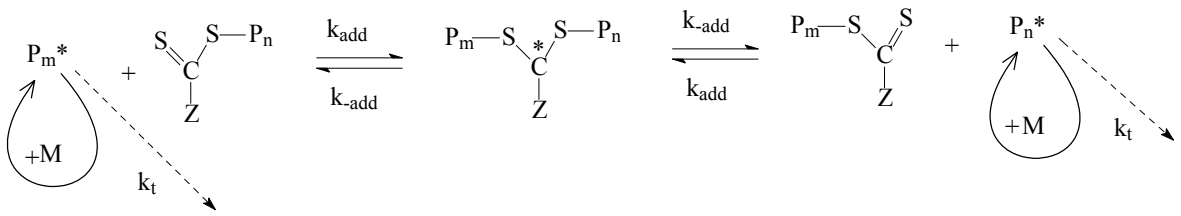


**Scheme 4.1**: The central RAFT equilibrium

Well controlled RAFT homopolymerizations of PBA and PMMA have been reported using the employed RAFT agents.[12,13,14] Now, due to MMA's low homopropagation rate coefficient ($k_p$), and since the α-olefins undergo degradative chain transfer of allylic hydrogens, the copolymerization reaction was highly unlikely. Further, to initiate the RAFT reactions, a normal free radical thermal initiator (like α,α'-azobisisobutyronitrile, AIBN) was employed, hence there was a large probability that the copolymerization if occurring, may not be controlled, since as previously stated, chain transfer and termination events dominate during free radical polymerization. But, in spite of the challenges posed, copolymers of the polar monomers with 1-octene with narrow MMD were obtained. Another advantage, which the RAFT technique offers, is that the polymer can be used directly without any cumbersome purification steps.

## *4.2 Experimental Section*

### *4.2.1 Materials*

Methyl methacrylate (MMA, Merck, 99+%), butyl acrylate (BA, Merck, 99+%) and 1-octene (Aldrich, 98%) were distilled and stored over molecular sieves at –15 ºC. *p*-Xylene (Aldrich, 99+% HPLC grade) and methyl ethyl ketone (Aldrich, 99+% HPLC grade) were stored over molecular sieves and used without further purification. The RAFT agents, S,S'-Bis(α,α'-dimethyl-α''-acetic acid)trithiocarbonate[12] and 2-cyanopropyl-2-yl dithiobenzoate[11] were synthesized as described in literature. Tetrahydrofuran (THF, Aldrich, AR), was used as supplied. α,α'-Azobisisobutyronitrile (AIBN, Merck, >98%) was recrystallized twice from methanol before use. 2,2'-Azobis(2,4- dimethylvaleronitrile) (V-65, Wako, >99%) was used as received.

### *4.2.2 Analysis and Measurements*

***4.2.2.1 Determination of Conversion and MMD***: Monomer conversion was determined from the concentration of the residual monomer measured via gas chromatography (GC). A Hewlett-Packard (HP-5890) GC, equipped with a HP Ultra 2 cross-linked 5% Me-Ph-Si column (25 m × 0.32 mm × 0.52 μm) was used. *p*-Xylene was employed as the internal reference. The GC temperature gradient used is given in Figure 4.1.

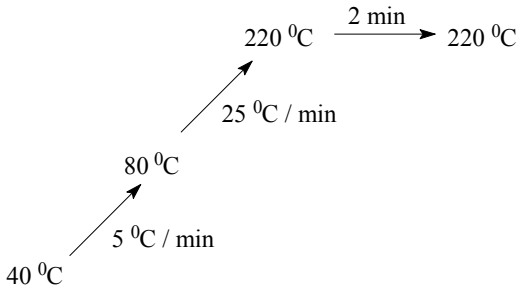


**Figure 4.1:** GC temperature gradient.

Molar mass (MM) and molar mass distributions (MMD) were measured by size exclusion chromatography (SEC), at ambient temperature using a Waters GPC equipped with a Waters model 510 pump, a model 410 differential refractometer (40 ºC), a Waters WISP 712 autoinjector (50 μL injection volume), a PL gel (5 μm particles) 50 × 7.5 mm guard column and a set of two mixed bed

columns (Mixed-C, Polymer Laboratories, 300 × 7.5 mm, 5 μm bead size, 40 ºC) . THF was used as the eluent at a flow rate of 1.0 mL/min. A set of two linear columns (Mixed-C, Polymer Laboratories, 30 cm, 40 ºC) was used. Calibration was carried out using narrow MMD polystyrene (PS) standards ranging from 580 to $7 \times 10^6$ g/mol. The molecular weights were calculated using the universal calibration principle and Mark-Houwink parameters[15] [PMMA: $K = 9.55 \times 10^{-5}$ dL/g, a = 0.719; PBA: $K = 1.22 \times 10^{-4}$ dL/g, a = 0.700; PS: $K = 1.14 \times 10^{-4}$ dL/g, a = 0.716]. Molecular weights were calculated relative to the relevant homopolymer (in this case PBA or PMMA). Data acquisition and processing were performed using Waters Millenium 32 software.

***4.2.2.2 GPEC Analysis:*** GPEC measurements were carried out on an Alliance Waters 2690 separation module with a Waters 2487 dual λ absorbance detector and a PL-EMD 960 ELSD detector (nitrogen flow 5.0 L/min, temperature 70 ºC). A Nova-Pak Cyano-Propyl (CN HP) 4 μm column (3.9 mm × 150 mm, 60 Å, Waters) was used at 40 ºC. The gradient employed is detailed in Table 4.1. The column was reset at the end of the gradient to initial conditions between 25 and 30 mins. HPLC grade solvents were obtained from BioSolve. A Varian 9010 solvent delivery system was used to maintain a stable flow rate of the eluents. Dilute polymer solutions were made in THF (10 mg/mL) and a sample of 10 μL was used for analysis. Chromatograms were analyzed using the Millennium 32 software version 3.05.

**Table 4.1:** Linear Ternary gradient used for GPEC

| Step | Time (min) | $\Phi_{water}$ | $\Phi_{acetonitrile}$ | $\Phi_{THF}$ | Flow (ml/min) |
|---|---|---|---|---|---|
| 1 | Initial | 0.4 | 0.6 | 0 | 0.5 |
| 2 | 20 | 0 | 1 | 0 | 0.5 |
| 3 | 25 | 0 | 0 | 1 | 0.5 |
| 4 | 30 | 0.4 | 0.6 | 0 | 0.5 |

The eluent compositions are given in volume fraction (Φ).

***4.2.2.3 MALDI-TOF-MS:*** Measurements were performed on a Voyager-DE STR (Applied Biosystems, Framingham, MA) instrument equipped with a 337 nm nitrogen laser. Positive-ion spectra were acquired in reflector mode. DCTB (trans-2-[3-(4-tert-butylphenyl)-2-methyl-2-propenylidene]malononitrile) was chosen as the matrix. Sodium trifluoracetate (Aldrich, 98%) was added as the cationic ionization agent. The matrix was dissolved in THF at a

concentration of 40 mg/mL. Sodium trifluoracetate was added to THF at a concentration of 1 mg/mL. The dissolved polymer concentration in THF was approximately 1 mg/mL. In a typical MALDI-TOF-MS experiment, the matrix, salt and polymer solutions were premixed in the ratio: 5 μL sample: 5 μL matrix: 0.5 μL Salt. Approximately 0.5 μL of the obtained mixture was hand spotted on the target plate. For each spectrum 1000 laser shots were accumulated.

***4.2.2.4 NMR:*** $^{13}C$ nuclear magnetic resonance (NMR) spectra were recorded on a Varian 400 spectrometer, in deuterated chloroform ($CDCl_3$) at 25 ºC. All chemical shifts are reported in ppm downfield from tetramethylsilane (TMS), used as an internal standard (δ=0 ppm).

### *4.2.3 Choice of RAFT agent*

S,S'-Bis(α,α'-dimethyl-α''-acetic acid)trithiocarbonate was chosen for its high chain transfer efficiency in radical polymerization,[12] and it is known from literature that well controlled PBA can be synthesized using the isobutyric acid group as the initiating species.[12]

2-cyanopropyl-2-yl dithiobenzoate was employed because it is known from literature to yield well controlled PMMA, resulting from its high chain transfer coefficient coupled with the fact that the cyanoisopropyl group is a good initiating species for MMA polymerization.[11]

## *4.3 Synthetic Procedures*

***4.3.1 RAFT copolymerization:*** A typical copolymerization of BA and 1-octene was carried out as follows: The RAFT agent (0.11 g; 0.4 mmol) and AIBN (0.003 g; 0.02 mmol) were accurately weighed and then transferred to a 25 mL three-neck round-bottom flask. Then a solution of *p*-xylene (3.83 g; 0.03 mol), butyl acrylate (0.94 g; 7.3 mmol) and 1-octene (0.82 g; 0.7.3 mmol) were added. Methyl ethyl ketone (3.22 g; 0.04 mol) was added to totally solubilize the RAFT and make the system homogeneous. After the reaction mixture was bubbled with argon for 30 min, the flask was immersed in a thermostated oil bath maintained at 80 ºC. The reaction was carried out under a flowing argon atmosphere. The initiator AIBN (0.003 g; 0.02 mmol) was added at three pre-determined time intervals during the copolymerization. Samples were withdrawn at suitable time periods throughout the polymerization. The sample was immediately diluted with THF. Some of this diluted sample was transferred immediately into a GC vial and further diluted

with THF, so as to determine the monomer conversion using GC. The remaining sample was used for SEC and MALDI-TOF-MS measurements.

## *4.4 Results and Discussion*

***4.4.1 RAFT copolymerization:*** Conventional free radical copolymerizations (FRP) and RAFT copolymerizations of BA and 1-octene (Oct) were examined as summarized in Table 4.2. Table 4.3 shows the results for the MMA and 1-octene copolymers.

From the data in table 4.2 and 4.3, the following observations can be made; **(i)** a significant fraction of 1-octene was incorporated during the RAFT experiments. **(ii)** Narrow MMDs were obtained for the RAFT reactions, which implied that no peculiarities were caused by the incorporation of the 1-octene. **(iii)** The experimentally determined molar masses ($M_n$) coincided well with the theoretically calculated $M_n$ values for the RAFT systems. The almost linear increase of $M_n$ as a function of monomer conversion is indicative of the fact, that there are a constant number of growing chains during the polymerization (Figure 4.2 and 4.4). In figure 4.3, the development of MMD with reaction time is shown. The shift towards the high molar mass is clearly observed. This further testifies the living character. **(iv)** When the mol% of the olefin was increased in the monomer feed, its incorporation was higher in the copolymer, but the overall conversion decreased (Figure 4.5 and 4.6). **(v)** Comparable FRP reactions, resulted in polymers with broad MMDs.

**Table 4.2:** Copolymers of BA/1-Octene

| Entry | BA (mol%) | Octene (mol%) | Overall Conv. (%) [d] | 1-octene incorp. (mol%) [d] | $M_n$ (g/mol) | PDI |
|---|---|---|---|---|---|---|
| 1 [*,a] | 75 | 25 | 70.0 | 8.4 | $2.8 \times 10^3$ | 1.3 |
| 2 [*,b] | 50 | 50 | 53.0 | 22.0 | $2.4 \times 10^3$ | 1.3 |
| 3 [#,c] | 75 | 25 | 73.0 | 7.2 | $6.6 \times 10^3$ | 2.9 |
| 4 [#,c] | 50 | 50 | 52.0 | 16.4 | $5.2 \times 10^3$ | 2.4 |

[*] - RAFT reactions, [#] - Free radical polymerization (FRP). *Solvents for the copolymerizations* – Mixture of methyl ethyl ketone (MEK) and *p*-xylene in 1:1 volume ratio. Volume of {monomer}/{solvent} = 0.25 / 1. Reaction temperature = 80 ºC. *RAFT copolymerizations* - [Monomer] : [S,S'-Bis(α,α'-dimethyl-α''-acetic acid)trithiocarbonate][12] : [AIBN] = 36.8 : 1 : 0.18. ***a*** – Reaction time = 10 hrs. ***b*** – Reaction time = 11 hrs. 30 mins. *FRP copolymerizations* – α,α'-azobisisobutyronitrile, AIBN (10 mmol/L). ***c*** – Reaction time = 11 hrs.

***d*** – Calculated from values, obtained from gas chromatography (GC) measurements.

**Table 4.3:** Copolymers of MMA/1-Octene

| Entry | MMA (mol%) | Octene (mol%) | Overall Conv. (%) [a] | 1-octene incorp. (mol%) [a] | $M_n$ (g/mol) | PDI |
|---|---|---|---|---|---|---|
| 1 * | 75 | 25 | 55.0 | 8.6 | $2.9 \times 10^3$ | 1.3 |
| 2 * | 50 | 50 | 44.0 | 20.0 | $1.7 \times 10^3$ | 1.3 |
| 3 # | 75 | 25 | 73.4 | 6.4 | $1.8 \times 10^4$ | 3.1 |
| 4 # | 50 | 50 | 57.5 | 16.2 | $1.0 \times 10^4$ | 4.2 |

* - RAFT reactions, # - Free radical polymerization (FRP). *Solvent for the copolymerizations – p*-xylene.

*RAFT copolymerizations* - [Monomer] : [2-cyanopropyl-2-yl dithiobenzoate][11]: [V-65, 2,2'-Azobis(2,4-dimethylvaleronitrile)] = 47.6 : 1: 0.125. Volume of {monomer}/{solvent} = 1 / 0.5. Reaction temperature = 50 °C. Reaction time = 20 hrs.

*FRP copolymerizations* – α,α'-Azobisiosbutyronitrile, AIBN (10 mmol/L). Volume of {monomer}/{solvent} = 0.5 / 1. Reaction temperature = 90 °C. Reaction time = 25 hrs.

***a*** – Calculated from values, obtained from gas chromatography (GC) measurements.

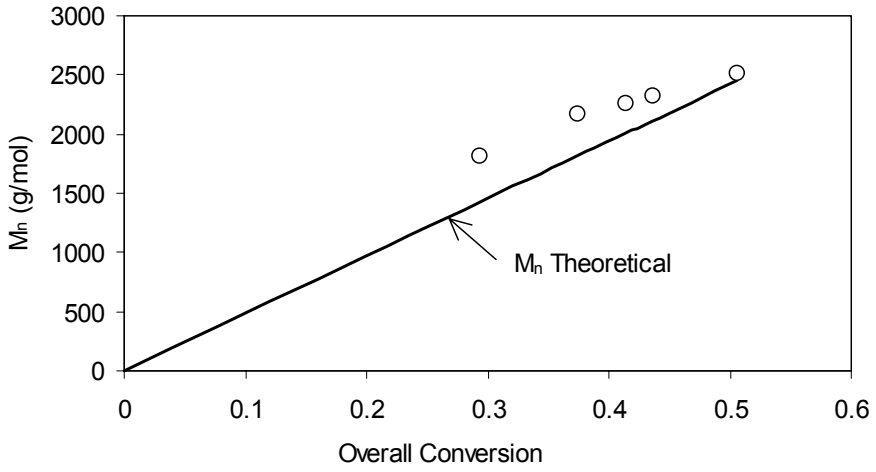


**Figure 4.2:** Plot of molar mass ($M_n$) *vs* overall conversion for the RAFT mediated copolymerization of BA and 1-Octene ($f_{Octene}$ = 0.25). Reaction temperature = 80 °C. [Monomer] **:** [S,S'-Bis(α,α'-dimethyl-α''-acetic acid)trithiocarbonate] **:** [AIBN] = 36.8**:**1**:**0.05.

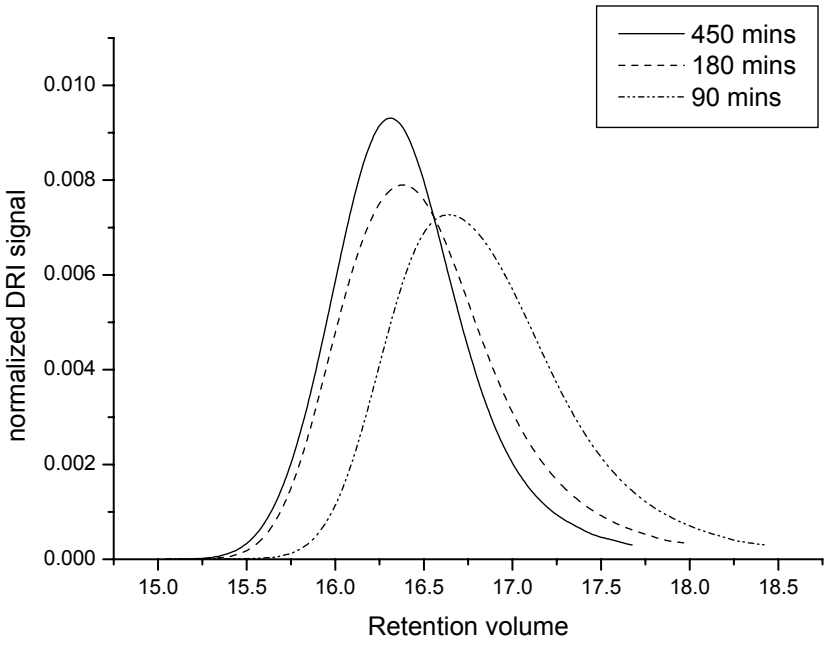


**Figure 4.3:** Development of MMD in the RAFT mediated copolymerization of BA and 1-Octene ($f_{oct}$ = 0.25). Reaction temperature = 80 °C. [Monomer]**:**[S,S'-Bis(α,α'-dimethyl-α''-acetic acid)trithiocarbonate]**:**[AIBN] = 36.8**:**1**:**0.05.

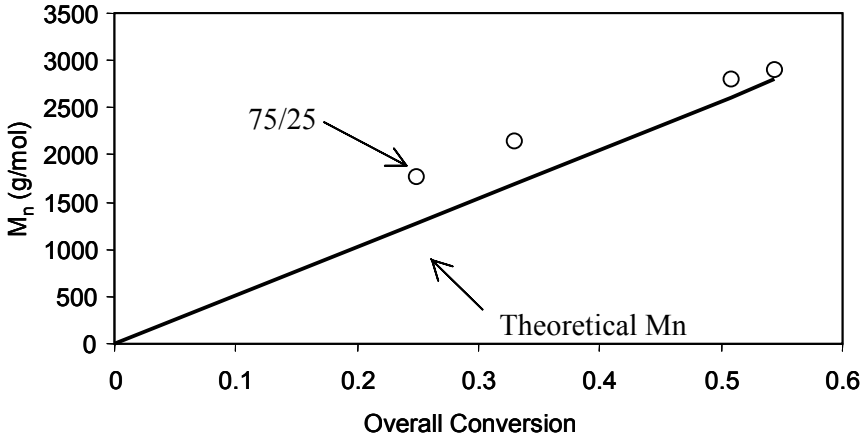


**Figure 4.4:** Plot of molar mass ($M_n$) *vs* overall conversion for the RAFT mediated copolymerization of MMA and 1-Octene ($f_{Octene}$ = 0.25). Reaction temperature = 50 °C. [Monomer]**:**[2-cyanopropyl-2-yl dithiobenzoate]**:**[V-65] = 47.6**:**1**:**0.125.

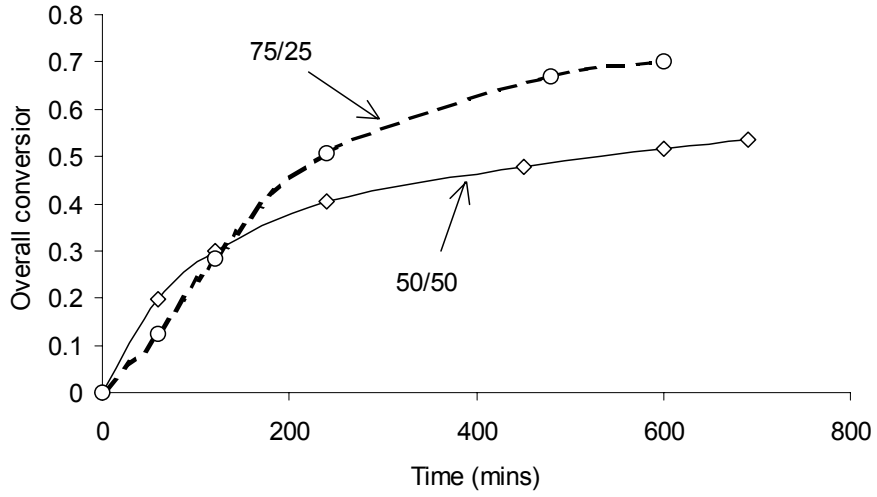


**Figure 4.5:** Plot of overall conversion *vs* time for the RAFT mediated copolymerization of BA and 1-Octene. For 75/25, $f_{Octene}$ = 0.25 and for 50/50, $f_{Octene}$ = 0.50. Reaction temperature = 80 °C. [Monomer]**:**[S,S'-Bis(α,α'-dimethyl-α''-acetic acid)trithiocarbonate]**:**[AIBN] = 36.8**:**1**:**0.18.

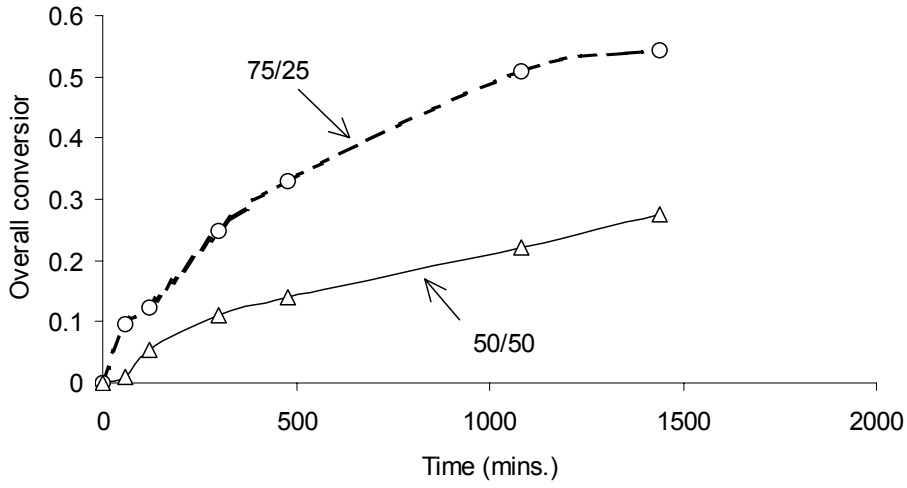


**Figure 4.6:** Plot of overall conversion *vs* time for the RAFT mediated copolymerization of MMA and 1-Octene. For 75/25, $f_{Octene}$ = 0.25 and for 50/50, $f_{Octene}$ = 0.50. Reaction temperature = 50 °C. [Monomer]**:**[2-cyanopropyl-2-yl dithiobenzoate]**:** [V-65 (2,2'-azobis(2,4- dimethylvaleronitrile))] = 47.6**:**1**:**0.125.

### *4.4.2 Copolymer Characterization:*

The formation of real copolymers was shown using matrix assisted laser desorption-ionization time-of-flight mass spectrometry (MALDI-TOF-MS) and $^{13}C$ NMR spectroscopy. Reverse phase gradient polymer elution chromatography (GPEC) with water and acetonitrile as eluent was employed for selective separation based on chemical composition.

#### *4.4.2.1 Copolymers of BA/Octene:*

Figure 4.7 is the MALDI-TOF-MS spectrum of a BA/Octene copolymer. Figure 4.8 is an expansion of a selected portion from the MALDI-TOF-MS spectrum in figure 4.7. The polymer chains were all cationized with sodium. All the polymer chains were assigned to various chemical compositions, constituting of varying BA (B) and 1-octene (O) units. All copolymer chains can be divided into having four pairs of end groups. The peak assignments of Figure 4.8, described in Table 4.4 are made using the following strategies; **(1)** comparison of the experimental and the theoretically calculated masses, **(2)** comparison of the theoretical isotopic distribution with the observed distributions.

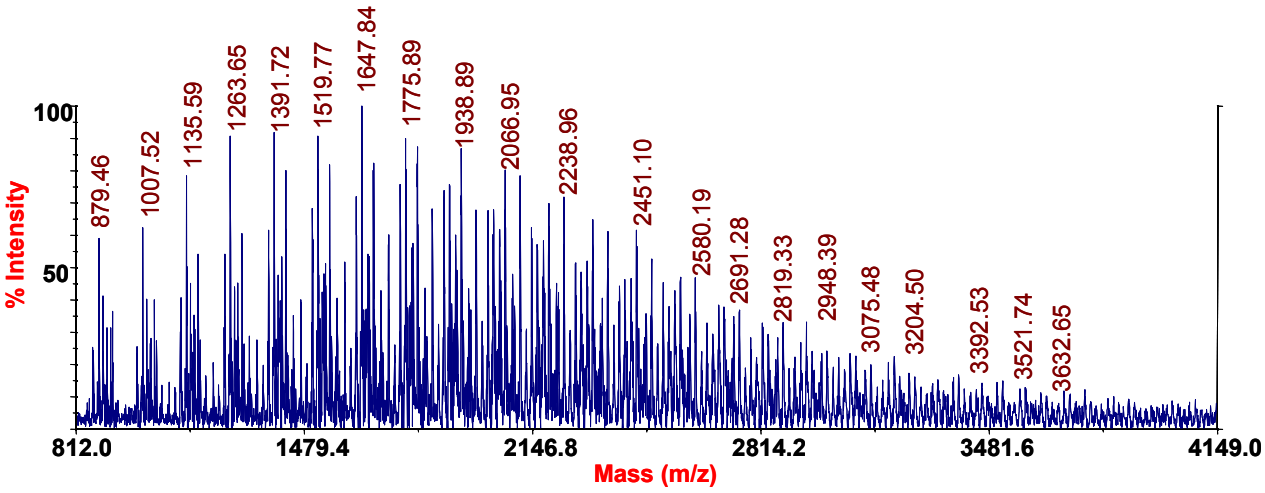


**Figure 4.7:** MALDI-TOF-MS spectrum for the BA/Octene copolymer synthesized using RAFT ($f_{Octene}$ = 0.5. $F_{Octene}$ = 0.22). [Reflector mode; Matrix - DCTB (trans-2-[3-(4-tert-butylphenyl)-2-methyl-2-propenylidene]malononitrile)].

During the RAFT copolymerization, the polymeric chains can propagate in both directions, since, S,S'-Bis(α,α'-dimethyl-α''-acetic acid)trithiocarbonate is a bifunctional RAFT agent, resulting in end group E1 as shown in Figure 4.9(a). The end group pairs E2 and E3

originated as a result of the exchange reaction between the proton of the COOH group and a sodium cation during MALDI-TOF-MS analysis. In the case of end group pair E2**,** only one proton was exchanged for the sodium and for end group pair E3 both protons were exchanged. Hence, for copolymer chains having identical chemical compositions, the copolymer chains with end groups E2 and E3 are detected at higher masses differing by 22 Daltons and 44 Daltons respectively, as compared to chains having E1 as the end group. The initiator AIBN is added at pre-determined time intervals during the copolymerization so as to generate radicals and keep the RAFT polymerization process active. Hence, some chains can be initiated by the primary cyanoisopropyl radical. The structure for end group pair E4 represents a case wherein one of the end groups is the AIBN fragment [Figure 4.9(b)]. In Figure 4.10 a comparison is made between the observed mass distributions and the theoretical isotopic mass distribution.

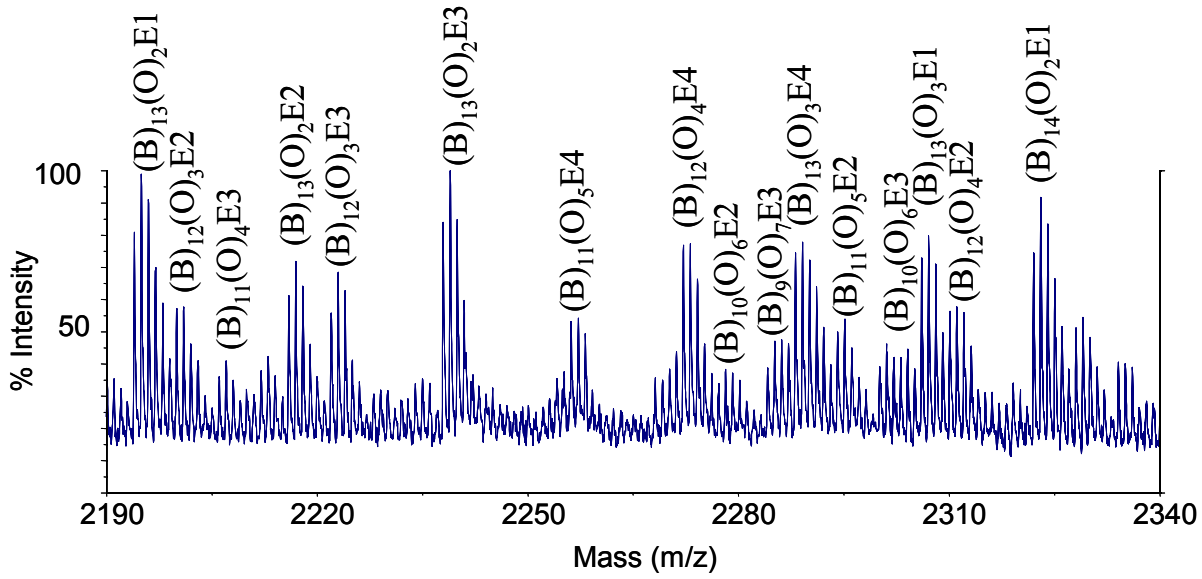


**Figure 4.8:** Expansion of the MALDI-TOF-MS spectrum for the BA/Octene copolymer synthesized using RAFT ($f_{Octene}$ = 0.5. $F_{Octene}$ = 0.22). [Reflector mode; Matrix - DCTB (trans-2-[3-(4-tert-butylphenyl)-2-methyl-2-propenylidene]malononitrile)].

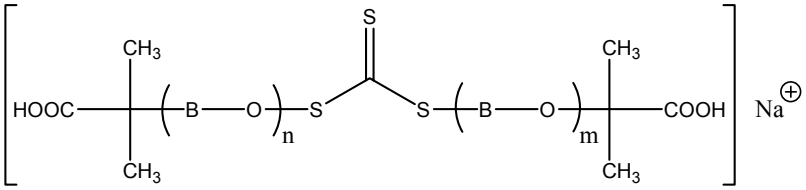


**(a) E1**

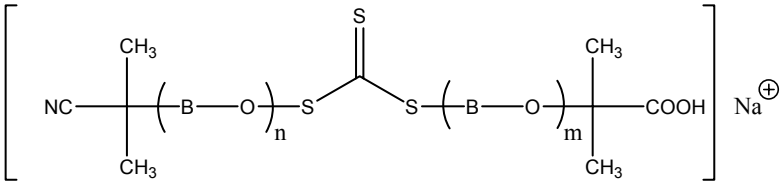


**(b) E4**

**Figure 4.9:** The end group pairs E1 and E4 observed during MALDI-TOF-MS analysis of the BA/Octene copolymers. B and O are the abbreviations for butyl acrylate and 1-octene respectively.

**Table 4.4:** Peak assignment of the MALDI-TOF-MS spectrum shown in Figure 4.8

| Peak | BA units | Octene units | Observed Mass (Da) | Theoretical Mass (Da) | $Na^+$ |
|---|---|---|---|---|---|
| $B_{13}O_2E1$ | 13 | 2 | 2195.0061 | 2195.3369 | 1 |
| $B_{13}O_2E2$ | 13 | 2 | 2216.9749 | 2017.3188 | 2 |
| $B_{13}O_2E3$ | 13 | 2 | 2238.9600 | 2039.3008 | 3 |
| $B_{11}O_5E4$ | 11 | 5 | 2257.1845 | 2257.2921 | 1 |

*It is evident from the MALDI-TOF-MS spectrum that several units of 1-octene were incorporated within the polymer chain.* This clearly proves that octene behaves as a comonomer during the polymerization. The understanding for the successful copolymerization in the RAFT systems, can be attributed to the reactivity of the octene radical during the copolymerization. It is likely that for propagating radicals with a terminal 1-octene unit, the time constant for crosspropagation is smaller than that for $k_{add}$ (Scheme 4.1). In other words, chains with a 1-octene terminal unit exclusively undergo crosspropagation. This behaviour is in the same lines as that observed for the copolymerization of MA/Octene using ATRP, described in Chapter 2.

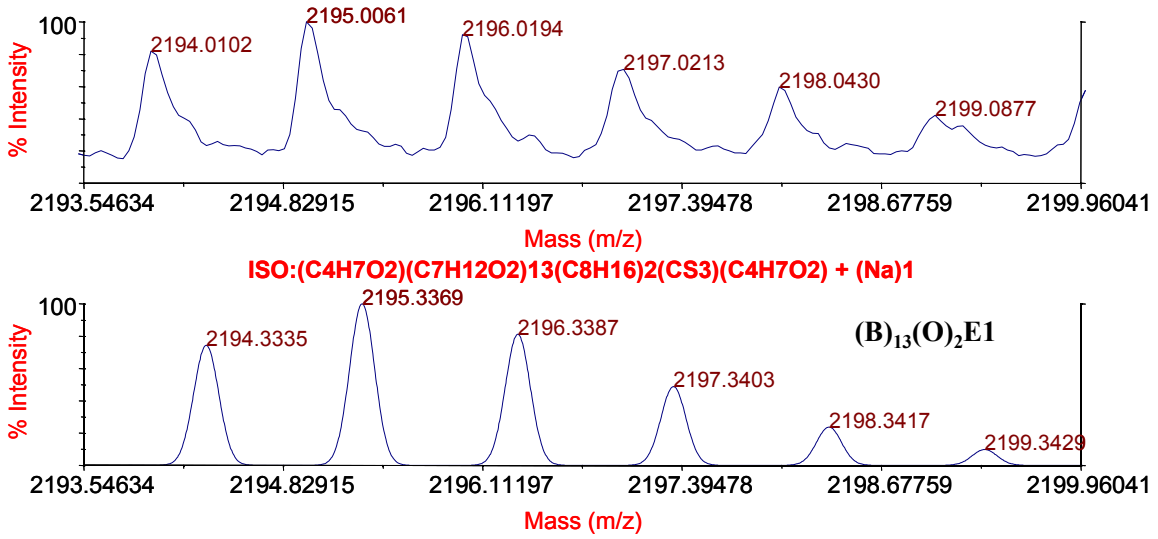


**Figure 4.10:** Detail of the MALDI-TOF-MS spectrum for the BA/Octene copolymer synthesized using RAFT. $f_{Octene}$ = 0.50, $F_{Octene}$ = 0.22. Isotopic mass distributions : observed (above) and theoretical (below), for a polymer chain having end group **E1** and having 13 monomeric units of butyl acrylate (B) and 2 monomeric units of octene(O).

In the $^{13}C$ NMR spectrum for BA/1-octene copolymer, two signals are observed in the carbonyl region (δ 174.5 and 175.9 ppm) [Figure 4.11]. The peak at δ 174.5 ppm, is assigned to the carbonyl carbon present in long BA runs. The peak at δ 175.9 ppm is assigned to a BA carbonyl adjacent to an octene unit. The current assignments are based on a publication, wherein a $^{13}C$ NMR spectrum of methyl acrylate/α-olefin was assigned.[4(a)] The presence of this peak also provides further evidence that the octene has been incorporated into the same polymer chains as BA. The signal to noise ratio for the spectrum can be vastly improved by increasing the polymer solution concentration and the number of scans.

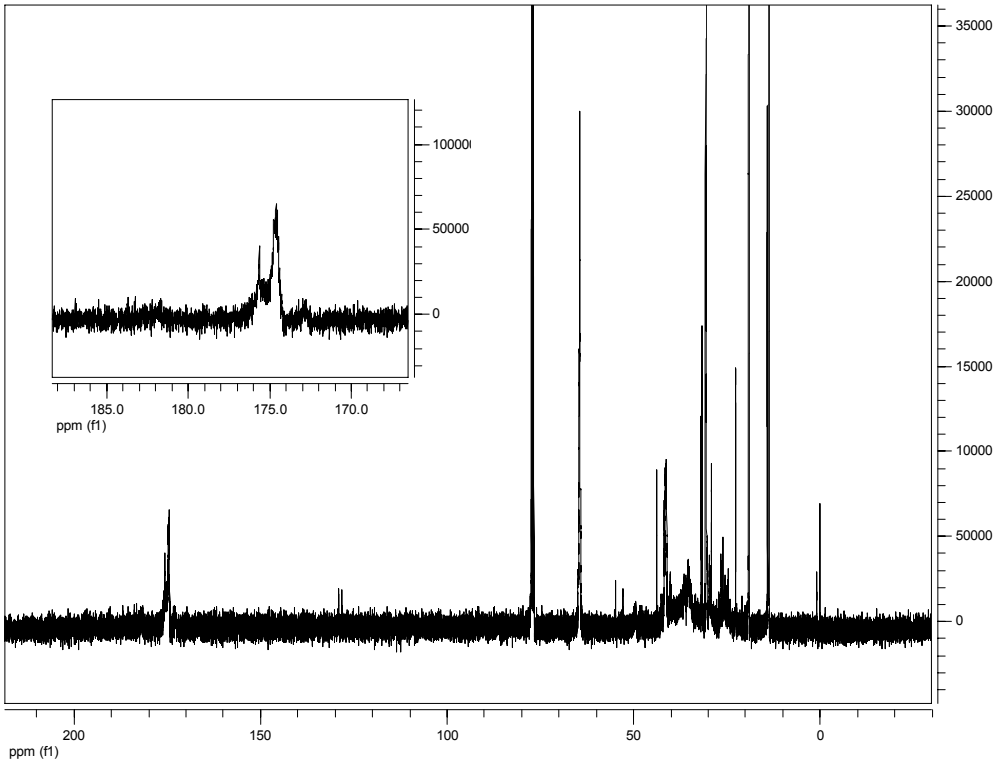


**Figure 4.11:** $^{13}C$ NMR spectrum for a P[(BA)-co-(Octene)] synthesized using RAFT in $CDCl_3$ recorded under fast pulse conditions. ($f_{Octene}$ = 0.5, $F_{Octene}$ = 0.22). $M_n$ = $2.4 \times 10^3$ g/mol, PDI = 1.3.

***4.4.2.2 Copolymers of MMA/Octene:*** The difference in the chemical composition between PMMA homopolymer and the copolymer of P(MMA-co-Octene) was demonstrated by using GPEC. In GPEC, separation of the polymers is based on differences in column interactions, as in the case of isocratic chromatography, but also depends on precipitation and redissolution mechanisms as the eluent composition changes gradually in time. Hence, it is possible to separate polymers depending on molar mass, chemical composition and chain(-end) functionality. The GPEC trace in figure 4.12 clearly indicates well-resolved peaks from the homopolymer of MMA and the copolymer of MMA and 1-octene, wherein 8.6 mol% of octene was incorporated. The molecular weights and the end groups are almost identical for both polymers, hence a clear unbiased comparison was possible. The difference in the elution behavior was a direct indication of a chemical composition difference between the homopolymer and the copolymer.

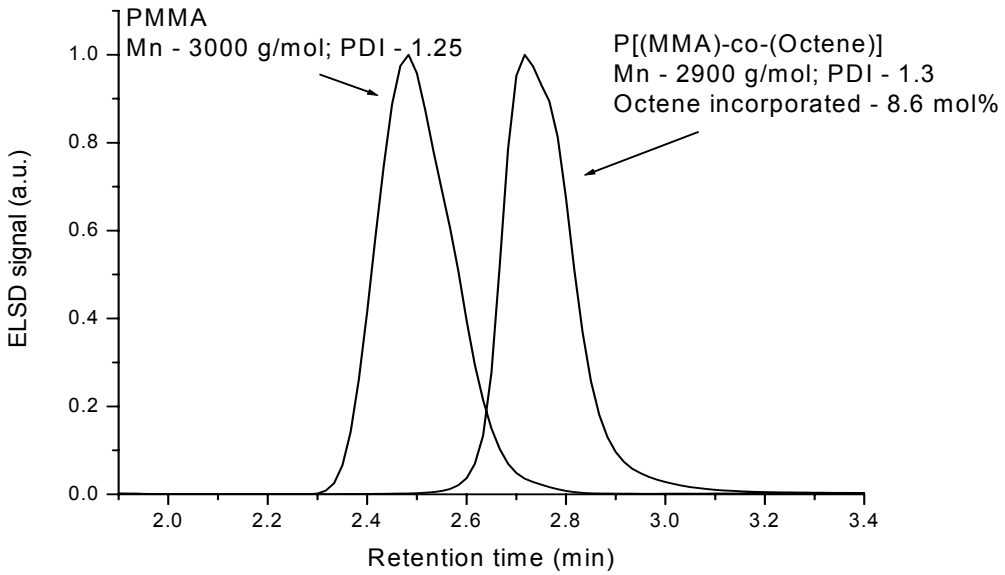


**Figure 4.12:** GPEC traces of PMMA and of P[(MMA)-co-(1-Octene)]. Eluent = Water/acetonitrile (40/60 to 0/100 in 20 mins). CN-modified Si-column.

## *4.5 Conclusion*

The RAFT copolymerizations of BA and MMA with 1-octene were investigated. Well-controlled copolymers with 25 mol% incorporation of the olefin into the polymer chain were obtained. Narrow MMDs were obtained for the RAFT experiments, which suggested normal RAFT behavior, with no peculiarities caused by the incorporation of the olefin. S,S'-Bis(α,α'-dimethyl-α''-acetic acid)trithiocarbonate and 2-cyanopropyl-2-yl dithiobenzoate were found to be the suitable RAFT agents for the BA/Octene and MMA/Octene RAFT copolymerizations respectively.

The formation of the copolymer was established using MALDI-TOF-MS, $^{13}C$ NMR and GPEC. The fact that several units of octene were incorporated, clearly indicates that octene acts as a comonomer, as opposed to a chain transfer agent. This was attributed, to the rapidity of the crosspropagation of octene-terminated polymeric radicals with the polar monomer.

## *4.6 References*


1) Padwa, A. R.; *Prog. Polym. Sci.*, **1989**, *14*, 811.

2) *The Elements of Polymer Science and Engineering*; Rudin, A; 2nd Edition, Academic Press, **1999**, p 218.

3) Ittel, S. D., Johnson, L. K., Brookhart, M.; *Chem. Rev.*, **2000**, *100*, 1169. Wang, C.; Friedrich, S.; Younkin, T. R.; Li, R. T.; Grubbs, R. H.; Bansleben, D. A.; Day, M. W.; *Organometallics*, **1998**, *17*, 3149. Yasuda, H.; *Prog. Polym. Sci.,* **2000**, *25*, 573.

4) **(a)** Tian, G.; Boone, H. W.; Novak, B. M.; *Macromolecules*, **2001**, *34*, 7656. **(b)** Elyashiv, S.; Sen, A; *Polymer Preprints*, **2001,** *42(2)*, 423.

5) Liu, S; Elyashiv, S.; Sen, A; *J. Am. Chem. Soc.*, **2001**, *123*, 12738.

6) Venkatesh, R., Klumperman,B.; *Macromolecules*, **2004**, *37*, 1226.

7) Chiefari, J., Chong, Y. K., Ercole, F., Krstina, J., Jeffery, J., Le, T. P. T., Mayadunne, R. T. A., Meijs, G. F., Moad, C. L., Moad, G., Rizzardo, E., Thang, S. H.; *Macromolecules*, **1998**, *31*, 5559.

8) Donovan, M. S., Lowe, A. B., Sumerlin, B. S., McCormick, C. L.; *Macromolecules*, **2002**, *35*, 4123.

9) Barner-Kowollik, C., Davis, T., Heuts, J. P. A., Stenzel, M. H., Vana, P., Whittaker, M.; *J. Polym. Sci., Part A: Polym. Chem.*, **2002**, *41*, 365.

10) de Brouwer, H., Schellekens, M. A. J., Klumperman, B., Monteiro, M. J., German, A. L.; *J. Polym. Sci., Part A: Polym. Chem.*, **2000**, *38*, 3596.

11) Le, T. P., Moad, G., Rizzardo, E., Thang, S. H.; *PCT Int Appl*., **1998**, WO98/01478.

12) Lai, J. T., Filla, D., Shea, R.; *Macromolecules*, **2002**, *35*, 6754.

13) Moad, G., Chiefari, J., Chong, Y. K., Krstina, J., Mayadunne, R. T. A., Postma, A., Rizzardo, E., Thang, S. H.; *Polym. Int*., **2000**, *49*, 993.

14) Chong, Y. K., Krstina, J., Le, T. P. T., Moad, G., Postma, A., Rizzardo, E., Thang, S. H.; *Macromolecules*, **2003**, *36*, 2256.

15) Beuermann, S.; Paquet, D. A., Jr.; McMinn, J. H.; Hutchinson, R. A.; *Macromolecules*, **1996**, *29*, 4206.

# Chapter 5

## *Reversible addition-fragmentation chain transfer (RAFT):*

## *The fate of the Intermediate Radical*

**Abstract:** Electron spin resonance (ESR) spectroscopy was employed to determine the intermediate radical concentration for AIBN initiated and cumyl dithiobenzoate mediated butyl acrylate (BA) and styrene (Sty) polymerizations. It was determined that the intermediate radical concentration during the BA polymerization was an order of magnitude higher as compared to that for Sty. The reason was attributed to the faster fragmentation rate of the formed intermediate radicals in the Sty system. For the BA systems, the formed intermediate radicals were detected at long reaction times in the virtual absence of the initiator. A successful combination of SEC and MALDI-TOF-MS techniques was employed, to study and understand the termination reactions occurring (if any) during the RAFT process. First, the cumyl dithiobenzoate mediated BA polymerization was investigated, where products from the polymeric RAFT agent and polymeric chains initiated by the 2-cyanoisopropyl radical (derived from AIBN) were identified. Further, model reactions using the synthesized poly (butyl acrylate) [PBA-RAFT] with AIBN were performed. Interestingly, the intensity of the chains with the unassigned end group (E4) clearly increased. The clear increase in intensity reflects that, the unassigned peak most probably resulted due to termination reaction(s) occurring during the RAFT process. But, the preferred mode of termination still remained unanswered. So as to overcome the limitations of the AIBN system, *"the ATRP-way"* of creating radicals using model compounds was investigated. PBA-Br was chosen as the model compound. The MALDI-TOF-MS spectra for the fractionated polymer, clearly proved the formation of the 4 arm and 3 arm star polymers, which resulted from the termination of the BA intermediate radical formed during the RAFT process. More importantly, structures can be assigned to the terminated products. The intensities of the observed distributions decrease in the order of the end group cumyl (Cu) > ethyl isobutyryl (EiB) > 2-cyanoisopropyl (CiP). This work indicates that indeed the intermediate radicals formed during the cumyl dithiobenzoate mediated BA polymerization, resulted in stable and long living intermediate radicals. But at the same time, these intermediate radicals are also prone to termination, resulting in the formation of 3 and 4 arm star polymers. Thus, for the present system, a combination of the two events may contribute to the retardation, which is normally observed during RAFT polymerizations.

## *5.1 Introduction*

The RAFT process is a highly versatile controlled radical polymerisation technique that can be applied to most monomers, which can be polymerised under free radical conditions.[1] The RAFT

---

Manuscripts in preparation.

process relies on the rapid central addition-fragmentation equilibrium between propagating and intermediate radicals, and chain activity and dormancy as shown in Scheme 5.1(c).

Initiation

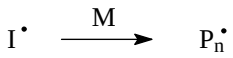


(a) Chain transfer

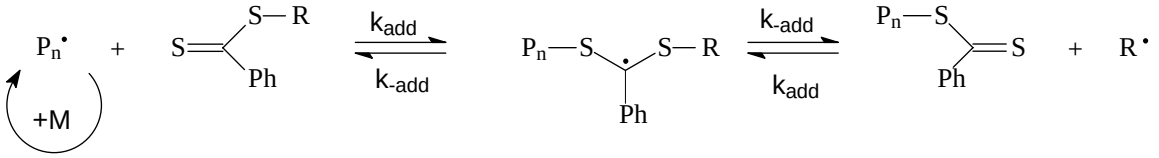


(b) Re-initiation and Propagation

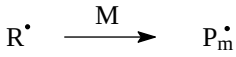


(c) Chain equilibrium

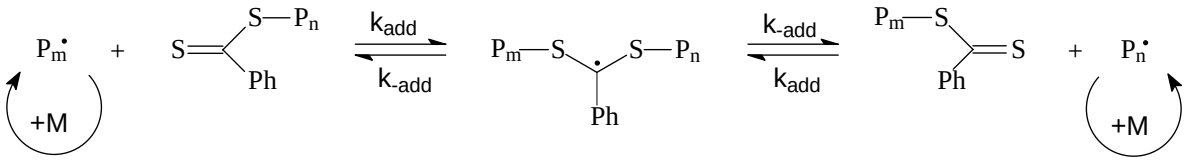


Termination

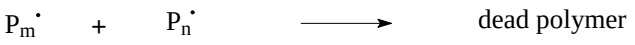


**Scheme 5.1**: Proposed mechanism for the RAFT process without intermediate radical termination.

As mentioned previously in the general introduction, research and debate are focused on the retardation phenomenon (implying, decrease in the rate of polymerization in the presence of the RAFT agent, as compared to a RAFT agent-free polymerization), which may occur at the initial stages of the RAFT polymerization (inhibition or initialization) or during the course of the RAFT polymerization (which is related to the fate of the formed intermediate radical). These effects have been explained by a number of factors in terms of the mechanism of the RAFT process;[2] **(i)** slow fragmentation of the adduct radical formed from addition to the original RAFT, **(ii)** slow re-initiation by the expelled radical, **(iii)** preference of the expelled radical to add to the RAFT agent as opposed to the monomer, **(iv)** formation of single monomer adduct RAFT species,[3] **(v)** slow

fragmentation of the polymeric intermediate radical,[4,5,6] **(vi)** preference of the expelled polymeric radical to add to the RAFT agent as opposed to the monomer, **(vii)** termination of the polymeric intermediate radical (see Scheme 5.2).[7,8,9,10]

**Cross-Termination**

3 arm star

**Self-Termination of Intermediate radicals**

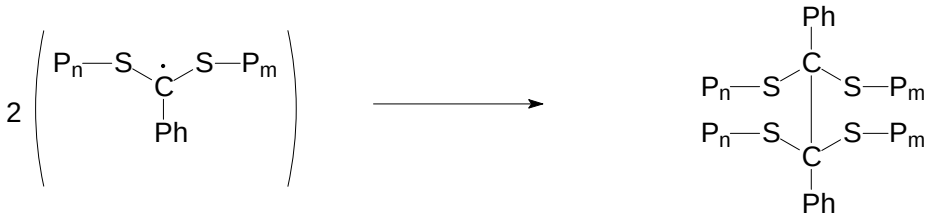


4 arm star

**Scheme 5.2:** Termination mechanism used to explain the formation of 3 and 4 arm stars.

Focusing the discussion on the fate of the intermediate radical, Barner-Kowollik and co-workers attributed the retardation during the RAFT polymerization to the slow fragmentation of the intermediate radical, due to the high intermediate radical stability and hence longer lifetimes.[4,5] For the bulk polymerization of styrene using α,α'-azobisisobutyronitrile (AIBN) and cumyl dithiobenzoate (CDB) at 60 ºC, the rate coefficient for fragmentation ($k_f$) was deduced to be around $3 \times 10^{-2}$ $s^{-1}$. On employing cumyl phenyldithioacetate (altering the activating group in the RAFT agent), $k_f$ was found to be around $2.7 \times 10^{-1}$ $s^{-1}$. On the other hand, using the same experimental system, Monteiro and co-workers explained the observed retardation as a result of cross-termination between propagating and intermediate radicals.[7] The estimated $k_f$ was ~ $10^5$ $s^{-1}$. Recent publications using model experiments[8] and $^{13}C$ NMR techniques[10] confirm the formation of the cross-termination products [see Figure 5.19(2b) and 5.19(3)].

The work described in this chapter, has been done in order to resolve (or at least try to resolve) this ongoing debate. Poly (butyl acrylate) (PBA) will be used as the model for most of the study. Observations from electron spin resonance (ESR) experiments, followed by termination reactions with model experiments are described. Matrix assisted laser desorption/ionization – time of flight – mass spectrometry (MALDI-TOF-MS) technique, coupled with size exclusion chromatography, is employed for polymer characterization. Mass spectrometry techniques provide the sensitivity and resolution, together with structural information to determine even the smallest amount of product. In the past, MALDI-TOF-MS has been employed to study RAFT generated polymers.[11,12,13]

## *5.2 Experimental Section*

### *5.2.1 Materials*

Butyl acrylate (BA, Merck, 99+%) and styrene (Sty, Aldrich, 99+%) were distilled under reduced pressure and stored over molecular sieves at –15 ºC. Toluene (Aldrich, 99+% HPLC grade), benzene (Aldrich, 99+% HPLC grade) and tert-butyl benzene (Aldrich, 99%) were stored over molecular sieves and used without further purification. The RAFT agent, 2-phenylprop-2-yl dithiobenzoate (or cumyl dithiobenzoate, CDB)[2] was synthesized as described in literature. N,N,N',N'',N'' pentamethyldiethylenetriamine (PMDETA, Aldrich, 98%), copper (I) bromide (CuBr, Aldrich, 99.98%), copper (II) bromide ($CuBr_2$, Aldrich, 99%), copper powder (Cu(0), Aldrich, 99%), ethyl-2-bromoisobutyrate (EBriB, Aldrich, 98%), 2,2,6,6-tetramethyl-1-piperidinyloxy (TEMPO, Aldrich), aluminum oxide (activated, basic, for column chromatography, 50-200 μm) and tetrahydrofuran (THF, Aldrich, AR) were used as supplied. α,α'-Azobisisobutyronitrile (AIBN, Merck, >98%) was recrystallized twice from methanol before use.

### *5.2.2 Analysis and Measurements*

***5.2.2.1 Determination of MMD***: Molar mass (MM) and molar mass distributions (MMD) were measured by size exclusion chromatography (SEC), at ambient temperature using a Waters GPC equipped with a Waters model 510 pump, a model 410 differential refractometer

(40 ºC), a Waters WISP 712 autoinjector (50 μL injection volume), a PL gel (5 μm particles) 50 × 7.5 mm guard column and a set of two mixed bed columns (Mixed-C, Polymer Laboratories, 300 × 7.5 mm , 5 μm bead size, 40 ºC) was used. THF was used as the eluent at a flow rate of 1.0 mL/min. Calibration was carried out using narrow MMD polystyrene (PS) standards ranging from 580 to $7 \times 10^6$ g/mol. The molecular weights were calculated using the universal calibration principle and Mark-Houwink parameters[14] [PBA: $K = 1.22 \times 10^{-4}$ dL/g, a = 0.700; PS: $K = 1.14 \times 10^{-4}$ dL/g, a = 0.716]. Molecular weights were calculated relative to the relevant homopolymer (in this case PBA). Data acquisition and processing were performed using Waters Millenium 32 software.

In some instances, the polymers obtained after the model reactions were fractionated prior to MALDI-TOF-MS analysis, using a SEC apparatus, which constituted of a four-column set, PLgel Mixed-B (Polymer Laboratories, 10μ), PLgel Mixed-C (Polymer Laboratories, 5μ), two PLgel Mixed-D (Polymer Laboratories, 5μ) and a guard column (Plgel, Polymer Laboratories, 5μ). The system also consisted of an isocratic pump (Gyncotek P580, Separations, flow rate of 1.0 mL/min), UV detector (Spectra Physics Linear$^{TM}$ UV-VIS 200, 254 nm), Differential Refractive Index and viscosity detector (dual detector 250,Viscotek) and a light scattering detector (RALLS, Viscotek). THF was used as a solvent at a flow rate of 1.0 mL/min. A fraction collector (Millipore) was used to collect 120 fractions at equal volume intervals of 18 droplets. The system was calibrated using narrow MMD PS standards ranging from 580 to $2 \times 10^6$ g/mol.

***5.2.2.2 MALDI-TOF-MS:*** Measurements were performed on a Voyager-DE STR (Applied Biosystems, Framingham, MA) instrument equipped with a 337 nm nitrogen laser. Positive-ion spectra were acquired in reflector mode. DCTB (trans-2-[3-(4-tert-butylphenyl)-2-methyl-2-propenylidene]malononitrile) was chosen as the matrix. Sodium trifluoracetate (Aldrich, 98%) was added as the cationic ionization agent. The matrix was dissolved in THF at a concentration of 40 mg/mL. Sodium trifluoracetate was added to THF at a concentration of 1 mg/mL. The dissolved polymer concentration in THF was approximately 1 mg/mL. In a typical MALDI experiment, the matrix, salt and polymer solutions were premixed in the ratio: 5 μL sample: 5 μL matrix: 0.5 μL Salt. Approximately 0.5 μL of the obtained mixture was hand spotted on the target plate. For each spectrum 1000 laser shots were accumulated.

***5.2.2.3 ESR:*** ESR spectra were recorded on a JEOL JES RE-2X spectrometer, using a universal X-band-width, 100 kHz field modulation, with 0.32 G amplitude, and 1 mW

microwave power. The measurement temperatures were controlled using a JEOL DVT2 variable temperature unit. Data acquisition and analysis were performed with the JEOL ESPRIT 330 data analysis system. The concentration of the observed radicals was estimated by calibration (calibration range between $10^{-4}$ to $10^{-8}$ mol/L) with TEMPO in the reaction medium at the reaction temperature [for example, for BA polymerization, the reaction medium was BA and benzene, and the reaction temperature was 363 K (90 °C)].

## *5.3 Synthetic Procedures*

***5.3.1 ESR:*** The sample solution containing benzene (0.53 mL, 6.0 mmol), BA (0.53 mL, 3.6 mmol), cumyl dithiobenzoate (CDB) (0.028 g, 0.1 mmol) and AIBN (5 mg, 0.03 mmol) was placed in a quartz ESR tube and purged with nitrogen for 5 mins., prior to measurements. The reactions were carried out within the ESR spectrometer cavity, which was maintained at the reaction temperature of 363 K.

***5.3.2 RAFT polymerization:*** The RAFT agent, CDB (0.272 g; 1.0 mmol) and AIBN (0.033 g; 0.2 mmol) were accurately weighed and then transferred to a 25 mL three-neck round-bottom flask. Then a solution of toluene (4.6 g; 0.05 mol) and BA (4.73 g; 0.037 mol) was added. The reaction mixture was degassed by sparging with argon for 30 min. Then, the flask was immersed in a thermostated oil bath maintained at 70 °C. The reaction was carried out for 5 hrs. under a flowing argon atmosphere. The monomer conversion was determined using GC.

***Details:*** Final Conversion = 30 %, $M_n$ = 2025 g/mol, $M_w$ = 2344 g/mol, PDI = 1.15.

***5.3.3 ATRP polymerization:*** A typical polymerization was carried out in a 25 mL three-neck round-bottom flask. Toluene (9.0 g, 0.08 mol), BA (4.67 g, 0.037 mol), CuBr (0.095 g, 0.66 mmol) and $CuBr_2$ (0.035 g, 0.15 mmol) were accurately weighed and transferred to the flask. The ligand, PMDETA (0.14 g, 0.83 mmol) was then added. The reaction mixture was degassed by sparging with argon for 30 min. The flask was immersed in a thermostated oil bath maintained at 70 °C and stirred for 10 min. A light green, slightly heterogeneous system was obtained. The initiator, EBriB (0.33 g, 1.7 mmol), was then added slowly via a degassed syringe. The reaction was carried out for 4 hrs. under a flowing argon atmosphere. The final polymer was

diluted with THF, passed through a column of aluminum oxide prior to SEC and MALDI-TOF-MS measurements.

***Details*:** $M_n$ = 2405 g/mol, $M_w$ = 2828 g/mol, PDI = 1.17.

### *5.3.4 Model reactions of PBA-Br with PBA-RAFT:*

A typical model reaction was carried out in a 10 mL two-neck round-bottom flask. PBA-Br [$M_n$ = 2405 g/mol, $M_w$ = 2828 g/mol, PDI = 1.17] (0.05 g, 0.02 mmol), PBA-RAFT [$M_n$ = 2025 g/mol, $M_w$ = 2344 g/mol, PDI = 1.15] (0.052 g, 0.02 mmol), CuBr (0.246 g, 1.7 mmol), Cu(0) (0.109 g, 1.7 mmol) and *tert*-butyl benzene (1.6 g, 12 mmol) were accurately weighed. The ligand, PMDETA (0.433 g, 2.5 mmol) was then added. The reaction mixture was degassed by sparging with argon for 30 min. Then, the flask was immersed in a thermostated oil bath maintained at 80 °C. The reaction was carried out for 3 hrs., under a flowing argon atmosphere. The final polymer was diluted with THF, passed through a column of aluminum oxide prior to SEC and MALDI-TOF-MS measurements.

## *5.4 Results and Discussion*

One of the objections to previously published model termination work for the RAFT styrene system[8] was that, the lifetime of the intermediate radical was short – lived due to the fast fragmentation process.[15] This point has been countered in another recent publication.[16] But, apart from all this, the current work with ESR clearly indicates that the radical lifetime for the BA intermediate species is much longer and the concentration much higher as compared to the Sty species. Hence, the BA system was chosen for the model termination reactions, since, if any cross-termination of the intermediate radical was to occur, it would be more pronounced in this case.

The ESR work is initially described, wherein, the intermediate radical concentrations for the individual BA and styrene systems are determined. Then the model compound reaction of PBA-RAFT with AIBN has been investigated, followed by the PBA-Br reactions. A combination of SEC and MALDI-TOF-MS techniques, have been employed for the polymer characterization.

### *5.4.1 ESR:*

ESR spectroscopy is a very powerful tool for the investigation of radical polymerization.[17] In recent years, this technique has been used effectively to reveal the mechanism of the RAFT polymerization.[18,19,20,21] In this section, ESR is applied for the AIBN initiated, cumyl dithiobenzoate mediated BA and Sty homopolymerization, to observe the

intermediate radical concentration as a function of time. Radical concentration as a function of monomer conversion is also compared for the two systems. The monomer conversion was obtained from offline lab experiments, employing similar formulations.

***5.4.1.1 BA System:*** Figure 5.1(a) depicts the ESR spectrum obtained for the RAFT intermediate radical [Figure 5.1(c)] formed during the BA polymerization after 15 mins. at 90 °C. The observed signal can be simulated reasonably with hyperfine splitting constants shown in the structure in Figure 5.1(c) and was consistent to those reported in previous studies.[18] Figure 5.1(b) is the simulated spectra for the intermediate radical. However, the line widths of the experimental ESR spectrum are too broad to determine the hyperfine splitting constants of γ-protons from the propagating polymeric chain ends attached to the sulfur atoms of Figure 5.1(c). Relatively broad line width implies the formation of mid-chain type radical. The propagating radical concentration was too low to be directly observed with the current equipment.

Radical concentration can be estimated from double integration of the observed spectra. The typical radical concentration *vs* time profile is shown in Figure 5.2. The propagating radical concentration was too low to be directly observed with the current equipment. The radical concentration *vs* monomer conversion profile is also shown in Figure 5.3. The observations from the plots are, **(i)** the concentration of the intermediate radical was in the order of $10^{-6}$ M. There was an increase in the intermediate radical concentration with time, then, upon passing through a maximum, the radical concentration gradually decreased. The radical concentration quickly reached a steady state (evident from Figures 5.2 and 5.3). The steady state condition persisted for about 60 mins. into the reaction, after which there was a gradual decrease in radical concentration. The decrease in the radical concentration with time, is attributed to the rapid consumption of the initiator radicals, since the half-life time for AIBN was only around 35 mins. at 90 °C. **(ii)** The intermediate radicals were present even after 5 hrs of reaction, which was very surprising, since, from the given literature on the rate coefficient for decomposition ($k_d$) of AIBN, almost no initiator would be expected to remain. The long lifetime of the intermediate radical has also been reported in a previous article.[21] In that paper, the cumyl dithiobenzoate mediated styrene polymerization was investigated. Though in that particular study, high initiator and RAFT concentration were employed to maximize ESR signals. A reversible radical deactivation step was suggested to explain the presence of this radical after such long reaction times in the virtual absence of the initiator. **(iii)** From Figure 5.4, it was clear that monomer conversion still occurred at later stages of the polymerization, though the rate of polymerization was quite slow. Now, $R_p \propto [R^*]$, where $R_p$ is the

rate of polymerization and [$R^*$] stands for radical concentration. Hence, this reduction in polymerization rate is ascribed to the relatively low radical concentration at the later stages.

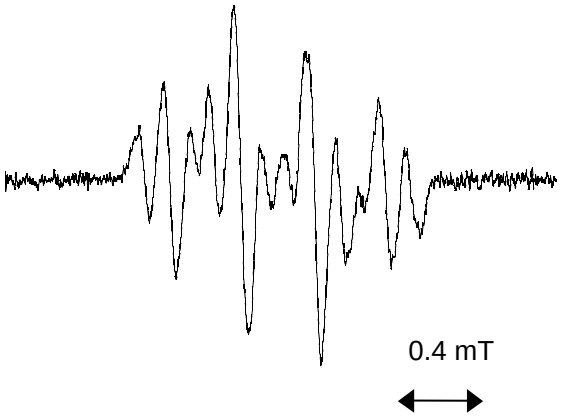


**(a)**

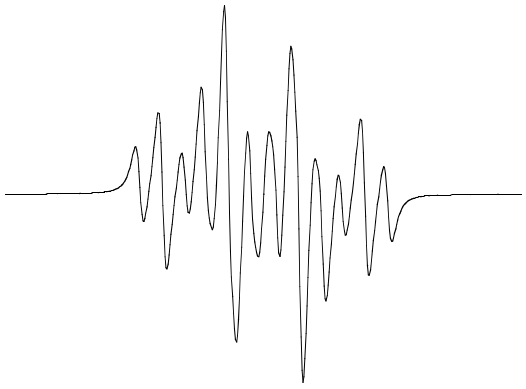

**(b)**

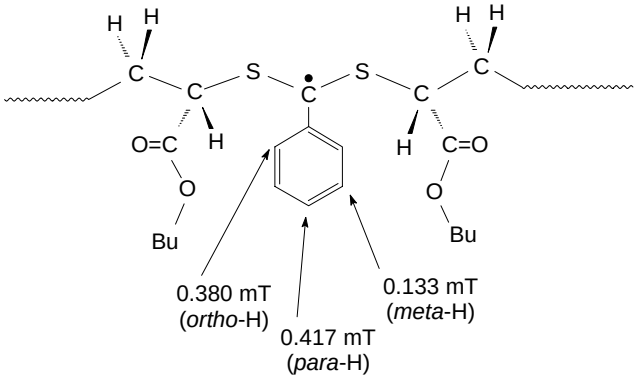


**(c)**

**Figure 5.1:** ESR spectra for the RAFT intermediate radical. **(a)** Obtained during the homopolymerization of BA at 90 °C. [BA] = 3.6 mmol, [RAFT] = 0.12 mmol, [AIBN] = 0.03 mmol. **(b)** Simulated spectrum. **(c)** Structure of the obtained intermediate radical with the hyperfine splitting spectral parameters for the phenyl protons.

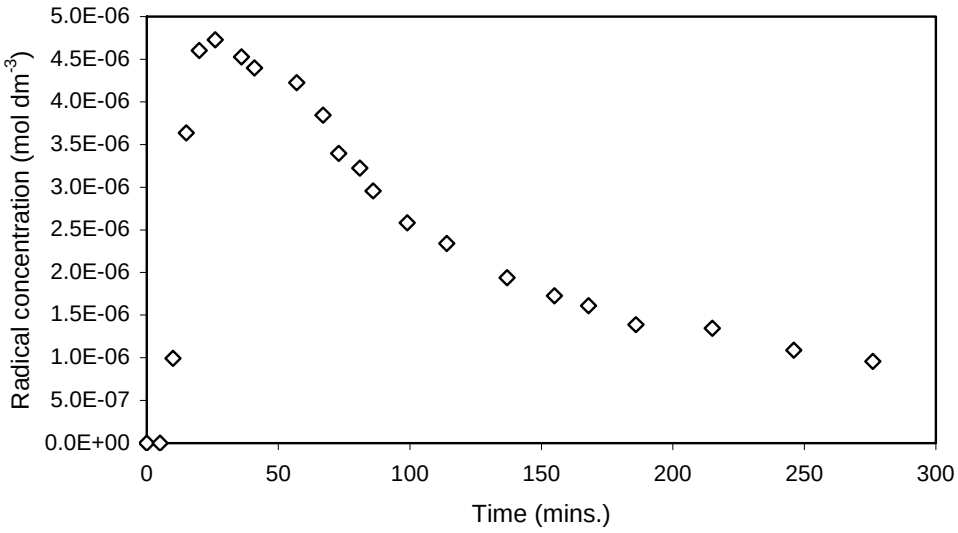


**Figure 5.2:** Plot of intermediate radical concentration *versus* time for BA polymerization at 90 °C. [BA] = 3.6 mmol, [RAFT] = 0.12 mmol, [AIBN] = 0.03 mmol.

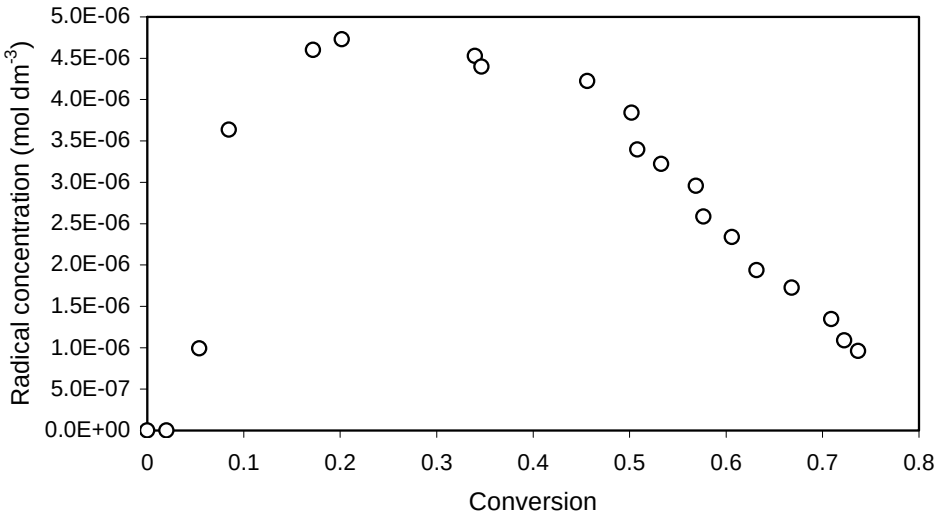


**Figure 5.3:** Plot of intermediate radical concentration *versus* conversion for BA polymerization at 90 °C. The monomer conversions were determined from lab experiments.

In Figure 5.4, the plot of $M_n$ versus conversion for the lab experiments are shown. The experimentally determined molar masses ($M_n$) coincide reasonably well with the theoretically calculated $M_n$ values for the RAFT system. The linear increase of $M_n$ as a function of monomer conversion is indicative of the living character of the polymerization. Relatively narrow MMD are obtained for the RAFT reaction. After 50 % conversion, very low amount of radicals are generated

from thermal decomposition of AIBN. It is expected that the long-living intermediate and the short-living propagating radicals only exist after 50 % conversion. Some of propagating radicals go back to the intermediate radical form; however some of the propagating radicals may terminate by coupling reactions. Increase of PDI in the later stage of the polymerization may imply the absence of newly generated initiating radicals and presence of terminated species. Decrease of radical concentrations of intermediate radicals is consistent with the increase of termination reactions. Controlled increase in the value of $M_n$ during 50-80 % conversion may indicate smaller contribution of side reactions including termination.

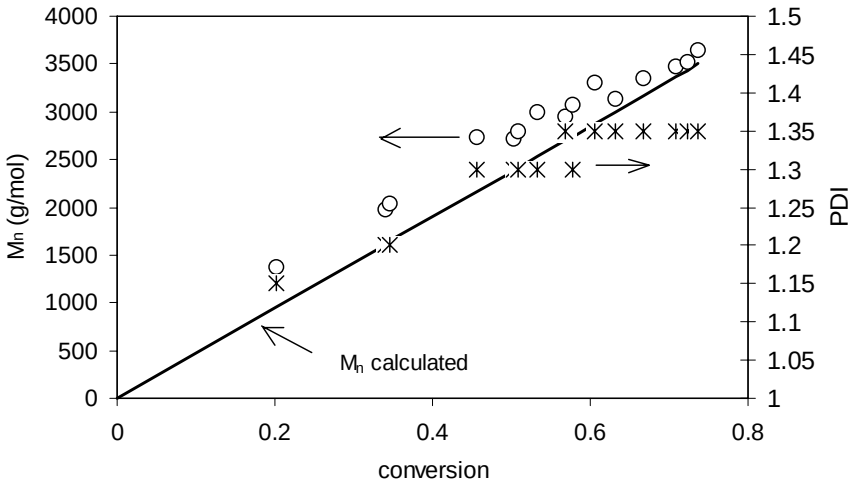


**Figure 5.4:** Plot of $M_n$ *versus* conversion for the BA polymerization at 90 °C.

***5.4.1.2 Styrene System:*** Similar to that for the BA, Sty polymerizations were also carried out. Figure 5.5 depicts the ESR spectrum obtained for the RAFT intermediate radical formed during the Sty polymerization after 26 mins. at 90 °C. The observed signal was consistent to those reported in previous studies.[18] Since, like in the BA case, the line widths of the ESR spectrum were too broad to determine the hyperfine splitting constants of γ- protons on the propagating polymeric chain ends, attached to the sulfur atoms, the simulated spectrum was based on the same parameters as given in Figure 5.1(c). Therefore, the simulated spectrum is similar to that shown in Figure 5.1(b).

Recently though, well-resolved ESR spectrum for the styrene intermediate radical during RAFT polymerization at 0 °C was reported.[20] The initiation was done by UV irradiation. The observed signal was considered to be similar to the ESR signal reported in a previous publication[18] to which the obtained signal in Figure 5.5 is consistent, only that, the spectroscopic resolution was

much higher at low temperatures, which enabled the deduction of the structures for the propagating radicals. Spectral parameters, like hyperfine splittings and g-factor, for the two signals, were determined and compared.[20]

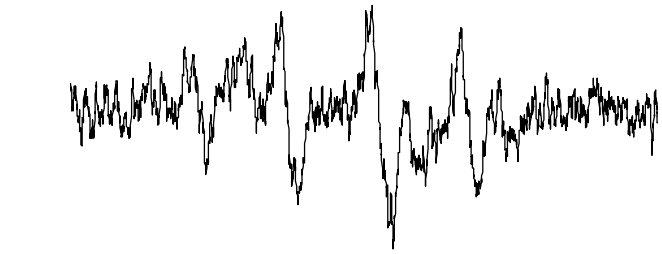

**(a)**

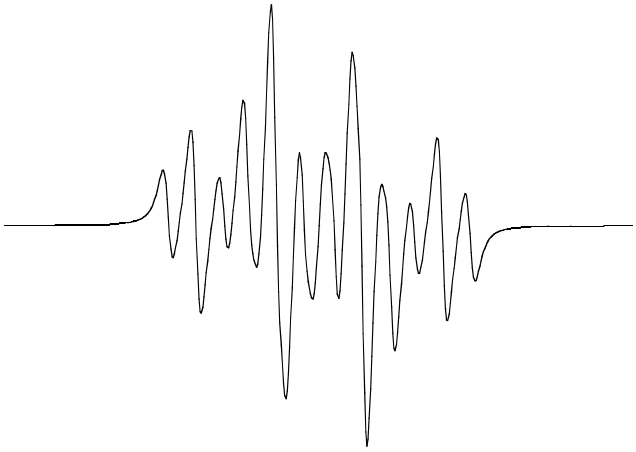

**(b)**

**Figure 5.5:** ESR spectra for the RAFT intermediate radical. **(a)** Obtained during the homopolymerization of Sty at 90 °C. [Sty] = 4.0 mmol, [RAFT] = 0.09 mmol, [AIBN] = 0.027 mmol., **(b)** Simulated spectrum.

Further, the radical concentration *vs* time profile and the radical concentration *vs* monomer conversion profile are shown in Figures 5.6 and 5.7 respectively. The observations from the plots are, **(i)** the concentration of the intermediate radical is in the order of $10^{-7}$ M. The obtained value is in accordance with previously reported values for this system.[8,21] The long inhibition time at the onset of the polymerization, may now be explained in terms of the initialization time required for the RAFT mono-adduct to be formed.[3] For the Sty system, just as for the BA system, there is an increase in the intermediate radical concentration with time, followed by a gradual decrease. **(ii)** However, unlike the BA system, the Sty intermediate radicals were not visible anymore after about 2 hrs. Maybe, the radical concentrations were below the detection limit of the instrument. Hence, the long lifetime for the Sty intermediate radical, which had been observed in the previous

work,[21] can clearly attributed to the high initiator and RAFT concentration which were employed.[21] But, the proposed reversible radical deactivation step has still to be unequivocally proven.

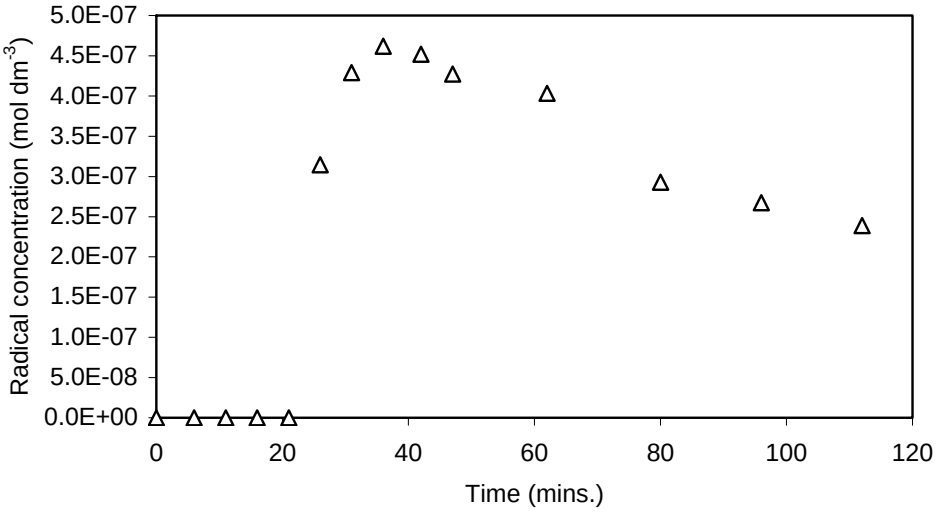


**Figure 5.6:** Plot of intermediate radical concentration *versus* time for Sty polymerization at 90 °C. [Sty] = 4.0 mmol, [RAFT] = 0.09 mmol, [AIBN] = 0.027 mmol.

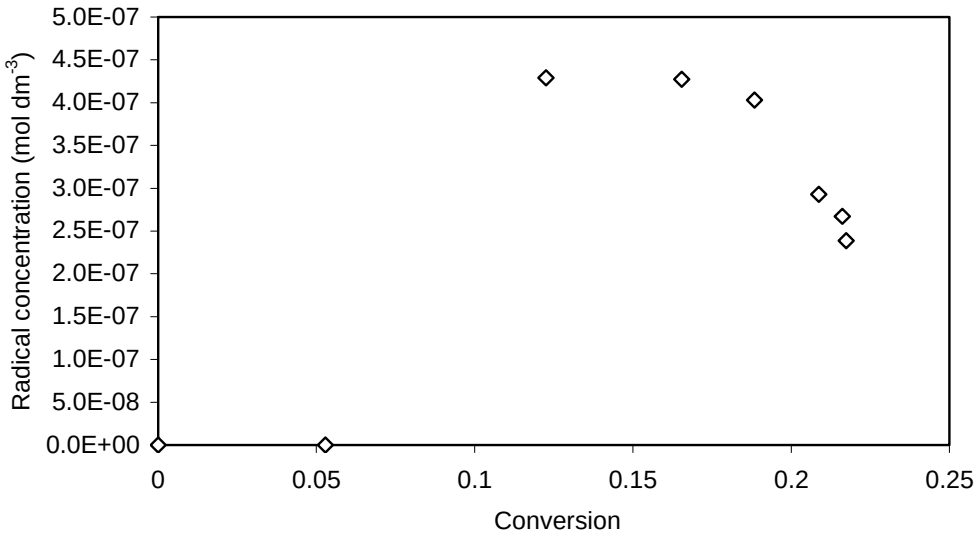


**Figure 5.7:** Plot of intermediate radical concentration *versus* conversion for Sty polymerization at 90 °C. The monomer conversions were determined from lab experiments.

Now, from all the data described above, comparison of the BA and Sty RAFT systems becomes very easy. As shown in plots Figure 5.8 and 5.9, in which the radical concentration *vs* time and conversion are overlaid for the 2 systems, it is more than evident that the intermediate radical

concentration for BA is significantly higher as compared to that for Sty. The intermediate radical concentration depends on the relative rates of the radical formation and destruction. A lower radical concentration could result either from a smaller rate constant for its formation or higher rate constant for fragmentation. From literature, it is known that radical stability and steric factors are important parameters for good RAFT leaving groups. Further, for the leaving groups, the fragmentation rate constants decrease in the series tertiary >> secondary >> primary.[2] In the present case, both the BA and Sty propagating radicals are secondary in nature, but, the Sty radical has increased stability due to resonance. Therefore, the fragmentation rate for the Sty system will be much higher as compared to the BA system and hence, a lower intermediate radical concentration is observed. Thus, as previously indicated, the BA system with the longer lifetime of the intermediate radical was chosen for the model termination reactions, since, if any cross-termination of the intermediate radical was to occur, it would be more pronounced in this case.

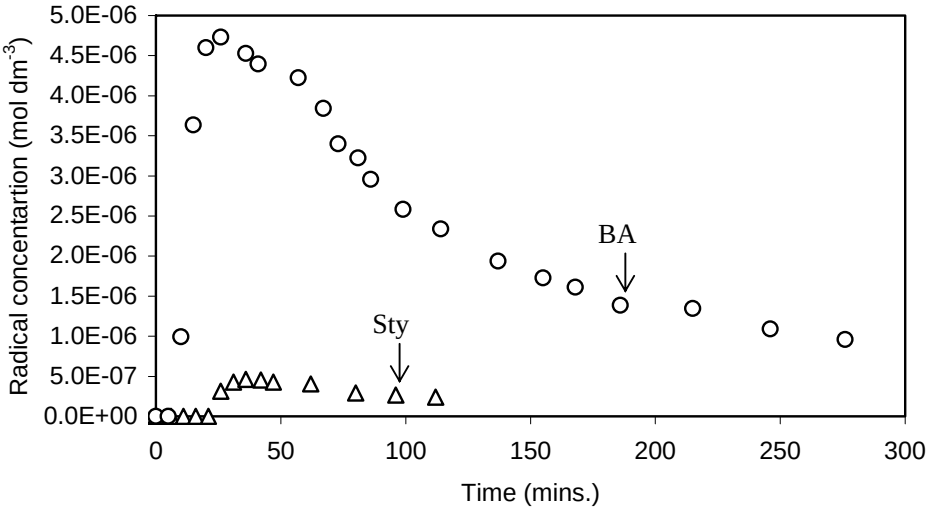


**Figure 5.8:** Plot of intermediate radical concentration *versus* time for BA and Sty RAFT mediated polymerization at 90 °C.

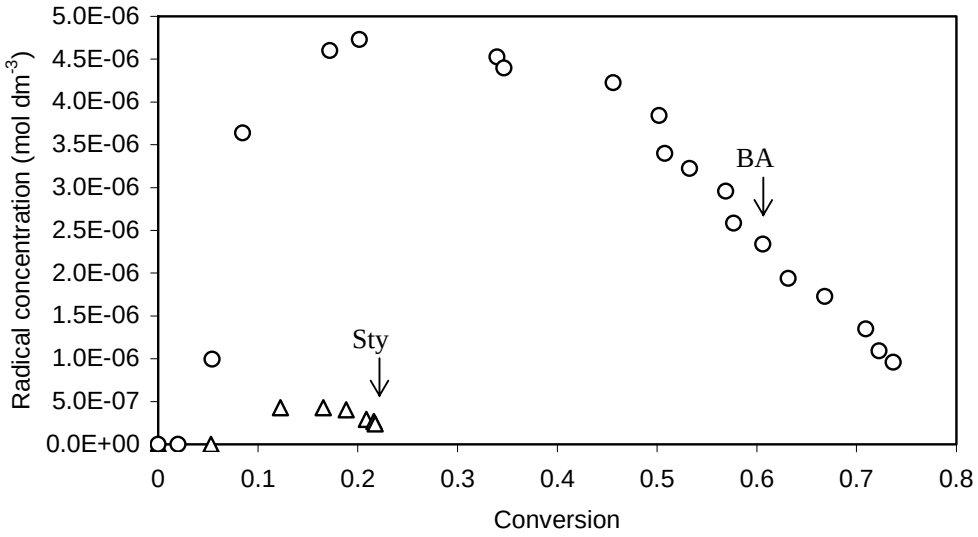


**Figure 5.9:** Plot of intermediate radical concentration *versus* conversion for BA and Sty RAFT mediated polymerization at 90 °C.

## *5.4.2 Termination Reactions*

MALDI-TOF-MS and SEC are the techniques employed to determine the course of the termination reaction. For all reactions, PBA-RAFT (synthesis described in Section 5.3.2) was employed as the model macro-RAFT. Hence, it was important to first assign the peaks observed in the MALDI-TOF-MS spectrum of this sample. The peak assignments for all the MALDI-TOF-MS spectra described in this section, were made using the following strategies; **(i)** comparison of the observed masses with those theoretically calculated, and **(ii)** comparison of the observed isotopic distributions with theoretical isotopic distributions.

Figure 5.10 is an expansion of a selected portion of the PBA-RAFT spectrum. Sodium trifluoracetate was added as the cationic ionization agent. Hence, the majority of the polymer chains were cationized with sodium, and therefore were detected at a m/z value 23 Daltons above the theoretically calculated mass. Interestingly, most polymer chains can be divided into having four pairs of end groups (E1, E2, E3, E4) [see Figure 5.10 and Table 5.1].

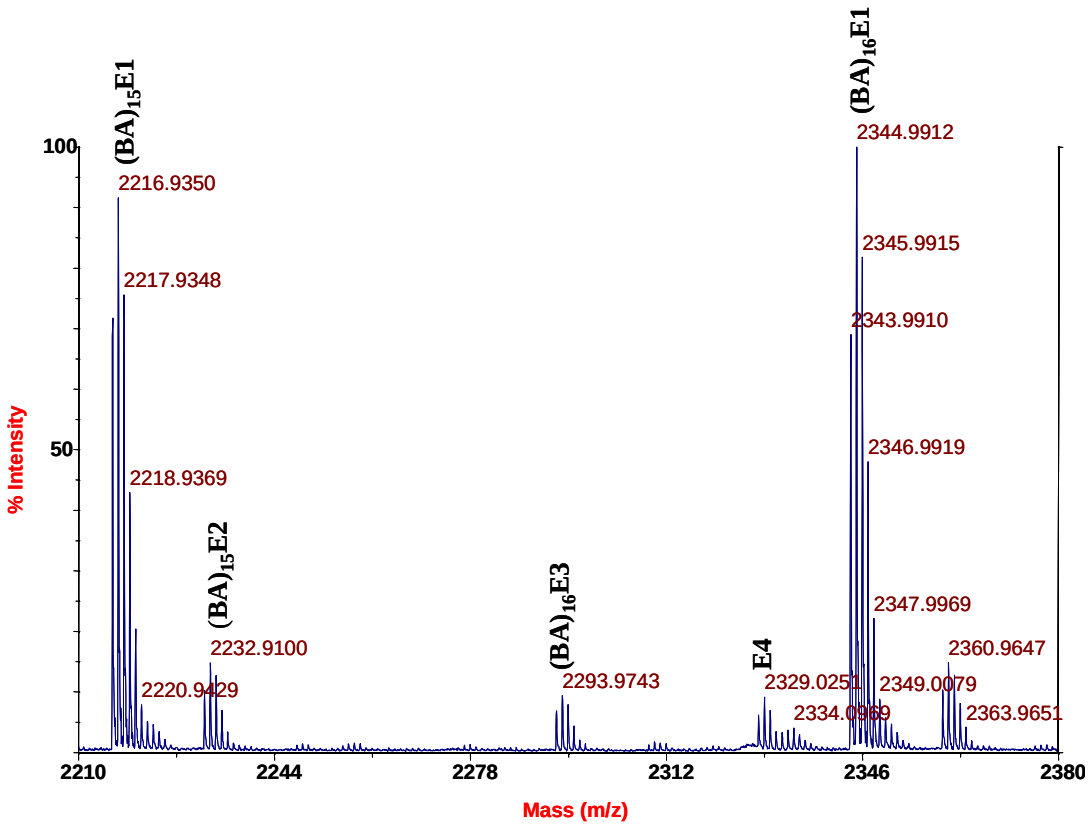


**Figure 5.10:** MALDI-TOF-MS spectrum for PBA-RAFT. [Spectrum acquired in reflector mode, Matrix : DCTB].

Usually, the detected signals after subtraction of the mass of the cationization reagent ($Na^+$), should be in agreement with the expected masses of the polymer chains, which can be calculated according to Equation (I). End group **E1** was assigned to Equation (I).

$$M_{homo} = 119.18 + (m \times 128.17) + 153.23 \quad \text{(I)}$$

where, 119.18 and 153.23 are the average masses of the end groups from the leaving group (cumyl fragment) and the dithiobenzoate activating group respectively (since cumyl dithiobenzoate was used as the RAFT agent). 128.17 is the average mass of BA and m the number of the monomer unit in the chain.

Some chains can also be cationized by potassium, in which case, the detected signals after subtraction of the mass of the cationization reagent ($K^+$), should be detected at a m/z value 39 Daltons above the theoretically calculated mass. The theoretical mass for end group **E2** can be calculated using Equation (I) itself, where the only difference is that in end group E2, the cation is now potassium.

Since, the initiator AIBN was used to generate radicals to start and keep the RAFT polymerization active, a few chains can also be initiated by this primary cyanoisopropyl radical. The presence of this species is consistent with previous studies.[11,13,22] The end group **E3** can be assigned by employing Equation (II). Sodium is the cation.

$$M_{homo} = 68.09 + (m \times 128.17) + 153.23 \qquad \text{(II)}$$

where, 68.09 and 153.23 are the average masses of the end groups from the cyanoisopropyl fragment and the dithiobenzoate activating group respectively. 128.17 is the average mass of BA and m the numbers of the monomer in the chain.

End group **E4** could not be assigned to any of the possible structures, including 3 or 4 arm stars, or even the intermediate radical. The closest plausible match has been that of a 3- arm star, formed as a result of cross-termination of a propagating chain having a cumyl end group with an intermediate radical, having two polymeric chains attached to it also with cumyl end groups. The mass, however, was 1.5 Da lower than the observed mass and is considered for our purpose outside the error of the MALDI-TOF-MS measurement. The error for the other assigned peaks was within 0.5 Da. In a recent publication,[22] it was suggested that small amounts of peroxides present in stabilized THF (which is used as an eluent in SEC), could aid in the exchange reaction of the double bonded sulfur atom in the RAFT dithiobenzoate moiety by oxygen, to result in a peak, which is 16 Da lower than the structure shown in Figure 5.11 (a). This proposed structure is shown in Figure 5.12. But, as shown later, on carrying out the termination reactions with AIBN, the intensity of the chains with the end group E4 increased, suggesting that this peak resulted due to termination reactions.

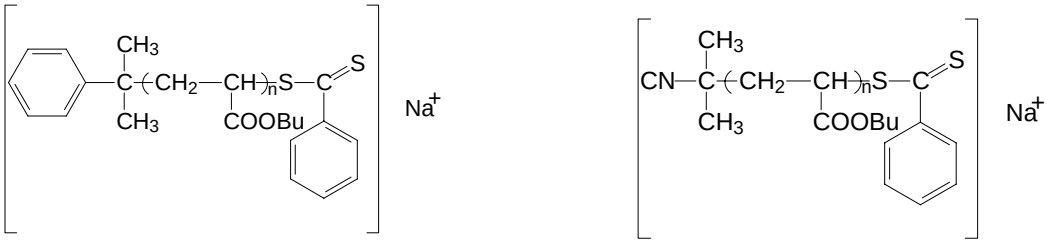


(a) **E1** (b) **E3**

**Figure 5.11:** The observed structures for the RAFT polymeric chains, during MALDI-TOF-MS measurements. Equation I assigned to (a) E1 and Equation II assigned to (b) E3 respectively.

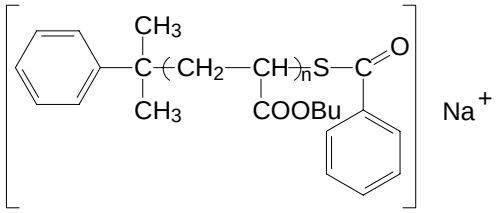


**Figure 5.12:** The proposed structure after exchange of the double bonded sulfur atom by oxygen.

Table 5.1 details the observed and theoretical mass differences. Figures 5.13 and 5.14 clearly compared the isotopic mass distributions for the polymer chains having the assigned end groups to those theoretically calculated. As is evident there is an excellent correlation.

**Table 5.1:** Peak assignment of the MALDI-TOF-MS spectrum shown in Figure 5.10

| Peak | BA units | Observed Mass (Da) | Theoretical Mass (Da) | $K^+$ | $Na^+$ |
|---|---|---|---|---|---|
| $(BA)_{15}E1$ | 16 | 2344.9912 | 2345.4016 | - | 1 |
| $(BA)_{15}E2$ | 15 | 2232.9100 | 2233.2918 | 1 | - |
| $(BA)_{16}E3$ | 16 | 2293.9743 | 2294.3655 | - | 1 |

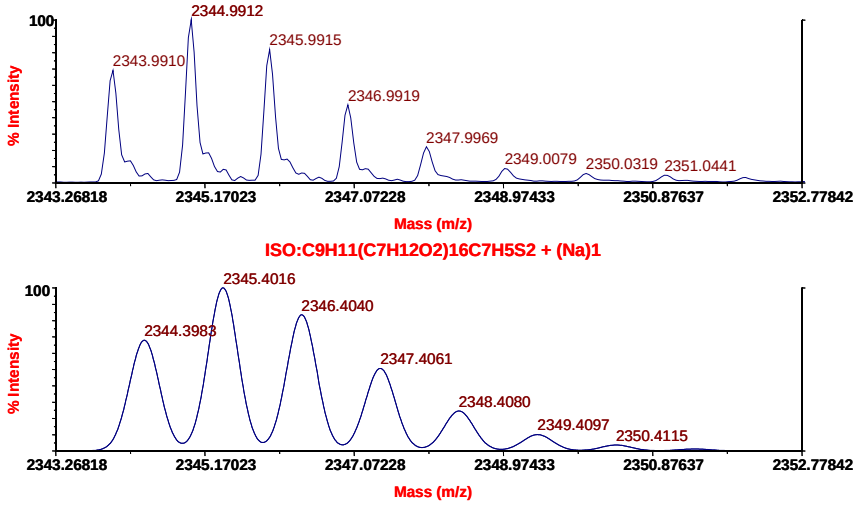


**Figure 5.13:** Detail of the MALDI-TOF-MS spectrum of PBA-RAFT, polymeric chains with end group **E1**. Isotopic mass distributions **:** Observed (above) and Theoretical (below).

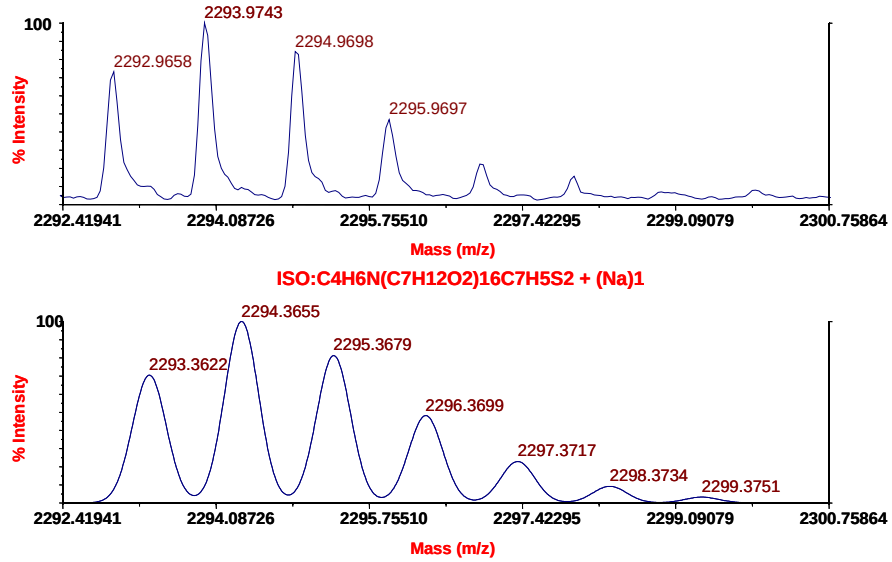


**Figure 5.14:** Detail of the MALDI-TOF-MS spectrum of PBA-RAFT, polymeric chains with end group **E3**. Isotopic mass distributions **:** Observed (above) and Theoretical (below).

***5.4.2.1 Reactions with AIBN:*** Two reactions were carried out with differing ratios of PBA-RAFT to AIBN in t-butyl benzene at 80 °C. Table 5.2 gives the resulting $M_n$, $M_w$ and PDI for these reactions. As the AIBN ratio is increased to 1, the $M_n$ increased from 2025 to 2131 and $M_w$ increased from 2344 to 2530. This can be more clearly seen from the SEC chromatograms (Figure 5.15). The data suggest there must be termination reactions to produce polymer with higher molecular weight than that of the original PBA-RAFT.

**Table 5.2:** AIBN induced termination reactions

| Entry | Ratio [PBA-RAFT] / [AIBN] | $M_n$ (g/mol) | $M_w$ (g/mol) | PDI |
|---|---|---|---|---|
| (1) | No AIBN (PBA-RAFT) | 2025 | 2344 | 1.15 |
| (2) | 6[a] | 2071 | 2421 | 1.16 |
| (3) | 1[a] | 2131 | 2530 | 1.18 |

*a)* *Reaction Temperature = 80 ℃, Reaction time =3 hrs. Solvent =* tert-*butyl benzene.*

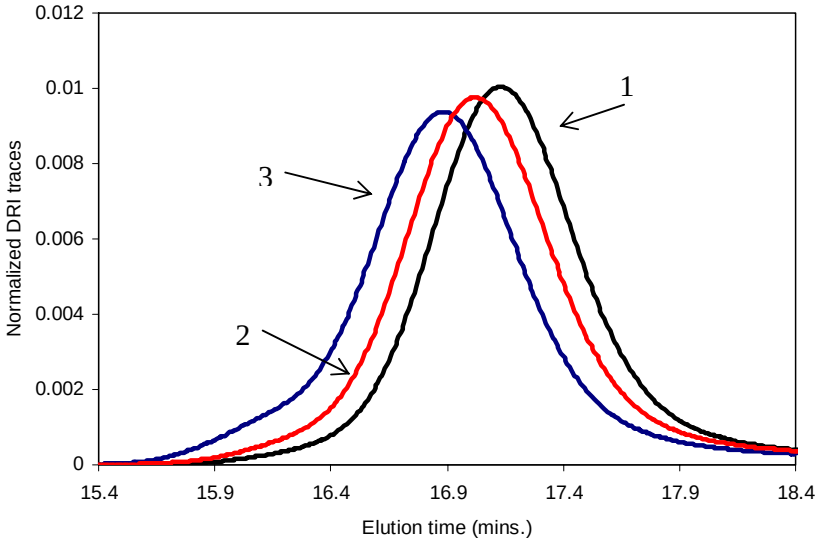


**Figure 5.15:** Plot of normalized DRI traces *versus* elution time for the AIBN termination experiments. (For labels, see Table 5.2).

On comparing the MALDI-TOF-MS spectra of the three polymers in Table 5.2 (see Figure 5.16), there are some interesting observations. The first is that the intensity of the peaks bearing the dithiobenzoate moiety as the terminal end-group decreased as the ratio of AIBN was increased. This indicates that the PBA-RAFT does go through the equilibrium reaction in Scheme 5.1(c), terminating to produce a polymer of higher molecular weight. The second, and more interesting, is that the intensity of the polymer chain at **E4** also increased as the ratio of AIBN was increased. This suggests that, either new chains are terminating to form **E4** or the amount of **E4** remained unchanged but increases relative to the loss of **E1** and **E3**. The evidence supports that **E4** is a termination product to form a dead species that does not participate further in the polymerization process.

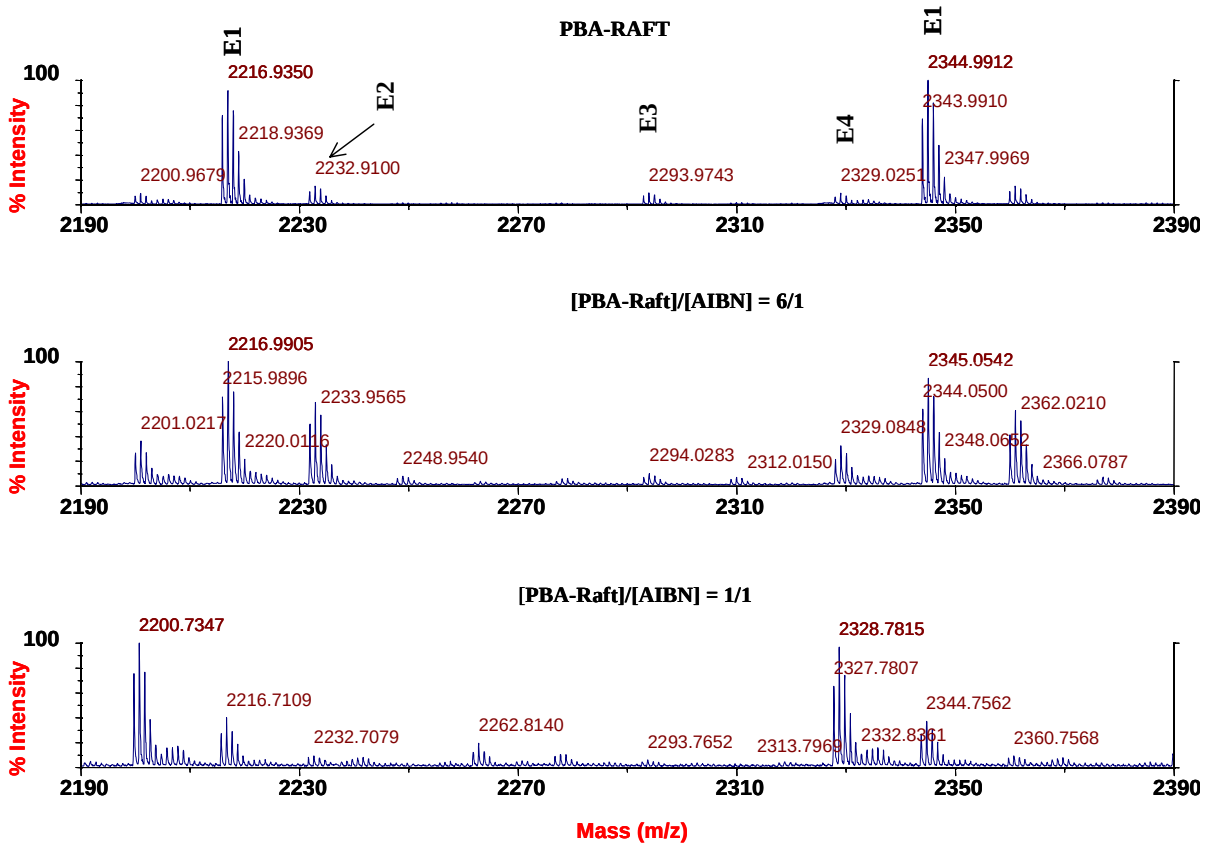


**Figure 5.16:** Comparison of the expanded regions of the MALDI-TOF-MS spectra obtained from the PBA-RAFT and the AIBN termination experiments. [Spectrum acquired in Reflector mode, Matrix **:** DCTB]

In hindsight, it was realized that there was one major drawback in the macro-RAFT - AIBN systems, i.e. the cyanoisopropyl radical will fragment significantly faster from the intermediate radical, than the polyacrylate chain. The cyanoisopropyl radical being tertiary in nature, is more stable, as opposed to the acrylate, which is a secondary radical. Hence, the cyanoisopropyl group will be preferentially expelled from the intermediate radical. This has two main consequences:

1) The intermediate radical concentration will be lower than in the equivalent acrylate RAFT mediated polymerization.
2) The cyanoisopropyl is the only "propagating" radical in the system.

So as to overcome this problem and to further explore cross-termination, it was decided to use the Fukuda[8] model experiments by carrying out reactions of PBA-Br with CuBr/PMDETA and Cu(0) in the presence of PBA-RAFT. Should intermediate radical termination not participate in the

RAFT mechanism then 3 and 4 arm stars should, in principle, not be produced. Fukuda has shown that in the case of styrene systems that 3 arm stars are observed using this method.

***5.4.2.2 Reactions with PBA-Br:*** The experimental procedure is described in Section 5.3.4. The PBA-Br ($M_n$ = 2405 g/mol, $M_w$ = 2828 g/mol, PDI = 1.17), was activated by the CuBr/PMDETA complex, to form the PBA propagating radical. This will now add to the PBA-RAFT to form the intermediate radical. Since, the radical reactivity is similar, there will be no preferred fragmentation pathway. The formed intermediate radical can now fragment, exist as a radical or terminate. In this way, the system will mimic the RAFT polymerization without chain growth. Cu(0) was added to prevent the accumulation of Cu(II) species.

The model termination reactions were performed using varying concentrations of PBA-RAFT and PBA-Br. Figure 5.17 details the SEC chromatograms after the model termination reactions. After the reaction, two well-separated peaks appeared, one of which corresponds to the original PBA-RAFT and the other one to the resultant terminated species. The new peak has an $M_n$ of ~ 8000 g/mol, which points towards the formation of termination products as a result of cross termination reactions. In a previous publication,[8] for the Sty system, the characterization of the cross terminated polymers was achieved using a SEC equipped with a multiangle laser light scattering (MALLS) detector. But, the changes in the hydrodynamic volume upon branching might slightly hinder the effectiveness of this technique. Hence, the MALDI-TOF-MS technique was chosen, since now the absolute mass can be determined. Prior, to MALDI-TOF-MS analysis, the final samples were fractionated. The fractionation procedure is detailed in Section 5.2.2.1.

Figure 5.18 is the MALDI-TOF-MS spectrum for the fractionated polymer sample (current fraction collected in the high MM region). The details for the examined fraction are $M_n$ = 6710 g/mol, $M_w$ = 6830 g/mol and PDI = 1.018. In spite of the narrow MMD, a clear tri-modality in MALDI-TOF-MS distribution was observed. The overall distributions can be grouped into; **(i)** The low mass region (mass range ~2000 Da), constituted of terminated chains present in the starting compounds (PBA-RAFT and PBA-Br respectively), which do not participate in the reactions. **(ii)** Middle mass range (mass range ~4000 – 6000 Da), consisted of terminated products obtained from bimolecular or cross termination during the reaction. **(iii)** High mass range (mass range ~ 8000 Da), comprised exclusively of cross termination products. The observed tri-modality in the MALDI-TOF-MS distributions, clearly highlighted the pitfalls of the SEC and exposed its limitations in this particular case for the branched polymers.[8] Now, on further examination within

the individual mass ranges, several distributions are clearly visible. This is due to the different end groups resulting from the termination reactions.

In the present study, the discussion will be restricted to the peaks present in the mass ranges between 4000 – 8000 Da. For, it is in this region, where the peaks arising from the terminated products would be expected to manifest. Figure 5.19 gives an overview of the possible terminated species, which could result during the reactions.

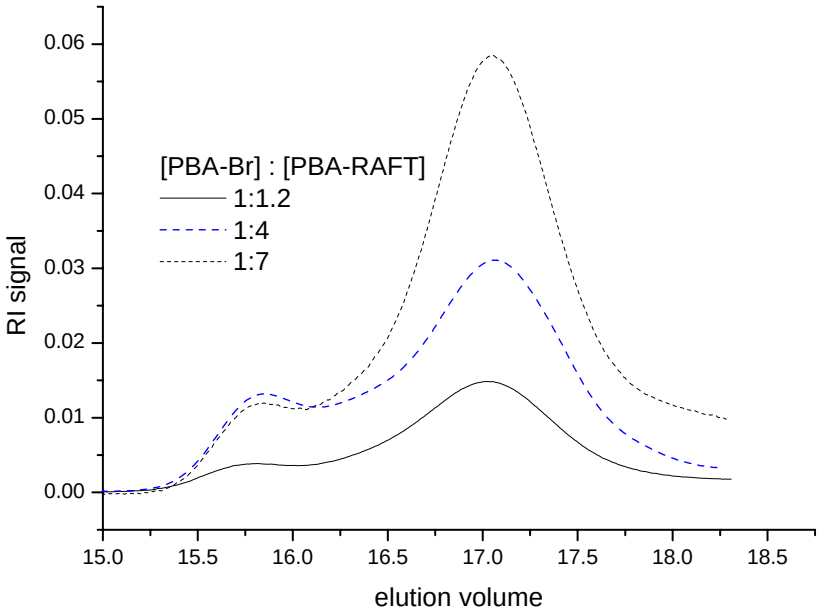


**Figure 5.17:** Normalized DRI traces *versus* elution volume obtained from SEC measurements, for the final polymers obtained after the termination reactions. For the termination reaction, [PBA-Br] : [PBA-RAFT]: [Cu(I)Br] : [Cu(0)] : [PMDETA] = 1 : 1.2/4/7 : 82: 82 : 120. Reaction time = 3 hrs., Reaction temperature = 80 °C.

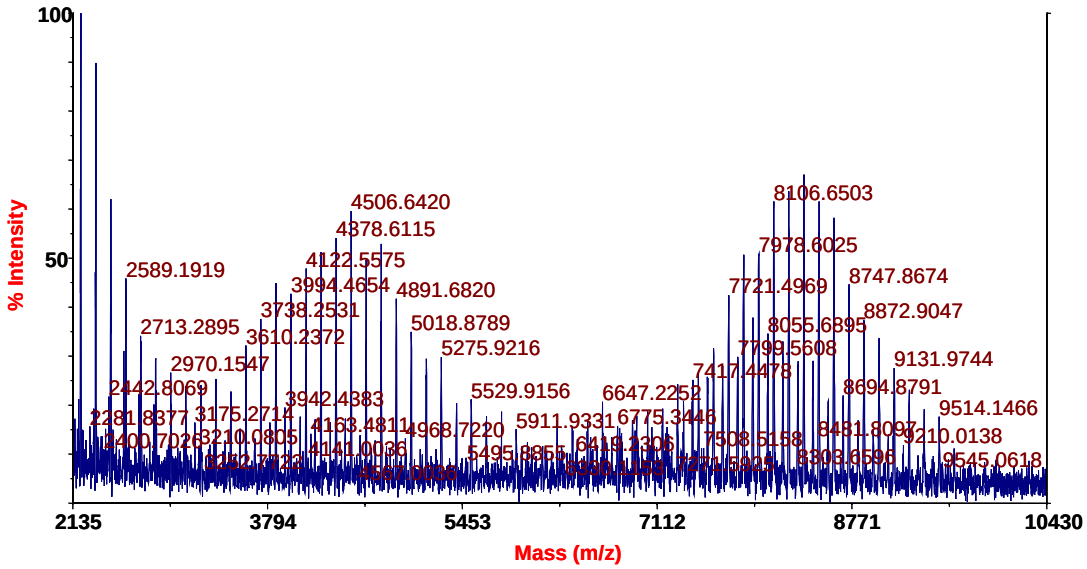


**Figure 5.18:** MALDI-TOF-MS spectrum for the fractionated polymer. (Details from SEC, $M_n$ = 6710 g/mol, $M_w$ = 6830 g/mol and PDI = 1.018). [Spectrum acquired in Reflector mode, Matrix : DCTB].

Figure 5.20 is an expansion of the Figure 5.18 in the high mass range (mass range ~ 8000 Da). As is evident, there seem to be two distinct distributions upon expansion. The individual distributions appear to be very broad. With increasing number of monomer repeat units (or higher degree of polymerization), the isotopic distribution usually broadens, due to the increased contribution from the different isotopes (e.g $^{12}C$ and $^{13}C$). The broadening could also result from overlapping between two isotopic distributions. In the present case, it is a combination of the two possibilities. Apart from the high degree of polymerization, the mass for the end groups cumyl (119.19 Da) and ethyl isobutyryl (115.15 Da) only differ by 4.04 Da. Further, as shown in Figure 5.21 these are the end groups which are predominantly present, hence, the isotopic distributions overlap.

In the high mass range, the polymeric chains will only result from the cross termination of intermediate radicals, resulting in the formation of the 4 arm star. Only in this way, can such high masses be obtained (4 × 2000 = 8000). Figure 5.21 depicts the structures to which the current peaks have been assigned. Figures 5.22 and 5.23, clearly compare the isotopic mass distributions for the polymer chains, having the assigned end groups, to those theoretically calculated. It is evident that there is an excellent correlation.

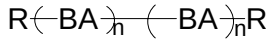

**(1)** Bimolecular Termination

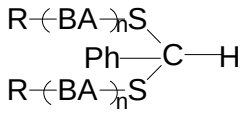

**2(a)**

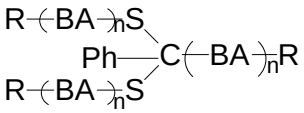

**2(b)**

**(2)** Termination of Intermediate radical with a proton **(a)** and a propagating polymeric chain **(b)** [Leads to the formation of a 3 arm star polymer in case of 2(b)].

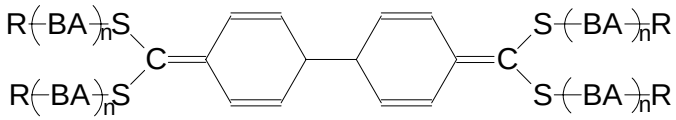

**3(a)**

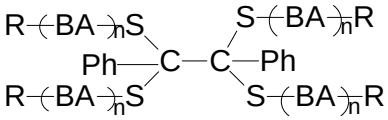

**3(b)**

**(3)** Cross termination of 2 Intermediate radicals. It can occur either through the phenyl activating group **(a)** or via the carbon centered radical **(b)**, resulting in the formation of 4 arm star polymers.

where,

**Ph –** Phenyl (it is the activating group in the cumyl dithiobenzoate).

**R –** could be **(a)** Cumyl, **(b)** 2-cyanoisopropyl or **(c)** ethyl isobutyryl group, derived from the RAFT agent, AIBN and EBriB (ATRP initiator) respectively.

**(a)** Cumyl **(Cu)**

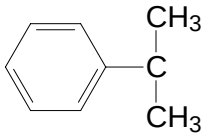

**(b)** 2-cyanoisopropyl **(CiP)**

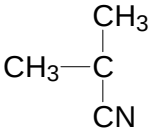

**(c)** ethyl isobutyryl **(EiB)**

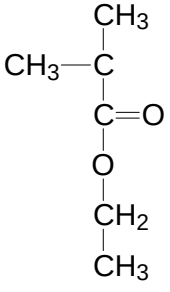

**Figure 5.19:** Overview of possible terminated polymeric products.

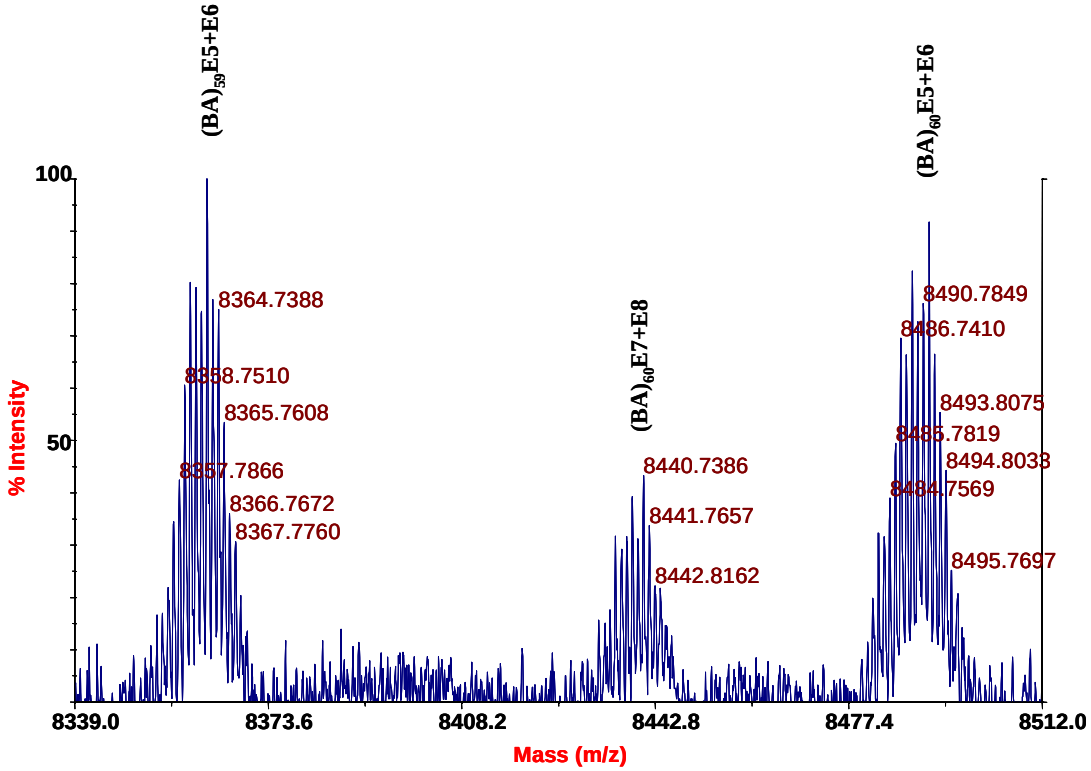


**Figure 5.20:** Expansion of the MALDI-TOF-MS spectrum from Figure 5.18, for the fractionated polymer in the high mass region. [Spectrum acquired in Reflector mode, Matrix : DCTB].

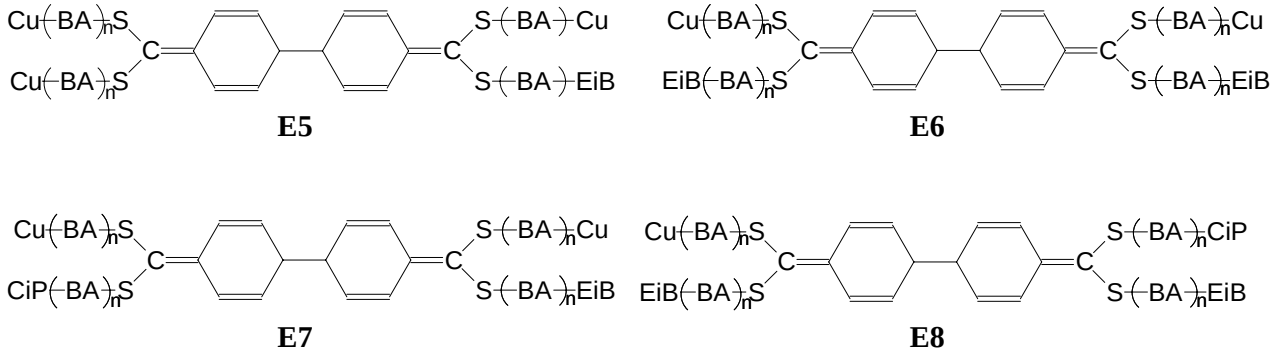


where, **Cu** – Cumyl; **CiP** - 2-cyanoisopropyl; **EiB** - ethyl isobutyryl; derived from the RAFT agent, AIBN and EBriB (ATRP initiator) respectively. For structures please refer to Figure 5.19. ***Cation – Na*$^+$.**

**Figure 5.21:** Observed 4 arm star terminated polymeric products. (The end group arrangement within each structure need not be in the same order, but for sake of simplicity it is depicted in this way).

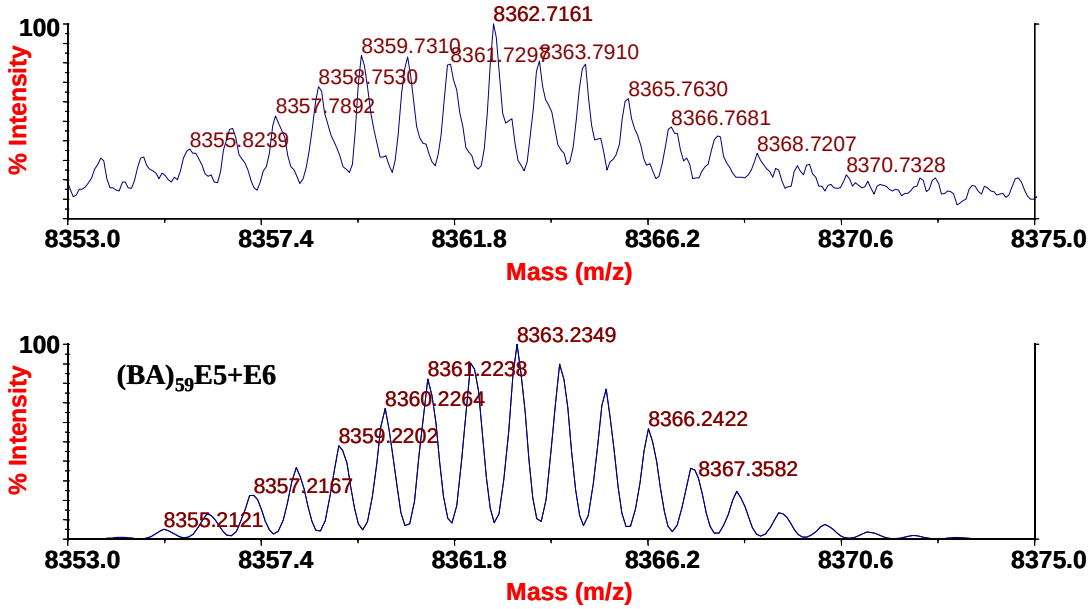


**Figure 5.22:** Detail of the MALDI-TOF-MS spectrum of fractionated polymer in the high mass region. Overlapping polymeric chains with end groups **E5** and **E6** (see Fig. 5.21). Isotopic mass distributions : Observed (above) and Theoretical (below). The ratio of the intensities for the distributions having end groups E5 and E6 is 2/1, respectively.

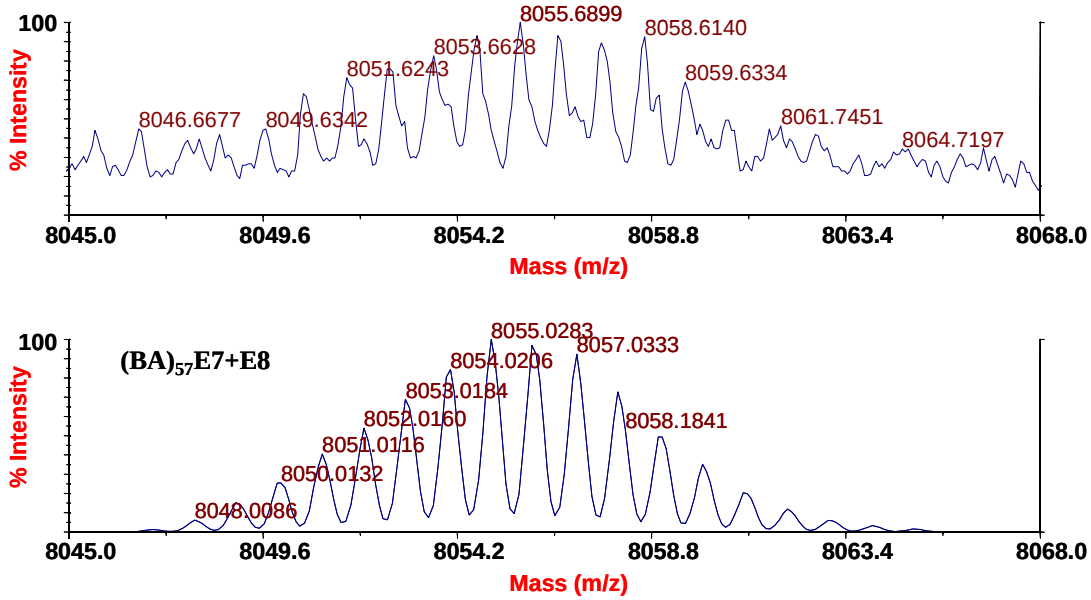


**Figure 5.23:** Detail of the MALDI-TOF-MS spectrum of fractionated polymer in the high mass region. Overlapping polymeric chains with end groups **E7** and **E8** (see Fig. 5.21). Isotopic mass distributions : Observed (above) and Theoretical (below). The ratio of the intensities for the distributions having end groups E7 and E8 is 2/1, respectively.

Now, as explained previously, the PBA-Br was activated by the CuBr/PMDETA complex, to form the PBA propagating radical. This will add to the PBA-RAFT to form the intermediate radical. Hence, the EiB (originating from the ATRP initiator) can clearly exist as one of the primary end groups. Further, the ratio of [PBA-RAFT]/[PBA-Br] in the present reaction was maintained at 4/1. Therefore, it is not surprising to see that the isotopic distributions for the structures, which predominantly have the cumyl end groups (E5), had the highest intensity. From Figures 5.10 and 5.11(b), for the synthesized PBA-RAFT, it was observed that a few chains were initiated by the cyanoisopropyl (CiP) radical, originating from AIBN. Hence, the polymeric chains with the CiP end group are also observed. But the intensity and presence of these chains were quite low in the starting PBA-RAFT itself. Hence, it is not surprising that the intensity of the distribution, possessing polymeric chains having the CiP end group, is lower, as observed in Figure 5.20.

Figure 5.24 is an expansion of the Figure 5.18 in the middle mass range (mass range ~ 4000-6000 Da). In this case too, there seem to be two distinct distributions, having broad isotopic patterns. The reason for the broad distributions, has already been discussed previously. The polymeric chains in the mass range of 4000 Da would be expected to result either from bimolecular termination between propagating radicals [Figure 5.19 (1)] or from termination of the intermediate radical with a proton [Figure 5.19(2a)] ($2 \times 2000 = 4000$). But, it was not possible to assign the observed peaks using the expected structures resulting from the above reactions. Interestingly, the peaks in this region were ascribed to the structures originating from the termination of the intermediate radical with a propagating polymeric radical, resulting in the formation of a 3 arm star polymer [Figure 5.19 (2b)]. In hindsight, the intermediate radical concentration for the BA systems is in the order of $10^{-6}$ M (as determined from the ESR experiments), which is at least an order or two higher than the propagating radical concentration. Thus, there is a higher probability for termination to occur via the intermediate radical. But, the resulting 3 arm star polymer distribution should have a maximum in the mass range of ~6000 Da ($3 \times 2000 = 6000$). Hence, this observation is indeed puzzling. But, since the other possible and plausible end groups did not fit the observed masses, coupled with the high concentration for the intermediate radicals, the possibility then only narrows down to the 3 arm star polymers, since in the absence of monomer, there is no other option. Figure 5.25 depicts the structures to which the current peaks have been assigned. Figures 5.26 and 5.27 clearly compare the isotopic mass distributions for the polymer chains having the assigned end groups to those theoretically calculated. As is evident there is an excellent correlation. In this case too, the intensities decrease in the series Cu > EiB > CiP.

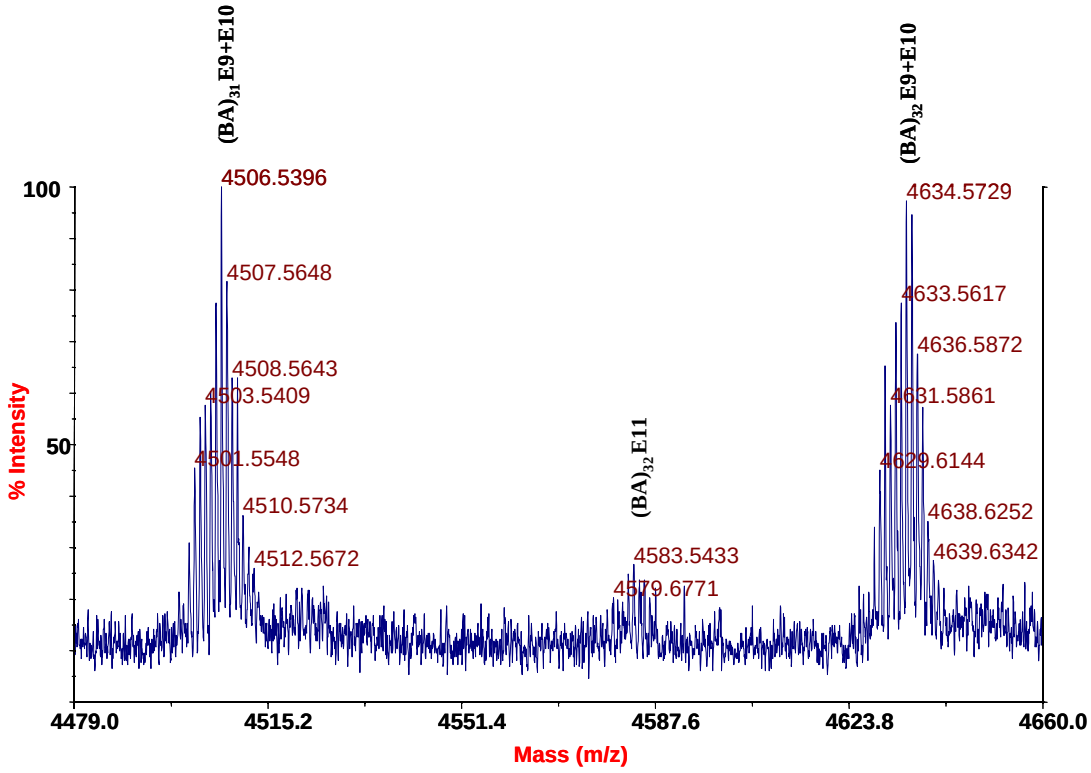


**Figure 5.24:** Expansion of the MALDI-TOF-MS spectrum from Figure 5.18, for the fractionated polymer in the middle mass region. [Spectrum acquired in Reflector mode, Matrix : DCTB].

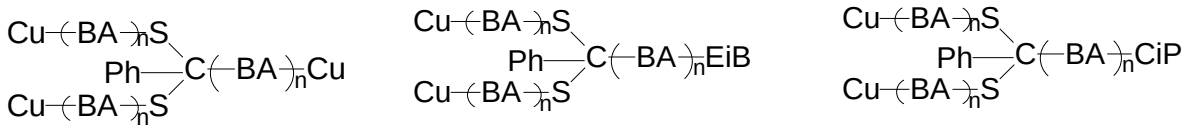


**E9** **E10** **E11**

where, **Cu** – Cumyl; **CiP** - 2-cyanoisopropyl; **EiB** - ethyl isobutyryl; derived from the RAFT agent, AIBN and EBriB (ATRP initiator) respectively. For structures please refer to Figure 5.19. ***Cation – Na*$^+$.**

**Figure 5.25:** Observed 3 arm star terminated polymeric products. (The end group arrangement within each structure need not be in the same order, but for sake of simplicity it is depicted in this way).

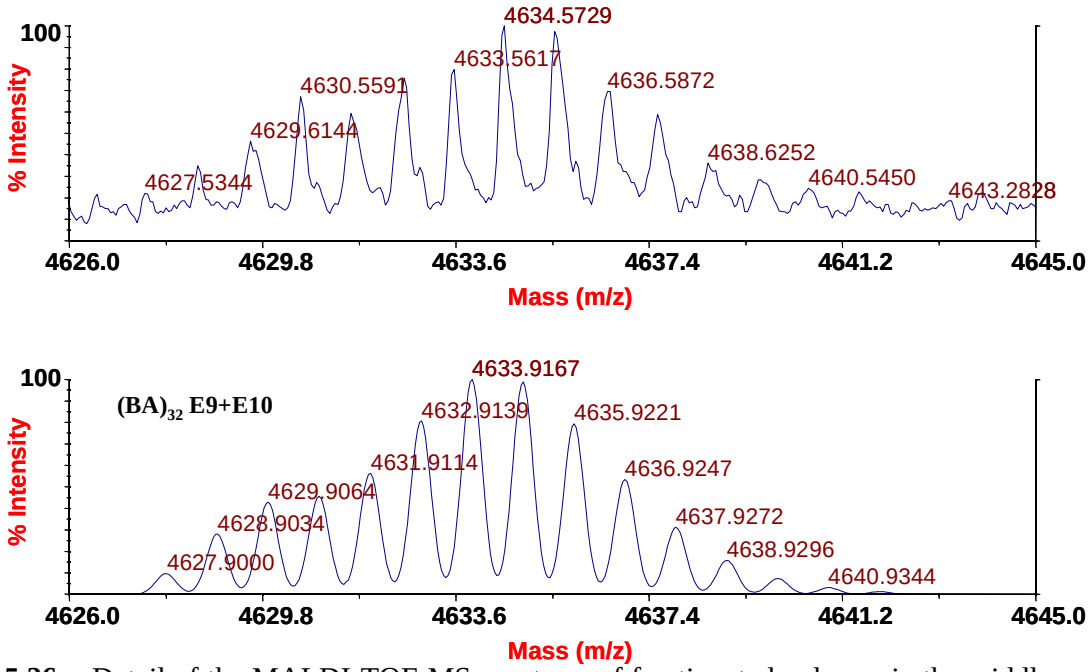


**Figure 5.26:** Detail of the MALDI-TOF-MS spectrum of fractionated polymer in the middle mass region. Overlapping polymeric chains with end groups **E9** and **E10** (see Fig. 5.25). Isotopic mass distributions : Observed (above) and Theoretical (below). The ratio of the intensities for the distributions having end groups E9 and E10 is 2/1, respectively.

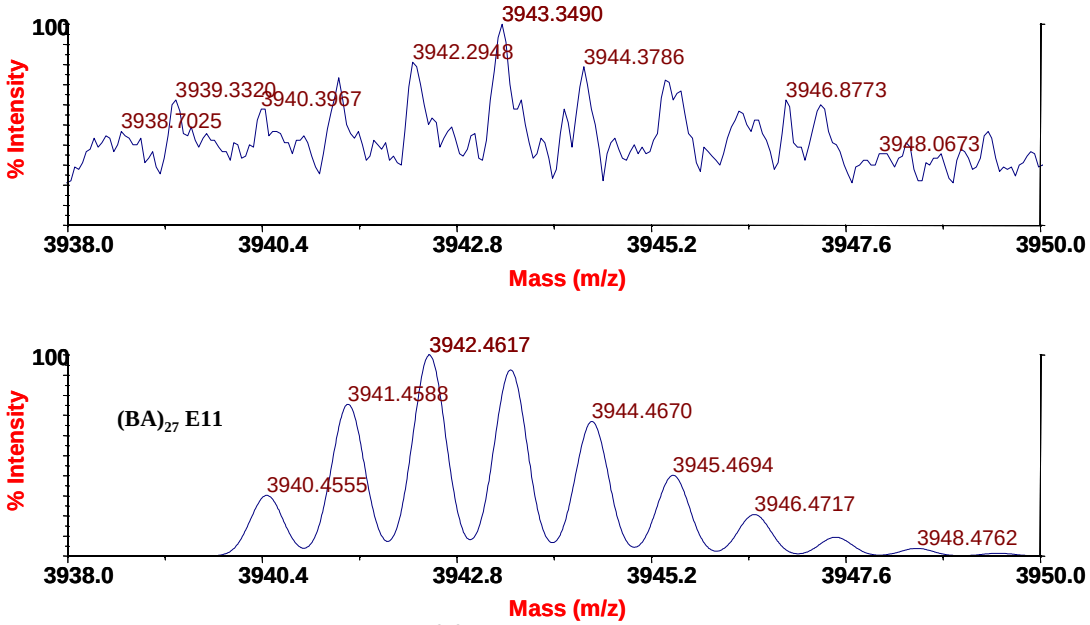


**Figure 5.27:** MALDI-TOF-MS spectrum of fractionated polymer in the middle mass region, with end groups **E11** (see Fig. 5.25). Isotopic mass distributions : Observed (above) and Theoretical (below).

Figure 5.28 gives an insight into the intensity of the distributions for the observed terminated species, having the various end groups in the MALDI-TOF-MS spectrum for the fractionated polymer (Figure 5.18). It is very difficult to plot the individual intensities for the overlapping isotopic distributions. Hence the intensities from the overlapping series are plotted together, taking into account the most prominent peak in that particular series (e.g. E5 + E6, E7 + E8 and E9 + E10). As is evident from the plot, **(i)** there is minimal overlap between the peaks in the different mass ranges. This clearly indicates that the terminated species present in the two series were obtained as a result of different termination pathways. That is to say, the terminated species obtained in the high mass range (~ 8000 Da) resulted due to termination between two intermediate radicals and in the middle mass range (~ 4000 – 6000 Da) termination was due to the cross termination of the intermediate radical with a propagating macro-radical. **(ii)** The intensities for all the observed series decreased in the order Cu > EiB > CiP (see Figure 5.25). **(iii)** There is another series, which is present between the mass ranges of 6000 – 8000 Da. This series has a very low intensity and the resolution for the same was quite poor for clear isotopic distribution and peak identification. The mass of this series is slightly lower than that for a 4 arm star polymer, so it might well be a 3 arm star polymer. The terminated products with 3 Cu end groups have already been accounted for (Figure 5.25). So the only possibility might be a 3 arm star polymer with 3 EiB groups, since 3 × 2400 = 7200. [For possible structure, see Figure 5.19 (2b), where R is now EiB].

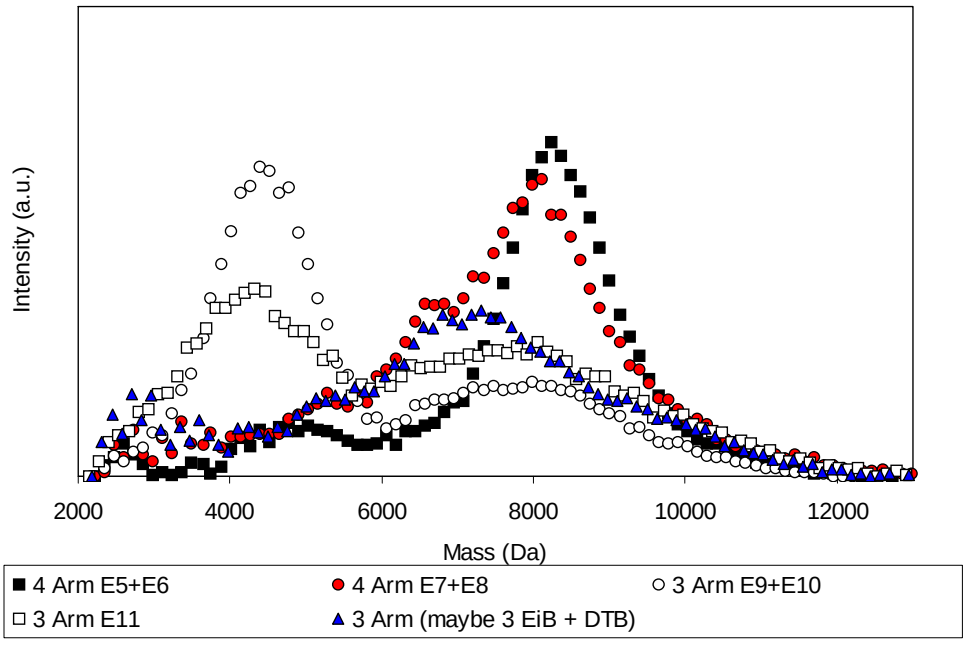


**Figure 5.28:** Plot of the intensities of the distributions for the observed terminated species, having the various end groups in the MALDI-TOF-MS spectrum (Figure 5.18).

## *5.5 Conclusion*

ESR was employed to determine the intermediate radical concentration for AIBN initiated and cumyl dithiobenzoate mediated BA and Sty polymerizations. It was determined that the intermediate radical concentration during the BA polymerization was an order of magnitude higher as compared to that for Sty. The reason is attributed to the faster fragmentation rate of the formed intermediate radicals in the Sty system, which is ascribed to the increased stability of the styrene radical due to resonance, as opposed to the BA radical. Hence, Sty is a better leaving group. In the BA systems, the formed intermediate radicals are detected at long reaction times in the virtual absence of the initiator. High - resolution ESR spectra for the RAFT intermediate radical for the BA and Sty systems at 0 °C were obtained. This assists in the detailed structure analysis.

A successful combination of SEC and MALDI-TOF-MS techniques was employed, to study and understand the termination reactions occurring (if any) during the RAFT process. First, the cumyl dithiobenzoate mediated BA polymerization was investigated, where products from the polymeric RAFT agent and polymeric chains initiated by the 2-cyanoisopropyl radical (derived from AIBN) were identified. Further, model reactions using the synthesized PBA-RAFT with AIBN were performed. The intensity of the peaks, corresponding to polymer chains still bearing the dithiobenzoate RAFT moiety as the terminal end group, clearly decreased as the concentration of AIBN was increased. Thus the central equilibrium in the RAFT process occurred. More interestingly, the intensity of the chains with the unassigned end group E4 clearly increases. The clear increase in intensity reflects that, the unassigned peak most probably results due to termination reaction(s) occurring during the RAFT process. But, the preferred mode of termination still remained unanswered at this point.

So as to overcome the limitations of the AIBN system, *"the ATRP-way"* of creating radicals using model compounds was investigated. PBA-Br was chosen as the model compound. The MALDI-TOF-MS spectra of the fractionated polymer, clearly prove the formation of the 4 arm and 3 arm star polymers, which resulted from the termination of the BA intermediate radical, formed during the RAFT process, with another intermediate radical or a propagating macro-radical. More importantly, structures were assigned to the terminated products. The intensities of the observed distributions decreased in the order of the end group Cu > EiB > CiP.

This work clearly indicates that indeed, the intermediate radicals formed during the cumyl dithiobenzoate mediated BA polymerization result in stable and long living intermediate radicals.

But at the same time, these intermediate radicals are also prone to termination, resulting in the formation of 3 and 4 arm star polymers. Thus, for the present system, a combination of the two events may contribute to the retardation, which is normally observed during the RAFT polymerizations.

## *5.6 References*


1) Le, T. P., Moad, G., Rizzardo, E., Thang, S. H.; *PCT Int Appl*., **1998**, WO98/01478.

2) Moad, G., Chiefari, J., Chong, Y. K., Krstina, J., Mayadunne, R. T. A., Postma, A., Rizzardo, E., Thang, S. H.; *Polym. Int*., **2000**, *49*, 993.

3) McLeary, J. B., Calitz, F. M., McKenzie, J. M., Tonge, M. P., Sanderson, R. D., Klumperman, B.; *Macromolecules*, ACS ASAP.

4) Barner-Kowollik, C., Quinn, J. F., Morsley, D. R., Davis, T. P., *J. Polym. Sci., Part A: Polym. Chem.*, **2001**, *39*, 1353.

5) Barner-Kowollik, C., Quinn, J. F., Uyen Nguyen, T. L., Heuts, J. P. A., Davis, T. P.; *Macromolecules*, **2001**, *34*, 7849.

6) Coote, M. L., Radom, L., *J. Am. Chem. Soc.*; **2003**, *125*, 1490.

7) Monteiro, M. J., de Brouwer, H.; *Macromolecules*, **2001**, *34*, 349.

8) Kwak, Y., Goto, A., Tsujii, Y., Murata, Y., Komatsu, K., Fukuda, T.; *Macromolecules*, **2002**, *35*, 3026.

9) Wang, A. R., Zhu, S.; *Macromol. Theory Simul.*; **2003**, *12*, 196.

10) Calitz, F. M., McLeary, J. B., McKenzie, J. M., Tonge, M. P., Klumperman, B., Sanderson, R. D., *Macromolecules*, **2003**, *36*, 9687.

11) Schilli, C., Lazendoerfer, M., Müller, A. H. E.; *Macromolecules*, **2002**, *35*, 6819.

12) Ganachaud, F., Monteiro, M. J., Gilbert, R. G., Dourges, M-A., Thang, S. H., Rizzardo, E.; *Macromolecules*, **2000**, *33*, 6738.

13) Destarac, M., Charmot, D., Franck, X., Zaed, S. Z.; *Macromol. Rapid Commun.*, **2000**, *21*, 1035.

14) Beuermann, S.; Paquet, D. A., Jr.; McMinn, J. H.; Hutchinson, R. A.; *Macromolecules*, **1996**, *29*, 4206.

15) Barner-Kowollik, C., Coote, M. L., Davis, T. P., Radom, L., Vana, P.; *J. Polym. Sci., Part A: Polym. Chem.*, **2003**, *41*, 2828.

16) Wang, A. R., Zhu, S., Kwak, Y., goto, A., Fukuda, T., Monteiro, M. J; *J. Polym. Sci., Part A: Polym. Chem.*, **2003**, *41*, 2833.

17) Kamachi, M., *J. Polym. Sci., Part A: Polym. Chem.*, **2002**, *40*, 269.

18) Hawthorne, D. G., Moad, G., Rizzardo, E., Thang, S.H.; *Macromolecules*, **1999**, *32*, 5457.

19) Alberti, A., Benaglia, M., Laus, M., Macciantelli, D., Sparnacci, K.; *Macromolecules*, **2003**, *36*, 741.

20) Du, F-S., Zhu, M-Q., Guo, H-Q., Li, Z-C., Li, F-M, Kamachi, M., Kajiwara, A.; *Macromolecules*, **2002**, *35*, 6739.

21) Calitz, F. M., Tonge, M. P., Sanderson, R. D.; *Macromolecules*, **2003**, *36*, 5.

22) Toy, A. A., Vana, P., Davis, T. P., Barner-Kowollik, C.; *Macromolecules*, **2004**, *37*, 744.

# Chapter 6

## *Copolymerization of allyl butyl ether (ABE) with acrylates via controlled radical polymerization*

**Abstract:** The atom transfer radical copolymerization (ATRP) and reversible addition-fragmentation chain transfer (RAFT) polymerization of acrylates (methyl acrylate, MA and butyl acrylate, BA) with allyl butyl ether (ABE) was investigated. Well-controlled copolymers constituting almost 20 mol% of ABE were obtained using ethyl-2-bromoisobutyrate (EBriB) as initiator. Narrow molar mass distributions (MMDs) were obtained for the ATRP experiments. The comparable free radical (co)polymerizations (FRP) resulted in broad MMDs. Increasing the fraction of ABE in the monomer feed led to an increase in the level of incorporation of ABE in the copolymer, at the expense of the overall conversion. Similarly, the RAFT copolymerizations using S,S'-bis(α,α'-dimethyl-α''-acetic acid)trithiocarbonate also resulted in excellent control on the polymerization with significant incorporation of ABE within the copolymer chains. The formation of the copolymer was confirmed using matrix assisted laser desorption / ionization – time of flight – mass spectrometry (MALDI-TOF-MS). From the obtained MALDI-TOF-MS spectra for the ATRP and RAFT systems, it was evident that several units of ABE were incorporated into the polymer chain. This was attributed to the rapidity of crosspropagation of ABE-terminated polymeric radicals with acrylates. This further indicated that ABE is behaving as a comonomer, and not simply as a chain transfer agent under the employed experimental conditions.

## *6.1 Introduction*

An elegant way to modify polymer properties is by the introduction of polar functional groups into an otherwise non-polar material.[1] Hence, the realm of olefin copolymerization especially with polar vinyl monomers is an area of intense research in polymer chemistry.

From the free-radical perspective, the homopolymerization of allylic monomers like allyl acetate or allyl butyl ether is very unlikely and if it does occur, it polymerizes at rather low rates. This effect is a consequence of degradative chain transfer, wherein, the propagating radical in such a polymerization is very reactive, while the allylic C-H in the monomer is quite weak, resulting in chain transfer to monomer. The weakness of the allylic C-H bond arises from the high resonance stability of the allylic radical that is formed. This formed allylic radical is too stable to reinitiate

---

Venkatesh, R., Vergouwen, F., Klumperman, B.; *J. Polym. Sci., Part A: Polym. Chem.*, In Press.

polymerization and will undergo termination by reaction with another allylic radical or more likely, with propagating radicals.[2] Recently, it is was observed that allyl ethyl ether acts as a strong retarder for the polymerization of methyl methacrylate initiated at 60 ºC by α,α'-azobisisobutyronitrile.[3]

This paper is a detailed study on the copolymerization of allyl butyl ether (ABE) with acrylates (methyl acrylate, MA and butyl acrylate, BA) using different free radical techniques. Comparison of reaction kinetics between conventional free radical polymerization (FRP) and atom transfer radical polymerization (ATRP) was carried out. A heterogeneous transition metal/ligand system is employed for the ATR polymerizations. The effect of monomer feed composition and influence of ABE on the radical polymerization was investigated. Further, the reversible addition-fragmentation chain transfer (RAFT) technique was also employed for the copolymerization reactions. So as to initiate the RAFT reactions, normal free radical thermal initiators (like α,α'-azobisisobutyronitrile) are employed, hence there was a large probability that the copolymerization, if occurring, may not be controlled, since chain transfer and termination events dominate during free radical polymerization. The incorporation of ABE in the copolymer chains was confirmed using mass spectrometry.

Controlled radical techniques have revolutionized free radical polymerization because it allows for the generation of macromolecular architectures such as comb, block, and star copolymers having narrow MMD. In recent years, controlled radical techniques have been employed for the (co)polymerization of monomers which always had been thought of as improbable to polymerize via a radical mechanism.[4,5,6] ATRP[7,8,9,10] is one of the techniques employed to obtain living (or controlled) radical polymerization. In copper mediated ATRP, the carbon-halogen bond of an alkyl halide (RX) is reversibly cleaved by a $Cu^{I}X$/ligand system resulting in a radical (R*) and $Cu^{II}X_2$/ligand (deactivator). The radical will mainly either reversibly deactivate, add monomer or irreversibly terminate (Scheme 6.1).

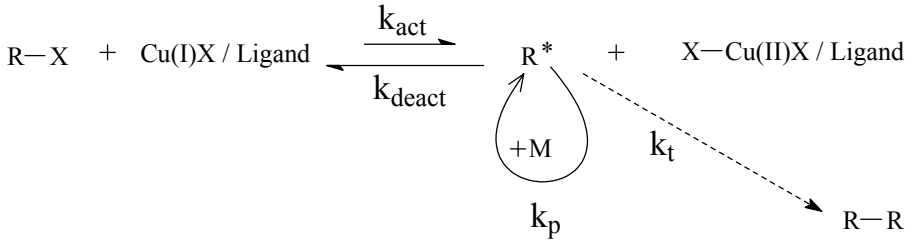


**Scheme 6.1:** ATRP Mechanism

The RAFT process is a highly versatile controlled radical polymerization technique that can be applied to most monomers, which can be polymerized under free radical conditions.[11,12,13,14,15,16,17] The RAFT process relies on the rapid central addition-fragmentation equilibrium between propagating and intermediate radicals, and chain activity and dormancy, as shown in Scheme 6.2.

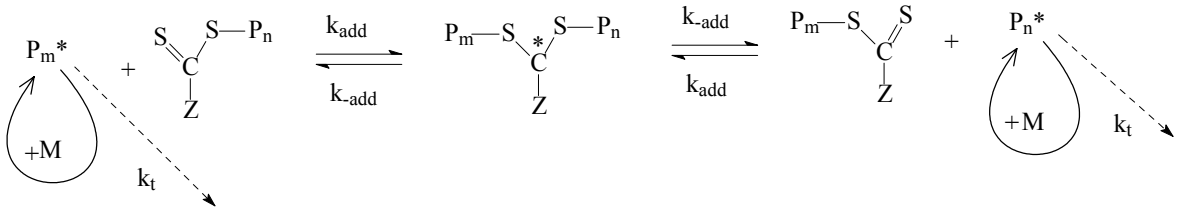


**Scheme 6.2:** RAFT Mechanism

Matrix assisted laser desorption/ionization – time of flight – mass spectrometry (MALDI-TOF-MS) technique, size exclusion chromatography and NMR are employed for polymer characterization. Mass spectrometry techniques provide the sensitivity and resolution, together with structural information to determine even the smallest amount of product. For low molar mass polymers, the determination of end groups is possible, which provides valuable information on the reaction mechanism. In the past, MALDI-TOF-MS has been employed to study ATRP and RAFT generated polymers.[18,19,20,21,22,23]

## *6.2 Experimental Section*

### *6.2.1 Materials*

Methyl acrylate (MA, Merck, 99+%), butyl acrylate (BA, Merck, 99+%) and allyl butyl ether (ABE, Aldrich, 98%) were distilled and stored over molecular sieves at –15 ºC. *p*-Xylene (Aldrich, 99+% HPLC grade) and methyl ethyl ketone (Aldrich, 99+% HPLC grade) was stored over molecular sieves and used without further purification. N,N,N',N'',N''-pentamethyldiethylenetriamine (PMDETA, Aldrich, 99%), ethyl-2-bromoisobutyrate (EBriB, Aldrich, 98%), copper (I) bromide (CuBr, Aldrich, 98%), copper (II) bromide ($CuBr_2$, Aldrich, 99%), aluminum oxide (activated, basic, for column chromatography, 50-200 μm), tetrahydrofuran

(THF, Aldrich, AR), 1,4-dioxane (Aldrich, AR) were used as supplied. α,α'-Azobisisobutyronitrile (AIBN, Merck, >98%) was recrystallized twice from methanol before use. The RAFT agent S,S'-bis(α,α'-dimethyl-α''-acetic acid)trithiocarbonate was synthesized as described in literature.[24]

## *6.2.2 Analysis and Measurements*

***6.2.2.1 Determination of Conversion and MMD:*** Monomer conversion was determined from the concentration of the residual monomer measured via gas chromatography (GC). A Hewlett-Packard (HP-5890) GC, equipped with a HP Ultra 2 cross-linked 5% Me-Ph-Si column (25 m × 0.32 mm × 0.52 μm) was used. *p*-Xylene was employed as the internal reference. The GC temperature program used is given in Figure 6.1.

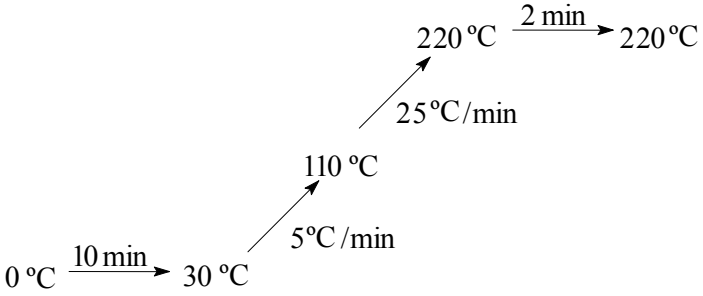


**Figure 6.1:** GC temperature program.

Molar mass (MM) and molar mass distributions (MMD) were measured by size exclusion chromatography (SEC), at ambient temperature using a Waters GPC equipped with a Waters model 510 pump and a model 410 differential refractometer (40 ºC). THF was used as the eluent at a flow rate of 1.0 mL/min. A set of two mixed bed columns (Mixed-C, Polymer Laboratories, 30 cm, 5 μm bead size, 40 ºC) was used. Calibration was carried out using narrow MMD polystyrene (PS) standards ranging from 600 to $7 \times 10^6$ g/mol. The molecular weights were calculated using the universal calibration principle and Mark-Houwink parameters [25] [PMA: $K = 1.95 \times 10^{-4}$ dL/g, a = 0.660; PBA: $K = 1.22 \times 10^{-4}$ dL/g, a = 0.700; PS: $K = 1.14 \times 10^{-4}$ dL/g, a = 0.716]. Molecular weights were calculated relative to the relevant homopolymer (in this case PMA or PBA). Data acquisition and processing were performed using Waters Millenium 32 software.

***6.2.2.2 NMR:*** $^1$H nuclear magnetic resonance (NMR) spectra were recorded on a Varian 400 spectrometer in deuterated chloroform ($CDCl_3$) at 25 ºC. All chemical shifts were reported in ppm downfield from tetramethylsilane (TMS), used as an internal standard ($\delta = 0$ ppm).

***6.2.2.3 MALDI-TOF-MS:*** Measurements were performed on a Voyager-DE STR (Applied Biosystems, Framingham, MA) instrument equipped with a 337 nm nitrogen laser. Positive-ion spectra were acquired in reflector mode. DCTB (trans-2-[3-(4-tert-butylphenyl)-2-methyl-2-propenylidene]malononitrile) was chosen as the matrix. Potassium trifluoracetate (Aldrich, 98%) or sodium trifluoracetate (Aldrich, 98%) was added as the cationic ionization agent. The matrix was dissolved in THF at a concentration of 40 mg/mL. Potassium trifluoracetate was added to THF at a concentration of 1 mg/mL. The dissolved polymer concentration in THF was approximately 1 mg/mL. In a typical MALDI experiment, the matrix, salt and polymer solutions were premixed in the ratio: 5 μL sample: 5 μL matrix: 0.5 μL salt. Approximately 0.5 μL of the obtained mixture was hand spotted on the target plate. For each spectrum 1000 laser shots were accumulated.

## *6.3 Synthetic Procedures*

***6.3.1 ATRP Copolymerization of MA and ABE:*** A typical polymerization was carried out in a 50 mL three-neck round-bottom flask. *p*-Xylene (11.5 g, 0.10 mol), MA (2.3 g, 0.03 mol), ABE (3.1 g, 0.03 mol), Cu(I)Br (0.107 g, 0.75 mmol) and Cu(II)$Br_2$ (0.018 g, 0.08 mmol) were accurately weighed, and transferred to the flask. The ligand, PMDETA (0.14 g, 0.83 mmol) was then added. After the reaction mixture was bubbled with argon for 30 min, the flask was immersed in a thermostated oil bath kept at 80 ºC and stirred for 10 min. A light green, slightly heterogeneous system was then obtained. The initiator, EBriB (0.32 g, 1.6 mmol) was added slowly via a degassed syringe. The reactions were carried out under a flowing argon atmosphere. Samples were withdrawn at suitable time periods throughout the polymerization. A pre-determined amount of the sample was transferred immediately after withdrawal into a GC vial and diluted with 1,4-dioxane, so as to determine the monomer conversion using GC. The remaining sample was diluted with THF, passed through a column of aluminum oxide prior to SEC and MALDI-TOF-MS measurements.

### *6.3.2 RAFT Copolymerization of BA and ABE:*

The RAFT agent S,S'-bis(α,α'-dimethyl-α''-acetic acid)trithiocarbonate (0.11 g; 0.4 mmol) and AIBN (30 mg; 0.02 mmol) were accurately weighed and then transferred to a 25 mL three-neck round-bottom flask. Then a solution of *p*-xylene (3.6 g, 0.03 mol), BA (0.94 g, 7.3 mmol) and ABE (0.84 g, 7.3 mmol) was added. Methyl ethyl ketone (3.42 g, 0.04 mol) was added to totally solubilize the RAFT agent and make the system homogeneous. After the reaction mixture was bubbled with argon for 30 min, the flask was immersed in a thermostated oil bath kept at 80 ºC. The reaction was carried out under a flowing argon atmosphere. A second batch of initiator AIBN (30 mg; 0.02 mmol) was added after two hours of reaction time during the copolymerization. Samples were withdrawn at suitable time periods throughout the polymerization. The sample was immediately diluted with THF. Some of this diluted sample was transferred immediately into a GC vial and further diluted with THF, so as to determine the monomer conversion using GC. The remaining sample was used for SEC and MALDI-TOF-MS measurements.

## *6.4 Results and Discussion*

### *6.4.1 Copolymerization of MA/ABE:*

AIBN-initiated and ATR copolymerizations of MA and ABE were examined as summarized in Table 6.1.

**Table 6.1:** Copolymers of MA/ABE

| Entry | $f_{ABE}$ (mol fraction) | $F_{ABE}$ (mol fraction)[d] | Overall conversion | $M_n$ (g/mol) | PDI ($M_w/M_n$) |
|---|---|---|---|---|---|
| 1[#,a] | 0.25 | 0.10 | 0.80 | $5.2 \times 10^3$ | 3.0 |
| 2[#,b] | 0.50 | 0.22 | 0.60 | $3.4 \times 10^3$ | 2.4 |
| 3[*,c] | 0.25 | 0.09 | 0.73 | $2.2 \times 10^3$ | 1.25 |
| 4[*,c] | 0.50 | 0.20 | 0.51 | $1.5 \times 10^3$ | 1.25 |

*-ATRP reactions; #-Free radical polymerization (FRP). For FRP reactions, AIBN is used as initiator. Reaction temperature = 80 ºC. Volume {solvent}/{monomer}=1/0.5.

***a)*** AIBN (5 mmol/L); Reaction time = 25 hrs 30 mins. ***b)*** AIBN (3 mmol/L); Reaction time = 32 hrs.

***c)*** Targeted $M_n$ = 3000 g/mol; [monomer]:[EBriB]:[CuBr]:[PMDETA] = 32:1:0.5:0.5; Reaction time = 24 hrs.

***d)*** Calculated from monomer conversion as measured by GC and confirmed by proton NMR.

From the data in Table 6.1, several observations can be made **(i)** ABE does copolymerize via a free radical mechanism. Homopolymerization of ABE was attempted in both FRP and ATRP, but no polymer was obtained. The reason for this is that allylic monomers undergo degradative chain transfer of allylic hydrogens.[2] The stable allylic radical derived from the monomer is slow to reinitiate and prone to terminate. **(ii)** It is known that the polymerization of acrylates occurs readily by free-radical polymerization to yield high-MM homopolymers.[26] The copolymerizations under FRP conditions, show relatively low MM. This indicates that allyl butyl ether acts as a chain transfer agent for the free radical polymerization. **(iii)** The experimentally determined MM in the case of polymerizations under ATRP conditions coincide nicely with the calculated values (Figure 6.2). The linearity clearly indicates that there were a constant number of growing chains during the polymerization. **(iv)** Narrow MMDs were obtained in the ATRP experiments, which points at conventional ATRP behavior, i.e. no peculiarities caused by the incorporation of ABE. **(v)** As the fraction of ABE is increased in the monomer feed, its incorporation is higher in the copolymer (*compare entries 1 & 2, 3 & 4*). Two effects can cause this phenomenon. Due to composition drift, the fraction of ABE in the remaining monomer increases, which leads to a decrease in the average propagation rate constant. When the fraction of ABE increases, the probability of endcapping a ABE moiety at the chain end with a bromide increases. When this happens the chain would be expected to be virtually inactive, since there are no substituent groups in ABE to stabilize the formed radical. Hence, the ATRP equilibrium prefers to be on the dormant side. Thus, a higher fraction of the ABE in the monomer feed, results in lower overall conversion in conjunction with lower MM (*compare entries 1 & 2, 3 & 4*). **(vi)** The observation in Figure 6.3 that the rates of polymerization in ATRP and in conventional FRP are nearly identical is largely a coincidence. The more or less arbitrary choice of polymerization conditions (temperature and exact recipe) happens to be such that this coincidence occurs.* However, the fact that the ratios at which the two comonomers are consumed seem to be in close agreement (Table 6.1) points to a great similarity between the reactivity ratios for both polymerization techniques.

*[* The indication "more or less arbitrary … polymerization conditions" does not refer to the selection of the conditions. It is just meant as an indication that the coincidence of the conversion - time curves is a result of the chosen conditions, which have not deliberately been tuned to cause this coincidence of conversion – time plots]*

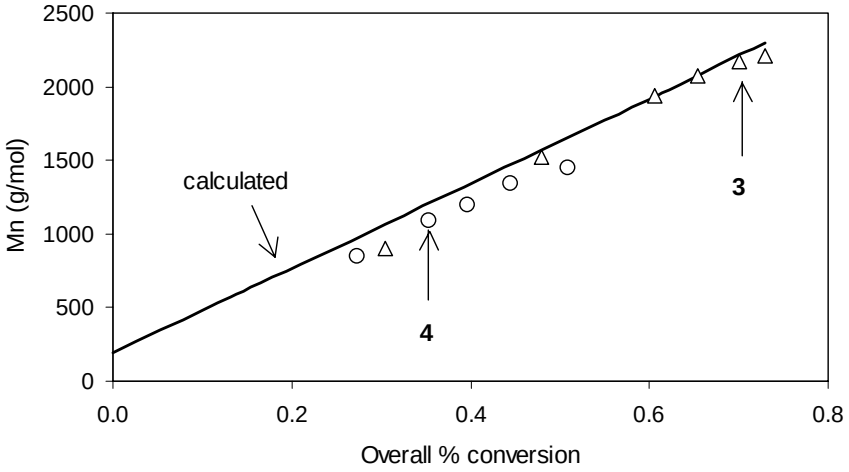


**Figure 6.2:** Plot of $M_n$ vs overall fractional conversion. Legends : (3) $f_{ABE} = 0.25$. (4) $f_{ABE} = 0.50$ (For details see Table 6.1). $M_n$ calculated = $M_{initiator}$ + [(($M_{MA}$ × ($[MA]_0$ / $[I]_0$)) × MA monomer conversion) + (($M_{ABE}$ × ($[ABE]_0$ / $[I]_0$)) × ABE monomer conversion)].

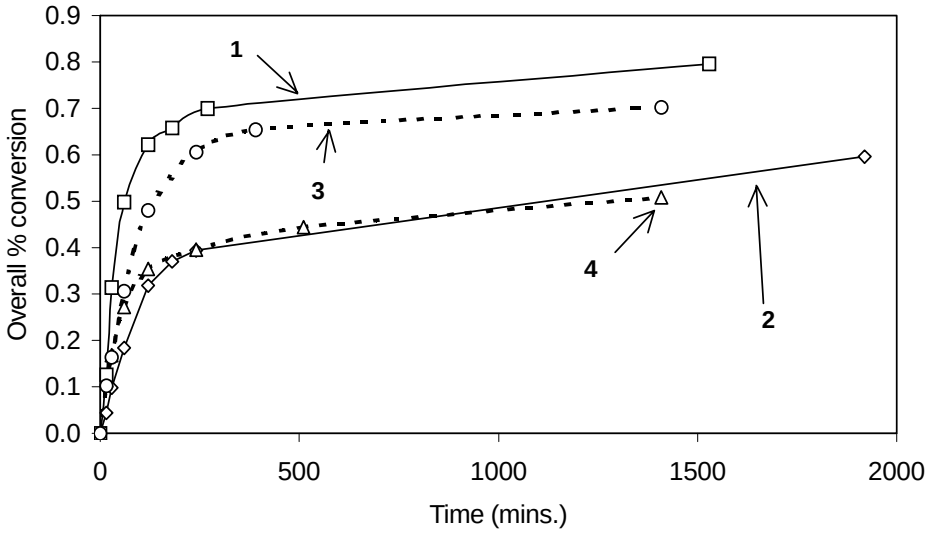


**Figure 6.3:** Plot of overall monomer conversion versus time for the copolymerizations. Legends : (1) FRP: $f_{ABE}$ = 0.25 (2) FRP: $f_{ABE}$ = 0.50. (3) ATRP: $f_{ABE}$ = 0.25. (4) ATRP: $f_{ABE}$ = 0.50. (For details see Table 6.1).

### *6.4.2 RAFT Copolymerization of BA/ABE:*

RAFT copolymerizations of BA and ABE were also examined as summarized in Table 6.2. S,S'-bis(α,α'-dimethyl-α''-acetic acid)trithiocarbonate was used as the RAFT agent because (1) it has a high chain transfer efficiency which results in good control over the radical polymerization,[24] (2) the leaving group is the

isobutyric acid group and it is known from literature that well controlled poly(butyl acrylate) can be synthesized using this group as the initiating species,[24] (3) telechelic carboxylic acid terminated polymers are obtained.

The RAFT copolymerizations result in significant incorporation of ABE into the polymer chain coupled with narrow MMDs. From Figure 6.4, the almost linear increase of $M_n$ as a function of monomer conversion is indicative of the fact, that there are a constant number of growing chains during the polymerization. As previously observed for the ATRP and FRP systems, a higher fraction of ABE in the monomer feed results in lower overall conversion coupled with lower MM.

**Table 6.2:** RAFT Copolymerization of BA/ABE

| Entry | $f_{ABE}$ | $F_{ABE}$[a] | Overall conversion | Mn (g/mol) | PDI ($M_w/M_n$) |
|---|---|---|---|---|---|
| 1 | 0.25 | 0.07 | 0.63 | $2.7 \times 10^3$ | 1.3 |
| 2 | 0.50 | 0.16 | 0.40 | $1.9 \times 10^3$ | 1.3 |

Targeted $M_n$ = 5000 g/mol; [monomer]:[RAFT]:[AIBN] = 37:1:0.09; Reaction temperature = 80 ºC; Reaction time = 4 hrs. ***a***) Calculated from values, obtained from GC measurements.

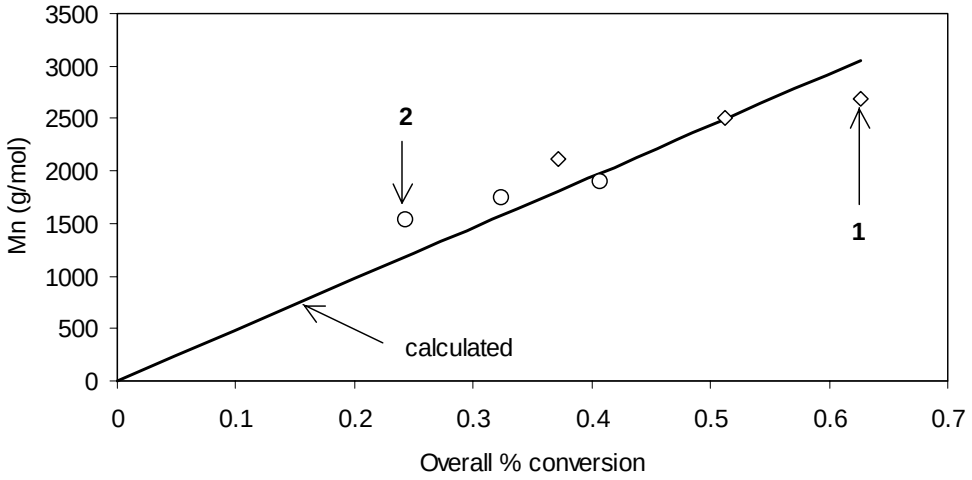


**Figure 6.4:** Plot of $M_n$ vs overall fractional conversion. Legends - (1) $f_{ABE}$ = 0.25. (2) $f_{ABE}$ = 0.50. (For details, see Table 6.2). $M_n$ calculated = $M_{RAFT}$ + [(($M_{BA}$ × ([BA]$_0$ / [RAFT]$_0$)) × BA monomer conversion) + (($M_{ABE}$ × ([ABE]$_0$ / [RAFT]$_0$)) × ABE monomer conversion)]

### 6.4.3 *Polymer Characterization:*

The synthesized copolymers were characterized using matrix assisted laser desorption / ionization – time of flight – mass spectrometry (MALDI-TOF-MS) and $^{1}H$ NMR spectroscopy. Determination of the accurate (relative) molar masses of synthetic polymers is often difficult to achieve. Detailed information of molecular structure, such as identification of end groups, can be even more difficult. Even though, polymers with a molecular weight of several hundred thousand Daltons can be characterized by MALDI-TOF-MS, most of the investigations with this technique focus on the mass range where single polymer chains are resolved.[27] The resolved mass range depends on the molar mass range of the repeating units and on the resolution of the mass spectrometer. From the absolute mass of each signal of the polymer distribution, the polymer composition can be deduced directly in favorable cases.

#### 6.4.3.1 *Copolymers of MA/ABE synthesized using ATRP:*

Figure 6.5 shows the MALDI-TOF-MS spectrum of the MA/ABE copolymer (Table 6.1, entry 4). The overlap of several distributions is clearly visible. The copolymers have the heterogeneity in the degree of polymerization, corresponding to a distribution in chain length, coupled with the heterogeneity in the chemical composition.

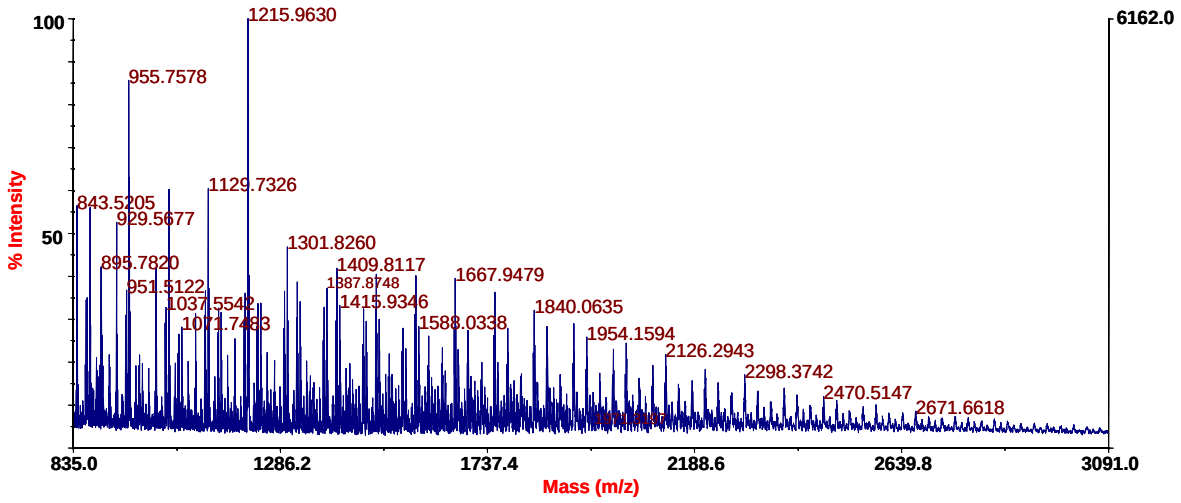


**Figure 6.5:** MALDI-TOF-MS spectrum for MA/ABE copolymer. $f_{ABE}$ = 0.50, $F_{ABE}$ = 0.20. (Table 6.1, entry 4). [Spectrum acquired in the reflector mode, Matrix : DCTB].

Figure 6.6 is an expansion of a selected portion of the spectrum shown in Figure 6.5. The peak assignments of Figure 6.6, described in Table 6.3 are made using the following strategies; **(1)** comparison with the homopolymer spectrum of MA; **(2)** comparison of the experimental masses and those theoretically calculated; **(3)** comparison of the theoretical isotopic distribution with the observed distributions. All the copolymer chains were assigned to various chemical compositions, containing varying numbers of MA (M) and ABE (A) units. Interestingly all copolymer chains can be divided into having four pairs of end groups (E1, E2, E3 and E4).

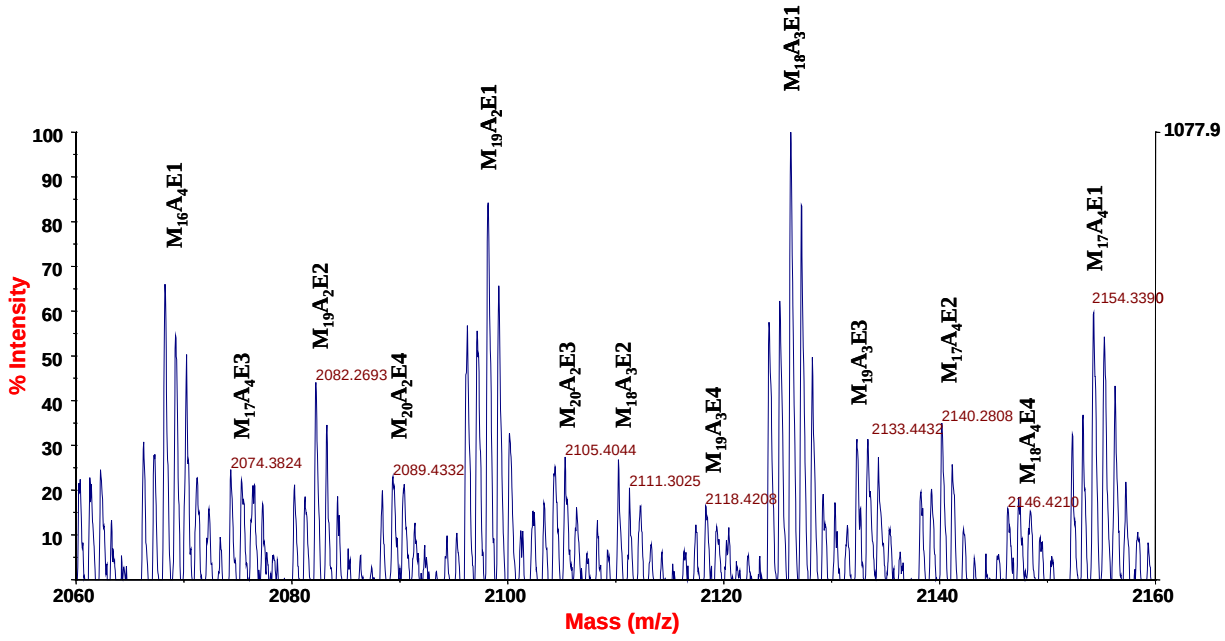


**Figure 6.6:** Expansion of the MALDI-TOF-MS spectrum for MA/ABE copolymer synthesized using ATRP. $f_{ABE}$ = 0.50, $F_{ABE}$ = 0.20. (Table 6.1, entry 4). [Spectrum acquired in the reflector mode].

Usually, the detected signals after subtraction of the mass of the cationization reagent, should be in agreement with the expected masses of the copolymer chains, which can be calculated according to Equation 1:

$$M_{copo} = 115.15 + [(m \times 86.09) + (n \times 114.18)] + 79.90 \qquad (1)$$

where, 115.15 and 79.9 are the average masses of the end groups from the initiator fragment and the bromine respectively (since EBriB was used as the ATRP initiator), 86.09 and 114.18 are the average masses of the MA and ABE repeating units, respectively, and m and n the numbers of the monomers in the chain.

Potassium trifluoracetate (KTFA) was used as the cationic ionization agent, hence the polymer chains cationized with potassium were detected at a m/z valued 39 Daltons above the theoretically calculated mass. The polymer chains with the primary end group E1 are well assigned using Equation 1 and potassium as the cation. The next most abundant series with the end group E2 can also be assigned using Equation 1, but now the chains are cationized with sodium, and hence are detected at 23 Daltons above the theoretically calculated mass. The assignments of the peaks were confirmed by using sodium trifluoroacetate (NaTFA) as the cationic ionization agent. When NaTFA was used instead of KTFA the overall quality of the spectrum decreased, but a clear increase in the abundance of chains cationized with sodium was observed relative to those cationized with potassium.

In MALDI-TOF-MS, during ionization (in the employed range of laser intensity) it is observed that some of the terminal Br fragments. Other groups have already reported the loss of the halide in the form of HBr during MALDI-TOF-MS analysis of poly(acrylates) produced by ATRP.[15] In this event, Equation 2 can be employed, which is a slight modification to Equation 1. The difference between the two Equations is that Equation 1 accounts for the Br at the chain end whereas Equation 2 does not.

$$M_{copo} = 115.15 + [(m \times 86.09) + (n \times 114.18)] + 1.00 \qquad (2)$$

where, 115.15 and 1.00 are the average masses of the end groups from the initiator fragment and of a hydrogen atom respectively, 86.09 and 114.18 are the average masses of the MA and ABE repeating units, respectively, and m and n the numbers of the monomers in the chain.

The polymer chains with end groups E3 and E4 can now be very clearly assigned using Equation 2 and the cation as potassium and sodium respectively. The values summarized in Table 6.3 show the comparison between the theoretical and observed masses for the different end groups. In Figure 6.8 a comparison is made between the observed mass distributions and the theoretical isotopic mass distribution. As observed, there is an excellent correlation.

Thus, it is evident from Figure 6.6 that several units of ABE have been incorporated in the polymer chain. This indicates that ABE is behaving as a comonomer, and not simply as a chain transfer agent. The origin of the comonomer incorporation has been discussed previously for the copolymerization of acrylate and octene (see Chapter 2).[28] In the previous case, there is a large difference in the activation rate parameters between dormant chains that carry an acrylate terminal group *versus* those with an octene terminal group. In the present case the situation is somewhat

similar. It is likely that for propagating radicals with a terminal ABE unit, the time constant for crosspropagation is smaller than that for deactivation. In other words, chains with an ABE terminal unit exclusively undergo crosspropagation with MA.

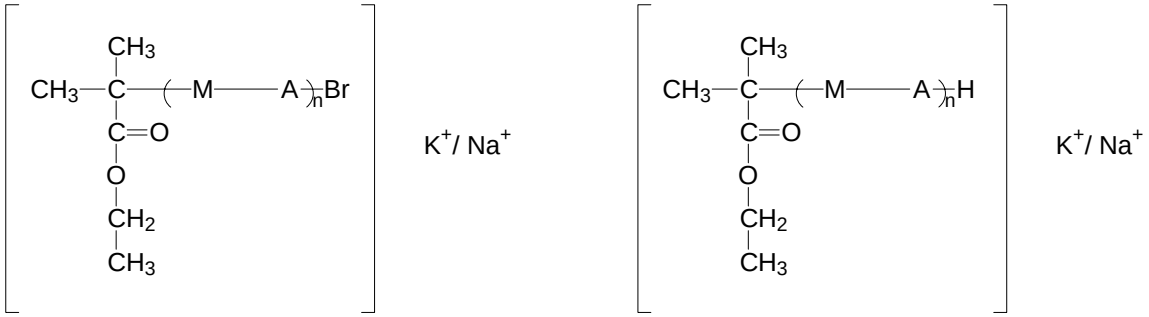


**(a) E1 and E2** **(b) E3 and E4**

**Figure 6.7:** The obtained end groups observed during MALDI-TOF-MS measurements , **(a)** represents the structure for end groups E1 and E2, the only difference is that, E1 is cationized by potassium ($K^+$) and E2 is cationized by sodium ($Na^+$) respectively; **(b)** represents the structure for end groups E3 and E4, the only difference is that E3 is now cationized by potassium ($K^+$) and E4 is cationized by sodium ($Na^+$) respectively. M and A are the abbreviations for methyl acrylate and allyl butyl ether respectively.

**Table 6.3:** Peak assignment of the MALDI-TOF-MS spectrum shown in Figure 6.6

| Peak | MA units | ABE units | Observed Mass (Da) | Theoretical Mass (Da) | $K^+$ | $Na^+$ |
|---|---|---|---|---|---|---|
| $M_{17}A_4E1$ | 17 | 4 | 2154.3390 | 2154.440 | 1 | - |
| $M_{19}A_2E2$ | 19 | 2 | 2082.2693 | 2082.1393 | - | 1 |
| $M_{20}A_2E3$ | 20 | 2 | 2105.4044 | 2105.4361 | 1 | - |
| $M_{20}A_2E4$ | 20 | 2 | 2089.4332 | 2089.3258 | - | 1 |

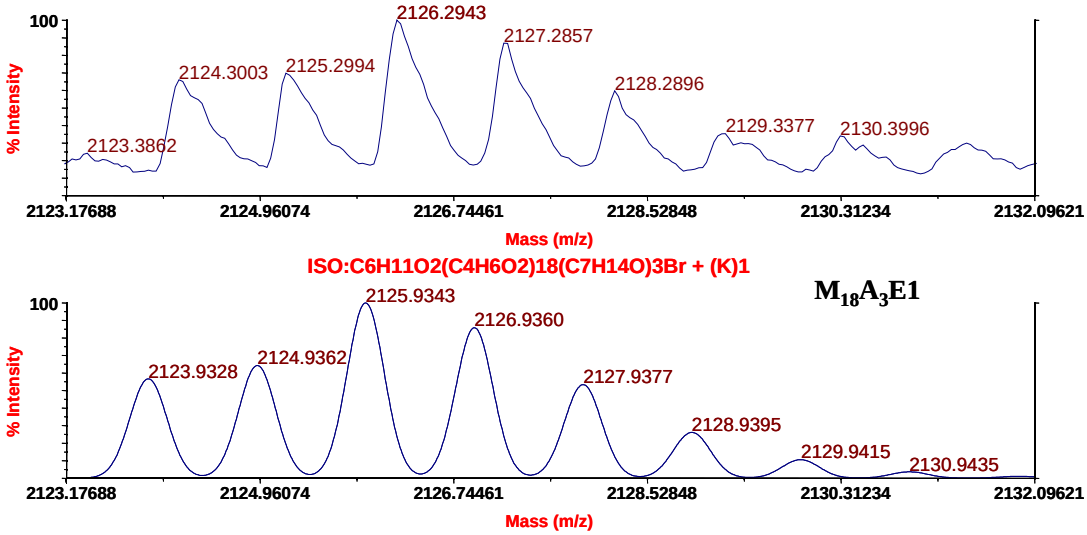


**Figure 6.8:** Detail of the MALDI-TOF-MS spectrum for MA/ABE copolymer synthesized using ATRP. $f_{ABE}$ = 0.50, $F_{ABE}$ = 0.20. (Table 6.1, entry 4). Isotopic mass distributions : observed (above) and theoretical (below) for a polymer chain having end group E1 and having 18 monomeric units of methyl acrylate (M) and 3 monomeric units of allyl butyl ether (A).

The $^{1}$H NMR spectrum of the MA/ABE copolymer is shown in Figure 6.9. The methoxy peak at $\delta$ 3.6, the MA methine peak at $\delta$ 2.3, and the ABE methyl triplet at $\delta$ 0.8 are easily distinguished and can be used to calculate the copolymer composition. The region from $\delta$ 1.0 - 2.0 includes the poorly resolved peaks attributed to methine and methylene hydrogens on the polymer backbone and the methylene hydrogens of the ABE side chain.

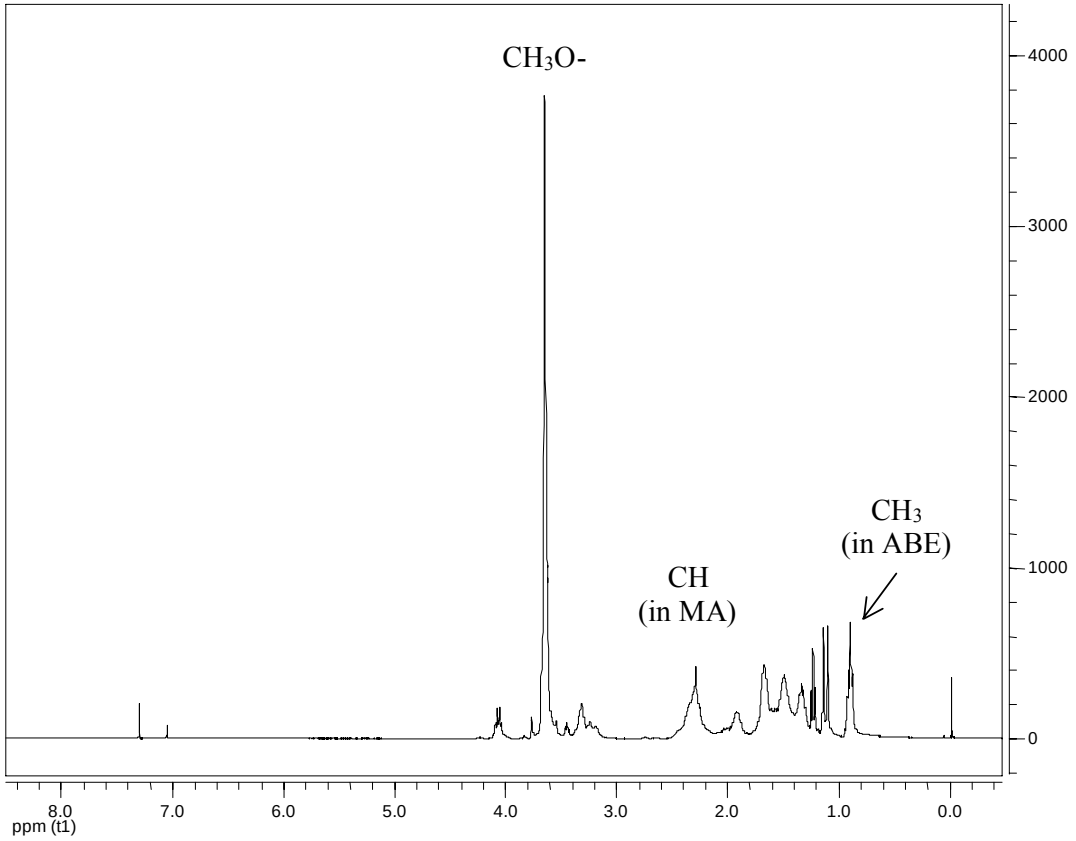


**Figure 6.9:** $^{1}$H NMR spectrum for MA/ABE copolymer synthesized using ATRP ($F_{ABE}$ = 0.20). $M_n$ = 1500 g/mol, PDI = 1.25 (for further details, please see Table 6.1, entry 4).

***6.4.3.2 Copolymers of BA/ABE synthesized using RAFT:*** Figure 6.10 shows the MALDI-TOF-MS spectrum for the BA/ABE copolymer (Table 6.2, entry 2). Similar to the MALDI-TOF-MS spectrum of the ATRP synthesized copolymers, the overlap of several distributions is clearly visible, as a result of the heterogeneity in the degree of polymerization and chemical composition distribution. Figure 6.11 is an expansion of a selected portion from the obtained MALDI-TOF-MS spectrum in Figure 6.10 for the BA/ABE copolymer. The polymer chains were all cationized with sodium. All the polymer chains were assigned to various chemical compositions, containing varying numbers of BA (B) and ABE (A) units. The majority of the copolymer chains can be divided into having four pairs of end groups (E1, E2, E3 and E4) [see Figure 6.11].

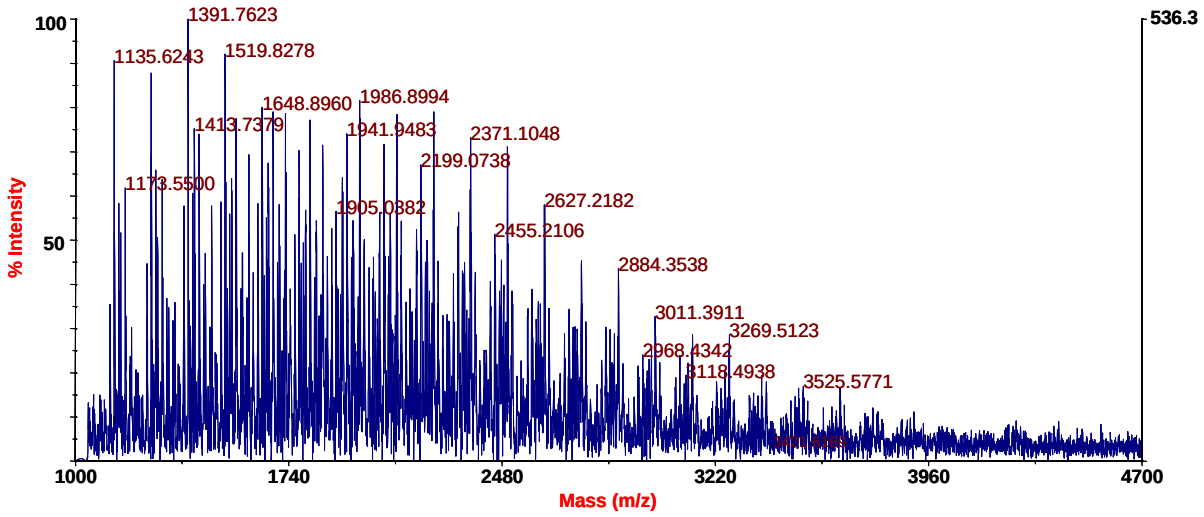


**Figure 6.10:** MALDI-TOF-MS spectrum for BA/ABE copolymer. $f_{ABE}$ = 0.50, $F_{ABE}$ = 0.16. (Table 2, entry 2). [Spectrum acquired in the reflector mode].

Since, S,S'-bis(α,α'-dimethyl-α''-acetic acid)trithiocarbonate is a bifunctional RAFT agent, during the RAFT process the polymeric chains can propagate in two directions. The structures in Figure 6.12 do not necessarily reflect the true comonomer sequence, but for sake of simplicity the structures are depicted in this way. The primary end group pair E1 is a result of the successful RAFT polymerization. The end group pairs E2 and E3 originated as a result of the exchange reaction between the proton of the COOH group and a sodium cation during MALDI-TOF-MS analysis (see Figure 6.12). In the case of end group pair E2 only one proton has been exchanged for the sodium and for end group pair E3 both protons have been exchanged. Hence, for copolymer chains having identical copolymer composition, the copolymer chains with end groups E2 and E3 are detected at higher masses differing by 22 Daltons and 44 Daltons respectively, as compared to the chains having E1 as the end group.

The initiator AIBN is added at a pre-determined time interval during the copolymerization to continuously generate radicals and keep the RAFT polymerization process active. Hence, some chains can be initiated by the primary cyanoisopropyl radical. The structure for end group pair E4 represents a case wherein both the end groups originate from the AIBN fragment. End group pair E4 is depicted in Figure 6.12 (iv).

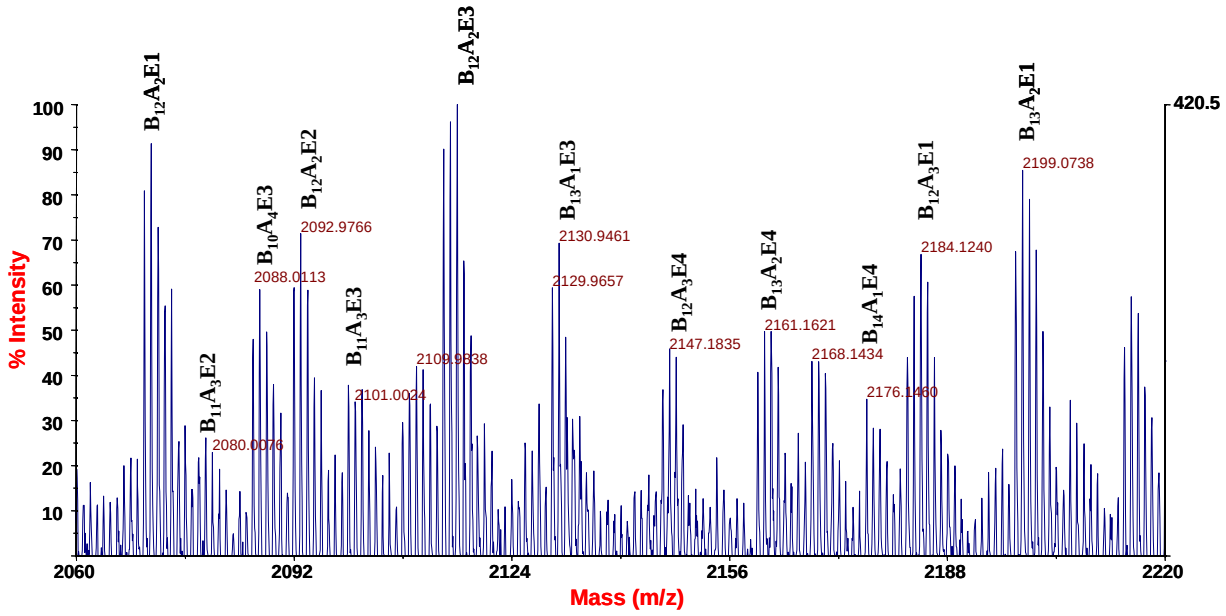


**Figure 6.11:** Expansion of the MALDI-TOF-MS spectrum for BA/ABE copolymer synthesized using RAFT. $f_{ABE}$ = 0.50, $F_{ABE}$ = 0.16. (Table 2, entry 2). [Spectrum acquired in the reflector mode].

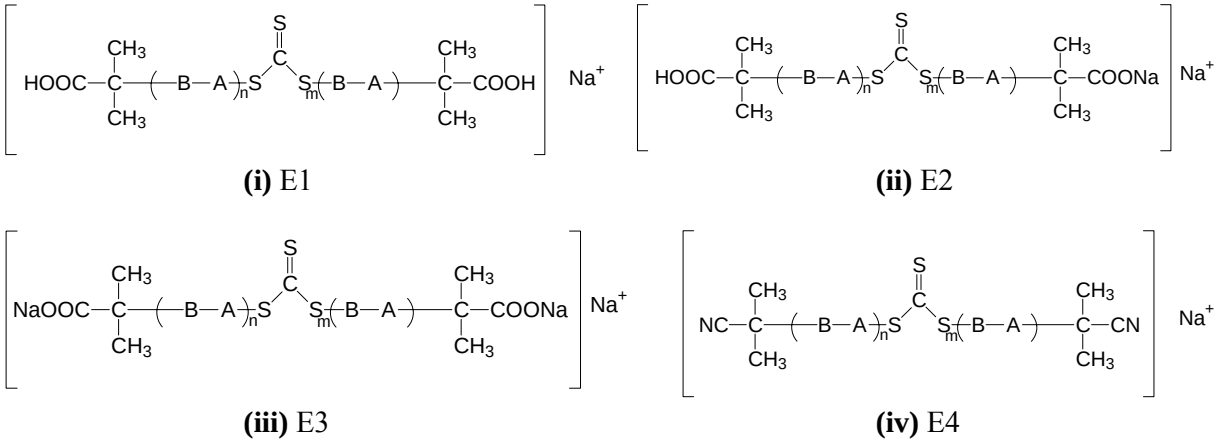


**Figure 6.12:** The obtained end groups observed during MALDI-TOF-MS measurements , **(i), (ii), (iii)** and **(iv)** represent the structure for end groups E1, E2, E3 and E4 respectively. B and A are the abbreviations for butyl acrylate and allyl butyl ether respectively.

The peak assignments of Figure 6.11, described in Table 6.4 are made using the following strategies; **(1)** comparison with the homopolymer spectrum of BA; **(2)** comparison of the experimental masses and those theoretically calculated; **(3)** comparison of the theoretical isotopic distribution with the observed distributions.

**Table 6.4:** Peak assignment of the MALDI-TOF-MS spectrum shown in Figure 6.11

| Peak | BA units | ABE units | Observed Mass (Da) | Theoretical Mass (Da) | $Na^+$ |
|---|---|---|---|---|---|
| $B_{12}A_2E1$ | 12 | 2 | 2071.0146 | 2071.2117 | 1 |
| $B_{12}A_2E2$ | 12 | 2 | 2092.9751 | 2093.1936 | 2 |
| $B_{10}A_4E3$ | 10 | 4 | 2088.0113 | 2087.806 | 3 |
| $B_{12}A_3E4$ | 12 | 3 | 2147.1835 | 2147.3269 | 1 |

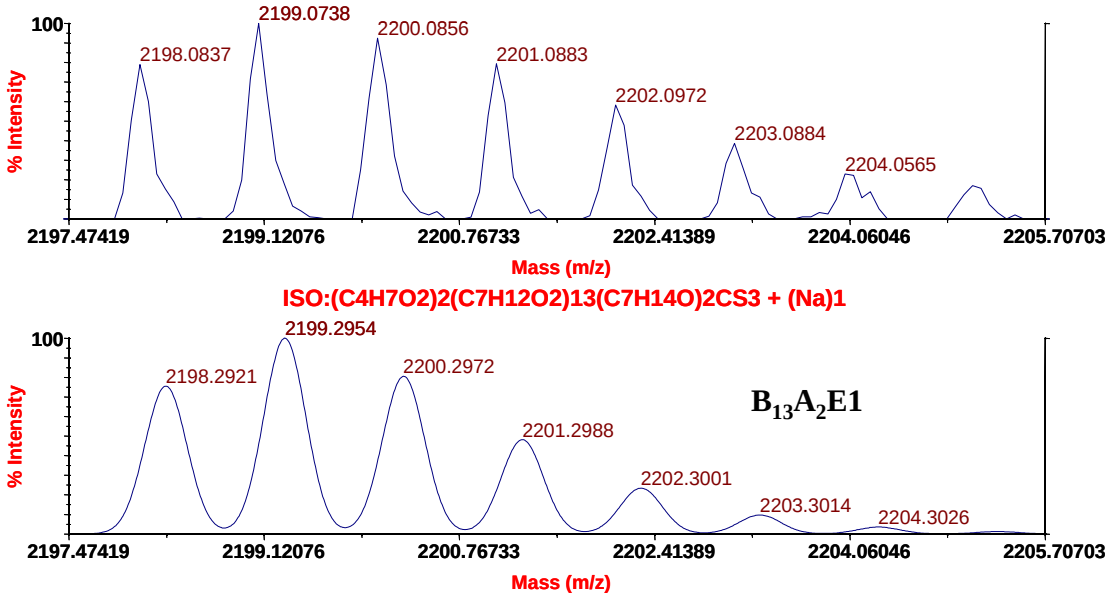


Figure 6.13: Detail of MALDI-TOF-MS spectrum for BA/ABE copolymer synthesized using RAFT. $f_{ABE}$ = 0.50, $F_{ABE}$ = 0.16. (table 2, entry 2). Isotopic mass distributions : observed (above) and theoretical (below), for a polymer chain having end group E1 and having 13 monomeric units of butyl acrylate (B) and 2 monomeric units of allyl butyl ether (A).

It is evident from Figure 6.11 that several units of ABE have been incorporated into the polymer chain. This further indicates that ABE is behaving as a comonomer, and not simply as a chain transfer agent.

## *6.5 Conclusions*

The atom transfer radical copolymerization (ATRP) and reversible addition fragmentation chain transfer of acrylates (MA and BA) with ABE was investigated. Well-defined copolymers containing almost 20 mol% of ABE were obtained using ethyl-2-bromoisobutyrate (EBriB) as initiator. Narrow MMDs were obtained for the ATRP experiments, which suggested conventional ATRP behavior, with no peculiarities caused by the incorporation of ABE**.** The comparable free radical (co)polymerizations (FRP) resulted in broad MMDs. The copolymerization under FRP conditions show relatively low molar mass polymers, as compared to the homopolymerization of acrylates, which occurs readily by free-radical polymerization to yield high-MM homopolymers. This indicates that ABE acts as a chain transfer agent for the free radical polymerization. Increasing the fraction of ABE in the monomer feed led to an increase in the level of incorporation of ABE into the copolymer, at the expense of the overall conversion.

Similarly, the RAFT copolymerizations using S,S'-bis(α,α'-dimethyl-α''-acetic acid)trithiocarbonate also results in excellent control of the polymerization with significant incorporation of ABE into the copolymer chains.

The fact that using controlled radical techniques (in the targeted mass range) results in significant incorporation of ABE within the polymer chains coupled with excellent control of the polymerizations, clearly indicates that ABE acts as a comonomer as opposed to a chain transfer agent.

The formation of the copolymer was established using matrix assisted laser desorption / ionization – time of flight – mass spectrometry (MALDI-TOF-MS). From the obtained MALDI-TOF-MS spectra for the ATRP and RAFT systems, it is evident that several units of ABE have been incorporated in the polymer chain. This is attributed to the rapidity of crosspropagation of ABE-terminated polymeric radicals with acrylates.

## 6.6 References


1) Padwa, A. R.; *Prog. Polym. Sci.*, **1989**, *14*, 811. *Functional Polymers: Modern Synthetic Methods and Novel Structures*; Patil, A. O.; Schulz, D.N.; Novak, B. M.; (Eds.); ACS Symposium Series 704; American Chemical Society: Washington, DC, **1998**.

2) Odian, G, *Principles of Polymerization*; John Wiley: New York, **1991**, p. 266.

3) Bevington, J. C., Huckerby, T. N., Hunt, B. J., Jenkins, A. D.; *J. Macromol. Sci.-Pure Appl. Chem.*, **2001**, *A38(10)*, 981.

4) Venkatesh, R., Klumperman, B.; *Macromolecules*, **2004**, *37*, 1226.

5) Liu, S., Elyashiv, S., Sen, A.; *J. Am. Chem. Soc.*, **2001**, *123*, 12738.

6) Donovan, M. S., Lowe, A. B., Sanford, T. A., McCormick, C. L.; *J. Polym. Sci., Part A: Polym. Chem.*; **2003**, *41*, 1262.

7) Kato, M., Kamigaito, M., Sawamoto, M., Higashimura, T.; *Macromolecules*, **1995**, *28*, 1721.

8) Wang, J. S., Matyjaszewski, K.; *Macromolecules*, **1995**, *28*, 7901.

9) Kamigaito, M., Ando, T., Sawamoto, M.; *Chem. Rev*., **2001**, *101*, 3689. Matyjaszewski, K., Xia, J.; *Chem. Rev*., **2001**, *101*, 2921.

10) Haddleton, D. M., Crossman, M. C., Dana, B. H., Duncalf, D. J., Heming, A. M., Kukulj, D., Shooter, A. J.; *Macromolecules*, **1999**, *32*, 2110.

11) Le, T. P., Moad, G., Rizzardo, E., Thang, S. H.; *PCT Int Appl*., **1998**, WO98/01478.

12) Chiefari, J., Chong, Y. K., Ercole, F., Krstina, J., Jeffery, J., Le, T. P. T., Mayadunne, R. T. A., Meijs, G. F., Moad, C. L., Moad, G., Rizzardo, E., Thang, S. H.; *Macromolecules*, **1998**, *31*, 5559.

13) Moad, G., Chiefari, J., Chong, Y. K., Krstina, J., Mayadunne, R. T. A., Postma, A., Rizzardo, E., Thang, S. H.; *Polym. Int*., **2000**, *49*, 993.

14) Chong, Y. K., Krstina, J., Le, T. P. T., Moad, G., Postma, A., Rizzardo, E., Thang, S. H.; *Macromolecules*, **2003**, *36*, 2256. Chiefari, J., Mayadunne, R. T. A., Moad, C. L., Moad, G., Rizzardo, E., Postma, A., Skidmore, M. A., Thang, S. H.; *Macromolecules*, **2003**, *36*, 2273.

15) Donovan, M. S., Lowe, A. B., Sumerlin, B. S., McCormick, C. L.; *Macromolecules*, **2002**, *35*, 4123.

16) Barner-Kowollik, C., Davis, T., Heuts, J. P. A., Stenzel, M. H., Vana, P., Whittaker, M.; *J. Polym. Sci., Part A: Polym. Chem.*; **2002**, *41*, 365.

17) de Brouwer, H., Schellekens, M. A. J., Klumperman, B., Monteiro, M. J., German, A. L.; *J. Polym. Sci., Part A: Polym. Chem.*; **2000**, *38*, 3596.

18) Matyjaszewski, K, Nakagawa, Y., Jasieczeck C. B.; *Macromolecules*, **1998**, *31*, 1535. Coessens, V., Matyjaszewski, K.; *J. Macromol. Sci.- Pure Appl. Chem.*; **1999**, *A 36*, 653. Coessens, V., Matyjaszewski, K.; *J. Macromol. Sci.- Pure Appl. Chem.*; **1999**, *A 36*, 667.

19) Bednarek, M., Biedroń, T., Kubisa, P.; *Macromol. Chem. Phys.*; **2000**, *201*, 58.

20) Borman, C. D., Jackson, A. T., Bunn, A., Cutter, A. L., Irvine, D. J.; *Polymer*, **2000**, *41*, 6015.

21) Schilli, C., Lazendoerfer, M., Müller, A. H. E.; *Macromolecules*, **2002**, *35*, 6819.

22) Ganachaud, F., Monteiro, M. J., Gilbert, R. G., Dourges, M-A., Thang, S. H., Rizzardo, E.; *Macromolecules*, **2000**, *33*, 6738.

23) Destarac, M., Charmot, D., Franck, X., Zaed, S. Z.; *Macromol. Rapid Commun.*, **2000**, *21*, 1035.

24) Lai, J. T., Filla, D., Shea, R.; *Macromolecules*, **2002**, *35*, 6754.

25) Beuermann, S.; Paquet, D. A., Jr.; McMinn, J. H.; Hutchinson, R. A.; *Macromolecules*, **1996**, *29*, 4206.

26) Odian, G, *Principles of Polymerization*; John Wiley: New York, **1991**, p. 629.

27) Nielen, M. W. F.; *Mass Spectrom. Rev.*, **1999**, *18*, 309.

28) Venkatesh, R., Harrisson, S., Haddleton, D. M., Klumperman, B.; submitted to *Macromolecules*.

# Chapter 7

## *Novel 'bottle-brush' Copolymers*

## *via Controlled Radical Polymerization*

**Abstract:** A combination of reversible addition-fragmentation chain transfer (RAFT) polymerization and atom transfer radical polymerization (ATRP) techniques were applied for the synthesis of novel polymer brushes by using the "grafting from" approach. The procedure included the following steps: ***(1)*** Synthesis of 2-(2-bromoisobutyryloxy)ethyl methacrylate [BIEM], ***(2)*** RAFT homopolymerization of BIEM to obtain PBIEM as the polymer backbone. The RAFT copolymerization of BIEM and PEO macromonomer (PEOMA, $M_n$ ~ 450 g/mol, $DP_{PEO}$ = 9) was also performed to obtain a more hydrophilic polymer backbone. Well-controlled copolymers containing almost 25 mol% of PEOMA were obtained, and ***(3)*** ATRP homopolymerization of methyl acrylate (MA) and copolymerization of MA with 1-octene (Oct) using both PBIEM homopolymer and P[(BIEM)-co-(PEOMA)] as polyinitiators resulted in brushes with densely grafted homopolymer and copolymer side chains, respectively. Well-controlled copolymer side chains containing 15 mol% of 1-octene were obtained. Narrow molar mass distributions (MMD) were obtained for the ATRP experiments. The formation of the side chains was monitored using SEC and NMR. The copolymer composition in the side chain was established using $^1$H NMR. Contact angle measurements indicated that for the brush polymers, containing 1-octene in the side chain, there was a decrease in the surface energy, as compared with the brush polymers containing only the homopolymer of MA in the side chain. From the adhesion measurements, it was evident that the brush polymers containing the statistical copolymer of polar (MA) and non-polar (Oct) in the side chain, have a better interaction with predominantly non-polar substrates (polypropylene) as opposed to polymers without the non-polar Oct.

## *7.1 Introduction*

Polymer brushes can be grafted from flat, colloidal and irregular surfaces and also from each suitable repeat unit of the polymer backbone, generating molecular, 'bottle-brush' structures. Their properties depend on a variety of molecular parameters including the degrees of polymerization of the main ($DP_n$) and side chains ($DP_{SC}$), graft density, main chain topology, and chemical

---

Venkatesh, R., Yajjou, L., Kisin, S., Koning, C. E., Klumperman, B.; *manuscript under preparation.*

composition. Three synthetic routes to macromolecular brushes, which also have been applied to loosely grafted systems, are described in the literature[1] : **(i)** "grafting onto" (attachment of side chains to the backbone), **(ii)** "grafting through" (homo- and co-polymerization of macromonomers) and **(iii)** "grafting from" (grafting side chains from the backbone). The controlled synthesis of macromolecular brushes by "grafting from" a macroinitiator via ATRP[2,3] has been previously reported.[1,4,5,6,7]

Now, copolymers of α-olefins with polar monomers remain a pivotal area in polymer research, since the effect of incorporation of functional groups into an otherwise nonpolar material is substantial.[8,9] Recent publications were indicative of the fact that polar monomers can be copolymerized with α-olefins, resulting in significant incorporation of the α-olefin in the copolymer using controlled radical techniques.[10,11,12,13]

In this chapter, the successful homopolymerization and copolymerization of 2-(2-bromoisobutyryloxy)ethyl methacrylate [BIEM] with PEO macromonomer using the RAFT[14,15] technique is discussed. By using RAFT, the need to use protective group chemistry on the ATRP initiator moiety is avoided. Further, the results for the ATRP homopolymerization of methyl acrylate (MA) and copolymerization of MA with 1-octene (Oct), using both PBIEM homopolymer and P[(BIEM)-co-(PEOMA)] as polyinitiators are discussed in detail. Chemical composition was confirmed using nuclear magnetic resonance (NMR) spectroscopy. Finally, the polymer film properties of these 'bottle-brush' copolymers were explored using contact angle and adhesion measurements. Scanning Force Microscopy was employed to have an insight into the polymer architecture.

## *7.2 Experimental Section*

### *7.2.1 Materials*

BIEM was synthesized as described in Section 7.3.1. Poly(ethylene glycol) methyl ether methacrylate (PEOMA, $M_n$ ~ 450 g/mol, $DP_{PEO}$ = 9) was obtained from Aldrich. The macromonomer was purified by dissolving it in dichloromethane, and passing it through a column filled with aluminum oxide and inhibitor remover replacement packing. The solvent was then

evaporated and the purity checked by NMR before use. Methyl acrylate (MA, Merck, 99+%) and 1-octene (Oct, Aldrich, 98%) were distilled and stored over molecular sieves. *p*-Xylene (Aldrich, 99+% HPLC grade) and methyl ethyl ketone (Aldrich, 99+% HPLC grade) were stored over molecular sieves and used without further purification. N,N,N',N'',N''-pentamethyldiethylenetriamine (PMDETA, Aldrich, 99%), copper (I) bromide (CuBr, Aldrich, 98%), aluminum oxide (activated, basic, for column chromatography, 50-200 μm), tetrahydrofuran (THF, Aldrich, AR) and 1,4-dioxane (Aldrich, AR) were used as supplied.

## *7.2.2 Analysis and Measurements*

***7.2.2.1 Determination of Conversion and MMD:*** Monomer conversion was determined from the concentration of residual monomer measured via gas chromatography (GC). A Hewlett-Packard (HP-5890) GC, equipped with a HP Ultra 2 cross-linked 5% Me-Ph-Si column (25 m × 0.32 mm × 0.52 μm) was used. MEK was employed as the internal reference. The GC temperature gradient used is given in Figure 7.1.

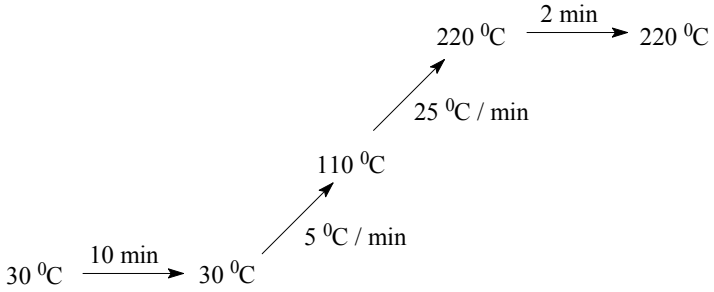


**Figure 7.1:** GC temperature gradient.

Molar mass (MM) and molar mass distributions (MMD) were measured by size exclusion chromatography (SEC), at ambient temperature using a Waters GPC equipped with a Waters model 510 pump, a model 410 differential refractometer (40 ºC), a Waters WISP 712 autoinjector ( 50 μL injection volume), a PL gel (5 μm particles) 50 × 7.5 mm guard column and a set of two mixed bed columns (Mixed-C, Polymer Laboratories, 300 × 7.5 mm , 5 μm bead size, 40 ºC) . THF was used as the eluent at a flow rate of 1.0 mL/min. Calibration was carried out using narrow MMD polystyrene (PS) standards ranging from 600 to $7 \times 10^6$ g/mol. The MM was calculated relative to PS standards. Data acquisition and processing were performed using Waters Millenium 32 software.

***7.2.2.2 NMR:*** $^{1}H$ nuclear magnetic resonance (NMR) spectra were recorded on a Varian 400 spectrometer, in deuterated chloroform ($CDCl_3$) at 25 ºC. All chemical shifts are reported in ppm downfield from tetramethylsilane (TMS), used as an internal standard ($\delta$=0 ppm).

***7.2.2.3 Preparative HPLC:*** The backbone main chain polymer was isolated using a preparative HPLC apparatus at ambient temperature, equipped with an Agilent binary pump (G1312A), an Agilent UV detector (G1314A) and a Rheodyne manual injector with 2 mL sample loop. THF was used as the eluent at a flow rate of 2.0 mL/min. An Ultragel column (Waters, 1000 Å, 19 x 300 mm) was used. UV: $\lambda$ = 254 nm.

***7.2.2.4 Contact Angle measurements:*** Static contact angles were obtained by means of the sessile drop method, using a Krüss G10 set-up. The probe liquids employed were water and ethylene glycol. The droplet was monitored by a CCD-camera and analyzed by Drop Shape Analysis software (DSA Version 1.0, Krüss). The complete profile of the sessile droplet was fitted by the software, which employed the tangent method for the determination of the contact angle. Reproducibility was within 1.0°. The Owens/Wendt method[16] has been employed to calculate the surface free energy of the polymer surface from contact angle measurements.

***7.2.2.5 Scanning Force Microscopy (SFM):*** The samples for SFM measurements were prepared by dip-coating from dilute solution of polymer in THF (0.05 g/L) onto freshly cleaved mica. The SFM images were taken with a Digital Instruments Dimension 3100 microscope operated in tapping mode.

***7.2.2.6 HPLC-MS:*** The individual monomer conversion during the RAFT homo- and co-polymerization were monitored using an HPLC-MS apparatus. HPLC instrument was an Agilent 1100 series (Agilent Technologies), equipped with degasser (G1322A), quaternary pump (G1311A), autosampler (G1313A), column compartment (G1316A) and UV-DAD detector (G1315B). The mass spectrometer (MS) was an Agilent MSD type SL (G1946D), equipped with an atmospheric pressure electrospray interface. A Superspher 100RP-18E column (Bischoff, 150 x 3 mm; particle size 4 μm) was used. The gradient employed is detailed in Table 7.1. The column was reset at the end of the gradient to initial conditions between 15 and 20 mins, and further equilibrated for 15 mins. HPLC grade solvents were obtained from BioSolve. Acetic acid was procured from

Merck. Dilute polymer solutions were made in THF (10 mg/mL) and a sample of 1 µL was used for analysis at 25 ºC. Data acquisition and processing were performed using HP Chemstation.

**Table 7.1:** Linear binary gradient used for HPLC-MS

| Step | Time (min) | $\Phi$ Methanol + 0.1% acetic acid | $\Phi$ Water + 0.1% acetic acid | Flow (mL/min) |
|---|---|---|---|---|
| 1 | Initial | 0.7 | 0.3 | 0.4 |
| 2 | 10 | 1.0 | - | 0.4 |
| 3 | 15 | 1.0 | - | 0.4 |
| 4 | 20 | 0.7 | 0.3 | 0.4 |

The eluent composition are given in volume fraction ($\Phi$).

| | | |
|---|---|---|
| Diode Array Detector (DAD): | $\lambda$ = 254 nm | |
| Spray Chamber Settings: | Drying gas temperature: | 350$^{o}$C |
| | Drying gas flow: | 13 L/min |
| | Nebuliser pressure: | 30 psi |
| | Capillary voltage: | 4000 V |
| MS: | SIM; mass = 301 + 607 | |

***7.2.2.7 Adhesion Measurements:*** Adhesion measurements were performed to study the interaction of the polymeric coatings with a PP substrate. Adhesive strength of the polymeric coatings on a polypropylene (PP) substrate was estimated by the direct pull-off test (DPO). Pull-off tests were carried out using a Universal Testing Machine 112 (TesT Gmbh). For DPO, studs of 8 mm in diameter were used. A precut in the Cu coating (sample preparation and deposition of the Cu coating is explained in section 7.3.4) was made prior to the test, so as to ensure that the pulled surface area is the same in all cases. The pulling rate was 1 mm/min. All measurements were repeated twice. Fractured surfaces were analyzed by means of scanning electron microscopy, SEM (JEOL JSM-840A Scanning Microscope). Back-scattered Electron Images were taken at 8 mm working distance with 15 kV accelerating voltage.

## 7.3 Synthetic Procedures

### 7.3.1 Synthesis of 2-(2-bromoisobutyryloxy)ethyl methacrylate [BIEM]:

This synthesis was carried out in a dry 250 mL three-neck round-bottom flask. 2-hydroxyethyl methacrylate, HEMA (10.0 g, 0.07 mol) and triethylamine, TEA (15.6 g, 0.15 mol) were dissolved in dichloromethane, DCM (97.8 g, 1.2 mol). The reaction mixture was stirred at 0 ºC and degassed by sparging with argon for 45 min. 2-bromoisobutyryl bromide (21.2 g, 0.09 mol) was added drop-wise over a period of 30 min. The reaction was carried out under a flowing argon atmosphere. The mixture was stirred at 0 ºC for 6 hours and then filtered to remove the formed solids (salt). The solids were washed with DCM. The filtrate was then washed with de-ionized water (2x 100 mL), 0.5 M $NaHCO_3$ (2x 100 mL) and saturated NaCl (2x 100 mL) solutions. Sodium sulphate, $Na_2SO_4$ was added for the removal of water traces. The $Na_2SO_4$ was filtered off and the DCM was removed under vacuum. The purity of the obtained product was checked by NMR. $^1$H NMR ($CDCl_3$): δ = 6.16 (1H), 5.62 (1H) [$CH_2$=C], 4.45 (4H) [-$CH_2$-OCO], 1.97 (3H) [α-$CH_3$), 1.95-1.96 (6H) [-C(Br)($CH_3$)$_2$].

### 7.3.2 RAFT polymerization:

A stock solution for the polymerization was prepared by accurately weighing the RAFT agent [2-cyanopropyl-2-yl dithiobenzoate][14] (0.015 g, 0.06 mmol), V-65 [2,2'-azobis(2,4-dimethylvaleronitrile)] (1.4 mg, 8× $10^{-3}$ mmol), *p*-xylene (4.1 g, 0.04 mol) and the monomer BIEM (1.0 g, 3.5 mmol). This stock solution was further divided into a number of gas chromatography (GC) vials. Each vial contained 0.25 mL of the stock solution. The GC vials were individually purged with argon for 45 s and then sealed with an aluminium cap (Alltech, clear lacquered, with center hole; Natural rubber red-orange/TEF transparent, 60 ºC shore A, 1.0 mm). All the vials were placed in a thermostated GC-vial reactor setup, maintained at 60 ºC. Vials were withdrawn from the setup at suitable time intervals. A pre-determined amount of sample was transferred immediately into a HPLC-MS vial and diluted with methanol. The remaining sample was diluted with THF and used for SEC analysis.

### 7.3.3 ATR polymerization:

A stock solution for the graft polymerization was prepared by accurately weighing the P[BIEM] (polyinitiator in this case) (0.12 g, 0.02 mmol), MEK (1.3 g, 0.02 mol), MA (0.06 g, 0.7 mmol), 1-octene (0.08 g, 0.7 mmol) and PMDETA (6.0

mg, 0.03 mmol). Copper (I) bromide (5.1 mg, 0.03 mmol) was then added. A relatively homogeneous mixture was obtained due to the polar nature of MEK. This stock solution was further divided into a number of gas chromatography (GC) vials. Each vial contained 0.25 mL of the stock solution. The GC vials were individually purged with argon for 45 s and then sealed with an aluminium cap (Alltech, clear lacquered, with center hole; Natural rubber red-orange/TEF transparent, 60 ºC shore A, 1.0 mm). All the vials were placed in a thermostated GC-vial reactor setup, maintained at 80 ºC. Vials were withdrawn from the setup at suitable time intervals. A pre-determined amount of sample was transferred immediately into another GC vial and diluted with p-xylene, so as to determine the monomer conversion using GC. The remaining sample was diluted with THF and passed through a column of aluminum oxide prior to SEC analysis.

### *7.3.4 Sample preparation:*

For Contact angle measurements, thin films of the comb copolymers were spin-coated on glass plates, using a polymer solution in THF with concentration 50 mg/mL. The solutions were filtered through a 0.2 μm Teflon filter prior to spin coating (5000 rpm for 40 s). The samples were placed in a vacuum oven at ambient temperature for 24 hrs, prior to contact angle measurements.

For adhesion measurements, polypropylene panels (1 mm, 2.5 × 4 cm) were coated with the comb copolymers (solution in THF, concentration 50 mg/mL) via spin coating. The polymer solutions were filtered through a 0.2 μm Teflon filter prior to spin coating (5000 rpm for 80 s). The samples were placed in a vacuum oven at ambient temperature for 24 hrs, prior to further treatment. Then on these coated panels, copper coating (0.5 μm) was deposited by magnetron sputtering technique (Alcatel SCM850 RF-magnetron-sputtering machine was employed). Radio frequency (RF) power of 500 W under the pressure of $3 \times 10^{-2}$ mbar was used for sputtering.

## *7.4 Results and Discussion*

The RAFT homopolymerization and copolymerization of BIEM is examined. Further, the ATRP of the side chains using the polyinitiators will be discussed, followed by chemical composition determination using NMR. Then the polymer film properties of these ‘bottle-brush’ copolymers will be examined.

### *7.4.1 Hompolymerization of BIEM and 'grafting through' Copolymerization of BIEM/PEOMA:*

The length distribution of the polymer brushes is only dependent on the MMD of the backbone. Thus, the synthesis of a polyinitiator with a narrow MMD is crucial. Loosely grafted copolymers were prepared by a 'grafting through' copolymerization of PEOMA and BIEM. The RAFT homo- and co-polymerization were examined as summarized in Table 7.2. 2-Cyanopropyl-2-yl dithiobenzoate was employed for the RAFT polymerization because it is known from literature to yield well-controlled PMMA, as a result of its high chain transfer coefficient coupled with the fact that the cyanoisopropyl group is a good initiating species for MMA polymerization.[17] By using RAFT technique, the need to use protective group chemistry on the ATRP initiator moiety is avoided. Further, the purification steps are also less cumbersome.

From Table 7.2, the important observations are, **(1)** the RAFT homopolymerization of BIEM was successful. Figure 7.1(a) illustrates that with conversion the entire distribution moves smoothly toward high MM values. **(2)** Similarly, the RAFT 'grafting through' copolymerization of BIEM and PEOMA also results in good control with 24 mol% incorporation of PEOMA. From the SEC chromatograms, it is clear that the entire distribution moves to higher MM with conversion [Figure 7.1(b)]. The copolymer was separated from the solvent and unreacted monomers by preparative HPLC (see Section 7.2.2.3). From the $^{1}$H NMR of the final copolymer in Figure 7.2, peaks from BIEM and PEOMA are clearly observed. On incorporation of the PEOMA into the copolymer, the hydrophilicity of the backbone is enhanced. **(3)** The 'grafting through' copolymerization of 2-(trimethylsilyloxy) ethyl methacrylate (HEMA-TMS) and a relatively high molecular weight PEO macromonomer has been previously reported using ATRP.[7] This resulted with a slight gradient in the composition along the backbone of the copolymer due to the differences in reactivity of the two monomers. A similar trend might be expected for the current BIEM and PEOMA system.

**Table 7.2:** RAFT Polymerization of BIEM

| Entry | $f_{BIEM}$ | $f_{PEOMA}$ | Overall Conversion | $F_{PEOMA}$ (mol fraction)[a] | $M_{n\ apparent}$ (g/mol)[b] | $M_n$ (calculated)[c] | PDI |
|---|---|---|---|---|---|---|---|
| 1 | 1.0 | - | 0.60 | - | $11.3 \times 10^3$ | $8.9 \times 10^3$ | 1.3 |
| 2 | 0.75 | 0.25 | 0.64 | 0.24 | $11.1 \times 10^3$ | $7.4 \times 10^3$ | 1.2 |

*Solvent for the polymerization* = *p*-xylene. [Monomer]:[2-cyanopropyl-2-yl dithiobenzoate][14]: [AIBN] = 53 : 1: 0.125. Volume of {monomer}/{solvent} = 1/7. Reaction temperature = 60 $^oC$. Reaction time = 24 hrs.

*a* Calculated from the area under the curve obtained from HPLC-MS measurements.

*b* From SEC, calibrated with PS standards.

*c* $M_n$ calculated = [((([M]$_0$/[Raft]$_0$) × $M_{monomer}$) × conversion) + $M_{Raft\ agent}$]

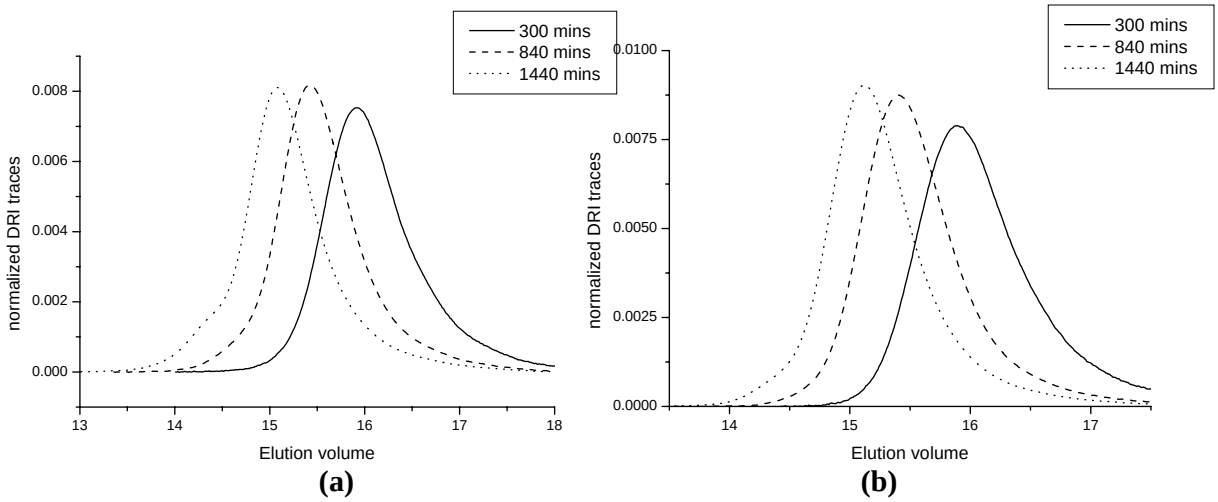


**Figure 7.1:** Development of MMD during the RAFT **(a)** homopolymerization of BIEM and **(b)** copolymerization of BIEM and PEOMA ($f_{PEOMA}$ = 0.25).

The $^1H$ NMR spectrum of the polyinitiator in Figure 7.2, clearly shows two typical peaks at 4.21 and 4.27 ppm (a and a'), which represent the methylene protons between two ester groups of the polyinitiator. The peak at 4.1 ppm is assigned to the -$OCH_2$ group in the PEOMA. The peaks between 3.6 and 3.8 ppm are attributed to the methylene groups present in the polyethylene oxide side chain. The peak assignments were made after comparison with the homopolymer spectrum of P(BIEM)[6] and PEOMA.

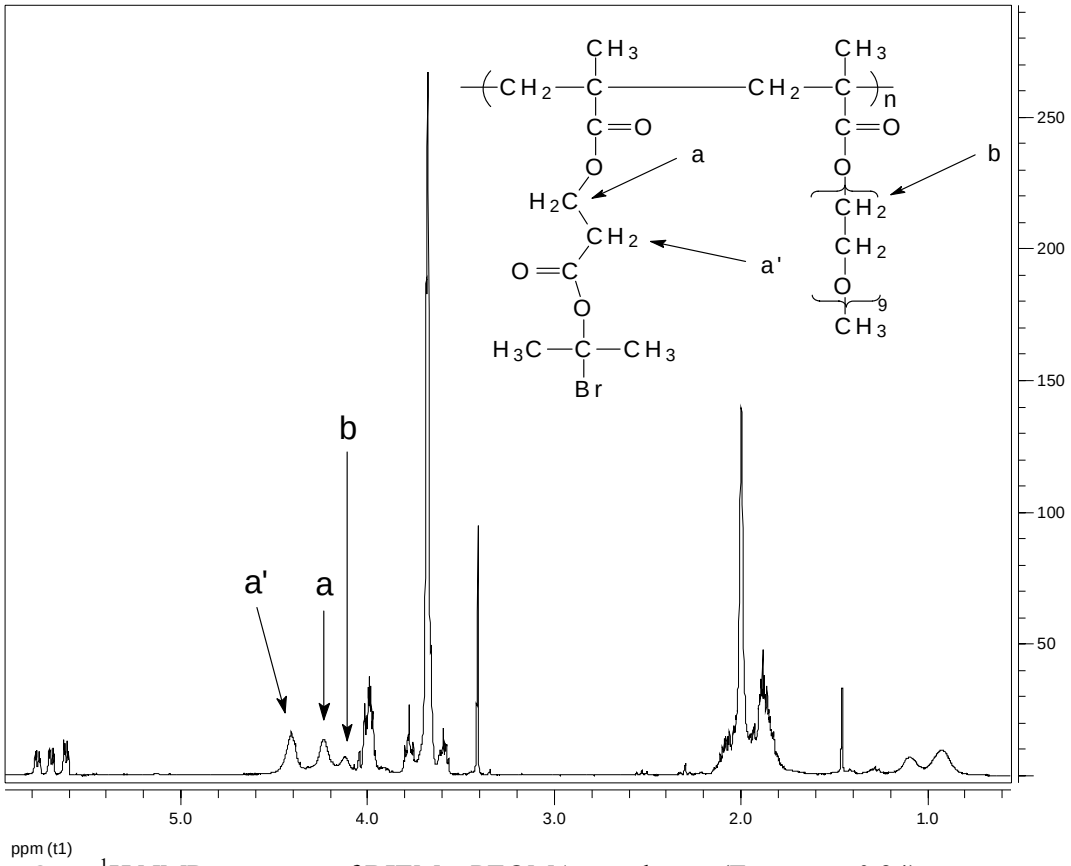


**Figure 7.2:** $^{1}$H NMR spectrum of BIEM – PEOMA copolymer ($F_{PEOMA} = 0.24$).

## *7.4.2 'Grafting from' polymerization using P(BIEM) and P(BIEM-co-PEOMA) as polyinitiators:*

Figure 7.3 illustrates the 'grafting from' polymerization process for the synthesis of brush polymers. Table 7.3 presents the results of ATRP using two different polyinitiators. Well-defined polymer brushes with homopolymer of MA and statistical copolymer side chains containing MA and 1-octene were obtained, as confirmed by the monomodal SEC chromatograms (Figure 7.4). The MMDs of the resulting brushes are relatively narrow in most cases (PDI < 1.4), indicating that the intermolecular coupling reactions during the polymerization are negligible and no peculiarities are caused by the incorporation of 1-octene. The polymerization of MA is fast and can go to relatively high conversion, as is observed in table 7.3. In literature too, during the synthesis of brush polymers, it has been observed that relatively high conversions are obtained for acrylate

polymerization, but no cross-linking occured.[6] Now, since the volume ratio of solvent to monomer is 9/1, a build-up in the viscosity at higher conversions is avoided. A higher fraction of octene in the monomer feed results in higher incorporation of octene into the copolymer, coupled with lower overall conversion and low MM.[12] Two effects can cause this phenomenon. Due to composition drift, the fraction of 1-octene in the remaining monomer increases, which leads to a decrease in average propagation rate constant. When the fraction of 1-octene increases, the probability of endcapping a 1-octene moiety at the chain end with a bromide increases. When this happens the chain will be virtually inactive, as shown with the model experiments (Chapter 2, Section 2.5).

Obviously, the $M_n$ values obtained from the SEC relative to linear PS standards were just the apparent ones. There is a change in the hydrodynamic volume of these brush polymers as a result of the branched and closely packed architectures. It is known that the hydrodynamic volume of the branched polymers decreases and therefore branched polymers elute later during SEC analysis as compared to their linear analogues of similar MM.[18,19]

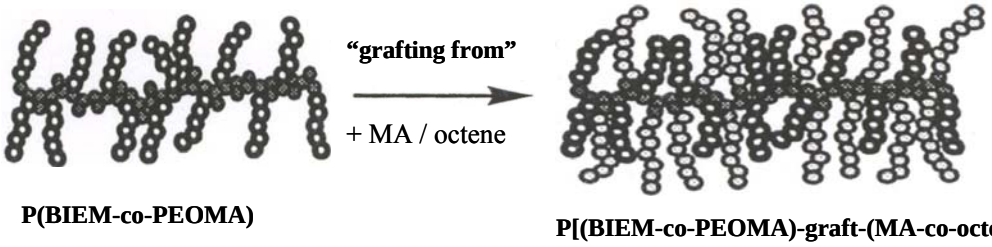


**Figure 7.3:** Preparation of brush polymers using the 'grafting from' approach.

**Table 7.3:** Synthesis of brush polymers via ATRP

| Entry | Polyinitiator | $f_{MA}$ | $f_{Octene}$ | $F_{Octene}$ (mol fraction)[a] | Overall Conversion | $M_{n\ apparent}$ (g/mol)[b] | PDI |
|---|---|---|---|---|---|---|---|
| 1 | P(BIEM) | 1 | - | - | 0.85 | $2.0 \times 10^4$ | 1.3 |
| 2 | P(BIEM) | 0.5 | 0.5 | 0.15 | 0.30 | $1.4 \times 10^4$ | 1.4 |
| 3 | P(BIEM-co-PEOMA) | 0.5 | 0.5 | 0.15 | 0.31 | $1.5 \times 10^4$ | 1.4 |

Reaction temperature = 80 ºC; Volume {solvent}/{monomer} = 1/9; Reaction time = 24 hrs.

[Monomer]:[Polyinitiator]:[CuBr]:[PMDETA] = 81:1:0.5:0.5

*a* Calculated from monomer conversion as measured by GC and confirmed by proton NMR.

*b* From SEC, calibrated with PS standards.

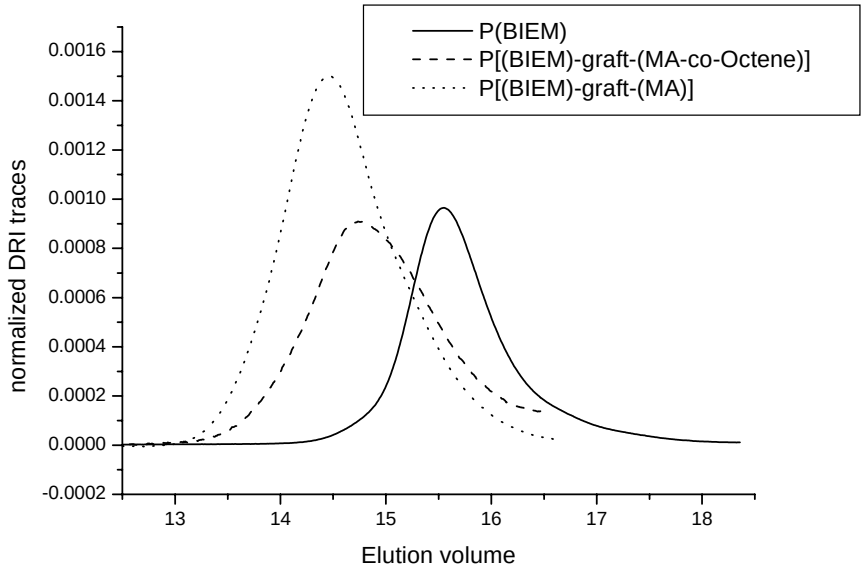


**Figure 7.4:** SEC traces of polyinitiator P(BIEM) and the corresponding short brushes with homopolymer of MA and copolymer of MA/Octene in the side chains. ($f_{Octene} = 0.50$). The chromatograms are scaled to conversion.

From the $^{1}H$ NMR spectrum in Figure 7.5 it is clear that the brush polymers have indeed been formed. The two typical peaks at 4.21 and 4.27 ppm (a and a'), which represent the methylene protons between two ester groups of the polyinitiator, as assigned in Figure 7.2, have disappeared. Instead, the methoxy peak at 3.6 ppm from MA and the octene methyl triplet at 0.8 ppm are easily distinguished and can be used to calculate copolymer composition. The region from 1.0 - 2.0 ppm includes the poorly resolved peaks attributed predominantly to the methine and methylene hydrogens present in the side chain (grafted copolymer) and the also from the methylene hydrogens present in the octene chain.

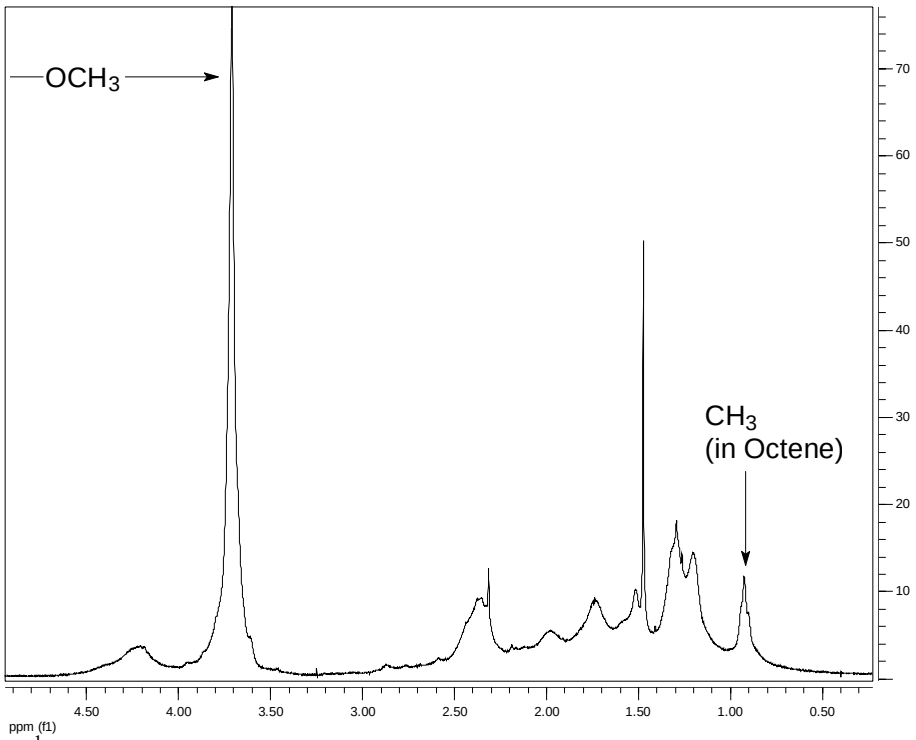


**Figure 7.5:** $^{1}$H NMR spectrum of P[(BIEM)-g- (MA-co-Octene)] brush copolymer ($F_{Oct}$ = 0.15).

***7.4.3 Scanning force microscopy (SFM) characterization of brush polymers:*** The brush polymers were further characterized by SFM in order to visualize the polymer architecture. All samples for SFM were prepared by dip-coating from dilute solutions using freshly cleaved mica as substrate.

Figure 7.6 shows the SFM images of the P[(BIEM)-g- (MA-co-Octene)] copolymer ($F_{Oct}$ = 0.15). From the image, only “islands” of polymer molecules are visible, single molecules are not observed. This may be attributed to the high concentration of the polymer, but since the density of the "islands" is not very high, this probably may not be the main reason. The polymer aggregation on mica could be one other reason. Basically, the interaction between MA and the polar mica substrate is not too strong. In literature, it was reported that the increase in humidity could rearrange PMMA molecules on mica surface.[20] PMA may also be expected to behave in a manner similar to PMMA. Further, the polymer side chains consist of a random copolymer of MA and octene. From literature, it is known that non-polar polymer molecules, such as polystyrene (PS), have weak interaction with mica surface, and hence the PS based polymers collapse on mica surface.[5,6] Similar

to PS, non-polar octene will not strongly interact with mica. Thus the presence of octene in the side chains will decrease the overall interaction between the polymer brush molecule and mica surface. Hence, the interaction might not be favorable enough to fix the structure during the sample preparation, which means solvent evaporation may induce aggregation.

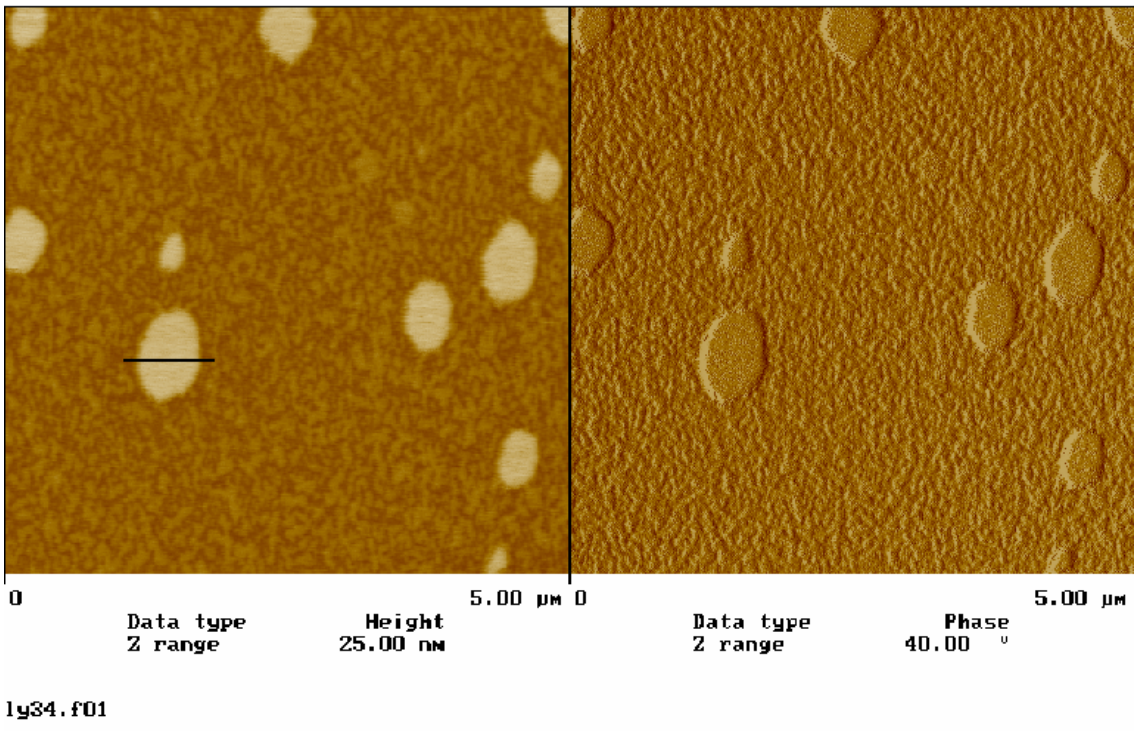


**Figure 7.6:** Tapping-mode SFM images for the P[(BIEM)-g- (MA-co-Octene)] brush polymer, dip coated from dilute THF solution on mica: (left) height image and (right) phase image. The cross-section analysis has been done along the line indicated in the SFM image. The height of the polymer "island" was found to be 5 nm.

***7.4.4 Contact angle measurements:*** Contact angles of water and ethylene glycol as wetting liquids (or probes) were measured for the P[(BIEM)-g-(MA-co-Octene)] ($F_{Oct}$ = 0.15) and P[(BIEM)-g- (MA)] copolymers (entries 1 & 2, in table 7.3), which were spin coated on glass plates. Since the backbone polymer chain employed for the 'grafting from' technique was the same, it was interesting to investigate the influence of octene in the side chain on the contact angle and the surface free energy measurements. From Figure 7.7 it is clear that the octene does have a significant influence on the contact angle and the surface energy of the polymer film. Incorporation of octene

slightly enhanced the hydrophobicity at the film surface and at the same time reduced the surface energy due to increased hydrophobicity.

On casting a film, when there is only MA in the side chain, the $–OCH_3$ from MA gets aligned at the air/film interface. If there is octene in the side chain, then at the interface the long non-polar alkyl side from the octene also gets preferentially aligned replacing some of the $–OCH_3$ from MA. This long alkyl side chain from octene renders more hydrophobicity at the interface due to its non-polar character. Hence the contact angle increased with the presence of octene in the polymer chain.

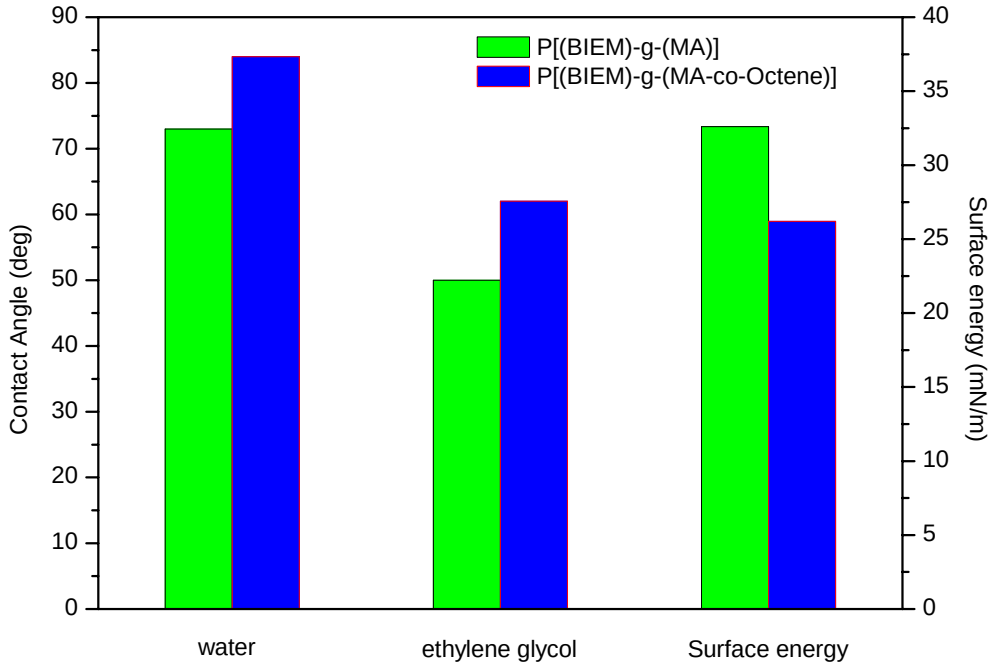


**Figure 7.7:** Results of contact angle measurements conducted on the brush copolymers (using water and ethylene glycol as probe liquids), which were spin coated on glass plates.

***7.4.5 Adhesion measurements:*** Adhesion measurements were performed on polypropylene (PP) panels coated with the P[(BIEM)-g-(MA-co-Octene)] ($F_{Oct}$ = 0.15) and P[(BIEM)-g- (MA)] copolymers (entries 1 & 2, in Table 7.3). It is known that non-polar materials are only compatible with polar resins after surface treatment. The reason for the incompatibility arises from the difference in the surface energies between the polar and non-polar parts.

From the contact angle measurements, it was evident that incorporation of octene into the polymer reduced the surface energy due to the non-polarity at the interface. Hence, it was

interesting to study the interaction of the octene in the polymeric side chain, if any, with the PP substrate. The adhesion measurements were repeated twice for each system (repeat experiments represented by 1 and 2). As is evident from Figure 7.8, larger force is required during the pull-off test to detach the polymeric film containing the octene in the side chain as opposed to having only MA in the side chain. Since the backbone polymer chain employed for the 'grafting from' technique was the same in both measurements, the difference in adhesive force can only be due to the different character of the groups in the side chains.

The SEM images for the fractured surfaces, from the PP non-coated (Figure 7.9) and PP coated with P[(BIEM)-g- (MA)] (Figure 7.10) seem to be similar. Hence, it might be concluded that the interface of break was the same in both cases (i.e. between the substrate and the polymer film). In other words, the adherance/interaction of the P[(BIEM)-g- (MA)] polymer on/with the substrate is not considerable. This is not surprising, since, the P[(BIEM)-g- (MA)] polymer is only composed of polar material and hence has a higher surface energy.

On the other hand, for the PP coated with P[(BIEM)-g-(MA-co-Octene)], the image looks quite different (Figures 7.11 and 7.12). It is observed that not all the polymeric coating gets detached from the substrate. From the pull-off and SEM results, it can be concluded that the small but significant fraction of octene in the side chain does preferentially interact with the PP substrate. The reason for this, as explained previously, may be attributed to the lower surface energy for a copolymer containing octene.

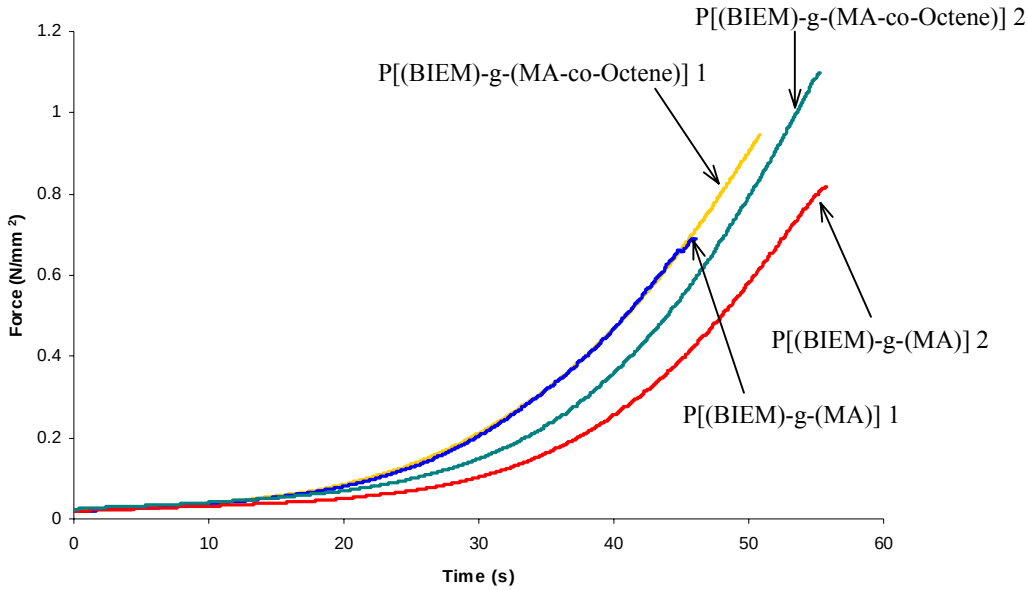


**Figure 7.8:** Plot comparing the force required during the pull off test *vs* time for the PP panels coated with P[(BIEM)-g-(MA-co-Octene)] ($F_{Oct}$ = 0.15) and P[(BIEM)-g- (MA)] copolymers. 1 and 2 indicate the repeated adhesion measurements carried out.

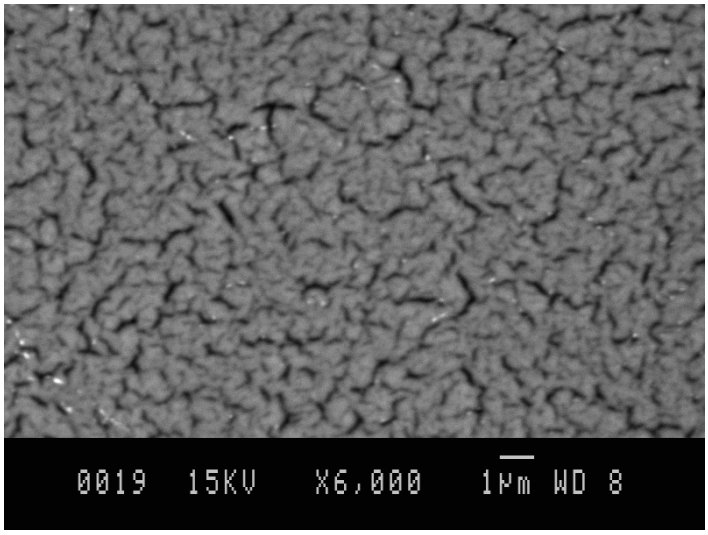


**Figure 7.9:** Backscattered scanning electron image for the fractured surface of a PP non-coated surface. Image is representative for the entire surface.

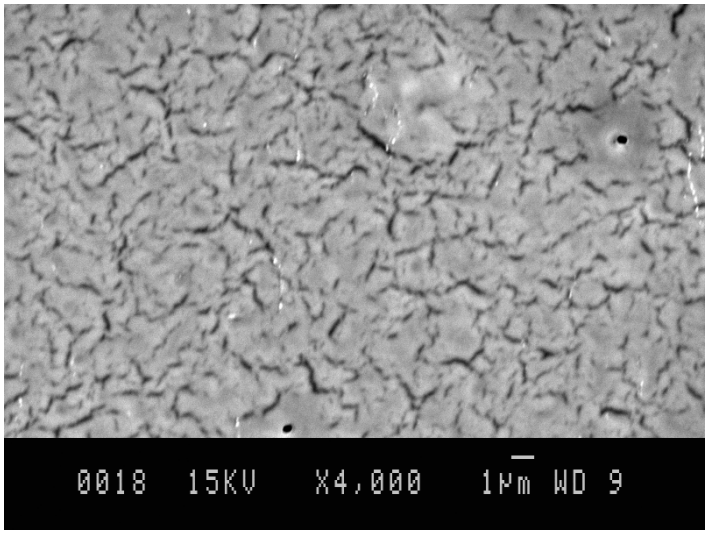


**Figure 7.10:** Backscattered scanning electron image for the fractured surface of a PP panel coated with P[(BIEM)-g- (MA)]. Image is representative for the entire surface.

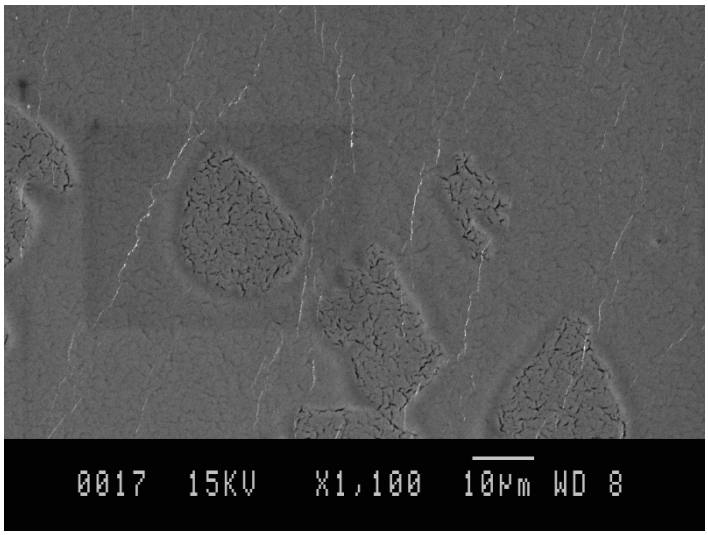


**Figure 7.11:** Backscattered scanning electron image for the fractured surface of a PP panel coated with P[(BIEM)-g- (MA-co-Octene)].

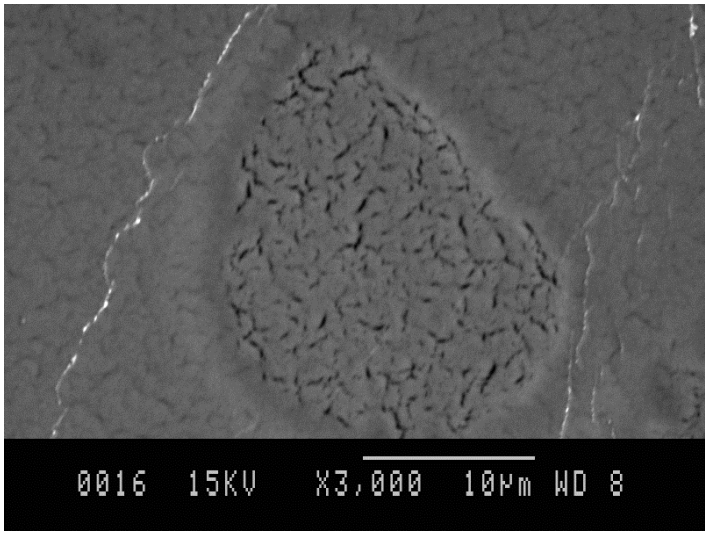


**Figure 7.12:** Backscattered scanning electron image for the fractured surface of a PP panel coated with P[(BIEM)-g- (MA-co-Octene)], at higher magnification.

## 7.5 Conclusions

A successful combination of RAFT and ATRP techniques was applied for the synthesis of novel polymer brushes by using the "grafting from" approach. The RAFT technique was employed for the backbone polymer synthesis. By using RAFT, the need to use protective group chemistry on the ATRP initiator moiety was avoided. RAFT homopolymerization of BIEM and 'grafting through' copolymerization of BIEM and PEOMA was successful and resulted in good control with 24 mol% incorporation of PEOMA.

Further, ATRP homopolymerization of methyl acrylate (MA) and copolymerization of MA with 1-octene (Oct), using both PBIEM homopolymer and P[(BIEM)-co-(PEOMA)] as polyinitiators, resulted in brushes with densely grafted homopolymer and copolymer side chains respectively. Well-controlled copolymer side chains containing 15 mol% of 1-octene were obtained. Narrow molar mass distributions (MMDs) were obtained for the ATRP experiments.

Contact angle measurements, using water and ethylene glycol as probe liquids, were performed for the P[(BIEM)-g-(MA-co-Octene)] ($F_{Oct}$ = 0.15) and P[(BIEM)-g- (MA)] copolymers. Incorporation of octene improved the hydrophobicity at the air/film interface and at the same time reduced the surface energy due to this enhanced hydrophobicity.

From the adhesion measurements, it was evident that the small but significant fraction of octene in the side chain does preferentially interact with the PP substrate and thus improve adhesion. The reason for this was attributed to the lower surface energy for the copolymer containing octene.

## 7.6 References

1) Börner, H. G., Duran, D., Matyjaszewski, K., da Silva, M., Sheiko, S. S.; *Macromolecules*, **2002**, *35*, 3387 and references therein.

2) Kato, M.; Kamigaito, M.; Sawamoto, M.; Higashimura, T.; *Macromolecules*, **1995**, *28*, 1721.

3) Wang, J. S.; Matyjaszewski, K.; *Macromolecules*, **1995**, *28*, 7901.

4) Beers, K. L., Gaynor, S. G., Matyjaszewski, K., Sheiko, S. S.; Moller, M.; *Macromolecules*, **1998**, *31*, 9413

5) Börner, H. G., Beers, K., Matyjaszewski, K., Sheiko, S. S.; Moller, M.; *Macromolecules*, **2001**, *34*, 4375.

6) Zhang, M., Breiner, T., Mori, H., Muller, A. H. E.; *Polymer*, **2003**, *44*, 1449.

7) Neugebauer, D., Zhang, Y., Pakula, T., Matyjaszewski, K.; *Polymer*, **2003**, *44*, 6863.

8) Padwa, A. R.; *Prog. Polym. Sci.*, **1989**, *14*, 811.

9) *Functional Polymers: Modern Synthetic Methods and Novel Structures*; Patil, A. O.; Schulz, D.N.; Novak,B. M.; (Eds.); ACS Symposium Series 704; American Chemical Society: Washington, DC, **1998**.

10) Liu, S; Elyashiv, S.; Sen, A; *J. Am. Chem. Soc.*, **2001**, *123*, 12738.

11) Venkatesh, R., Bastiaan, S., Klumperman, B.; submitted *Chem. Commun.*

12) Venkatesh, R., Harrisson, S., Haddleton, D. M., Klumperman, B.; submitted *Macromolecules*.

13) Venkatesh, R., Klumperman, B.; *Macromolecules*, **2004**, *37*, 1226.

14) Chiefari, J., Chong, Y. K., Ercole, F., Krstina, J., Jeffery, J., Le, T. P. T., Mayadunne, R. T. A., Meijs, G. F., Moad, C. L., Moad, G., Rizzardo, E., Thang, S. H.; *Macromolecules*, **1998**, *31*, 5559.

15) Chong, Y. K., Krstina, J., Le, T. P. T., Moad, G., Postma, A., Rizzardo, E., Thang, S. H.; *Macromolecules*, **2003**, *36*, 2256. Chiefari, J., Mayadunne, R. T. A., Moad, C. L., Moad, G., Rizzardo, E., Postma, A., Skidmore, M. A., Thang, S. H.; *Macromolecules*, **2003**, *36*, 2273.

16) Owens, D. K., Wendt, R. C.; *J. Appl. Polym. Sci.*; **1969**, *13*, 1741.

17 Moad, G., Chiefari, J., Chong, Y. K., Krstina, J., Mayadunne, R. T. A., Postma, A., Rizzardo, E., Thang, S. H.; *Polym. Int.*, **2000**, *49*, 993.

18) Billingham, N. C.; *Molar Mass Measurement in Polymer Science*, Kogan Press Ltd., **1977**, p.220.

19) Rabek, J. F.; *Experimental Methods in Polymer Chemistry*, John Wiley and Sons, **1980**, p.438.

20) Kumaki, J., Hashimoto, T.; *J. Am. Chem. Soc.*, **2003**, *125*, 4907.

# Chapter 8

## *Highlights and Technological Assessment*

## *8.1 Highlights*

In a recently published book on Radical Polymerization,[1] one of the questions posed within the Future Outlook and Perspectives chapter was *"Can we increase chemoselectivity of olefin polymerization and compete with metallocene and Ziegler-Natta systems? Or if not, how can we combine polyolefins and polyacrylates and other polar monomers prepared by radical polymerization."* While addressing this question, the work described in this thesis is clearly one of the stepping stones in the right direction. In this work, using radical polymerization techniques the feasibility for the copolymerization of alpha-olefins and polar monomers has been proven.

The highlights of the work described in this thesis are:

(1) Copolymerization of (meth)acrylates and 1-octene using radical techniques (free radical polymerization (FRP), ATRP and RAFT), results in statistical copolymers comprising almost 25 mol% of 1-octene.

(2) Narrow molar mass distributions (MMD) are obtained for the ATRP and RAFT experiments, which suggest conventional controlled behavior, with no peculiarities caused by the incorporation of 1-octene. However, for the FRP reactions, broad MMDs are obtained, which indicate that 1-octene behaves as a chain transfer agent under FRP conditions. The chain transfer reactions within the targeted molar mass range for the ATRP and RAFT experiments are insignificant.

(3) The only preferred radical pathway during the ATRP and RAFT copolymerization of (meth)acrylate and 1-octene is the rapid crosspropagation of the octene terminal radicals. That is, for propagating radicals with a terminal octene unit, the time constant for crosspropagation is smaller than that for deactivation. In other words, chains with an octene terminal unit exclusively undergo crosspropagation with the polar monomer. When the chain is end-capped with an olefin, it is virtually inactive or extremely slow to re-initiate.

(4) For the current study, the feasibility of the ATR copolymerizations has been found to be independent of the employed ligands .

(5) Increasing the fraction of the olefin in the monomer feed, leads to an increase in the level of incorporation of the olefin into the copolymer, at the expense of the overall conversion.

(6) There is a good agreement between the reactivity ratios determined for the ATRP and FRP systems.

(7) Different chain topologies (block, graft) have been synthesized using the ATRP and RAFT techniques. Using conventional FRP this is not possible.

(8) In the graft copolymers, incorporation of octene into the side-chain slightly enhances the hydrophobicity at the air/film interface and at the same time reduces the surface energy due to this enhanced hydrophobicity. It has also been observed, that statistical copolymers consisting of both polar and non-polar parts have better interaction with predominantly non-polar substrates, as opposed to polymers comprising entirely of polar monomeric units.

(9) On the lines of the octene systems, copolymerization of acrylates and allyl butyl ether (ABE) using radical techniques (FRP, ATRP and RAFT), also results in statistical copolymers comprising almost 20 mol% of ABE. Narrow MMDs are obtained for ATRP and RAFT experiments. These results indicate the versatility of controlled radical polymerization (CRP), for the copolymerization of monomers, which always had been thought of as improbable or impossible to polymerize, via a radical mechanism.

The difference of six orders of magnitude for the fragmentation rate coefficient in similar cumyl dithiobenzoate mediated styrene polymerizations is yet to explained.[2,3] The work described in Chapter 5 tries to tackle this issue by investigating the fate of the formed intermediate radical during cumyl dithiobenzoate mediated BA polymerization. The work clearly indicates that indeed, the intermediate radicals, formed during the polymerization, result in stable and long living intermediate radicals. But at the same time, these intermediate radicals are also prone to termination, resulting in the formation of 3 and 4 arm star polymers. Thus, for the present system, a combination of the two events may contribute to the retardation, which is normally observed during RAFT polymerizations.

## *8.2 Technological Assessment*

The synthesis of the copolymer consisting of both an α-olefin and a polar vinyl monomer opens up a kaleidoscope of opportunities for possible industrial applications.

The synthesized copolymer can be employed in coating compositions for polar substrates. Good adhesion to the metal surfaces can be obtained due to the polar groups. At the same time, the α-olefin part of the copolymer may offer good protective properties due to the low surface energy. Examples of copolymers suitable for the use in coating compositions are copolymers of α-olefins with methyl (meth)acrylate, glycidyl (meth)acrylate, hydroxyethyl (meth)acrylate, and styrene.

The copolymer could also be used in coating compositions of non-polar surfaces. As such, coating compositions are usually relatively polar, hence, not compatible with non-polar surfaces (e.g. polypropylene and its (co)polymers). Therefore, parts made of polypropylene or its copolymers are usually subjected to some form of pre-treatment before coating, to increase their polarity. On using the synthesized copolymers, the α-olefin part will be compatible with parts made of polypropylene and its copolymers. At the same time, the surface is also rendered more polar, due to the presence of the polar groups. This improves the compatibility with the normal coatings. Hence, pre-treatment of these plastic parts would not be required, which in turn would lead to massive cost savings and improved quality of the coating of these parts. *The first encouraging but preliminary result, employing this line of thought are reported in Chapter 7.*

The copolymer may be used as a compatibilizer in polymer blends comprising of one or more relatively polar (co)polymers, for example poly(methyl methacrylate), polyacrylate, styrene - maleic anhydride copolymer and polystyrene, and one or more relatively apolar (co)polymers, for example polypropylene and polyethylene. Such blends are for example applied to combine the favorable properties of the relatively polar (co)polymer(s), for example hardness, scratch resistance, chemical resistance, dimensional stability and heat resistance, with the favorable properties of the relatively apolar (co)polymer(s), for example strength, low density, and relatively low cost price.

The synthesized copolymers can also be used as a tie resin in multi-layer films, offering the possibility to combine the barrier properties of at least two different films. For example,

multilayered films comprising a layer of one or more relatively apolar (co)polymer(s) (e.g. polypropylene and/or polyethylene), and a layer of one or more relatively polar (co)polymers (e.g. ethylene-vinyl alcohol copolymer).

## *8.3 References*

1) *Handbook of Radical Polymerization*, Matyjaszewski, K., Davis, T. P., (Eds.), John Wiley and Sons Inc., Hoboken, **2002**.

2) Wang, A. R., Zhu, S., Kwak, Y., goto, A., Fukuda, T., Monteiro, M. J; *J. Polym. Sci., Part A: Polym. Chem.*, **2003**, *41*, 2833.

3) Barner-Kowollik, C., Coote, M. L., Davis, T. P., Radom, L., Vana, P.; *J. Polym. Sci., Part A: Polym. Chem.*, **2003**, *41*, 2828.

# Summary

In the author's opinion, in the current day and age, polymer research can be broadly classified into two distinct sectors, one where novel monomers/polymers are synthesized for specific applications, and the other where the borders of existing monomers/polymers are constantly probed in the quest for improved polymer properties (example by altering the polymer microstructure), or for new applications. The work carried out and described in this thesis pertains to the latter sector. The synthesis of copolymers containing both polar and non-polar monomers has always received a great deal of attention due to its interesting polymer properties. A lot of research is being conducted on the copolymerization of α-olefins. However, the majority of the work done and results published have been restricted to transition metal catalyzed polymerizations, where via an insertion mechanism the polar monomer is incorporated into the polymer chain. Interesting polymer structures like block and graft copolymers have been synthesized. But still the big challenge lies in the synthesis of random or statistical copolymers, which is difficult due to the unfavorable reactivity ratios of the comonomer pairs in conjunction with the catalyst systems.

The first aim of the project was to explore the possibilities and limitations for the free radical copolymerization (FRP) between polar and non-polar monomers. The free radical approach is known to work exceedingly well for polar monomers, but the homopolymerization of α-olefins and allylic monomers (like allyl acetate or allyl butyl ether) is very unlikely and if it does occur, it polymerizes at considerably low rates. This effect is a consequence of degradative chain transfer, wherein, the propagating radical in such a polymerization is very reactive, while the allylic C-H in the monomer is quite weak, resulting in chain transfer to monomer. This formed allylic radical is too stable to reinitiate polymerization and will undergo termination by reaction with another allylic radical or more likely, with propagating radicals. Surprisingly, the initial results for the FRP were positive to the point that, even though the α-olefin acts as a chain transfer agent during the polymerization, a small but significant amount of the α-olefin is incorporated statistically into the polymer chains.

The next step was then to employ controlled radical polymerization (CRP) techniques, where the steady concentration of free radicals is established by balancing rates of activation and deactivation and thus the limitations of the FRP (like termination and transfer events) are minimized to a great extent. The atom transfer radical copolymerizations (ATRP) of an acrylate

with an α-olefin (1-octene) and also of a methacrylate with an α-olefin resulted in the formation of statistical copolymers containing almost 25 mol% of 1-octene. Within the targeted molar mass range, narrow molar mass distributions (MMD) were obtained for the ATRP experiments, which suggest conventional controlled behavior. The formation of the copolymers was monitored using various characterization techniques, viz., size exclusion chromatography (SEC), NMR, matrix assisted laser desorption/ionization-time of flight-mass spectrometry (MALDI-TOF-MS) and gas chromatography. MALDI-TOF-MS has been extensively used in the current investigation because mass spectrometry techniques provide the sensitivity and resolution, together with structural information to determine even the smallest amount of product. For low molar mass polymers, the determination of end groups is possible, which provides valuable information on the reaction mechanism.

Further, other CRP techniques, like reversible addition-fragmentation chain transfer (RAFT) polymerization were also explored for the synthesis of the copolymers. The RAFT mediated copolymerization of the polar (acrylate or methacrylate) monomer and α-olefin (1-octene) also resulted in excellent control, with the formation of statistical copolymers containing almost 20 mol% of 1-octene. This result clearly proved the versatility of the CRP techniques for the current system.

Then the next step was to try and understand this successful copolymerization mechanism. This was achieved by synthesizing model compounds which mimic the growing polymeric radicals during polymerization. The only preferred radical pathway during the ATRP and RAFT copolymerization of (meth)acrylate and 1-octene was ascribed to the rapid crosspropagation of the 1-octene terminal radicals. Because, when the chain with a terminal olefin is end-capped, it was virtually inactive or extremely slow to re-initiate.

On the lines of the α-olefin systems, copolymerization of monomers, which otherwise were thought of as improbable to polymerize via a radical mechanism were also explored. Copolymerization of acrylates and allyl butyl ether (ABE) using various radical techniques (FRP, ATRP and RAFT), results in statistical copolymers containing almost 20 mol% of ABE. Narrow MMDs were obtained for the CRP experiments.

To finalize this part of the project, different chain topologies like block, and graft copolymers were synthesized using the CRP techniques and the polar and non-polar monomers. The synthesized copolymers were then explored for possible industrial applications. The copolymer was used as a primer for non-polar surfaces. The α-olefin part is expected to be compatible with parts made of polypropylene and propylene copolymers. At the same time, the surface is also rendered more polar, due to the presence of the polar groups. This improves the compatibility with the usually polar top coats. The preliminary results clearly indicated the feasibility for the above line of thought.

RAFT like ATRP has become an important technique for producing polymers with controlled architectures, chain lengths and chain length distributions. Currently within the scientific community, there is a debate raging around the RAFT mechanism. The difference of six orders of magnitude (result of the different lines of thought) for the fragmentation rate coefficient in similar cumyl dithiobenzoate mediated styrene polymerizations is yet to be explained. The current work, tries to tackle this issue by investigating the fate of the formed intermediate radical during cumyl dithiobenzoate mediated BA polymerization. The work clearly indicates that indeed the intermediate radicals formed during the polymerization, result in stable and long living intermediate radicals. But at the same time, these intermediate radicals are also prone to termination, resulting in the formation of 3 and 4 arm star polymers [this has been proved using MALDI-TOF-MS]. Thus, for the present system, a combination of the two events may contribute to the retardation, which is frequently observed during RAFT polymerizations.

In conclusion, conventional FRP and CRP techniques have provided another, more convenient route for the synthesis of copolymers containing both polar and non-polar groups.

# Samenvatting

Volgens de auteur kan het onderzoek aan polymeren worden onderverdeeld in twee categorieën. Enerzijds worden er nieuwe monomeren en polymeren gesynthetiseerd voor specifieke applicaties, anderzijds worden de grenzen van bestaande monomeren/polymeren steeds verder verlegd door toepassing van technieken die leiden tot bijvoorbeeld een andere microstructuur. Het werk beschreven in dit proefschrift behoort tot de tweede categorie. De copolymerisatie van polaire en apolaire monomeren heeft altijd veel aandacht getrokken vanwege de interessante eigenschappen die dergelijke materialen bezitten. Veel onderzoek is verricht aan de copolymerisatie van α-olefinen. Echter, het overgrote deel van dit onderzoek beperkt zich tot overgangsmetaalgekatalyseerde polymerisatiereacties, waar via een insertiemechanisme het polaire monomeer wordt ingebouwd in de polymeerketen. Via deze techniek kunnen interessante polymeerstructuren, zoals blok- en graftcopolymeren worden gesynthetiseerd. De grote uitdaging ligt nog in de synthese van ideale of statistische copolymeren. Deze materialen zijn moeilijk toegankelijk vanwege de ongunstige reactiviteitsverhoudingen van de gewenste comonomeerparen in samenhang met de katalytische polymerisatietechnieken.

Het eerste doel van het project was om de mogelijkheden en limiteringen van vrije radicaalcopolymerisatie tussen polaire en apolaire monomeren te onderzoeken. Vrije radicaalpolymerisatie wordt veel toegepast voor polaire (vinyl)monomeren. Echter de copolymerisatie met α-olefinen en allylische monomeren (b.v. allylacetaat en allylbutylether) is erg onwaarschijnlijk. Als de copolymerisatie al verloopt zal deze gepaard gaan met een lage polymerisatiesnelheid . Deze lage snelheid is een gevolg van degradatieve ketenoverdracht waarbij het reactieve propagerende radicaal een allylisch waterstofatoom abstraheert van een comonomeer. Het gevormde allylische radicaal is te stabiel om herinitiatie van een polymeerketen te bewerkstelligen. Het zal derhalve een nevenreactie ondergaan zoals bijvoorbeeld terminatie met een ander allylisch radicaal of terminatie met een propagerend radicaal. Verrassenderwijs duidden de eerste resultaten uit de vrije radicaalcopolymerisatie erop dat de inbouw van α-olefinen in een vinylpolymerisatie mogelijk is.

De volgende stap in het onderzoek was het toepassen van gecontroleerde radicaalpolymerisatietechnieken. Hierbij wordt een radicaalconcentratie ingesteld door het uitbalanceren van activerings- en deactiveringsreacties. Hiermee werd getracht de beperkingen van vrije radicaalpolymerisatie in de synthese van de α-olefinecopolymeren te minimaliseren. De *atom*

*transfer radical copolymerizations* (ATRP) van een acrylaat met een α-olefine (1-octeen) en ook van een methacrylaat met een α-olefine resulteerden in een statistisch copolymeer met bijna 25 mol% 1-octeeninbouw. Binnen het onderzochte molmassagebied werden smalle molmassaverdelingen (MMDs) verkregen voor de ATRP experimenten. Dit duidt op de gebruikelijke beheersing van de polymerisatie die in het geval van ATRP wordt waargenomen. De vorming van een copolymeer werd bevestigd door een scala aan karakteriseringstechnieken (gelpermeatiechromatografie (GPC), kernspinresonantie spectroscopie (NMR), matrix-geassisteerde laser desorptie ionisatie-massaspectrometrie (MALDI-TOF-MS) en gaschromatografie). MALDI-TOF-MS werd uitgebreid gebruikt binnen het huidige onderzoek vanwege de hoge gevoeligheid en resolutie die de onderzoeker in staat stellen om gedetailleerde informatie over het onderzochte materiaal te verkrijgen. Voor polymeren met een lage gemiddelde molmassa biedt de techniek verder goede mogelijkheden om het karakter van de eindgroepen vast te stellen. Dit is van groot belang bij het onderzoek naar het polymerisatiemechanisme.

Naast ATRP werd ook gebruik gemaakt van reversibele additie-fragmentatie ketenoverdracht (RAFT) polymerisatie voor de synthese van de α-olefine copolymeren. Ook in het geval van RAFT werden succesvolle copolymerisaties uitgevoerd van 1-octeen met een acrylaat en met een methacrylaat. In dit geval werd circa 20 mol% 1-octeen ingebouwd in het copolymeer.

De volgende stap in het onderzoek was om een poging om te begrijpen waarom ATRP en RAFT zonder problemen kunnen worden uitgevoerd met 1-octeen als comonomeer. Hiertoe werden modelverbindingen gebruikt waarmee de activering van verschillende ketenuiteinden konden worden gesimuleerd. De conclusie van dit deelonderzoek was dat een α-olefine op het uiteinde van een groeiende keten (nagenoeg) altijd instantane propagatie met een vinylmonomeer ondergaat. Wanneer een keten met een terminale α-olefine wordt gedeactiveerd, leidt dit tot een eindgroep die effectief dood is (niet of nauwelijks opnieuw te activeren).

In het verlengde van de α-olefinen werd tevens onderzocht of allylbutylether (ABE) via ATRP en RAFT te copolymeriseren is met een acrylaat. Opnieuw bleek circa 20 mol% ABE in te bouwen te zijn. Verder werd in het geval van ATRP en RAFT een smalle molmassaverdeling gevonden.

Uiteindelijk werden verschillende ketentopologieën (blok- en graftcopolymeren) gesynthetiseerd via gecontroleerde radicaalpolymerisatietechnieken (ATRP en RAFT). De gesynthetiseerde polymeren werden vervolgens onderzocht op hun potentie in industriële toepassingen. Met name werd gekeken naar de werking als primer voor een apolair oppervlak. Van het α-olefinedeel van het polymeer wordt verwacht dat het interactie zal hebben met polypropeen of met propeencopolymeren. Het polaire deel van het molecuul zal interactie vertonen met de doorgaans polaire *top coat*. De eerste resultaten zijn hoopgevend. Er lijkt interactie op te treden met de apolaire ondergrond.

RAFT en ATRP zijn beide belangrijke technieken aan het worden voor de productie van polymeren met een goed gedefinieerde architectuur, ketenlengte en ketenlengteverdeling. Op dit moment ontspint er zich binnen de wetenschappelijke wereld een debat over de details van het RAFT mechanisme. Er zijn twee scholen ten aanzien van de verklaring van retardatiefenomenen die frequent worden waargenomen. Afhankelijk van het gekozen model is er een discrepantie van zes orden van grootte voor de fragmentatiesnelheidsconstante. Binnen het huidige onderzoek is een aantal modelexperimenten gedaan om vast te stellen wat het lot is van het zogenaamde intermediaire radicaal in een butylacrylaat polymerisatie met een dithiobenzoaat als RAFT reagens. Het werk toont aan dat er drie- en vierarmige sterren gevormd kunnen worden. Dit geeft aan dat de terminatie van intermediaire radicalen een rol kan spelen in de retardatiefenomenen. Het is gezien de hoogte van de radicaalconcentratie niet uit te sluiten dat ook langzame fragmentatie een rol speelt in de retardatie.

Concluderend kan gezegd worden dat vrije radicaalpolymerisatie, ATRP en RAFT polymerisatie interessante alternatieven bieden voor de synthese van copolymeren bestaande uit polaire vinylmonomeren en apolaire α-olefinen.

# Patents

1) Venkatesh, R., Klumperman, L., Process for the Copolymerization of alpha-olefins with Vinyl Monomers using thiocarbonylthio compounds as chain transfer agents, European Patent Application, EP 1384729, **2004**.
2) Venkatesh, R., Klumperman, L., Process for the Copolymerization of alpha-olefins with Vinyl Monomers, PCT Int. Application, WO 2003091297, **2004**.

# Scientific Papers

1) Venkatesh, R., Klumperman, B.; *Macromolecules*, **2004**, *37*, 1226.
2) Venkatesh, R., Vergouwen, F., Klumperman, B.; *J. Polym. Sci., Part A : Polym. Chem.,* In Press.
3) Venkatesh, R., Klumperman, B.; *Polymer Preprints (Am. Chem. Soc., Div. of Polymer Chemistry)*, **2003**, 44(1), 796.
4) Venkatesh, R., Harrisson, S., Klumperman, B., Haddleton, D. M.; *Polymer Preprints (Am. Chem. Soc., Div. of Polymer Chemistry)*, **2003**, 44(1), 798.

5) Venkatesh, R., Harrisson, S., Haddleton, D. M., Klumperman, B.; submitted *Macromolecules*.
6) Venkatesh, R., Staal, B. B. P, Klumperman, B.; submitted *Chem. Commun.*

7) Venkatesh, R., Yajjou, L., Kisin, S., Koning, C. E., Klumperman, B.; *manuscript under preparation.*
   **Title**: Bottle-brush copolymers via Controlled radical Polymerization.
8) Venkatesh, R., Vergouwen, F., Klumperman, B.; *manuscript under preparation.*
   **Title**: Atom Transfer Radical Copolymerization of α-Olefins with Methyl Acrylate**:** Determination of Activation Parameters.
9) Venkatesh, R., Kajiwara, A., Klumperman, B.; *manuscript under preparation.*
   **Title**: Electron Spin Resonance study on Reversible addition-fragmentation chain transfer (RAFT) mediated polymerization of Butyl Acrylate and Styrene.

10) Venkatesh, R., Staal, B. B. P, Klumperman, B., Monteiro, M. J.; *manuscript under preparation.*

**Title**: Characterization of 3 and 4 arm stars produced in the Reversible addition-fragmentation chain transfer (RAFT) polymerization of Butyl Acrylate.

11) Venkatesh, R., Kajiwara, A., de Brouwer, H., Klumperman, B., Monteiro, M. J.; *manuscript under preparation.*

**Title**: Reversible addition-fragmentation chain transfer (RAFT) kinetic study on cumyl dithiobenzoate mediated Butyl Acrylate polymerization.

12) Staal, B. B. P, Karanam, S., Venkatesh, R., Klumperman, B.; *manuscript under preparation.*

**Title**: Identification of chain-end groups via Matrix assisted laser desorption/ionization – time of flight – mass spectrometry (MALDI-TOF-MS) for poly (methyl methacrylate) synthesized by atom transfer radical polymerization (ATRP).

# Acknowledgements

Finally, its done. But still the most important part remains. Thanking the people who have been instrumental in getting it to its completion.

I would like to express my sincere gratitude to Bert, for clearly defining the research area, providing valuable suggestions during the experimental stages and finding time to read through the manuscript in spite of his tight schedule. Most importantly, I would like to thank him for his encouragement and his confidence in me and my abilities.

I would like to thank the Dutch Polymer Institute (DPI) for having financed this research project.

I am also indebted to the various project collaborators, Dr Simon Harrisson and Prof Dave Haddleton (Univ. of Warwick, UK) for assisting me with the online NMR experiments. Dr Atsushi Kajiwara (Nara University of Education, Japan) for his absolute dedication and sincerity in helping me navigate the world of ESR spectroscopy. I thoroughly enjoyed my experience in Japan (in the lab and outside it too). Dr Michael Monteiro (Univ. of Queensland, Australia), thanks a lot for everything boss. It was brilliant that you were there right from the onset. My 'Karma' must have been pretty good, hence we met. To, Dr Mariëlle Wouters (TNO), Dr Marshall Ming (TU/e) and Srđan Kisin (TU/e) for their suggestions and also for assisting me with the contact angle and adhesion experiments. Dr Richard Brinkhuis (Akzo Resins) for important pointers during the course of my PhD. Dr John Severn for the GC reaction setup. Thanks a lot matey.

Closer to home now, the SPC team, thanks are due to Prof Cor Koning for his encouragement and valuable suggestions during the course of the PhD. Also to Prof Alex van Herk, who always had some very pointed questions, but got me thinking nonetheless (apart from the chemistry I take with me some other memories too). The characterization team of Bas, Wieb and Marion, words cannot express my gratitude. It will be enough to say that this thesis would not have seen the light of the day, if it was not for you guys. Thanks!

Being in SPC has made me feel at home, I sincerely would like to thank all the past and present SPC team members for this. Thanks also to our dear secretaries Helly, Caroline and Pleunie. Life was made much easier with you guys around. Now the gang, Delphine, Vincent, Ellen, Maarten, Kirti, Joep, Jens, Raf, Wouter M, Jelena, Bas, Robin, Wouter G, Wieb, Matthijs and Rachel, thanks for everything. I owe you guys. During my time here, I also had to opportunity to work with some very good students, I would sincerely like to acknowledge them, Frank, Niels, Latifa and Eric. It was a pleasure working with you guys.

Coming to the Indian mafia, they are more family than friends, my special thanks to the past and present members, Ankur, Sreepad, Sachin, Suresh, Keshav, Rajesh, Manoranjan, Sreejit, Nilesh, Pankaj, Vidya, Mani, Kirti, Madhu and Jignesh. Thanks are also due to Lalit, Suchi, Anand, Baisakhi and Laxmikant for all their encouragement.

Finally, I am indebted to the moral support, absolute belief and encouragement provided by my parents and my family. Gayathri, I thank you for your understanding and support, and look forward to a brilliant married life with you by my side.

# Curricular Vitae

Rajan Venkatesh was born on the 7th of August 1975 in Mumbai, INDIA. In 1996, he completed his Bachelors in Chemistry with Distinction from Bombay University. After which he entered into the world of polymer research. He attained his Master of Science (by research) in Chemistry (Specialization – Polymer Chemistry) from the University Department of Chemical Technology (now, University Institute of Chemical Technology) at Mumbai in 1999. The title of the thesis was "Synthesis and Characterization of Functional Monomers, Polymers and Copolymers Based on Them". This was achieved under the able supervision of Prof Dr M A Shenoy. Thereafter, the outside world beckoned him and he moved across to the group of Prof Dr P A Lovell at the University of Manchester Institute of Science and Technology, Manchester, UK. He obtained his Master of Philosophy in Polymer Science and Technology in 2000. The title of the thesis was "Studies of Chain Transfer to Polymer in Acrylate Emulsion Copolymerizations".

In June 2000, he initiated his PhD project and took the first tentative steps into the arena of controlled radical polymerization, at the Eindhoven University of Technology, in The Netherlands. He has been working since in the Polymer Chemistry group, under the able guidance of Dr ir Bert Klumperman. As of the 1st of April 2004, he will be working as an R&D scientist for BASF AG at Ludwigshafen, in the Polymer Division.